PHD

Studies on the active sites and mechanisms of aspartate transaminase and malate dehydrogenase.

Smith, Geoffrey D.

Award date:
1978

Awarding institution:
University of Bath

Studies on the Active Sites and Mechanisms of

Aspartate Transaminase and Malate Dehydrogenase

Submitted by Geoffrey D. Smith

for the degree of Ph.D

of the University of Bath

1978

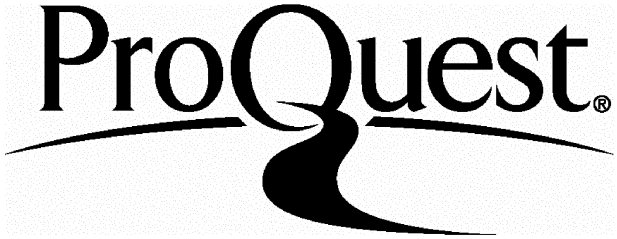

SUMMARY

Difluoro-oxaloacetate reacts with the aminic form of aspartate transaminase, forming a tight reversible complex as shown in steady state inhibition studies. Spectrophotmetric evidence indicates slow transamination of the analogue and allowed tentative identification of some of the reaction intermediates, together with the rate constants for their formation and removal. Difluoro-oxaloacetate forms an abortive complex with the aldimine form of transaminase giving rise to observable changes in the ^{19}F n.m.r. signal of the ligand. The pH dependences of line width and chemical shift show inflexion points at pH 5.4 and ph 8.5 implicating groups with pKs in these regions in binding dicarboxylate ligands to the active site. With the apoenzyme, the pH profile of the n.m.r. parameters lacks the inflexion point at pH 5.4, providing evidence that the Schiff-base nitrogen (pK 5.4) is one of the carboxylate binding sites. The direction of n.m.r. shifts implies a non-polar microenvironment at the active site.

Steady state kinetics of the NADH reduction of difluoro-oxaloacetate catalysed by malate dehydrogenase show that the fluoro-analogue is a good substrate for the enzyme and follows the same kinetic mechanism as that of oxaloacetate. Binding of the analogue both directly to the enzyme and in a ternary abortive complex was shown in protection experiments using iodoacetamide. The presence of the co-enzyme enhanced the affinity of the enzyme for the keto acid. The

^{19}F n.m.r. signal of difluoro-oxaloacetate shifts downfield and broadens in the presence of malate dehydrogenase and NAD.

Difluoro-oxaloacetate is an effective inhibitor of malate dehydrogenase, the inhibition is complex, and appears to result from the formation of abortive binary and ternary complexes, together with alternate product inhibition. DL-Difluoromalate was found not to be a substrate for malate dehydrogenase, but was a pure non-competitive inhibitor of difluoro-oxaloacetate reduction catalysed by malate dehydrogenase.

TABLE OF CONTENTS

	PAGE
SUMMARY	1
Study on aspartate transaminase	
INTRODUCTION	
Transamination; historical background	9
Physicochemical properties of cytoplasmic aspartate transaminase	11
Binding of the coenzyme to the protein	12
Reaction of aspartate transaminase with the natural substrates	14
Reaction of aspartate transaminase with pseudo-substrates	18
Mechanism of enzymic transamination	27
Nuclear magnetic resonance (n.m.r)	35
Covalently bound flourine as an ^{19}F n.m.r. probe	36
Fluorinated substrate analogues as ^{19}F n.m.r. probes	37
Background to the use of difluoro-oxaloacetate	40
MATERIALS	41
Methods	
Synthesis of difluoro-oxaloacetate	42
Assay of enzyme activity	44
Purification of aspartate transaminase	44
Preparation of the aminic form of aspartate transaminase	46
Preparation of the apoenzyme form of aspartate transaminase	46
Instrumentation	47
Measurement of fluoride ion	48
Computation	49

PAGE

RESULTS

Section 1: Kinetic and spectral studies on aspartate transaminase

Inhibition of aspartate transaminase by difluoro-oxaloacetate 50

The slow spectral change, 332 to 360 nm 55

Initial rates of the 332-360 nm spectral change 59

Transamination of difluoro-oxaloacetate 63

Estimation of fluoride released during the 332-360 nm spectral change 69

Determination of the aminic-aldimine enzyme equilibrium in the presence of difluoro-oxaloacetate 72

U.V. spectrum of aspartate transaminase in the presence of cysteine sulphinate and difluoro-oxaloacetate 76

The fast spectral change, 332-328 nm 76

Extent of the 332-328 nm spectral change 78

Rates of the 332-328 nm spectral change 81

Computer simulation of the 332-328 nm spectral change 87

Rapid spectrophotometric scans of a reaction mixture of aminic aspartate transaminase and difluoro-oxaloacetate 90

Section 2: ^{19}F nmr investigation of aspartate transaminase

Difluoro-oxaloacetate-aldimine enzyme complex

Spectrophotometric determination of dissociation constant 92

Determination of dissociation constant from ^{19}F chemical shift 95

Variation of n.m.r. parameters with pH 96

Interaction of aminic aspartate transaminase with high concentrations of difluoro-oxaloacetate 99

PAGE

Difluoro-oxaloacetate-apoenzyme complex

Determination of dissociation constant from ^{19}F chemical shift 104

Variation of n.m.r. parameters with pH 106

Perfluorosuccinate-aldimine enzyme complex

Determination of dissociation constant from the ^{19}F chemical shift 108

Effect of environmental changes on ligands

Variation with pH of the ^{19}F chemical shift of difluoro-oxaloacetate and perfluorosuccinate 111

Effect of polarity of the medium on the ^{19}F chemical shift of difluoro-oxaloacetate and perfluorosuccinate 113

DISCUSSION 116

Study on malate dehydrogenase 137

Introduction

Physicochemical properties 138

Active site amino acid residues 140

Interaction with co-enzyme 141

Enzyme reaction mechanism

Initial rate studies 142

Equilibrium studies 143

Effect of pH on the mechanism 145

Substrate inhibition and activation 145

Hydroxy-malonate inhibition 147

Reciprocating compulsory order mechanism 148

PAGE

Materials 150

Methods

Purification of mitochondrial malate dehydrogenase 151

Standard enzyme assay 154

Protein estimation 155

Purification of NAD 155

Preparation of DL-difluoromalate 155

Kinetic measurements 157

Results

Malate dehydrogenase catalysed reduction of difluoro-oxaloacetate 159

Protection of malate dehydrogenase against inactivation by iodoacetamide 164

By difluoro-oxaloacetate alone 167

By difluoro-oxaloacetate and NAD 170

By oxaloacetate alone 171

Determination of dissociation constant and Δ of difluoro-oxaloacetate, NAD, malate dehydrogenase complex by ^{19}F n.m.r. 172

Inhibition of malate dehydrogenase catalysed oxidation of L-malate by difluoro-oxaloacetate 175

Inhibition of malate dehydrogenase catalysed reduction of difluoro-oxaloacetate by DL-difluoro-malate 180

	PAGE
Discussion	185
Summary	206
Appendix 1	208
Appendix 2	212
References	215
Acknowledgements	229

Study on Aspartate Transaminase

Introduction

Transamination

Transamination may be defined as the intermolecular transfer of an amino group without the intermediate formation of ammonia. Non-enzymic transamination was shown (Herbst and Engel, 1934) to occur when an aqueous solution of α-aminophenylacetic and pyruvic acids was boiled, forming benzaldehyde, carbon dioxide and alanine; similar reactions were also shown to occur between pyruvic acid and other amino acids. Enzymic transamination was later demonstrated between glutamic and pyruvic acids in pigeon breast muscle (Braunstein and Kritzmann, 1937). With the advent of reagents of higher purity and improved analytical techniques, it was established that most naturally-occuring amino acids undergo enzymic transamination (Meister and Tice, 1950; Feldman and Gunsalus, 1950; Cammarata and Cohen, 1950). Transamination is now known to play a general role in amino acid metabolism, and may be respresented by the general equation.

$$R.CO.COO^- + R'.\underset{\displaystyle NH_3^+}{CH}.COO^- \rightleftharpoons R.\underset{\displaystyle NH_3^+}{CH}.COO^- + R'.CO.COO^- \qquad (1)$$

The mechanism of the non-enzymic reaction between α-aminophenylacetic acid and pyruvic acid obviously differs from enzymic transamination, as it is accompanied by decarboxylation. Transamination can occur when decarboxylation is prevented by esterification of both carboxyl groups, but this reaction requires an anhydrous medium (Brewer and Herbst, 1941). Non-enzymic transamination without decarboxylation was demonstrated in aqueous media by Snell (1944; 1945), who showed the occurrence of the reversible reaction (2) at physiological pH.

$$\text{glutamate} + \text{pyridoxal} \rightleftharpoons \alpha\text{-oxoglutarate} + \text{pyridoxamine} \qquad (2)$$

Pyridoxal phosphate (PLP) was subsequently found to be necessary in enzymic transamination (Schlenk and Snell, 1945; Lichstein, Gunsalus and Umbreit, 1945; Schlenk and Fisher, 1945; Kritzmann and Samarina, 1946). Jenkins, Yphantis and Sizer (1959) established that not only does highly purified aspartate aminotransferase contain two moles of PLP per mole enzyme, but also that resolution of the apoenzyme and coenzyme abolishes catalytic activity. Addition of PLP or pyridoxamine phosphate (PMP) to the apoenzyme restores the activity. The coenzymic role of these compounds was thus established.

The non-enzymic transamination reactions between amino acids and pyridoxal have been extensively studied because of their importance in understanding enzymic transamination. These studies have led to the formulation of a general mechanism for vitamin B6 catalysed reactions (Braunstein, 1960; Metzler, Ikawa and Snell, 1954). In each case, initial activation of the amino acid is postulated to occur through the formation of an aldimine Schiff's base between the amino acid and pyridoxal. This results in labilization of the bonds to the α-carbon atom of the amino acid and can lead to several reactions, including transamination. In this case a proton is transferred from the α-carbon to the coenzyme 4' carbon to give a ketimine, which is subsequently hydrolysed to the keto acid and pyridoxamine (Fig.1).

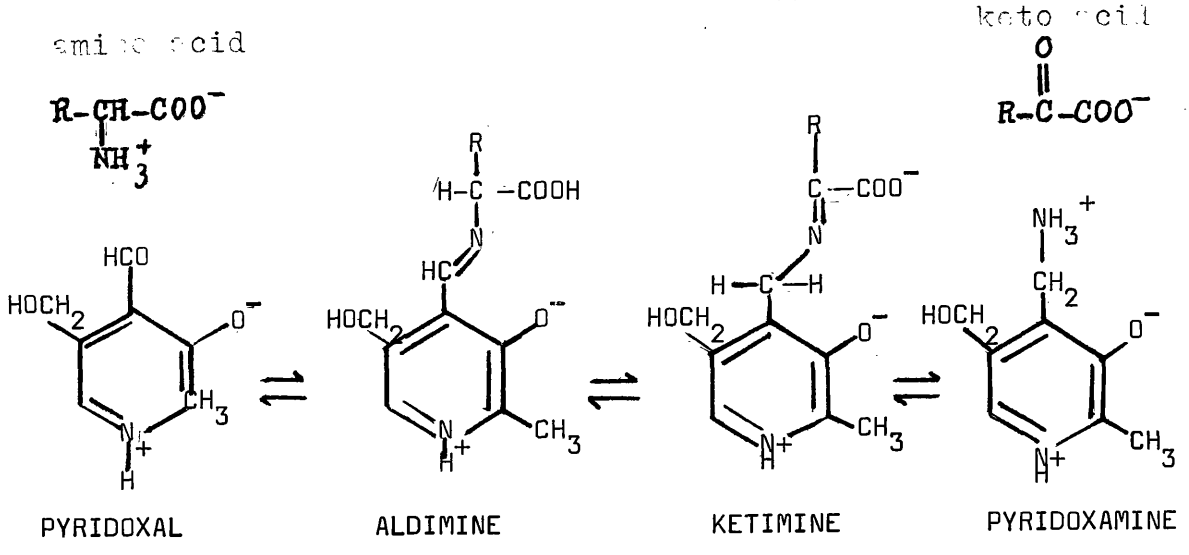

Fig.1 Mechanism for pyridoxal catalysed non-enzymic transamination after Metzler et al. (1954).

The rate of non-enzymic transamination can be increased by as much as 20-fold by the addition of certain metal ions (Metzler and Snell, 1952; Metzler, 1957; Heinert and Martell, 1963), and it is suggested that these act by forming chelates which maintain the complex in the planar state necessary for resonance stabilisation of the aldimine intermediate. Imidazole (Bruice and Topping, 1962; 1963) is also an effective catalyst for certain non-enzymic transamination reactions and acts in the absence of metal ions, suggesting the possible significance of imidazole groups of proteins in enhancing the catalytic action of PLP in the enzymic reaction. There are numerous indications that enzymic transamination operates by the same general mechanism as that given in Fig.1 (Jenkins and Sizer, 1957; Lis et al., 1960; Hammes and Fasella, 1962; Banks et al., 1963; Braunstein, 1964; Guirard and Snell, 1964).

Cytoplasmic aspartate aminotransferase (AAT)

Physicochemical properties

AAT (L-aspartate : 2-oxoglutarate aminotransferase, E.C. 2.6.1.1.) catalyses the reversible reaction:-

L-aspartate + α-oxoglutarate $\rightleftharpoons$ oxaloacetate + L-glutamate (3)

The complete amino acid sequence of cytoplasmic AAT (molecular weight 93,147) has been obtained (Ovchinnikov et al. 1973). The purified enzyme is electrophoretically separable into several subforms with differing kinetic and spectral properties (Martinez-Carrion et al., 1967; John and Jones, 1974). Each enzyme subform consists of two identical subunits, each carrying a coenzyme molecule. There is no evidence that the mechanism of transamination involves subunit

interactions, although under certain conditions asymmetry between the two subunits has been shown (Arrio-Dupont, 1972; Cournil and Arrio-Dupont, 1973; Harris and Bayley, 1975).

With PLP as coenzyme, AAT has the properties of a pH indicator, being colourless at alkaline pH (λ max 360 nm) and becoming yellow (λ max 430 nm) as the pH is lowered. The pK_a for this change is 6.2 (Sizer and Jenkins, 1963). At pH 10 the enzyme solution again turns yellow as a result of denaturation of the protein and release of free PLP. The absorption bands are optically active, and since PLP has a plane of symmetry the activity must arise from interaction with the apoenzyme (Torchinsky and Koreneva, 1963; Fasella and Hammes, 1964). Transamination is inhibited by certain dicarboxylic acids which form pH-dependant complexes with the PLP-enzyme. In a homologous series of α-dicarboxylic acids, glutarate was found to give maximum interaction (Jenkins, Yphantis and Sizer, 1959). As a result of the complex formation the pK_a of the decolorization is raised from 6.2 to approximately 8.0 (Sizer and Jenkins, 1959).

AAT can also be isolated with PMP as the prosthetic group. This form exhibits a pH-independent peak at 332 nm (Jenkins and Sizer, 1960).

Binding of the coenzyme to the protein

Transamination involves conversion of PLP-enzyme to PMP-enzyme. In the PLP-enzyme, PLP is covalently bound to the apoenzyme by an aldimine linkage to a lysine residue (Hughes, Jenkins and Fischer, 1962), which has recently been identified as lysine-258 (Ovchinnikov et al., 1973). Such a Schiff's base cannot be formed between PMP and the apoenzyme and this is reflected in the greater ease of resolution of the PMP-enzyme (Wada and Snell, 1962; Scardi et al., 1963).

However the mere existence of the PMP-enzyme complex implies the involvement of interactions other than Schiff's base in the attachment of coenzyme to protein. Although the phosphate group is dispensable in model systems, the apoenzyme has at least a thousand fold greater affinity for vitamin B6 phosphate esters than for the non-phosphorylated forms (Wada and Snell, 1962a). The phosphate group is likely to be present as the mono-anion, as only the mono-ionic form of inorganic phosphate competes with the cofactor for association with the apoenzyme (Banks et al., 1963).

The pH-dependant colour change for the PLP-enzyme has been attributed to the protonation of the aldimine Schiff's base nitrogen (Jenkins and Sizer, 1957; Martell, 1963). However the pK_a for this change is 6.2 compared with 10.5 for the free PLP-imine (Sizer and Jenkins, 1963). This difference could be partly accounted for by an interaction of the pyridine nitrogen with a proton-donating group on the apoenzyme. A positively-charged pyridine nitrogen would be expected to reduce the electron density on the Schiff's base nitrogen so making it less easily protonated. A tyrosine residue has been implicated as the group responsible for protonation of the pyridine nitrogen (Bocharov et al., 1968).

The methyl group in the 2 position of the pyridine does not seem to be of primary importance in binding. Coenzyme derivatives modified at this position bind strongly to the apoenzyme forming active holoenzymes (Bocharov et al., 1968). Kinetics of the association reaction between the apoenzyme and the coenzyme modified at position 2 with aliphatic substituents of increasing chain lengths, suggest a hydrophobic interaction with the protein (Bocharov et al., 1968).

The overall picture is summarised in Fig.2 in which the coenzyme is shown linked to the protein by most of its functional groups.

Ivanov and Karpeisky (1969) argue that catalytically-active AAT contains the bipolar form of the PLP aldimine which is thermodynamically unfavourable in the absence of the protein (Johnston et al., 1963) and can only be maintained by very tight binding of the coenzyme resulting from multiple interactions with the protein. The coenzyme is therefore maintained at the active site in a state of high energy and high potential reactivity.

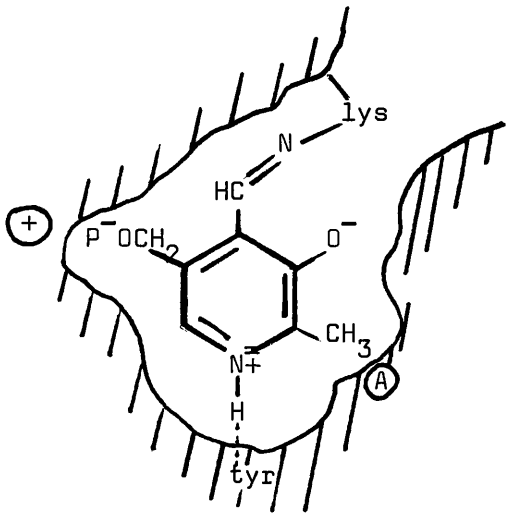

Fig.2 Schematic representation of the binding of PLP to the active site of AAT, after Braunstein (1970).
+ cationic group of apoenzyme; lys, lysine residue
tyr, tyrosine residue; A hydrophobic locus.

The mechanism of enzymic transamination

Reaction of cytoplasmic AAT with its substrates. The general mechanism for enzymic transamination as predicted by the Snell-Braunstein hypothesis (Braunstein, 1964; Guirard and Snell, 1964), can be represented as follows:

$$\text{Asp} + \text{E} \rightleftharpoons \text{EX} \rightleftharpoons \text{E'X} \rightleftharpoons \text{Ox} + \text{E'} \qquad (4)$$

$$\text{Og} + \text{E'} \rightleftharpoons \text{E'Y} \rightleftharpoons \text{EY} \rightleftharpoons \text{Glu} + \text{E} \qquad (5)$$

where Asp, Ox, Og and Glu represent aspartate, oxaloacetate, α-oxoglutarate and glutamate respectively. E and E' refer to free PLP and PMP enzyme, EX and EY are aldimine intermediates and E'X and E'Y are ketimine intermediates.

The details of this reaction mechanism have been investigated using four major approaches, namely steady-state kinetics, equilibrium studies at high enzyme and substrate concentration, chemical analysis of the enzyme-substrate mixtures and by fast reaction kinetics.

Extensive steady-state kinetic studies have been done on AAT (Velick and Vavra, 1962a,b; Banks et al., 1963; Wada and Morino, 1964; Henson and Cleland, 1964; Nisselbaum and Bodanski, 1964, 1966), and all the results obtained are consistent with the mechanism given above. A plot of V/K_m versus pH should reveal the pK_a of the group that affects k_1 in equation (4) (Frieden and Alberty, 1955). Using this plot, Velick and Vavra (1962a,b) showed that for amino acid substrates reacting with the aldimine enzyme, this group has a pK_a of 6.3, which is close to the value of 6.2 obtained from the spectrophotometric titrations of the aldimine enzyme (Sizer and Jenkins, 1963). The results indicated that only the non-protonated aldimine enzyme reacts with amino acid substrates. The maximal velocity of the reaction remains constant in the range pH 9 to 6 and then decreases with a pK_a of about 5.1.

Equilibrium studies of the enzyme with one or more of its substrates provided the first direct evidence that the mechanism of enzymic transamination involved a "shuttle" mechanism (Jenkins and Sizer, 1957, 1960). Spectrophotometric titrations have allowed determination of the dissociation constants of all four substrates from their initial enzyme complexes and of the equilibrium constants for each half reaction (equations (4) and (5)) (Jenkins and Taylor, 1965; Jenkins and D'Ari, 1966). Absorption maxima in the regions of 330, 365, 430 and 490 nm have been detected in the presence of substrates. The absorbances at 365 and 430 nm are attributed to

non-protonated and protonated aldimine Schiff's bases respectively and that at 330 nm to ketimine derivatives or to tetrahedral addition products between pyridoxal and the amino acid. Jenkins (1964) suggests that the absorbance at 490 nm may arise from a quinoid type intermediate such as that shown in Fig.3.

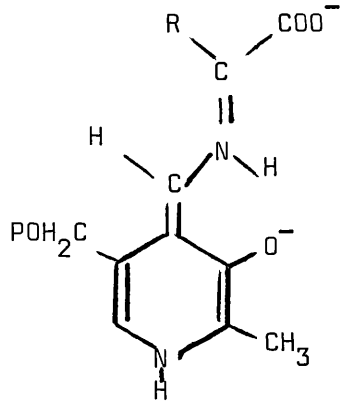

Fig.3 Structure of the mesomeric form of the quinoid-type intermediate after Jenkins (1964).

The existence of enzyme-substrate Schiff's bases has been confirmed in chemical studies by Riva et al., (1964), who treated the enzyme with $NaBH_4$ in the presence of substrates. Borohydride reduces the Schiff's base to a stable secondary amine and allows the isolation of phosphopyridoxal-glutamate and phosphopyridoxal-aspartate. A similar experiment with α-methyl aspartate (Fig.4) gave rise to pyridoxal-α-methylaspartate (Malakhova and Torchinskii, 1965). α-Methylaspartate is a

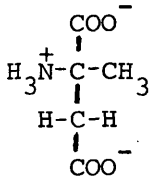

Fig.4 α-Methylaspartate

substrate analogue capable of reacting with the aldimine enzyme, but unable to undergo transamination because of the absence of a hydrogen atom on the α carbon.

Knowledge of the chemical nature of all discrete intermediates, of their order of formation and the kinetic and thermodynamic parameters describing their transformation, is required for an understanding of any reaction mechanism. Steady-state kinetics of enzyme-catalysed reactions are carried out under conditions of low enzyme concentration, which makes direct observation of intermediates virtually impossible. Increasing the enzyme concentration to a level where intermediates can be observed, normally increases the rate to such an extent that the techniques of stopped-flow and temperature jump have to be employed to follow the reaction. Attempts have been made to follow the reaction of AAT with its substrates by stopped-flow (Gutfreund, 1961; Hammes and Fasella, 1962), but the half-time of the reaction was shown to be < 5 msec. This is close to the resolution time of the technique and only allowed lower bounds of the bimolecular rate constants to be defined (10^5 $M^{-1}sec^{-1}$).

The temperature jump technique, with a shorter resolution time, has been employed to greater effect (Hammes and Fasella, 1962; Fasella and Hammes 1967). For each half reaction three separate relaxation processes have been observed. The slowest effect was concentration dependent only at low substrate concentration and is assumed to be related to the rate limiting step in the mechanism. The fact that the relaxation time of this step approaches a limit indicates that this is an intramolecular processes. The absorbance changes associated with this process are positive at 330 nm and negative at 360, 430 and 490 nm, suggesting that intermediates with spectral peaks at 360, 430 and 490 nm are on one side of the rate limiting step, while intermediates with spectral peaks at 330 nm are on the other side. Analysis of the relaxation times of the slow process provided four (two for each half reaction) first order rate constants.

The two other observed relaxation processes occurred, too rapidly to be quantitatively measured. One of these processes was attributed to the bimolecular reaction of amino acid and enzyme and lower limits of 10^{7} - 10^{8} $M^{-1}sec^{-1}$ for the second order rate constants were established. These values are close to the maximum possible value of 10^{9} $M^{-1}sec^{-1}$ (Alberty and Hammes, 1958) estimated by assuming a diffusion limited process. The wavelength dependence of the amplitude of the two fastest relaxation processes together with their concentration dependence indicates that the relationship of these processes to the bimolecular step in the reaction is not simple.

Reaction of AAT with pseudosubstrates. Although a significant amount of information has been obtained by study of the interaction of AAT with its natural substrates, many of the reaction steps are too fast to be measured by stopped-flow and temperature jump methods. More detail concerning the reaction mechanism can often be revealed by the use of substrate analogues. A substrate analogue incorporates some but not all of the molecular features of the natural substrate. It may bind reversibly or irreversibly to the enzyme, and either undergoes only part of the catalytic reaction, or if the complete cycle does occur, it proceeds much slower than with the natural substrates, enabling the fundamental steps to be dissected out of the mechanism.

Studies on AAT using substrate analogues can be broadly divided into two main groups involving reaction with the aldimine and reaction with aminic forms of the enzyme.

The natural substrates for the aldimine enzyme are 4 - 5 carbon L-amino acids with a carboxyl group in the position. Use of substrate analogues suggests that the α and ω carboxylate and the α amino groups all play a part in binding the substrate to the active site. For example,

analogues such as hydroxylamine and thiosemicarbazide which mimic the nucleophilic character of the amino group, bind to the active site even though they do not possess carboxylate groups (Velick and Vavra, 1962a; Sizer and Jenkins, 1963; Hammes and Fasella, 1963; Jenkins and D'Ari, 1966b). L-Alanine (Jenkins, 1961), L-serine and L-methionine (Novogrodsky and Meister, 1964), all lacking a ω carboxylate group, bind at the active site forming Schiff's bases, although the affinity for the enzyme is much less than that of the natural substrates. That both carboxylate groups contribute to the binding is shown by the potent competitive inhibition shown by dicarboxylic acids having a similar molecular geometry to that of the natural substrates (Haarhoff, 1969). The fact that maleate reacts strongly with the aldimine enzyme forming an abortive complex, yet fumarate does not, suggests that the carboxylate groups must be cis for effective binding (Jenkins, Yphantis and Sizer, 1959).

Each of the three substrate groups involved in binding probably interacts with a specific group on the holoenzyme. Of these binding sites only that interacting with the substrate amino group has been identified with precision. It has already been mentioned that the amino group is believed to be linked to the coenzyme 4'-carbon in the enzyme-substrate complex. It is generally thought that the formation of the enzyme-substrate aldimine complex is facilitated by the fact that in the holoenzyme the 4' carbon of the coenzyme exists as a Schiff's base with an ϵ-amino group of a lysine residue of the protein (Jenkins, Orlowski and Sizer, 1959b).

The carboxylate substrate groups are presumed to interact with two positively charged groups of the enzyme and studies with dicarboxylic

acid substrate analogues suggests that in the case of the analogues one of these groups is the protonated form of the aldimine nitrogen. Glutarate forms an abortive complex with the aldimine enzyme with λ max 435 nm. The dissociation constant of the enzyme-glutarate complex may be spectrophotometrically determined (Jenkins and D'Ari, 1966c) and has been shown to decrease with decreasing pH (Jenkins and D'Ari, 1966b). This pH effect is prevented by thiosemicarbazide (Jenkins and D'Ari, 1966b), a carbonyl reagent which breaks the aldimine linkage. These results support a model in which a carboxyl group of glutarate binds to the protonated form of the aldimine nitrogen.

Using ^{19}F n.m.r. spectroscopy, Martinez-Carrion, Cheng and Relimpio (1973), showed that the ^{19}F signal of perfluorosuccinate broadened on binding to deionised aldimine enzyme. The band broadening, an index of tightness of binding, was found to increase with decreasing pH and a line width-pH profile showed inflexion points at pH 5.2 and 8.4. The protonation of the internal aldimine chromophore of the deionised enzyme had been shown to occur with a pK_a of 5.4 (Cheng, Michuda-Kozak and Martinez-Carrion, 1971) and the n.m.r. data was taken as evidence that the protonated aldimine is the low pH binding site for one of the carboxylate groups of perfluorosuccinate. Proton n.m.r. allowed extension of these conclusions to succinate itself.

Jenkins and D'Ari (1966c) have shown that at high pH glutarate is bound by one carboxylate group and at low pH by both carboxylates, the low pH binding site being the protonated aldimine previously mentioned. Evidence as to the identity of the higher pH carboxyl binding site is more circumstantial. Buffer anions act as competitive inhibitors toward dicarboxylate substrates and analogues (Jenkins and D'Ari, 1966a), suggesting that one of the carboxylate groups binds

at the anion binding site. Studies with photo-inactivated enzyme (Cheng and Martinez-Carrion, 1972), have shown that a histidine residue at the active site is the most likely binding site for anions. In photo-inactivated AAT (Peterson and Martinez-Carrion, 1970), although the affinity of the enzyme for succinate and glutarate is reduced, there is no longer any competition for binding by anions. On the basis of this evidence Martinez-Carrion et al. (1973) suggest that a histidyl residue is the high pH binding site. It is difficult however to reconcile the usual pK range (5-7) of histidine residues with the pK of the high pH carboxylate binding site which is thought to be approximately 11 (Jenkins and D'Ari, 1968).

Jenkins and D'Ari (1968) have proposed a mechanism for dicarboxylate binding at high pH. In stopped-flow experiments the interaction of glutarate with the aldimine enzyme at high pH shows the appearance of a transient intermediate absorbing at 430 nm. These authors propose that one of the carboxylate groups binds first to the internal aldimine nitrogen causing its protonation and hence absorbence of the chromophore at 430 nm. The second carboxylate group then binds to a positively charged group on the protein displacing a counterion. The first carboxylate group then dissociates from the aldimine nitrogen, which would lose a proton, giving rise to a glutarate-aldimine enzyme complex absorbing at 360 nm. This scheme implies that not only are the enzyme-substrate bonds formed sequentially but also that they need not be present simultaneously to account for substrate specificty.

It must be pointed out however that the evidence with regard to the carboxylate binding sites has been obtained using dicarboxylic acids forming abortive complexes. It is possible that the binding mode of true substrates is different in view of the fact that in the productive binding mode a covalent complex is formed.

As mentioned previously, saturation of the enzyme with its substrates, reveals a number of absorption bands that have been attributed to an equilibrium mixture of various enzyme-substrate intermediates. These spectral bands show no optical activity, unlike the absorption bonds displayed by the aldimine enzyme in the absence of substrates (Fasella & Hammes, 1965; Torchinsky et al., 1968). This difference has been attributed to a conformational change at the active site and is related to catalytic activity in a mechanism to be discussed later.

In order to study the sequence of events leading to the formation of intermediates, the kinetics of the reaction between the aldimine enzyme and various substrate analogues have been studied.

In the presence of anions, α -methyl aspartate (Fig.4) reacts preferentially with the non-protonated aldimine form of the enzyme (Fasella, Giartosio & Hammes, 1966), as do the natural substrates, forming aldiminic enzyme substrate complexes. Each complex appears to exist in protonated and non protonated forms, the ratio of which is pH independent (Fasella et al., 1966); Hammes & Tancredi, 1967; Fonda and Johnson, 1970), suggesting intramolecular proton transfer.

Using stopped flow and temperature jump techniques, the reaction between aldimine enzyme and α-methyl aspartate has been resolved into at least three separate steps (Hammes & Haslam, 1968). Of the three relaxation processes observed, the fastest was concentration dependent, the other two reaching a limit with increasing concentration of substrate. Calculation of all six rate constants was possible, but anomalies in the variation of the fastest relaxation process at low substrate concentrations necessitated the introduction of substrate activation into the reaction mechanism. The initial reaction was interpreted

as being the interaction of the amino acid with the internal unprotonated Schiff's base to form a non-covalent complex, and the last complex was thought to be the Schiff's base linking ∝ -methyl aspartate with the coenzyme. The central complex was tentatively identified as a conformational isomer of the initial product (Fig.5).

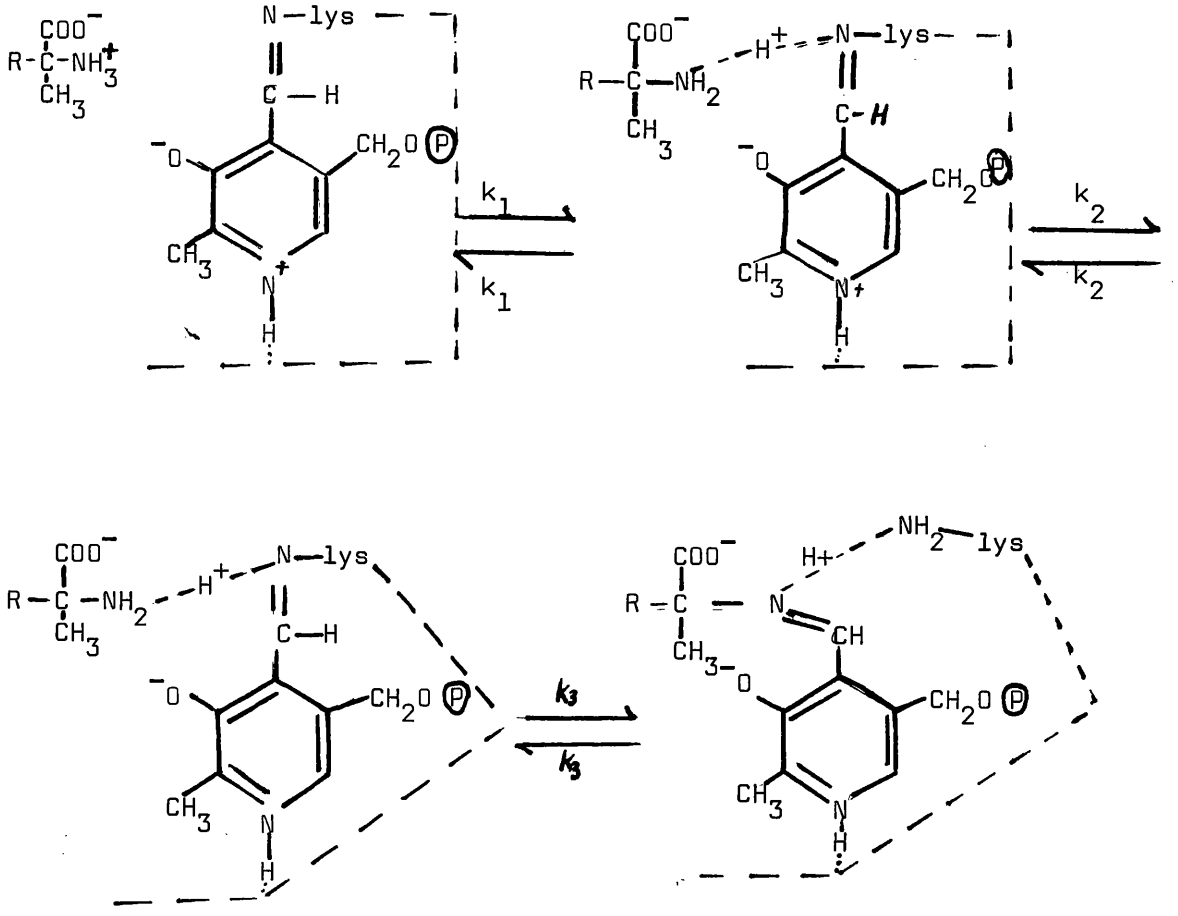

Fig.5 Postulated reaction mechanism for the interaction of L-∝ methyl aspartate and AAT. The dashed line schematically represents the protein. (Hammes & Haslam; 1968).

All three species appeared to have absorption peaks in both the 430 nm and 360 nm regions. It was suggested that a possible interpretation of these results was that each species exists as two rapidly equilibrating conformational isomers, possibly involving intramolecular proton transfer. The second order rate constant of 1×10^4 $M^{-1} sec^{-1}$ for the initial bimolecular process is considerably smaller than the lower

limits obtained using natural substrates.

Another analogue, erythro β-hydroxy aspartate (Fig.5) acts as a substrate for AAT, although the rate of transamination is considerably slower than that of the natural substrates. (Jenkins, 1961b). The equilibrium characteristics of the interaction between aldimine enzyme and erythro β-hydroxy aspartate have been extensively studied (Jenkins, 1961b, 1964). This interaction is characterised by the appearance of a strong absorption band at 492 nm, which has been assigned to the formation of a quinoid-type structure (cf. Fig.3) on the aldimine side of the rate limiting step.

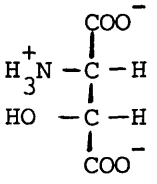

Fig.6 erythro-β-hydroxy aspartate.

Rapid reaction studies using this analogue were initially carried out by Czerlinski and Malkewitz (1965). A more detailed investigation was performed by Hammes and Haslam (1969), using temperature jump and stopped flow techniques at various wavelengths between 300-500 nm. Eleven relaxation processes were observed, of which eight appeared to be on the main reaction pathway. The data were evaluated on the basis of a simple sequential mechanism involving seven reaction intermediates. This allowed the determination of seven out of the eight pairs of rate constants. The values obtained for these rate constants are smaller than the corresponding values for the natural substrates but larger than the corresponding rate constants for α-methyl aspartate. On the basis of the sign and the wavelength dependence of the amplitudes of the relaxation process, assignment

of spectral maxima and structure were made for the majority of intermediates on the aldimine side of the rate limiting step. The rate limiting step was tentatively identified as being either the hydrolysis of or a conformational change of the ketimine intermediate. This differs from reaction of AAT with its natural substrates, in which the rate limiting step is thought to be the labilisation of the α-proton (Banks et al., 1968).

In the presence of a catalytic amount of aldimine ATT, the substrate analogue, threo-β-chloroglutamate (Fig.7), undergoes a β-elimination reaction producing Cl^-, NH_4^+ and α-oxoglutarate (Manning, Khomutov and Fasella, 1968).

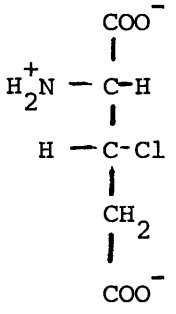

Fig.7 threo-β-chloroglutamate.

Observation of the reaction in a stopped-flow apparatus (Antonini et al., 1970) showed that the reaction occurred in two distinct phases, a fast initial phase reaching a metastable equilibrium in less than one second, followed by slow changes over a time period of about sixty seconds. The initial process was attributed to the formation of an enzyme substrate complex and the slow change to the breakdown of this complex with eventual formation of products and regeneration of free enzyme (Fig.8).

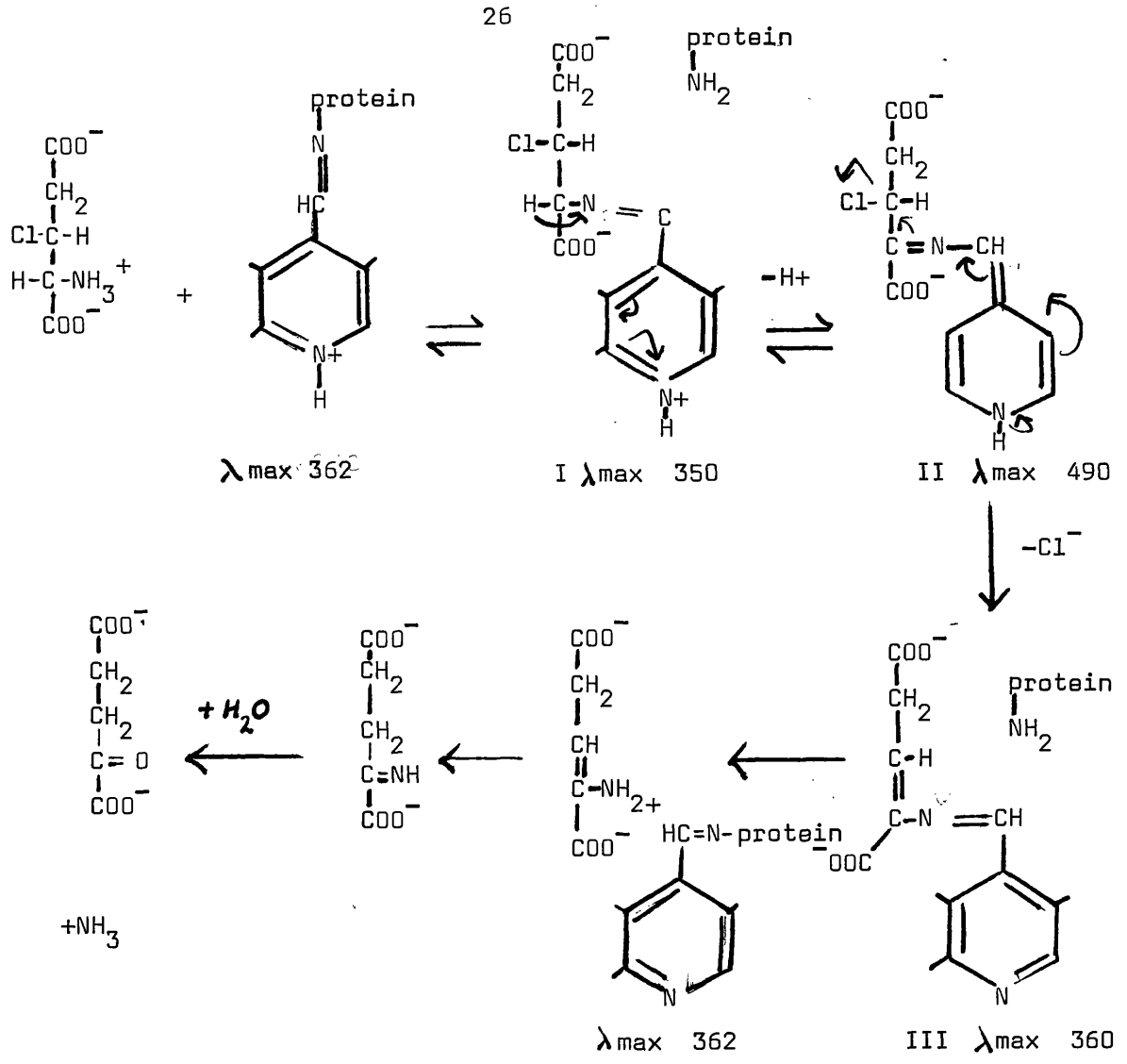

Fig.8 Proposed scheme for reaction between AAT and threo β-chloro-glutarate Antonini et al., 1970.

Suitable choice of reaction conditions enabled the fast reaction to be studied without complications due to the following slow process and analysis of the data allowed assignment of an absorption maxima at 350 nm and a possible structure (Fig.8, I) to the initial observable complex. The rate limiting step of the overall reaction was deduced to be the labilisation of the substrate α-hydrogen (I→II, Fig.8).

The value of $1.44 \times 10^{3} M^{-1} sec^{-1}$ obtained for the bimolecular rate constant of the initial complex formation is much lower than that of the natural substrates, but is of the same order as that obtained for α-methyl aspartate. The authors stress the possibility that an

earlier complex may exist at very low concentrations. In this case the apparent second order rate constant would contain both different steps in the process and direct comparison of data may not be possible.

Although the use of substrate analogues can never provide a completely accurate picture of aldimine enzyme-substrate intermediates, it has given indications as to the nature of some of the complexes and shown that there are many steps involved.

Possibly because of difficulties in obtaining stable analogues of α keto acid substrates, information regarding the formation of intermediates in the second half of the "shuttle" mechanism is rather sparse. The second order rate constants for the formation of the aminic enzyme-substrate complex are known to be greater than $10^{7} M^{-1} sec^{-1}$ (Fasella and Hammes, 1967). Specificity studies have shown (Banks et al., 1963) that α keto dicarboxylic acids bind more strongly than simple α keto acids, suggesting that both dicarboxylate groups are involved in binding. There are also significant differences in the binding behaviour of dicarboxylic acids with alternate forms of the enzyme. For instance, oxaloacetate binds more strongly than α-oxoglutarate to the aminic acid enzyme, but less strongly than α-oxoglutarate to the aldimine enzyme (Velick and Vavra, 1962a). Maleate and glutarate bind equally well to the aldimine enzyme (Jenkins et al., 1959) but maleate also binds well to the aminic enzyme (Valick and Vavra, 1962a) whereas glutarate does not (Jenkins, 1964). It has been suggested (Fasella and Turano, 1970) that these differences may reflect small changes in the geometry and charge distribution of the two forms of the holoenzyme.

Work on model systems (Metzler, Ikawa and Snell, 1954; Matsushima and Martell, 1967) suggests that aldimine and aminic enzyme complexes are

interconverted via labilisation of the substrate ∝C-H bond. This is facilitated by the positively-charged nitrogen which acts as an electron sink via the conjugated system of the coenzyme. The proton is eliminated leaving a carbanion (Gram and Guthrie, 1965; Auld & Bruice, 1967) which may be stabilised by a quinoid type intermediate (Schirch and Slotta, 1966). A second mesomeric carbanion form of this intermediate then accepts a proton on the 4' carbon of the coenzyme giving the ketimine (Fig.9).

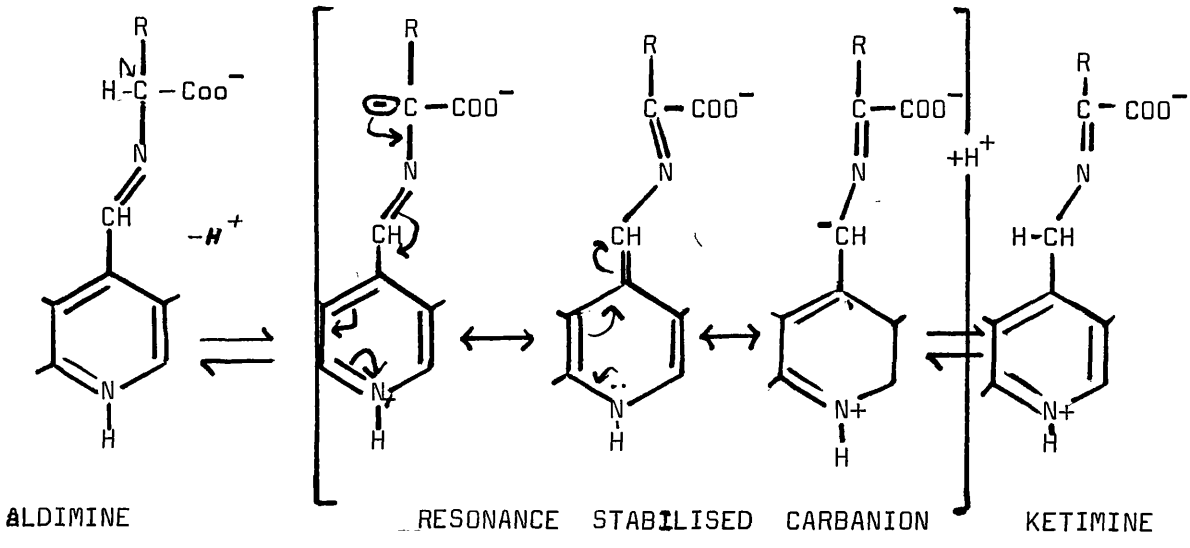

Fig.9 Scheme for aldimine-ketimine interconversion.

In the enzymic system evidence has been cited both supporting and opposing the existence of a carbanion intermediate. It has been suggested (Shlyapnikov and Karpeisky, 1969).that increased consumption of the tetranitromethane by AAT in the presence of substrate is evidence for carbanion formation, but it has been reported (Birchmeir, Zavralek and Christen, 1973) that in the presence of substrates a tyrosine residue becomes exposed to nitration

by tetranitromethane. However the use of oxidation-reduction indicators such as hexacyanoferrate (III) does appear to be consistent with the existence of the postulated carbanion intermediate (Healy and Christen, 1973). Kinetic isotope effects on the rate constants for Schiff's base interconversion on the other hand, have been interpreted as precluding a carbanion intermediate (Banks et al., 1968a; Doonan, Vernon and Banks, 1970).

According to Dunathan's hypothesis (1966), the labilisation of the proton on the α carbon atom requires that this bond be orientated perpendicular to the plane of the cofactor π-electron system (Fig.10).

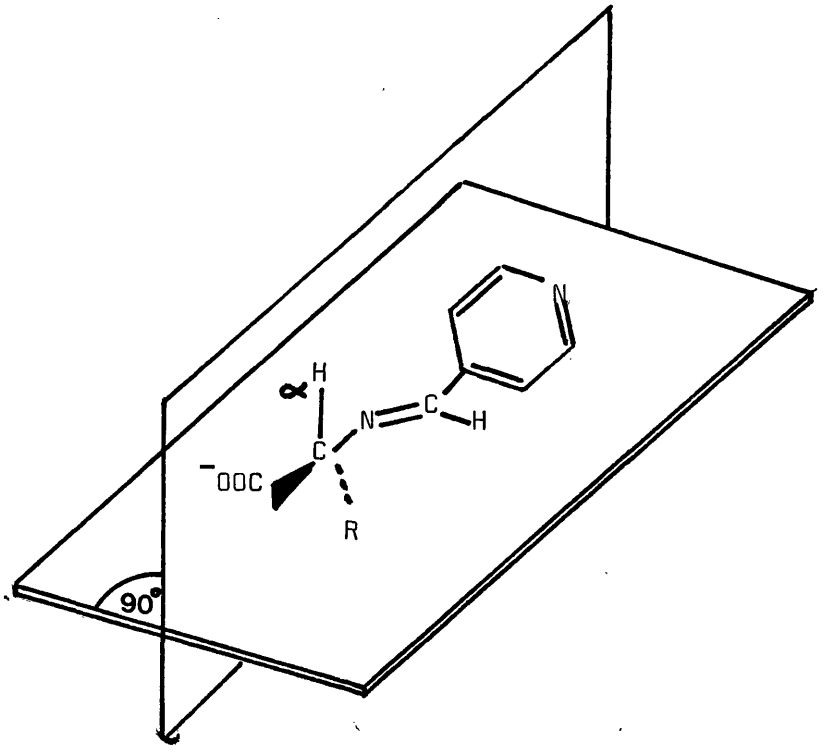

Fig.10 Diagramatic representation of coenzyme-substrate aldimine complex, with proton perpendicular to plane of coenzyme ring.

This conformation would be imposed by the geometry of the active site. Deuterium-labelled cofactors and substrates have been used to demonstrate that specifically the pro S hydrogen atom on the cofactor

4' carbon is involved in the prototropic shift (Dunathan, Davis and Kaplan, 1968a; Dunathan et al., 1968b; Besmer and Arigoni, 1969).

Using pyridoxamine-pyruvate transaminase and deuterated substrates (Ayling, Dunathan and Snell, 1968) conservation of the mobile proton was observed, indicating intramolecular proton transfer. Analysis of the percentage deuteron or proton transfer and the kinetic isotope effects, suggests that transfer in this enzyme may be via a lysine residue rather than via the imidazole ring of a histidine residue.

Although this evidence implicates a lysine residue as being responsible for proton transfer in pyridoxamine pyruvate transaminase, studies with photooxidised AAT using erythro-β-hydroxy aspartate indicate that proton transfer is via a histidine residue (Peterson and Martinez-Carrion, 1970).

A lysine residue has been found to be within a few angstroms of a histidyl residue at the active site of AAT (Turano et al., 1966). This same lysine which is normally bound to PLP in the holo-enzyme, is covalently modified by β-chloro-L-alanine (Morino and Okamoto 1973). Studies on the α-β elimination of β-chloro-L-alanine catalysed by AAT in the presence of formate ion (Morino, Osman and Okamoto, 1974), suggest the possibility that the formate ion is bound to the site normally occupied by the distal carboxylate of the natural substrate, i.e. a histidyl residue. This then produces a charge relay system, extending to the ϵ-amino group of the lysine which acts as a base abstracting the α-proton (Fig.11). A similar mechanism could be envisaged for proton abstraction in transamination.

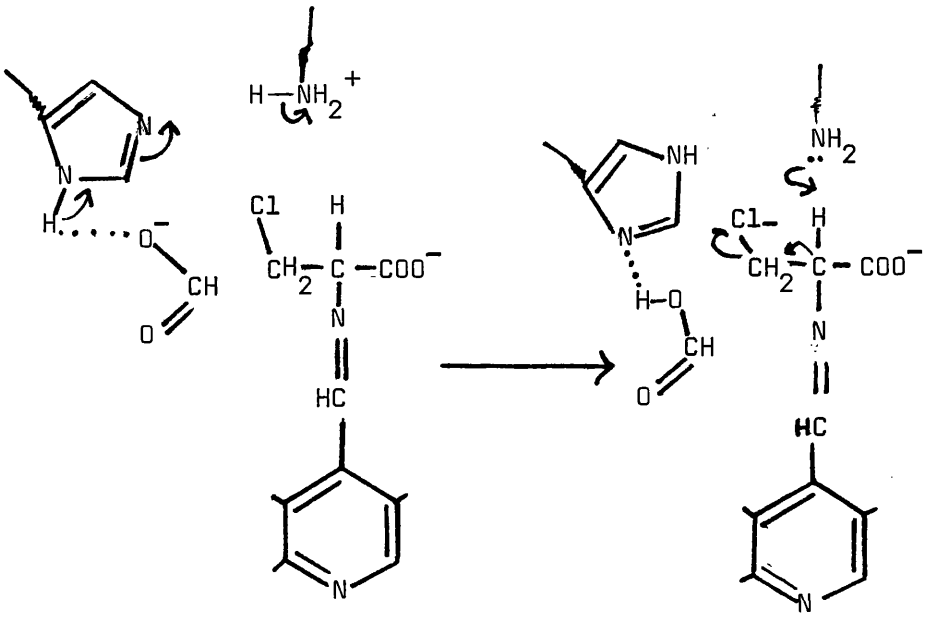

Fig.11 Suggested mechanism for the action of formate in α-β elimination of β-chloro-L-alamine (Morino, Osman and Okamoto).

Dynamic model for the mechanism of transamination

The evidence discussed suggests that enzymic transamination proceeds through a number of steps, each of which is catalysed by the concerted action of protein, coenzyme and substrate groups. The evidence is possibly best summarised in the dynamic model describing the sequence of event at the active site which has been presented by Ivanov and Karpeisky (1969). This is outlined in Fig.12.

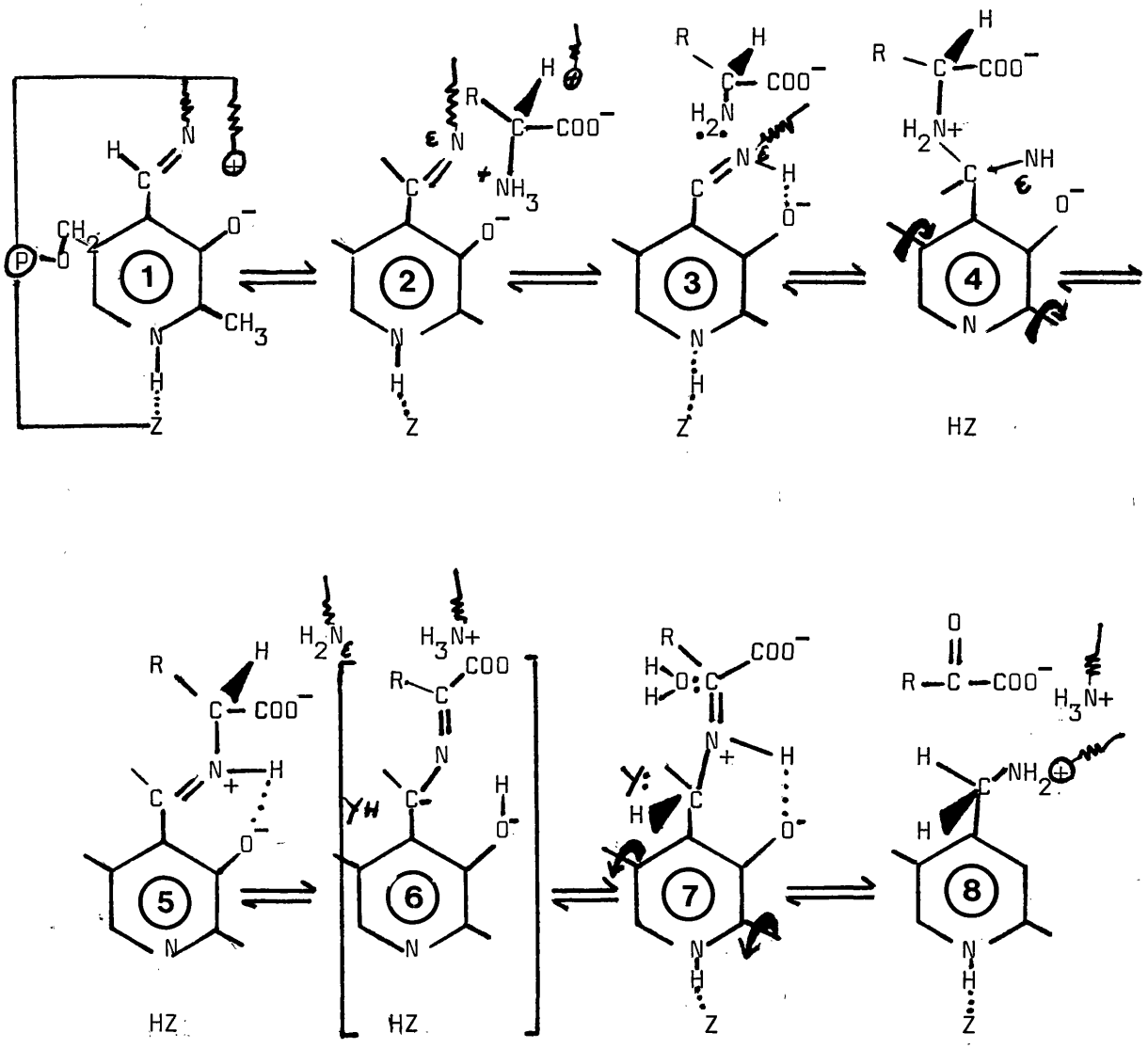

Fig.12

As part of the postulated mechanism the authors suggest the presence of a positively charged protein group in the vicinity of the internal aldimine linkage. Experiments with model systems suggest that protonation of the ring nitrogen will only be effective in reducing the pK_a of the Schiff's base nitrogen from 10.5 to ~8 (Johnston et al., 1963). The presence of a positive charge centre near the nitrogen could be an additional factor in lowering the pK_a further to the observed 6.2 (Sizer and Jenkins, 1963).

On formation of the initial non-covalent complex, it is suggested that the substrate α-carboxylate group binds to the previously-mentioned positively-charged centre. This decreases the pK_a of the substrate amino group to ~7.7 causing loss of a proton. Concomitantly the pK_a of the internal aldimine is raised to 8.0 (from 6.2) making it liable to protonation. Proton transfer then takes place (Fig.12 (3)). The protonated Schiff's base is then liable to nucleophilic attack by the lone pair electrons of the substrate amino group.

The initial distance between the centres of the amino group nitrogen and the formyl carbon is $\geq$ 3.5 Å. This distance must be reduced to ~1.5 Å in the formation of the intermediate tetrahedral adduct and subsequent aldimine formation. The authors suggest that this is most easily achieved by rotation of the coenzyme ring through an angle of approximately 40° about the axis formed by the 2 methyl and 5 methylene groups (Fig.12 (4)). Rotation is not restricted by other coenzyme linkages, since protonation of the internal aldimine will lead to a decrease in the basicity of the pyridine ring, resulting in proton transfer from the ring nitrogen to a protein group (probably a tyrosine residue) with disruption of the hydrogen bond during rotation. This rotation of the coenzyme could account for changes in the ORD and circular dichroism spectra, observed on addition of substrates to the enzyme.

On forming the covalent bond with the coenzyme 4' carbon the substrate amino nitrogen becomes positively charged, since the basicities of the two nitrogens attached to the formyl carbon are similar, proton exchange can take place. When the proton is located on the lysyl ϵ-nitrogen atom, disruption of the bond between this atom and the 4' carbon atom can take place. Thus the internal aldinine is

converted to the substrate aldimine.

In the aldimine-ketimine transition the involvement of two groups, acting as general acid-base catalysts is postulated. The non-protonated ε-amino group of the lysine that initially forms the internal aldimine is suggested as being the base responsible for abstraction of the proton of the α carbon, resulting in a resonance-stabilised carbanion (Fig.12 (6)). A proton-donating group can then protonate the coenzyme 4' carbon owing to the partial negative charge that has arisen on this atom due to carbanion formation (Fig.12 (6)). This atom then acquires a tetrahedral structure and the coenzyme can rotate back into the original plane with concomitant reprotonation of the pyridine nitrogen. This will decrease the electron density on the phenolic oxygen atom and the proton of the intramolecular hydrogen bond dissociates. Nucleophilic addition of a molecule of water at the α-carbon of the substrate then occurs yielding the α keto acid and protein bound pyridoxamine phosphate.

The amino group of PMP is now in close proximity to two cationic groups, the lysine ε-NH_2 and the protein cationic group previously mentioned, this leads to a decrease in the basicity of the NH_2 group of PMP, which remains unionised and is therefore capable of interaction with the keto substrate in the reverse half of the reaction.

Study of enzyme microenvironments

Nuclear magnetic resonance (n.m.r.) and electron spin resonance (e.s.r.) spectroscopy are among the most useful of the physical methods for probing the environment of the active site of enzymes in solution. Although e.s.r. spectroscopy is very sensitive (minimum probe concentration 10^{-7}-10^{-5}M), the chemical structures necessary for the stabilisation of unpaired electrons result in a physically large probe which may cause perturbations in the geometry of the macromolecule. N.m.r. probes are less sensitive (minimum probe concentration 10^{-3}M), but are usually much smaller than e.s.r. probes and potentially less disturbing.

Nuclear magnetic resonance. Certain nuclei absorb radiofrequency radiation when placed in a magnetic field, giving rise to an observable signal. The magnetic field experienced by a nucleus is modified by its environment and at a fixed radiofrequency the observed signals occur at slightly different values (chemical shifts) of the applied magnetic field. The absorption of radiofrequency radiation causes the nucleus to be promoted to an excited energy state from which the return to the ground state is defined by the relaxation time of the nucleus. The relaxation time depends on the mobility of the nucleus within its macromolecular complex and so together with the chemical shift, which depends on the local environment of the nucleus, is of major interest to biologists.

Chemical shift values are the positions of the resonance signals in the n.m.r. spectrum relative to an arbitrarily-defined reference signal. Exact determination of relaxation times T_1 and T_2 requires sophisticated instrumentation, but value of T_2 can to some extent be derived from the line width of the resonance signals.

The most common nucleus exhibiting magnetic resonance is ^1H. Proteins contain protons in many different environments and therefore their proton magnetic resonance (p.m.r.)spectra are invariably complex. Assignment of some proton peaks to particular amino acid residues has however been possible in the case of smaller proteins e.g., lysozyme and chymotrypsin (Cohen and Jardetsky, 1968; Bradbury and Wilairat, 1967). The observation of the p.m.r. spectra of ligands binding to macromolecules has also provided information about the nature of substrate binding in alcohol dehydrogenase (Hollis, Bolen and Kellum, 1966; Hollis, 1967), lysozyme (Thomas, 1966; Raftery et al., 1968;) and αchymotrypsin (Gerig, 1968). In general, although a few proton resonances are well resolved to high and low field, most of the information is buried in a broad envelope.

^{19}F-nuclei also exhibit magnetic resonance and are generally detectable at concentrations of $> 10^{-3}M$. The chemical shifts of fluorine are at least an order of magnitude larger than those of corresponding proton analogues (Emsley and Phillips, 1973) and the ^{19}F resonance signals occur outside the range of proton resonance, thus they will not be masked by the signals from protons. The similarity of size between the fluorine atom (van der Waals' radius 1.35Å) and the hydrogen atom (van der Waals' radius 1.09Å) has allowed substitution of fluorine into compounds of biological interest, with retention or enhancement of their biological activities, (Ciba Symposium, 1972). These characteristics provide the rationale for the use of fluorine as an n.m.r. probe.

Like protons, fluorine has been used in two different approaches as an n.m.r. enzyme probe. In the first, fluorine is covalently attached to one or more amino acid residues of the enzyme and changes in the ^{19}F spectrum observed as perturbations (e.g., ligands, changing pH)

are introduced. An example of this type of approach is the work of Huestis and Raftery (1971), where Lys-1 and Lys-7 of RNase S-peptide were covalently labelled with a trifluoroacetate group. Addition of the RNase S-protein caused a differential shift in the ^{19}F NMR signals of the two labelled lysine residues, confirming the X-ray data, which suggested that Lys-1 is near the surface of the protein and exposed to the solvent, whereas Lys-7 is buried inside the protein near the active site.

In the presence of the inhibitor, 3'-cytidine monophosphate, the chemical shift of the signal from Lys-7 varied with pH. Tentative conclusions were drawn concerning the role of histidine residues in the binding of the inhibitor.

The second approach which involves using a fluorinated substrate analogue, can also provide information as to the nature of the active site, because the chemical shift, linewidth and other characteristics of the bound ligand reflects the environment in the enzyme-substrate complex. Under conditions of slow chemical exchange, two signals corresponding to the free and bound substrate respectively, may be observed. This is illustrated by studies on the binding of a trifluoroacetylated derivative of chitotriose to lysozyme (Raftery, Huestis and Millet, 1971). At a concentration of 3mM analogue and 3mM enzyme, a slow exchange situation was obtained. pH Variation of the ^{19}F signals of the various trifluoroacetyl groups bound to the enzyme, indicated a conformational change in the enzyme-substrate complex due to hydrogen bond formation. The linewidth of the NMR signal is to some extent a measure of the tumbling time of the probe nucleus; broadlines are indicative of slow tumbling. Hence signals of probes bound to macromolecules may accordingly be very broad and difficult to observe.

In many of the cases of ligands binding to enzymes, the rate of exchange is fast, and although the bound substrate will be subject to the slow tumbling time of the macromolecules, both the chemical shift and line width of the observed signal are weighted averages of the two environments. Observation of the changes in the n.m.r. signal at various ratios of free and bound ligand enables the n.m.r. parameters of the bound ligand, as well as the dissociation constant of the complex to be deduced.

The binding of N-acetyl DL p fluorophenylalanine to chymotrypsin has been studied under fast exchange conditions (Spotswood, Evans and Richards, 1967). The ^{19}F spectrum of the free ligand is a complex multiplet. Addition of chymotrypsin results in two sets of resonances corresponding to the D and L isomers, the D-isomer being shifted to low field, the L-isomer not being displaced relative to the free ligand. The low field shift is suggested to be due to the binding of the aromatic ring in a hydrophobic pocket at the active site.

A similar approach was used by Zeffren and Reavill (1968), in studies of the interaction of D L-N-trifluoroacetylphenylalanine (TFAP) with chymotrypsin. Analysis of this system is easier than in the preceding case, because the ^{19}F resonance of TFAP is a single peak. Upon addition of the enzyme the spectrum is resolved into two peaks, both downfield from the signal of the free ligand. Dissociation constants for both enantiomers were calculated and comparison of the enzyme-induced shift with the shift of the inhibitor in a number of different solvent systems led to the conclusion that the active site in the vicinity of the trifluoroacetyl group is highly polar.

A more detailed analysis of the system was carried out by Sykes (1969), who measured the relaxation times of the ^{19}F signal from the bound ligand as well as the chemical shift. From this information

the rate constants for the exchange process were calculated.

The active site of aspartate-aminotransferase has been investigated by ^{19}F n.m.r., using trifluoroacetate as a probe for anion binding (Cheng and Martinez-Carrion, 1972), and perfluorosuccinate as a probe for the dicarboxylate binding site (Martinez-Carrion, Cheng and Relimpio, 1973). These experiments have been discussed previously.

Background to the use of difluoro-oxaloacetate in the studies reported in this thesis

Difluoro-oxaloacetate is an iso-steric analogue of oxaloacetate in which the CH_2 grouping of oxaloacetate is replaced by CF_2. Such analogues, containing one or more fluorine atoms in place of corresponding hydrogen atoms of a natural substrate, have been shown in many cases to mimic the biological activity of the latter (Ciba Foundation Symposium, 1972).

Difluoro-oxaloacetate was first prepared by Kun et al (1963) who showed that this analogue was an inhibitor of aspartate transaminase and was a substrate for malate dehydrogenase. Jenkins et al (1963) noted a shift in the spectral maximum of aspartate transaminase on addition of difluoro-oxaloacetate to the aminic form of the enzyme, but few experimental details were given. Preliminary studies (Briley et al, 1973) showed that addition of difluoro-oxaloacetate to the aminic form of aspartate transaminase resulted in a slow change in the absorption maximum of the enzyme from 332 to 360 nm.

These preliminary observations indicate the potential of difluoro-oxaloacetate as a kinetic probe for the reactions catalysed by aspartate transaminase and malate dehydrogenase. Furthermore, the single ^{19}F n.m.r. signal of difluoro-oxaloacetate should allow this substrate analogue to be used as a micro-environmental probe for the active sites of aspartate transaminase and malate dehydrogenase.

Materials

Perchloryl fluoride was obtained from Digby Chemical Service, London; diethyl oxaloacetate sodium enolate from Kodak Ltd., Kirkby, Liverpool; triethanolamine hydrochloride and L-cysteine sulphinic acid from Sigma, London; sodium hydride and perfluoro-succinic acid from Koch-Light Laboratories Ltd., Colnbrook, Bucks; NADH and lactate dehydrogenase from The Boehringer Corporation (London) Ltd. All other laboratory reagents were purchased from BDH Chemicals Ltd., Poole, Dorset, and were Analar grade. Pig Hearts were supplied by Scott-Bowyers Ltd., Trowbridge, Wiltshire, and were used within 2 h. of slaughter of the animals.

Methods

Synthesis of difluorooxaloacetate

The difluoro analogue may be prepared by the condensation of ethyl difluoroacetate and diethyl oxalate (Raasch, 1958) or by direct replacement of both hydrogen atoms on the -carbon atom of diethyloxaloacetate by fluorine with perchlorylfluoride (Kun et al., 1963). The latter procedure is preferable as the condensation reactions tend to give low yields (Kun et al., 1963). However the direct replacement reaction was also found to suffer from variable yields, probably because the ethoxide base acts as a nucleophile in addition to its function of removing protons from the diethyl oxaloacetate. The procedure described by Kun and coworkers was therefore modified.

Dry sodium enolate of diethyloxaloacetate (21 g) was suspended in 100 ml toluene : dioxane (2:1) and the stirred suspension was brought to $-10^{o}C$ by external cooling. Dry CO_2-free nitrogen was passed over the reaction mixture and after 10 min. perchloryl fluoride gas ($FClO_3$) was bubled into the mixture. The viscosity of the reaction mixture increased over a 25 min. period and the temperature was allowed to rise to -5^{o}-$0^{o}C$ to allow efficient stirring. Passage of $FClO_3$ was continued while a suspension of sodium hydride (4.8 gms. of 1:1 dispersion in mineral oil), in 10 ml. toluene/dioxane (2:1) was added dropwise. $FClO_3$ was passed into the reaction mixture for a further 30 min. Appearance of product was monitored by gas-liquid chromatography. The product showed as a single chromatographic peak, reaching a maximum height approximately 30 min. after the addition of sodium hydride.

When the reaction was complete as judged by GLC, the mixture was flushed with dry nitrogen for 10 min. and then added to 250 ml. diethylether. Enough distilled water was added to dissolve the

inorganic salts, followed by 100 ml. of saturated sodium chloride solution. The mixture was well shaken and the phases separated. The ethereal phase was extracted with 200 ml. water followed by 100 ml. saturated aqueous NaCl. The ethereal phase containing a large percentage of the product was put to one side and the aqueous washings retained. The aqueous phase from the initial extract was itself extracted with 3x250 ml. diethyl ether followed by 2x100 ml. benzene. Each organic extract was washed with the aqueous phases previously retained. All organic extracts were combined, dried over (Na_2SO_4), filtered and concentrated under reduced pressure. The concentrate contained two phases - the product of the reaction which is a brown coloured liquid, and also the mineral oil from the sodium hydride dispersion. The mineral oil was removed with a Pasteur pipette and the remaining liquid was distilled. Diethyldifluorooxaloacetate was collected as a colourless liquid distilling at 65°C and 0.5-1.0 mm. Hg. Yield 9.2 g. (41%). The product was homogeneous as judged by GLC.

The diethyl ester was hydrolysed by refluxing with 60 ml. 12% HCl for 1 h. The HCl was removed under reduced pressure leaving a thick syrup. A small volume of distilled water was added and the solution again taken to low volume under reduced pressure. The resulting syrup crystallised on storage. The product was dissolved in the minimum volume of boiling trifluoroacetic acid, dry benzene was added and the solution allowed to crystallise. This procedure gives the monohydrate of the acid. Yield 5.2 g. (68%), m.p. 116-117°C. Titration of the acid gave a molecular weight of 186.

Gas-liquid chromatography

In the preparation of diethyl difluorooxaloacetate, the appearance of product in the reaction mixture was followed by taking aliquots (100μl.),

diluting (to 1.0 ml.) with diethyl ether and analysing a sample (1 μl) of the diluted mixture by g.l.c. The sample was chromatographed on a stainless steel column (6 ft. x 0.25 in) containing 3% SE301 on Carbowax at 100°C.

Assay of enzyme activity

Enzyme assays were carried out by spectrophotometric estimation of oxaloacetic acid under conditions where the enolisation of the keto form is not partially rate limiting (Banks et al., 1963). The standard assay condition were as described by Banks et al.,(1968). The substrate solution contained 0.1M triethanolamine buffer, pH 7.5, L-aspartate (64.5 mM) and α-oxogluterate (6.85 mM)). Reactions were started by addition of enzyme to 3.0 ml of substrate solution at 25°C contained in a spectrophotometer cell (1 cm pathlength) and followed by absorbance changes at 260 nm. The unit of activity was taken as that amount of enzyme which, under the stated conditions, causes a rate of change of absorbance of 0.1 absorbance units/min.

Protein concentration

Protein concentrations of crude preparations were estimated by the 215:225 method (Layne, 1957) and of purified enzyme by the absorbance at 280 nm (Banks et al., 1968).

Extinction coefficients of enzyme forms

The molar extinction coefficients of the aldimine (7.6×10^3 $M, l^{-1} cm^{-1}$) and pyridoxamine ($8.1 \times 10^3 M l^{-1} C M^{-1}$) forms of AAT in 20 mM pyrophosphate buffer, pH 7.4 at 362 and 332 nm respectively were determined using the known extinction coefficients at pH 8.2 (Torchinsky et al., 1969).

Preparation of asparate aminotransferase (AAT)

The enzyme was prepared according to the method of Jenkins et al., (1959) using succinate buffer instead of Maleate buffer for the initial extraction and heat treatment (Turano et al., 1964). In addition

α-oxoglutarate (0.1 mM) was included in all buffers used in the preparation. The final product was extensively dialysed against double distilled water and freeze dried. The lyophilysate was stored under vacuum at +5°C. The isolation procedure is outlined in Scheme I.

Pig Heart Ventricles (2 Kg)

↓ Homogenised for 2 min. in 5 l. buffer (succinate EDTA, pH 6.0

Homogenate

↓ Heated with stirring at 72°C and maintained at this temp. for 25 min. 200 ml. 40 mM α-oxoglutarate added at 65°C. Cooled to 10°C. Filtered.

Filtrate

↓ $(NH_4)_2SO$ added to 50% saturation. Centrifuged at 3,000 x g for 45 min.

Supernatant

↓ $(NH_4)_2SO_4$ added to 67% saturation. Centrifuged at 3,000 x g for 45 min.

Precipitate

↓ Dissolved in min volume succinate buffer, pH 6.0 and dialysed against 15 l. running double distilled water.

Non-diffusible Material

↓ Concentrated to 20 ml. by vacuum dialysis, and 1 M phosphate buffer, pH 6.8 added to a concentration of 20 mM.

Concentrate

↓ Applied to hydroxylapatite column (2.5x40 cm) and eluted with 40 mM phosphate buffer, pH 6.8. Fractions containing AAT activity were pooled.

Active fractions

↓ 1.5 mM Kg added. $(NH_4)_2SO_4$ added until first permanent precipitate formed (approximately 55% saturation). Centrifuged at 5,000 g for 30 min.

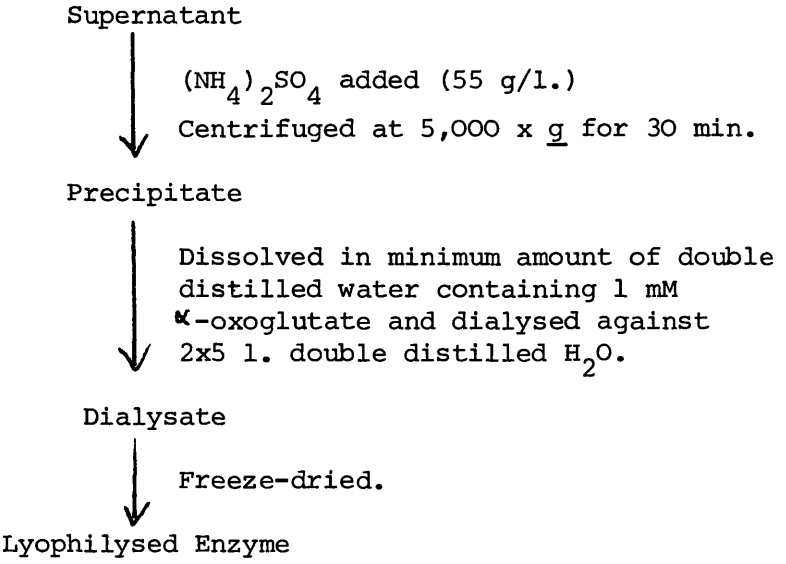

SCHEME I

A typical preparation from 2 Kg. ventricles gave 250 mg. AAT, specific activity 640 units/mg, with E 280 : E 362 7.25 at pH 7.4. This preparation gives a mixture of α, β and γ subforms of the aldimine enzyme.

Preparation of the aminic form of AAT

Conversion of the aldimine enzyme to the aminic form was achieved by the method of Jenkins and D'Ari (1966d). Cysteine sulphinate was added to aldimine transaminase in 20 mM pyrophosphate buffer pH 7.4, to give a molar ratio of 2:1. The resulting solution was passed through a Sephadex G-25 column (1x45 cm) at a rate of 1ml./min. and the eluate monitored at 280 nm. The protein peak was collected and the UV absorption maximum and the specific activity determined.

Preparation of Apoenzyme

The apoenzyme was prepared from aldimine enzyme via the aminic form as described by Scardi et al., (1963) except that 2.0 mM cysteine sulphinate substituted for glutamate. This procedure consistently achieved > 95% resolution as determined by residual transaminase activity. The apoenzyme could be reactivated with excess pyridoxal phosphate

(40μg/ml) in 50 mM acetate buffer, pH 7.8. At room temperature reactivation was complete within 5 min. The restorable activity was monitored throughout experiments using apoenzyme and was found to be $>$ 90% in experiments at pH 7.4 and $>$ 70% at lower pH. Concentrations of apoenzyme are quoted in terms of restorable activity.

Preparation of sample for n.m.r. measurements

For experiments at constant pH, enzyme (approx. 20 mg) was taken up in a small volume of 20 mM pyrophosphate buffer, pH 7.4, dialysed against 2x5 l. of the same buffer and concentrated (to 0.4 ml) by vacuum dialysis. For determinations at varying pH the enzyme was dialysed against 2x5 l. of double-distilled water prior to concentration.

Nuclear magnetic resonance measurements

^{19}F n.m.r. spectra were recorded at 94.1 MH_3 using a Jeol PS 100 n.m.r. spectrometer in 5 mm diameter sample tubes with co-axial capillary tubes containing either 2M difluorooxaloacetic acid or 2M perfluorosuccinic acid as internal lock. Chemical shifts were determined relative to the internal lock signal using an electronic counter and line widths were recorded as the peak width at half height. Where necessary the signal to noise ratios was enhanced using repeated scans with a Jeol JNM SB-3 signal to noise booster. Samples were maintained at $28\pm1^{o}C$.

Steady state kinetics and spectral scans

Steady state kinetics and spectral scans of the enzyme were done in a Pye Unicam SP 1800 at $25\pm1^{o}C$ unless otherwise stated.

Stopped flow measurements

Stopped flow measurements at fixed wave length were carried out at $25\pm1^{o}C$ using a Gibson-Durrum stopped flow spectrophotometer equipped

with a 2 cm observation tube. The dead time of the instrument was approximately 3ms. Progress curves were recorded on a Tectronix storage oscilloscope and permanent records made by taking polaroid photographs directly from the oscilloscope screen.

Scanning stopped flow measurements were made on the apparatus described by Holloway and White (1975). The instrument is a double-beam wavelength scanning stopped-flow U.V.-visible light spectrophotometer system that permits 800 absorption spectra/sec to be recorded, 2-8 ms after mixing the reactants. The analogue signal produced is digitised and fed into an 8K word data capture system, which can display selected spectra singly or superimposed on a storage oscilloscope. Permanent records of the oscilloscope display was made on 35 mm photographic film.

All solutions used in the stopped flow experiments were made up in degassed buffer to prevent bubble formation on mixing the reactants.

Measurement of Fluoride ion

Fluoride ion in solution was estimated using a combination fluoride electrode, Model 96-09 (Orion Research Inc.), coupled with a Radiometer pH meter (Model 26) using the expanded scale mode (full scale deflection = 100 mV). The measuring vessel was thermostatted to $25 \pm 1^{\circ}C$ and the electrode shielded from direct sunlight.

The concentration of fluoride was calculated from a plot of ψ against volume of NaF solution added (Macdonald, 1971) where

$$\psi = (V + v) \times 10^{\frac{E.F}{2.303\ RT}}$$

and V is the initial volume; v is the volume added; E is the e.m.f. recorded; F, R and T refer to the Faraday, Gas Constant and Absolute temperature respectively.

Computation

Iterative procedures involving solution of quadratics and linear regression of points on a straight line were performed using a programmable "Sumlock Statistician" (Computer Design Corporation, Los Angeles, California).

Evaluation of the data obtained from stopped flow experiments by the program CHEKMAT (Curtis and Chance, 1974) was done on the IBM computer at University College, London.

RESULTS

Steady State Kinetics

In its catalytic role, the aldimine form of aspartate transminase interacts with the amino acid substrates and is converted to the aminic form which reacts with keto acid substrates. This double-displacement mechanism may be represented as:

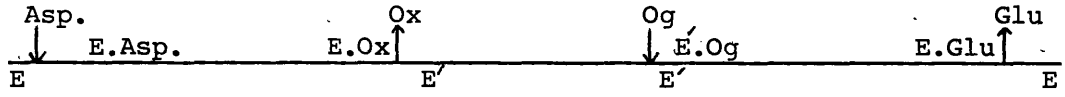

The equation for the initial velocity (v) of the reaction, according to this mechanism can be shown to be,

$$v = \frac{V_m}{1 + \frac{K^A}{[A]} + \frac{K^B}{[B]}} \qquad (1)$$

Where $[A]$ and K^A represent the concentration of the keto-acid and the Michaelis constant for the aminic enzyme-keto acid complex, respectively, and $[B]$ and K^B the concentration of the amino acid and Michaelis constant for the aldimine enzyme-amino acid complex. V_m is the maximum velocity. If an inhibitor combines reversibly with both forms of the enzyme, equation (1) then becomes,

$$v = \frac{V_m}{1 + \frac{K^A}{[A]}\left(1 + \frac{[I]}{K'_i}\right) + \frac{K^B}{[B]}\left(1 + \frac{[I]}{K_i}\right)} \qquad (2)$$

Where K'_i and K_i are the enzyme-inhibitor dissociation constants for the aminic and the aldimine forms of the enzyme respectively. Equation (2) may be rearranged to give:-

$$\frac{[A]}{v} = \frac{1}{V_m}\left(K^A + \frac{K^A[I]}{K_i'}\right) + \frac{[A]}{V_m}\left(\frac{K^B}{[B]} + \frac{K^B[I]}{[B]K_i} + 1\right) \quad (3)$$

or

$$\frac{[B]}{v} = \frac{1}{V_m}\left(K^B + \frac{K^B[I]}{K_i}\right) + \frac{[B]}{V_m}\left(1 + \frac{K^A}{[A]} + \frac{K^A[I]}{[A]K_i'}\right) \quad (4)$$

Thus if one substrate concentration is held constant, and the other varied at different concentrations of inhibitor, a plot of [A]/v versus [A] or [B]/v versus [B], will give rise to a series of straight lines in which both the slope and the intercept of the lines vary. If, however, the inhibitor interacts only with aminic form of the enzyme, then equations 3 and 4 become:

$$\frac{[A]}{v} = \frac{1}{V_m}\left(K^A + \frac{K^A[I]}{K_i'}\right) + \frac{[A]}{V_m}\left(1 + \frac{K^B}{[B]}\right) \quad (5)$$

and

$$\frac{[B]}{v} = \frac{K^B}{V_m} + \frac{[B]}{V_m}\left(1 + \frac{K^A}{[A]} + \frac{K^A[I]}{[A]K_i'}\right) \quad (6)$$

A plot of[A]/v versus [A] at a series of [I] concentrations will be a family of parallel lines; A plot of B /v versus [B] will give a family of straight lines having a common intercept on the [B]/v axis, but with varying slopes. A similar pair of equations may be obtained if the inhibitor interacts with only the aldimine form of the enzyme, but the variation of the slope or intercepts of the primary plots will be the reverse of the previous case. Thus the form(s) of the enzyme with which the inhibitor combines should be kinetically distinquishable. Studies on the effect of difluorooxaloacetate on the initial velocity (v) of AAT-catalysed transamination between aspartate and α-oxoglutarate were therefore carried out. Substrates and inhibitor were added to 0.1 M potassium phosphate buffer, pH 7.4 in a 1 cm pathlength quartz cuvette, to give a final volume of 3.0 ml. The reaction was initiated by the addition of 0.1 to 1.0 μg of enzyme. Transamination

was monitored by production of oxaloacetate, as described in the Methods section. The results of these experiments are presented in Fig.13 as plots of [S]/v against [S]. At varying α-oxoglutarate concentrations, constant aspartate and different fixed concentrations of difluorooxaloacetate, the plots were parallel lines (Fig.13a) indicating competitive inhibition (i.e. V^{app} is independent of inhibitor concentration). With aspartate as the variable substrate and constant α-oxoglutarate, the [S]/v versus [S] plots consisted of straight lines with a common ordinate intercept (Fig.13b) characteristic of uncompetitive inhibition (K_m^{app}/V^{app} is independent of inhibitor concentration).

The results are not consistent with equations (3) and (4) which predict mixed inhbitiion, but are in agreement with equations (5) and (6), i.e. at the concentrations of the experiments difluorooxaloacetate interacts primarily with the aminic form of aspartate transaminase.

Justification for this assumption was provided by a separate series of experiments on the effect of varying inhibitor concentration on the fractional inhibition, $\underline{i}$ at different fixed concentrations of α-oxoglutarate and constant aspartate. The results are shown in Fig.14 as a plot of $1/\underline{i}$ against $1/[I]$ where $\underline{i} = 1 - v_i/v_o$, v_i being the velocity in the presence of inhibitor and v_o the uninhibited velocity. The observed pattern of straight lines converging on a common ordinate intercept of unity is consistent with competitive and mixed inhibitors. These can be distinquished be a secondary plot of slope against α- oxoglutarate concentration. Rearrangement of equation (2) in fractional inhibition form gives,

$$\frac{1}{\underline{i}} = \frac{[A][B] + K^A[B] + K^B[A]}{\frac{K^A[B]}{K_i'} + \frac{K^B[A]}{K_i}} \cdot \frac{1}{[I]} + 1 \qquad (7)$$

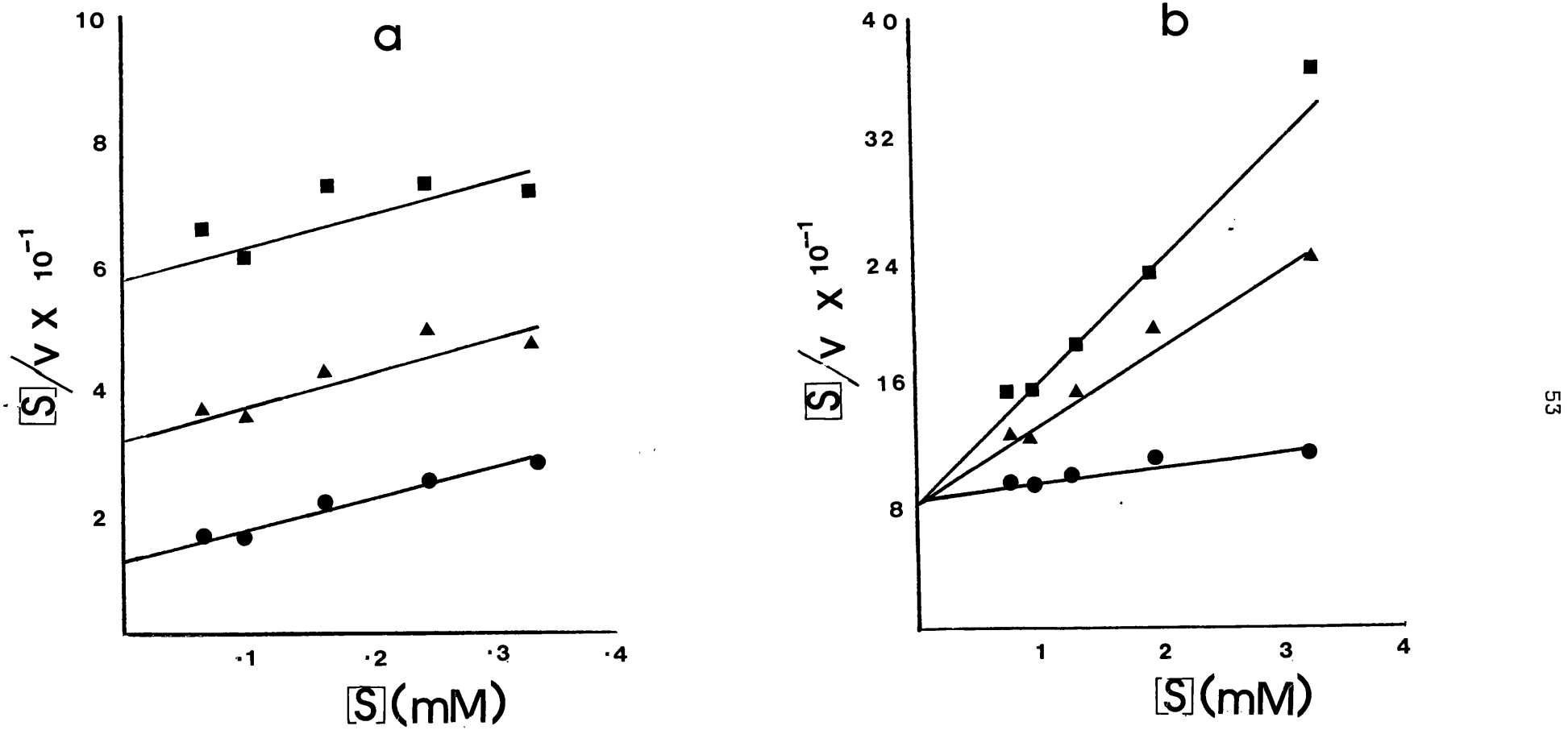

Fig. 13. Inhibition of transaminase by difluoro-oxaloacetate at varying substrate concentrations. a) Variable substrate, α-oxoglutarate; constant aspartate (33.0mM); difluoro-oxaloacetate concentrations: (●) 0, (▲) 20μM, (■) 40μM. The concentration of enzyme (sites) was 0.8nM. b) Variable substrate, aspartate; constant α-oxoglutarate (6.6mM); difluoro-oxaloacetate concentrations: (●) 0, (▲) 0.67mM, (■) 1.34mM. The enzyme concentration was 6.0nM. The lines were drawn using parameters calculated from K_m^{app} and V^{app} obtained from direct linear plots of initial velocity (v) against concentration of variable substrates (S). Further details are given in the Methods section.

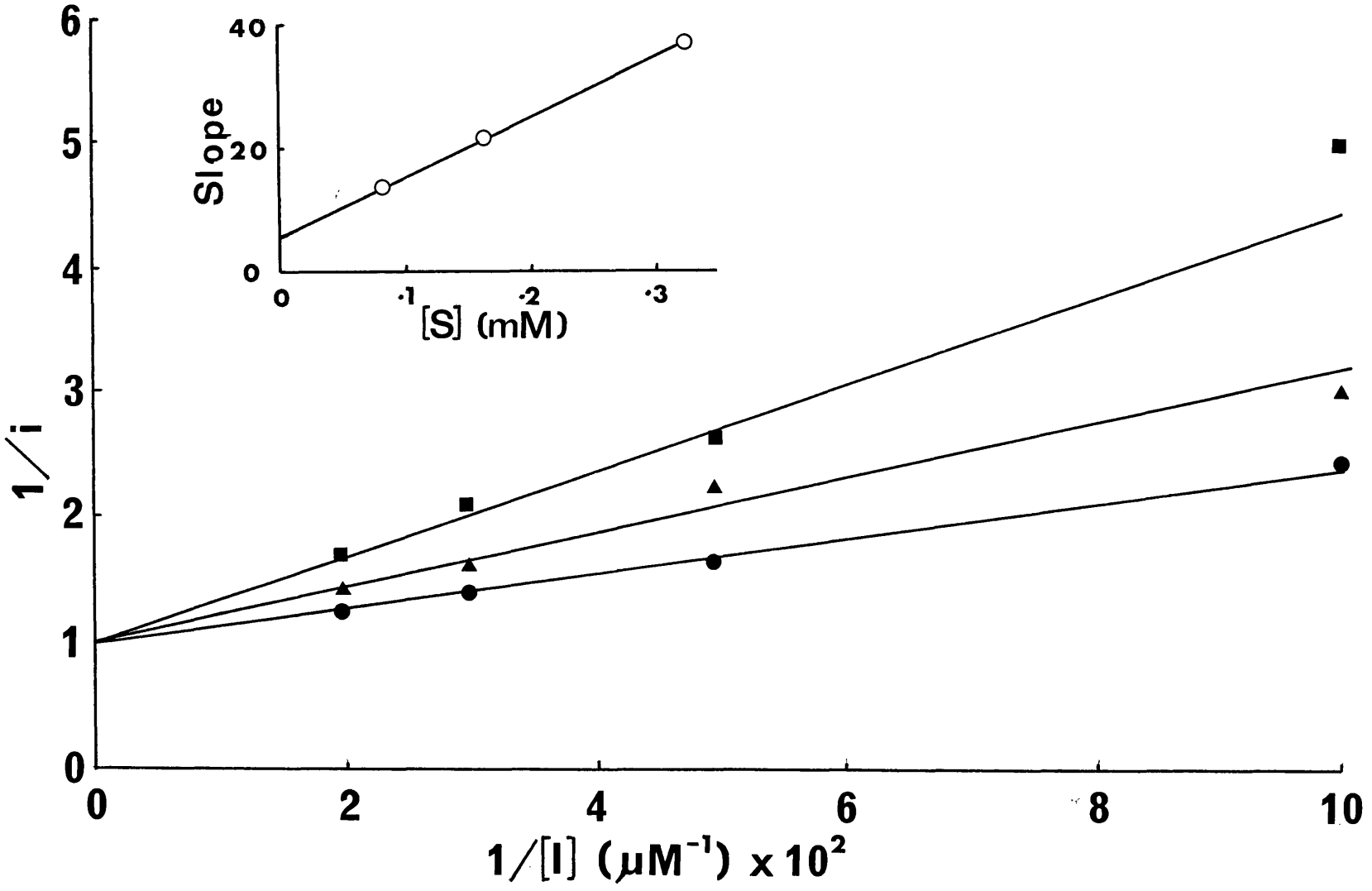

Fig. 14. Effect of difluoro-oxaloacetate on fractional inhibition of transaminase. Double reciprocal plot of fractional inhibition (i) against difluoro-oxaloacetate concentration: (●) 0.083mM, (▲) 0.166mM, (■) 0.33mM. The enzyme concentration was 1.0nM. The lines were drawn using parameters estimated from direct linear plots of i against [I] . Inset: Variation of the slope as a function of K-oxoglutarate concentration ([S]).

If equation (7) is applicable, the secondary plot of slope (K_i^{app}) versus [A] will not be linear. However if $K_i \gg [I]$, so that $[I]/K_i \simeq 0$, then equation (2) in fractional inhibition form, becomes,

$$\frac{1}{i} = \left(\frac{[A]K_i'}{K^A} \left(1 + \frac{K^B}{[B]} \right) + K_i' \right) \frac{1}{[I]} + 1 \qquad (8)$$

and a secondary plot of slope against [A] is linear, as observed, (Fig.14, inset), and gives an estimate of $K_i' = 5.85\,\mu M$ (ordinate intercept). A secondary plot of the slope (of the [B]/v versus [B] plot) against [I] was linear and gave an estimate of $K_i' = 8.93\,\mu M$; a secondary plot of the ordinate intercepts of the [A] /v versus [A] plot against [I] gave $K_i' = 9.96\,\mu M$.

If productive breakdown of the difluorooxaloacetate-aminic enzyme complex was significantly contributing to the steady state kinetics, non-hyperbolic variation of the initial rates with variation of inhibitor or α-oxoglutarate concentrations would result. In neither case was such kinetic behaviour detected, indicating that the measured K_i' is a good approximation to the true dissociation constant of the difluorooxaloacetate-aminic enzyme complex.

The slow spectral change

The addition of substrates or inhibitors to AAT often results in changes in the λmax of the absorption spectrum of the co-enzyme. The spectral changes can be utilised to obtain the dissociation constant of the enzyme-ligand complex (Jenkins and Taylor, 1965; Jenkins and D'Ari, 1966a). In order to further investigate the interaction of difluorooxaloacetate with the aminic form of AAT, difluoro-oxaloacetate (final concentration, 25μM) was added to a solution of the aminic enzyme (site concentration, 19μM) in 20mM sodium pyrophosphate buffer, pH 7.4, contained in a 1cm pathlength quartz cuvette, thermostatted at 25°C. Absorption spectra of the solution over the range 300-400nm were recorded

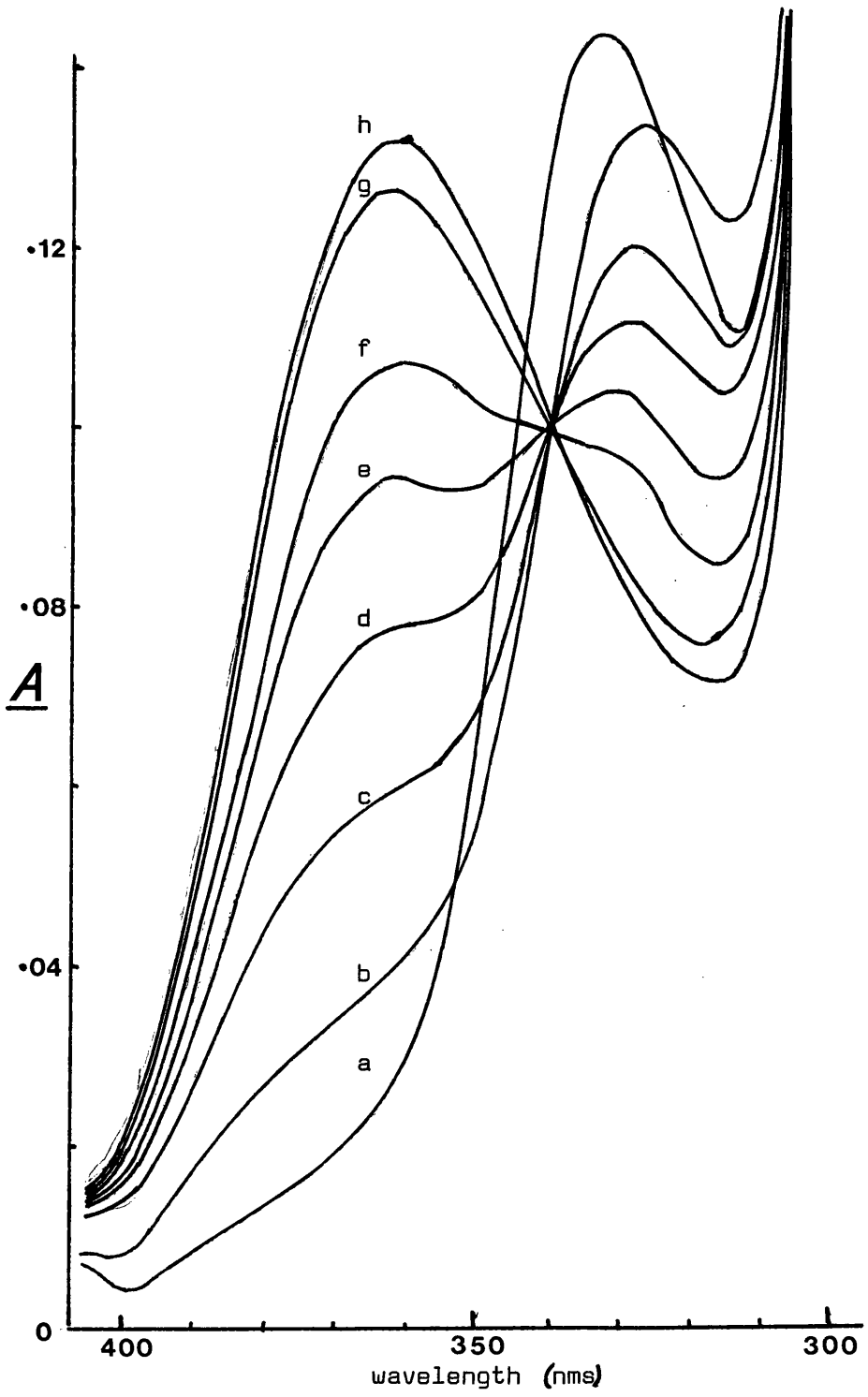

Fig. 15. Spectral changes on addition of difluoro-oxaloacetate to the aminic form of aspartate transaminase. The absorption spectra were obtained from successive scans (scan rate 0.5 nm/s) before (a) and after (b–h) addition of difluoro-oxaloacetate after the time intervals indicated: (b) 0.5 min; (c) 5 min; (d) 9 min; (e) 16 min; (f) 25 min; (g) 45 min; (h) 75 min. Other conditions are given in the text.

at 3 min. intervals. A slow spectral change was observed, the absorbance maximum in the 330nm region decreasing and a new maximum arising in the 360nm region (Fig. 15). The time course of the reaction was found to follow first order kinetics (Fig. 16), with a first order rate constant for the reaction of $1.06 \times 10^{-3} sec^{-1}$.

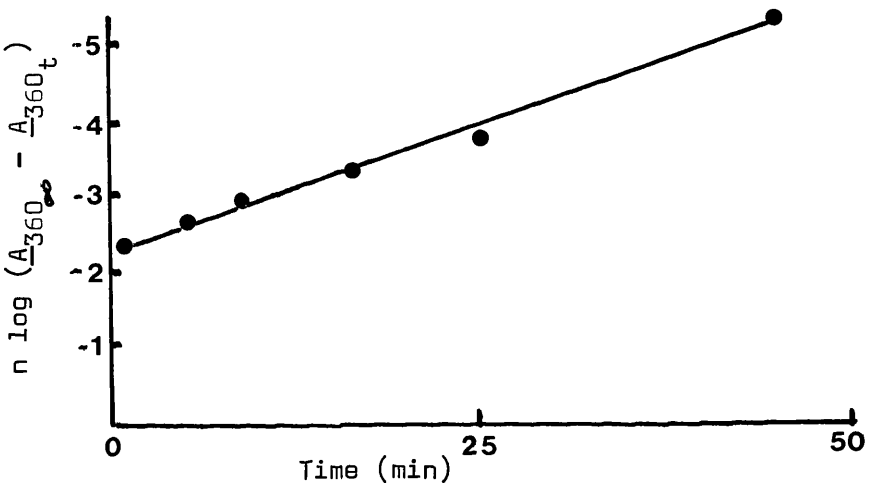

Fig. 16. Semi-logarithmic plot of absorbance changes shown in Fig. 15. The natural logarithm of ($\underline{A}_{360}$ - $\underline{A}_{360_t}$) was plotted against time.

When the spectral change was complete, addition of excess oxaloacetate (0.2mM) caused very little increase in the absorbance at 362nm suggesting that aminic enzyme had been fully reacted.

On repetition of the experiment at other concentrations of difluoro-oxaloacetate (3μM - 0.5mM), the value obtained for the first

order rate constant was found to increase with difluorooxaloacetate concentration reaching a maximum value ($1.78 \times 10^{-3} sec^{-1}$) at approximately 150 μM difluorooxaloacetate. Further increases in the concentration of the ligand produced only small variations in the first order rate constant (Fig.17).

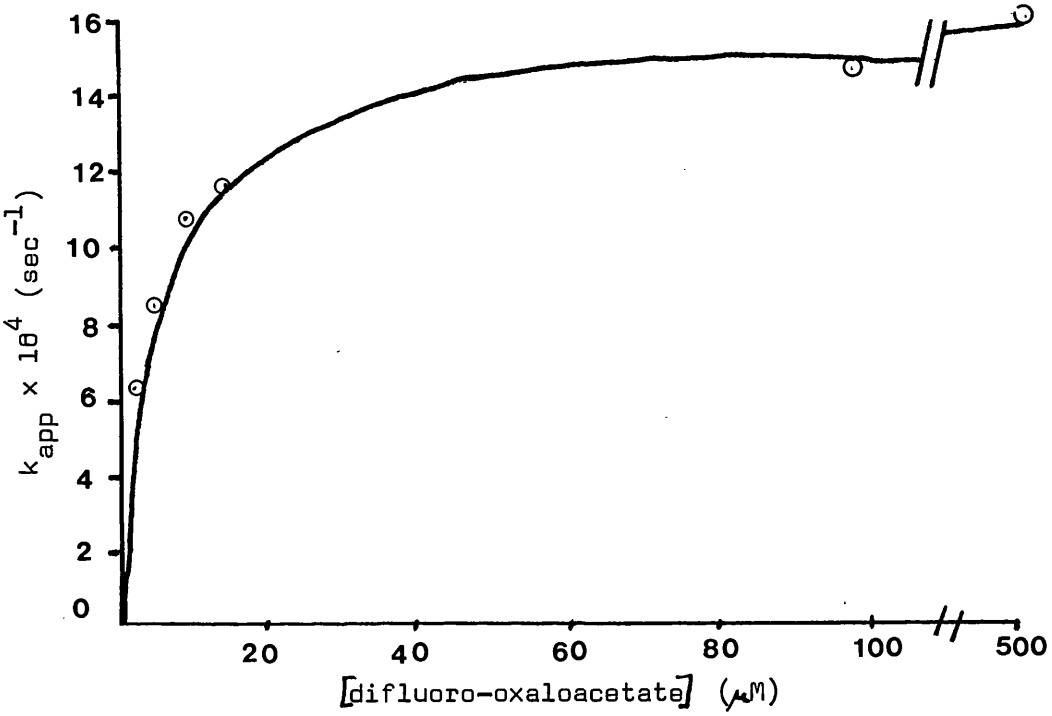

Fig. 17. Variation of the pseudo first-order rate constant with difluoro-oxaloacetate concentration. The conditions of the experiment are as for Figs. 15 and 16.

This behaviour is characteristic of the kinetic situation in which a complex is rapidly formed prior to the observed event (Equation 9a).

$$E' + I \underset{K_D}{\overset{\text{rapid}}{\rightleftharpoons}} A \xrightarrow[k_2]{\text{slow}} B \qquad (9a)$$

The maximum value for the first order rate constant is obtained when all of the enzyme is in the form of the complex before the slow event occurs; i.e. when $[I] \gg K_D$. Further evidence for this supposition is provided by the observation that the isosbestic point of the reaction

does not intersect the spectrum of aminic enzyme and there is also a rapid initial change of λ max from 332 nm to 328 nm, before the occurrence of the slow spectral change.

In a separate experiment the first order rate constant at high difluorooxaloacetate concentration (0.5 mM) was determined at 4 different temperatures. The log of the rate constants obtained was then plotted against the reciprocal of the absolute temperature (Fig.18) and the activation energy E (19.46 Kcal/mole), calculated from the slope according to the Arrhenius equation.

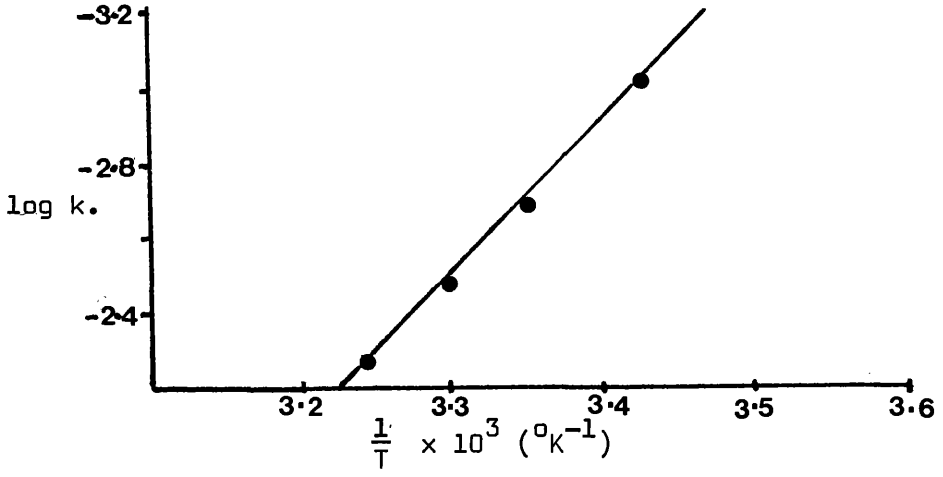

Fig. 18. Variation of the maximal first order rate constant (k) for the 332-360nm spectral change with temperature. The log of the first order rate constant is plotted against the reciprocal of the absolute temperature. The value for the first order rate constant was obtained as described for Fig.16. The enzyme concentration was 21 μM (sites). Other conditions are stated in the text.

Initial rates of the slow spectral change

A different approach to the problem of the characterization of this slow process, is via initial rate studies. The situation is complicated however, by the fact that in order to obtain measurable differences in the initial rates, concentrations of difluorooxaloacetate

must be lowered until they are of the same order as the enzyme concentration. Under these circumstances the assumptions implicit in the Michaelis Menten treatment are no longer valid and the data have to be treated in a different manner.

Considering equation (9)

$$E' + I \underset{k_{-1}}{\overset{k_1}{\rightleftharpoons}} A \xrightarrow{k_2} B \qquad (9b)$$

Assuming a steady state in A,

then $$\frac{d[A]}{dt} = 0 = [E'][I]k_1 - [A](k_{-1} + k_2)$$

let $$\frac{k_{-1} + k_2}{k_1} = K_m$$

then $$[A] = \frac{[E'][I]}{K_m}$$

If E_t is the total concentration of enzyme then $E_t = [E'] + [A]$

and $$[A] = \frac{[E_t - [A]][I_t - [A]]}{K_m}$$

where $[I_t]$ is initial concentration of difluorooxaloacetate

$$\therefore \quad [A]K_m = E_t[I_t] - E_t[A] - [I_t][A] + [A]^2$$

or $$[A]^2 - [A](E_t + [I_t] + K_m) + E_t[I_t] = 0 \qquad (10)$$

Now the initial rate of reaction $v = k_2[A]$ and a plot of v versus [A] should be a straight line through the origin.

A value for K_m may be obtained in the following way . The initial velocity v is determined for each of a series of values of $[I_t]$ and corresponding values of [A] are calculated by solution of the quadratic equation (10) using an assumed value of K_m. A plot

of v versus [A] is then fitted to a straight line through the origin (Bliss, 1967) and the error variance of the line obtained. The process is then repeated using different assumed values of K_m until the error variance of the straight line is minimised. The value of K_m corresponding to this minimum is taken as the true value.

1.0 ml. of a 16 μM solution of aminic AAT in 20 mM pyrophosphate buffer, pH 7.4, in a semi-micro quartz cuvette, was placed in the cell holder of a spectrophotometer, thermostatted at 25°C. The reaction was initiated by the addition of 3-10 μl of a 20 mM-stock solution of difluorooxaloacetate in pyrophosphate buffer, to give final concentrations in the range 35-200 μM. The reaction was monitored by following the change in optical density at 362 nm. The velocity in terms of μM/sec was calculated making the assumption that the extinction coefficient of the product is the same as the aldimine form of the enzyme, and that the extinction coefficient of A is the same as the extinction coefficient of the aminic form of the enzyme. As the extinction coefficients of both the aminic and the aldimine forms of the enzyme are known (Methods), the amount of product may be calculated from equation (11) derived as follows:-

$$E_t = [E'] + [A] + [B]$$

$$OD = \varepsilon_1\left([E'] + [A]\right) + \varepsilon_2[B]$$

$$OD = \varepsilon_1\left(E_t - [B]\right) + \varepsilon_2[B]$$

$$\therefore \quad [B] = \frac{OD - \varepsilon_1[E_t]}{\varepsilon_2 - \varepsilon_1} \qquad (11)$$

Treatment of the results as described above led to a convergence of the v versus [A] plots to a straight line as the assumed K_m was varied (Fig.19a). The best straight line, corresponding to K_m 7 μM is

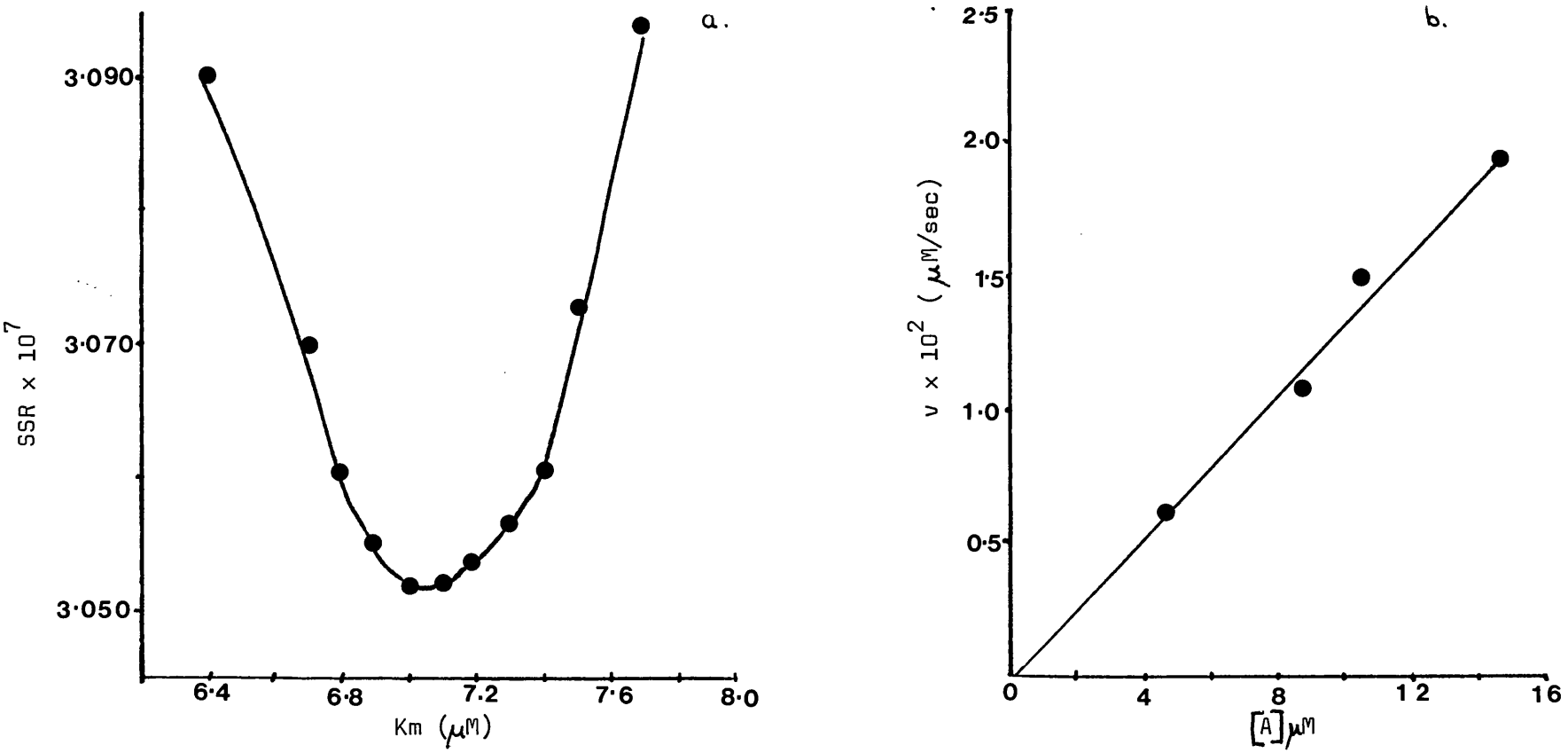

Fig. 19. Iterative solution for Km from the initial rates of the 332 to 360 nm spectral change. a) Variation in the sum of squares of residuals (SSR) as Km was varied. b) Plot of the initial rate versus [A] at the value of Km (7 μM) giving the minimum SSR.

shown in Fig.19b. The slope of the line is equal to k_2 (= 1.30 x 10^{-3} sec^{-1}), and is in good agreement with the maximum first order rate constant (1.22 x 10^{-3} sec^{-1}) obtained by conventional kinetic methods at high difluorooxaloacetate concentration (see previous section). If the assumption is made that $k_2 \ll k_{-1}$ then $K_m \simeq K_d$, and the similarity between the K_d and K_i obtained from the steady state inhibition experiments, suggest that the inhibition is caused by the reaction of difluorooxaloacetate with the aminic form of the enzyme to form complex A (Equation 9).

Transamination of difluorooxaloacetate

Although the steady state inhibition kinetics indicated that difluorooxaloacetate was not acting as a substrate for AAT, the slow spectral change implies a very slow transformation of difluorooxaloacetate to either a dead-end complex or to difluoroaspartate. If k_{cat} for transamination of difluorooxaloacetate is very much less than k_{cat} for the natural substrate then the substrate activity would not be detectable in the steady state kinetic plots.

In order to investigate the possibility of transamination of difluorooxaloacetate the optical density at 260 nm of a solution containing 0.03 mM aldimine enzyme, 30 mM-aspartate and 0.2 mM difluoro-oxaloacetate in 0.1M potassium phosphate buffer, pH 7.4 was monitored at 25°C reading against a blank containing only the enzyme and aspartate. Transamination of difluorooxaloacetate should result in continuous regeneration of aldimine enzyme from initially formed aminic enzyme so allowing continuous production of oxaloacetate (λ_{max} 260 nm) from aspartate.

Under these conditions a very slow rate (0 .00115 OD/min) was

observed. A spectral scan of the reaction mixture showed λ_{max} 328 nm. The ε_{260} of oxaloacetate is 5.7×10^{2} $l:M^{-1}cm^{-1}$ (Velick and Vavra, 1962a) and so the rate in terms of moles of oxaloacetate per sec per mole of enzyme may be calculated. This is 1.12×10^{-3} sec^{-1}, in good agreemnt with the first order rate constant obtained for the slow spectral change.

Although this experiment indicates that transamination of difluorooxaloacetate is occurring, similar more detailed studies were not possible in view of the difficulty of accurately measuring extremely slow rates in the presence of the high noise level generated by the large protein absorbance at 260 nm.

The amino acid, L-cysteine sulphinic acid, can act as an amino group donor for AAT. It reacts more rapidly than L-aspartate (Kearney and Singer, 1953) and as a result of rapid breakdown of the oxo-product, 3-sulphinylpyruvate, to SO_2 and pyruvate, the reaction is virtually irreversible (Jenkins and D'Ari, 1966d). This reaction can be coupled with lactate dehydrogenase (LDH), which reduces pyruvate to lactate with concomittant oxidation of NADH to NAD. Thus, provided that LDH and NADH are in excess, transamination can be followed by the disappearance of NADH (Scheme 2).

$$E' + \text{Ketoacid} \rightleftharpoons E + \text{Aminoacid}$$

$$E + CySO_2 \longrightarrow E' + \text{Pyruvate}$$

$$\text{Pyruvate} + \text{NADH} \xrightarrow{\text{LDH}} \text{Lactate} + \text{NAD}$$

Scheme 2 Cysteine sulphinate - coupled assay for transaminase activity

As measurements are made at 340 nm the high background absorbance resulting from protein is avoided and the large difference in extinction coefficients between NADH and NAD gives a 10 fold increase

in sensitivity compared with the method in which oxaloacetate production is followed at 260 nm.

The method was checked by measuring AAT-catalysed transamination between cysteine sulphinate and α-oxoglutarate. The reaction mixture contained 0.10 mM cysteine sulphinate; 0.10 mM NADH; 6.2×10^{-4} mM aldimine AAT (sites); 5 μg LDH in 20 mM pyrophosphate buffer, pH 7.4 at 25°C. The reaction was initiated by the addition of α-oxoglutarate to give a final concentration of 0.025 mM. The results are shown in Fig.20 in which the reaction is seen to be very rapid, going to completion as judged by the amount of NADH consumed (0.024 μMol.⁻¹).

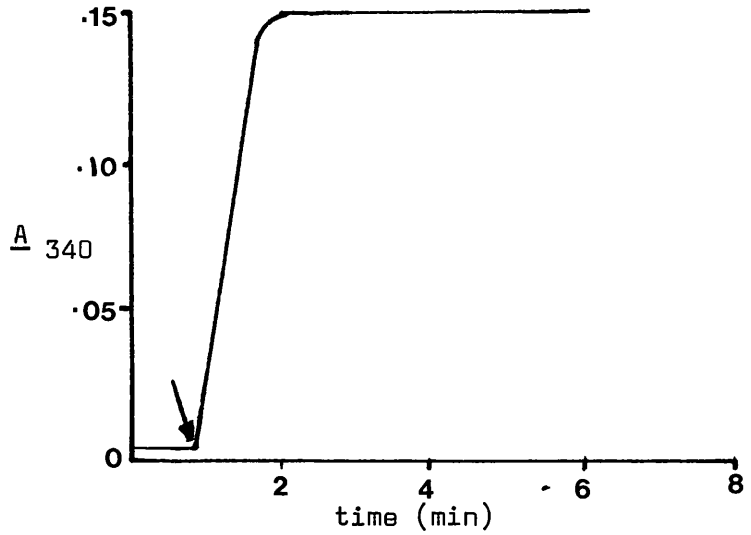

Fig. 20. Time course of NADH oxidation as an indicator of transamination between α-oxoglutarate and cysteine sulphinate catalysed by aspartate transaminase. The reaction was initiated by addition of α-oxoglutarate. The final volume in the cuvette was 1.0 ml.

The experiment was then repeated using difluorooxaloacetate as the ketoacid substrate. The reaction mixture contained 0.2 mM NADH; 0.5 mM difluorooxaloacetate; 5 μg LDH; 5.2×10^{-3} mM aldimine AAT in pyrophosphate buffer as before. The reaction was

initiated by the addition of aliquots of a cysteine sulphinate solution to give final concentrations as indicated in Fig.21. The consumption of NAD corresponding to cysteine sulphinate added is shown in Table 1.

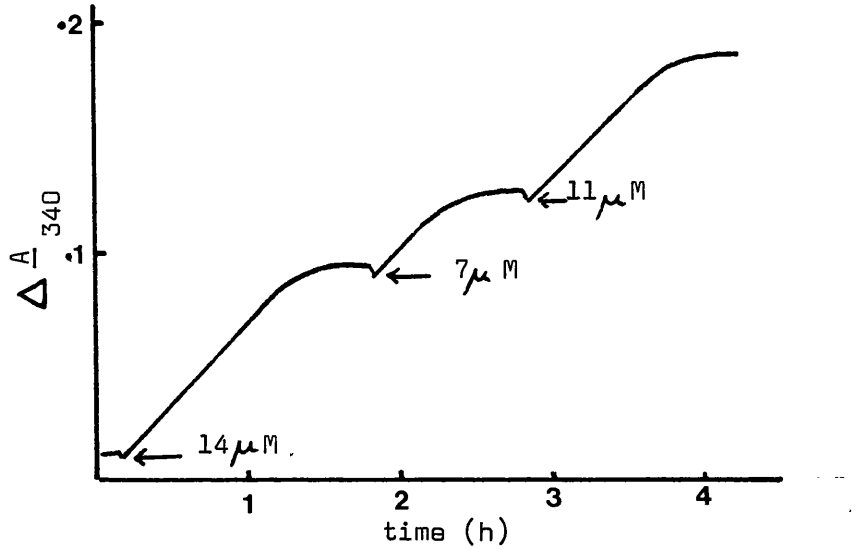

Fig. 21. Time course of NADH oxidation as a indicator of transamination between difluoro-oxaloacetate and cysteine sulphinate catalysed by aspartate transaminase. The reaction was initiated by the addition of cysteine sulphinate to give the concentrations indicated on the figure.

Cysteine sulphinate added (μ moles)	NADH consumed (μ moles)
0.02	0.0196
0.014	0.0120
0.0105	0.0096
0.007	0.0069

Table 1

As the initial cysteine sulphinate concentration is greater than the enzyme concentration and is completely used up in each step of the reaction, a catalytic reaction must be taking place.

No reaction is observed in the absence of enzyme. The rate of the reaction is linear for the greater part of the progress curves and a first order rate constant for the process can be calculated. This is 1.38 x 10^{-3} sec^{-1} at 5.2 μM enzyme and 1.28 x 10^{-3} sec^{-1} at 2.6 μM enzyme, in good agreement with the first order rate constant obtained from the slow spectral change and from the observation of oxaloacetate production at high enzyme concentration. Comparing this rate constant with the rate constant (530 sec^{-1}) obtained for the rate-limiting step of transamination of the natural substrate pair, aspartate-α-oxoglutorate (Fasella and Hammes, 1967), the constant for transamination of difluorooxaloacetate is smaller by a factor 4.3 x 10^{5}. Under these circumstances, substrate activity of difluorooxaloacetate will not be detected in the steady state inhibitor studies.

Conclusive evidence that transamination of difluorooxaloacetate was in fact taking place, was obtained by the isolation of the product of the reaction.

1 ml of 0.5 M ammonium acetate buffer, pH 7.4, containing aldimine AAT (10 mg), difluorooxaloacetate (50 mM) and cysteine sulphinate (40 mM), was incubated at room temperature for four days. The reaction mixture was then subjected to vacuum dialysis, and the non-diffusible material washed with double distilled water (2x5 ml), vacuum dialysing to low volume after each washing. The diffusate, now protein free, was collected and freeze dried. The freeze dried product was dissolved in 0.5 ml of distilled water and its ^{19}F n.m.r. spectrum recorded. The result is shown in Fig.22. The single sharp peak of difluorooxaloacetate is very much reduced in height compared with that given under comparable conditions by 50 mM difluorooxaloacetate, and the spectrum also shows the appearance of a doubled quartet. This new spectrum is typical of an AB.X

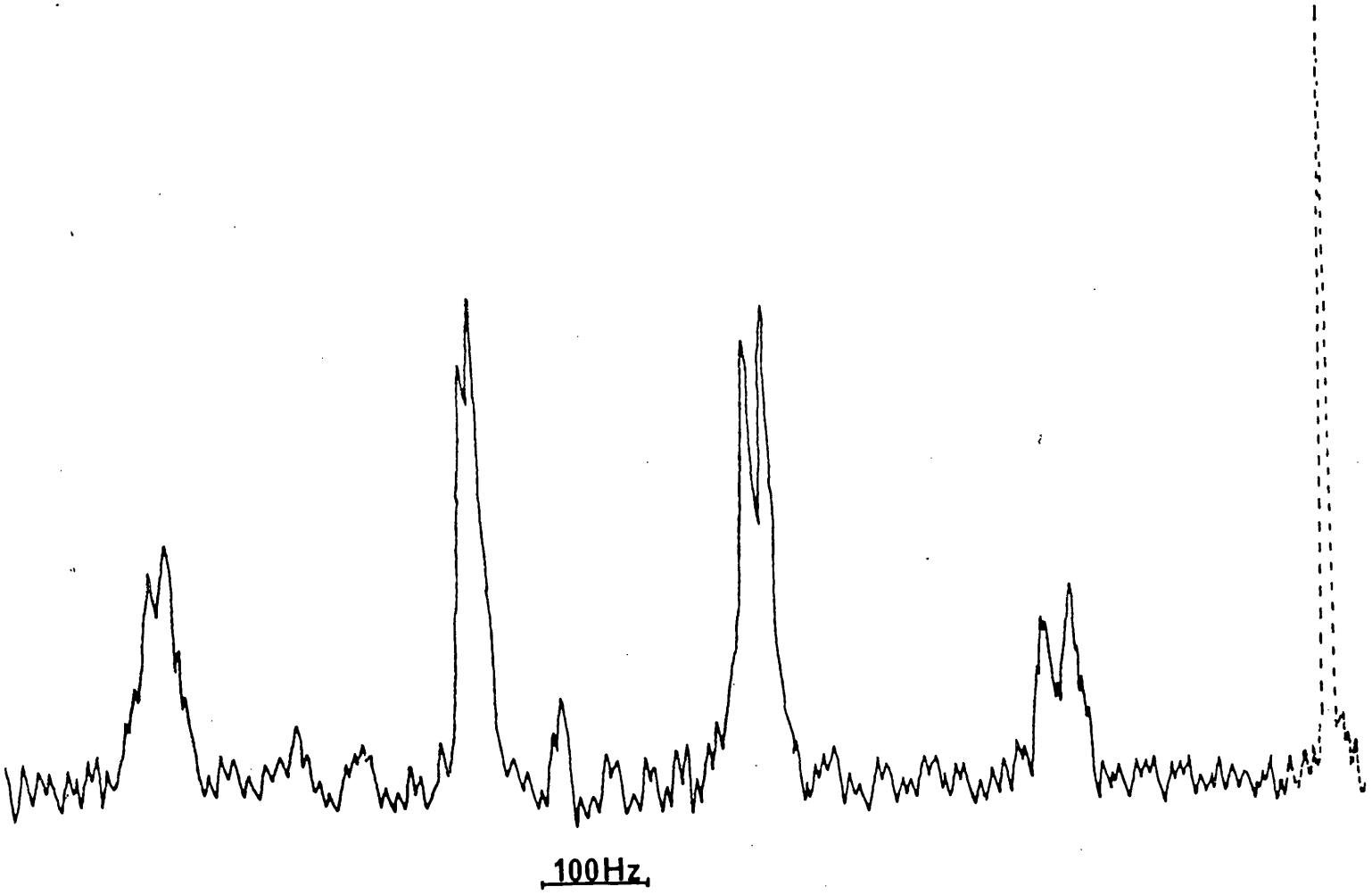

Fig. 22. ^{19}F n.m.r. spectra of difluoroaspartate and difluoro-oxaloacetate. The spectra were obtained under the conditions described in the text and are the average of 16 spectral scans. The singlet (- - -) is the spectrum of the unchanged difluoro-oxaloacetate.

system (Emsley et al., 1965) and corresponds to that expected from difluoroaspartate. The introduction of the amino group into the molecule generates an assymetric centre, thus the two fluorine atoms in the β position are no longer chemically equivalent and will exhibit spin-spin coupling, giving rise to a quartet. Each fluorine is in turn coupled to the α hydrogen atom so that each signal of the quartet will be split again, giving rise to a doubled quartet.

The n.m.r. parameters characterising the spectrum of difluoroaspartate are given in Table 2.

J_{AX}	J_{BX}	$\nu_A - \nu_B$	J_{AB}
8.3 Hz	20.7 Hz	456 Hz	270 Hz

Table 2

Possible AAT catalysed β-elimination of difluorooxaloacetate

Although AAT-catalysed transamination of difluorooxaloacetate to difluoroaspartate was demonstrated (see previous section), the possibility existed that the aminic - aldimine enzyme conversion could be accompanied also by β-elimination of fluoride ion as shown in Fig.23. Similar elimination mechanisms have been suggested for chloroglutamate (Antonini et al., 1970), β-chloroalanine (Morino et al., 1974) and β-fluorooxaloacetate (Kun et al., 1960).

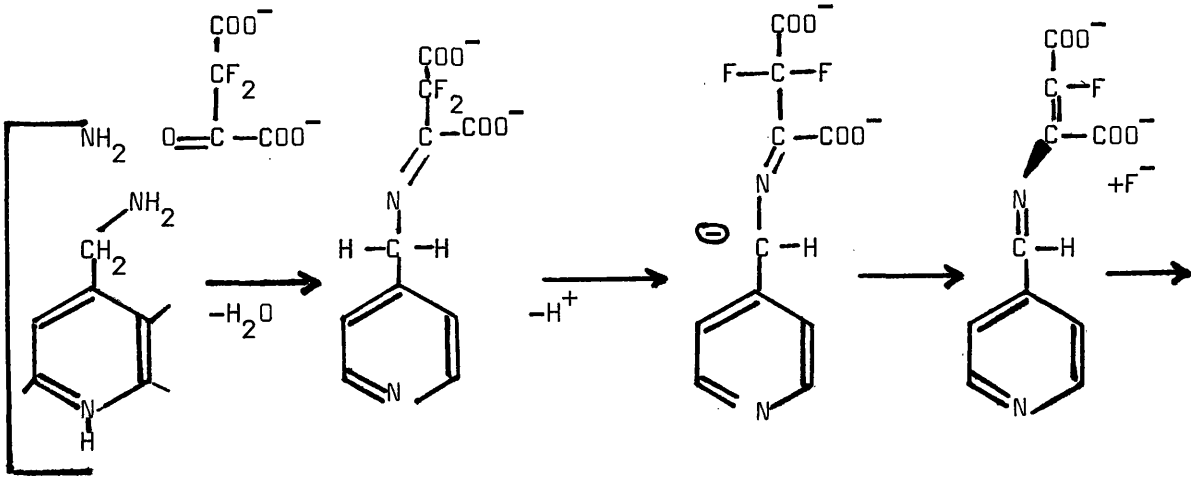

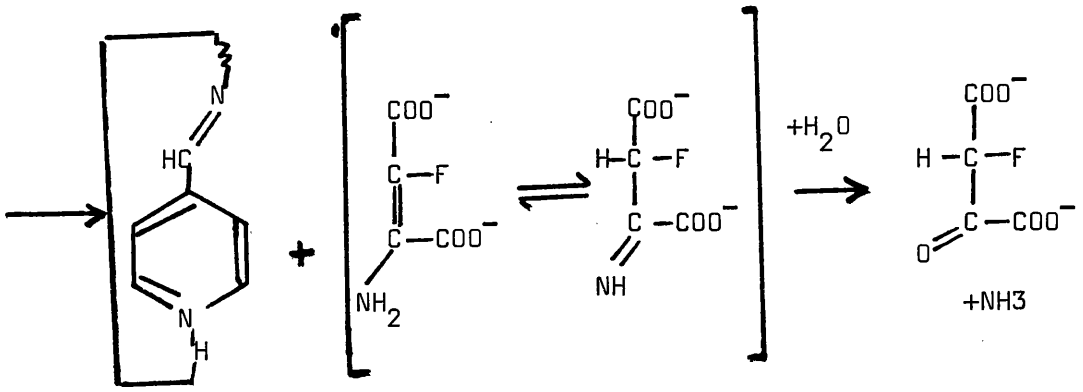

Fig. 23. Possible mechanism for reaction of difluoro-oxaloacetate with the aminic form of aspartate aminotransferase, resulting in the β-elimination of fluoride.

As β-elimination should result in the production of fluoride, this possible reaction pathway was investigated by determining the fluoride content of an aminic enzyme-difluorooxaloacetate reaction mixture using a fluoride electrode. Difluorooxaloacetate was added to a solution (1 ml) of aminic AAT (1.6×10^{-4} M in sites) in 20 mM pyrophosphate buffer, pH 7.4, to give a final concentration of 3.2 mM. The reaction was followed by monitoring the changes at 360 and 330 nm and was complete after 1 hour. The fluoride content of the reaction mixture was measured using a fluoride electrode as described in the Methods section. Aliquots of the reaction mixture were removed before addition of difluorooxaloacetate and at the completion of the reaction and suitably diluted for assay of enzyme activity. The fluoride contents of 3.2 mM difluorooxaloacetate in 20 mM

pyrophosphate buffer and of 1.6 x 10^{-4}M aminic AAT in 20 mM pyrophosphate buffer were also measured. The results are shown in Fig.24 and Table 3.

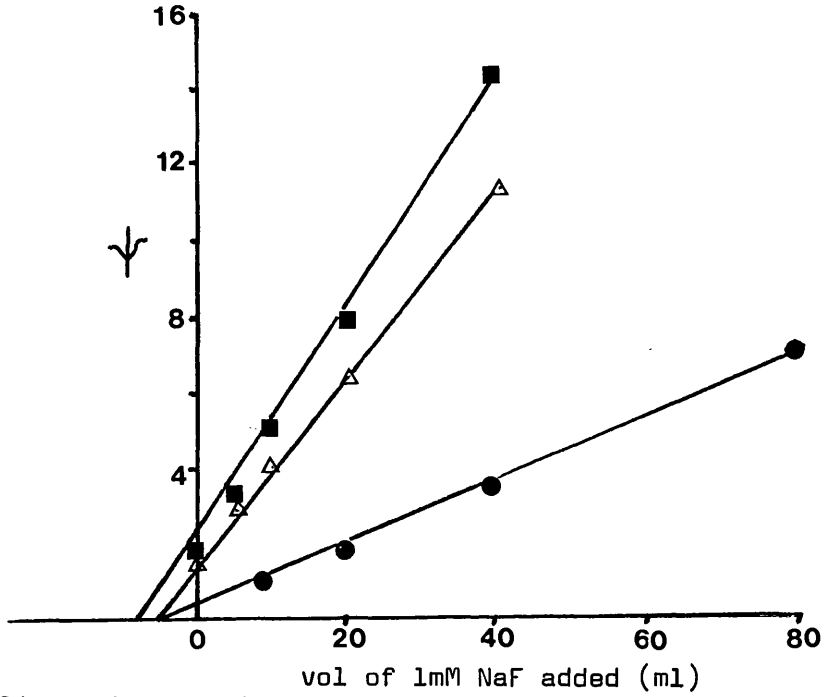

Fig. 24. Determination of fluoride ion in a reaction mixture of difluoro-oxaloacetate and the aminic form of aspartate transaminase. Plot of ψ (see Methods) versus μl of 1 mM NaF solution added: (●) .16mM aspartate transaminase; (△) 3.2 mM difluoro-oxaloacetate; (■) .16 mM aspartate transaminase + 3.2 mM difluoro-oxaloacetate after 1 hour.

Solution	$[F^-]\mu$ Molar
a) Aminic AAT + F_2OAA	7.5 ±0.1
b) Aminic AAT	4.6 ±0.4
c) F_2OAA	5.4 ±0.3

Table 3

The sum of the results for solution b & c (Table 3) gives the total fluoride concentration expected if no β-elimination takes place. Comparing this with the result obtained for solution a (Table 3), it can be seen that slightly less fluoride is found for solution a than for the sum of the two controls. This is probably experimental error since the method becomes increasingly inaccurate

below 10^{-5}M F^-. Thus within the limitations of the technique, no fluoride produced by β-elimination can be detected.

After suitable dilution the aliquots taken from the reaction mixture before and after reaction with difluorooxaloacetate, showed no detectable difference in enzyme activity, indicating that irreversible inactivation of the enzyme had not taken place.

Determination of the position of the aminic-aldimine enzyme equilibrium in the presence of difluorooxaloacetate

The studies of the slow spectral changes occurring on reaction of aminic AAT with difluorooxaloacetate indicate that this event represents the rate limiting step in transamination of difluorooxaloacetate. Experiments were undertaken to determine the position of equilibrium attained following the slow spectral change.

Cysteine sulphinate rapidly reacts irreversibly with aldimine AAT to form pyruvate. Provided that the reaction of cysteine sulphinate with aldimine AAT is very much faster than the rate limiting step for transamination of difluorooxaloacetate and that difluorooxaloacetate and cysteine sulphinate concentrations are much greater than their respective K_m values, it can be shown (Appendix 1) that the rate of production of pyruvate from cysteine sulphinate added to an aminic AAT-difluorooxaloacetate reaction mixture at "equilibrium", will be biphasic.

The equations predict that there will be an initial "burst" of pyruvate production equal to the amount of aldimine enzyme (or any rapidly interconverted species) formed in the pre-equilibrium before addition of cysteine sulphinate. This will be followed by a slow steady-state production of pyruvate representing the transamination of difluorooxaloacetate to difluoroaspartate. Extrapolation of this

steady state rate to zero time will give the amount of pyruvate liberated in the "burst". Using this experimental method it should therefore be possible to determine the extent of the slow spectral reaction.

Difluorooxaloacetate was added to a series of tubes containing 17.5 - 3.9μM (sites) aminic AAT in 1.5 ml 20 mM-pyrophosphate buffer, pH 7.4, to give a final concentration of 75.0μMolar. These solutions were incubated at 25°C for 2 h. after which time no further changes in their UV spectra could be detected. Aliquots (1 ml) of each reaction mixture were removed and placed each in a semimicro quartz cuvette. LDH (0.2μg) and NADH (to a final concentration of 80μM) were then added and a base line recorded at 339 nm. This wavelength is the isosbestic point for the slow spectral change. The reaction was initiated by the addition of cysteine sulphinate to give a final concentration of 200μMolar, and followed by the decrease in absorbance at 339 nm. A representative progress curve is shown in Fig.25. The total amount of enzyme present is plotted against the extent of the "burst" (Fig.26a) and against the steady state rate (Fig.26b).

Fig.26a demonstrates that the extent of the "burst" is linear with total enzyme, the slope of this graph is equal to 1.0 demonstrating that the aminic enzyme is essentially irreversibly converted to aldimine enzyme in the equilibrium mixture containing difluorooxaloacetate. The steady state rate should equal $[E_o]k_3$ (Appendix 1). Thus the slope of the graph in Fig.26b gives k_3; this equals $1.25 \times 10^{-3} sec^{-1}$, in good agreement with previous estimates for the rate constant of the rate-limiting step for transamination of difluorooxaloacetate.

Fast spectral change

Initial experiments on the interaction of difluorooxaloacetate and the aminic form of AAT indicated that a fast change in the λ_{max}

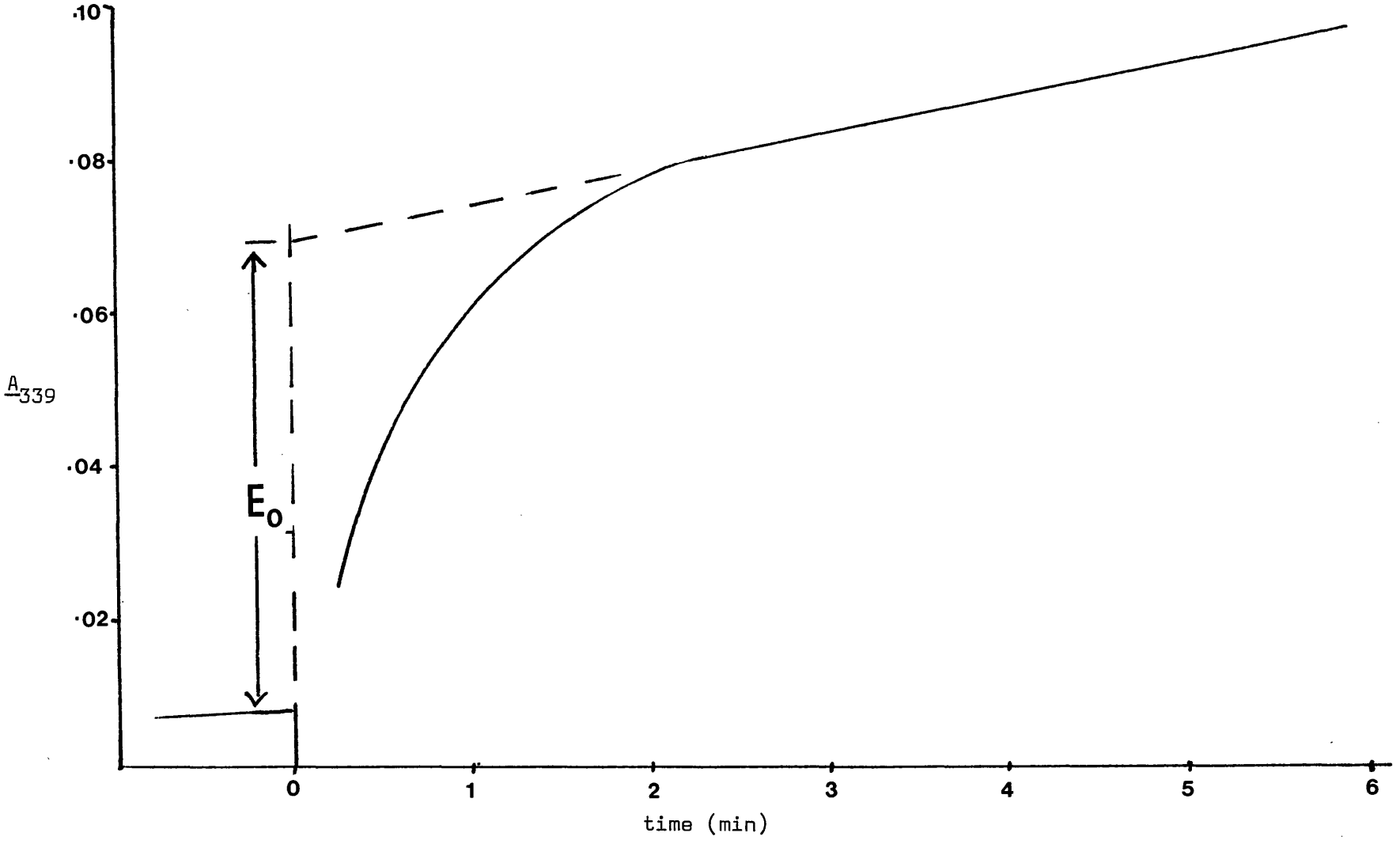

Fig. 25. Time course of NADH oxidation following addition of cysteine sulphinate to a mixture of difluoro-oxaloacetate and the aminic form of aspartate transaminase at equilibrium. The example shown is the "burst" produced from a reaction mixture originally containing 11 μM aminic form of aspartate transaminase. All other conditions are stated in the text.

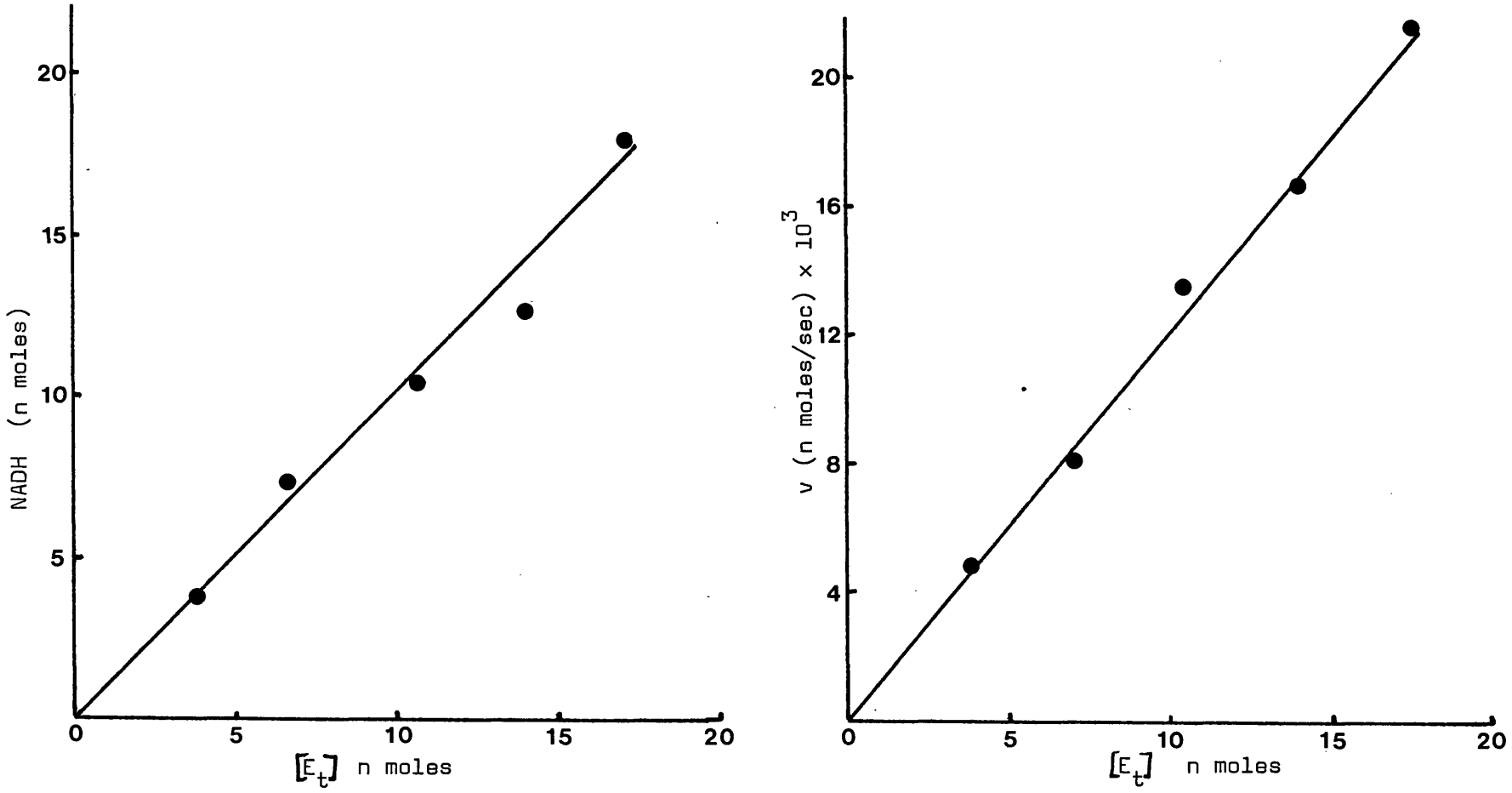

Fig. 26. Variation of parameters in the "burst" experiments (Fig. 25), with total enzyme concentration. (a), Plot of amount of NADH oxidised in the transient phase against enzyme concentration. (b) Plot of steady-state rate against total enzyme concentration.

of the enzyme absorbance (from 332 to 328 nm) took place before the previously discussed slow spectral change (ca 330 $\longrightarrow$ 360 nm).

In the presence of high concentrations of difluorooxaloacetate (0.2 mM) and cysteine sulphinate (2 mM), the UV spectrum of 21 μM aldimine AAT showed λ_{max} 328 nm and was invariant with time over a period of 1h. (Fig.27a). The difference spectrum between this reaction mixture and 21 μM aldimine enzyme with 2.0 mM cysteine sulphinate exhibited a maximum at 310 nm and a minimum at 345 nm (Fig.27b).

Rapid addition and mixing ($\sim$ 5 sec) of difluorooxaloacetate (20.50 μM) with 20 μM aminic AAT in a conventional spectrophotometer, following the increase in absorbance at 310 nm or the decrease in absorbance at 345 nm, showed that the process of formation of the species absorbing at 328 nm was observable, the reaction being complete after approximately 15 sec. However, accurate analysis of the reaction was not possible using this method and therefore the reaction was studied by stopped-flow techniques.

The aminic form of AAT (46.2 μM solution in 20 mM pyrophosphate buffer, pH 7.4) was rapidly mixed with an equal volume of difluoro-oxaloacetate solution (40-160 μM solution in buffer) in a stopped-flow spectrophotometer, and the reaction observed by following the decrease in absorbance at 345 nm. A representative progress curve of the reaction is shown in Fig.28.

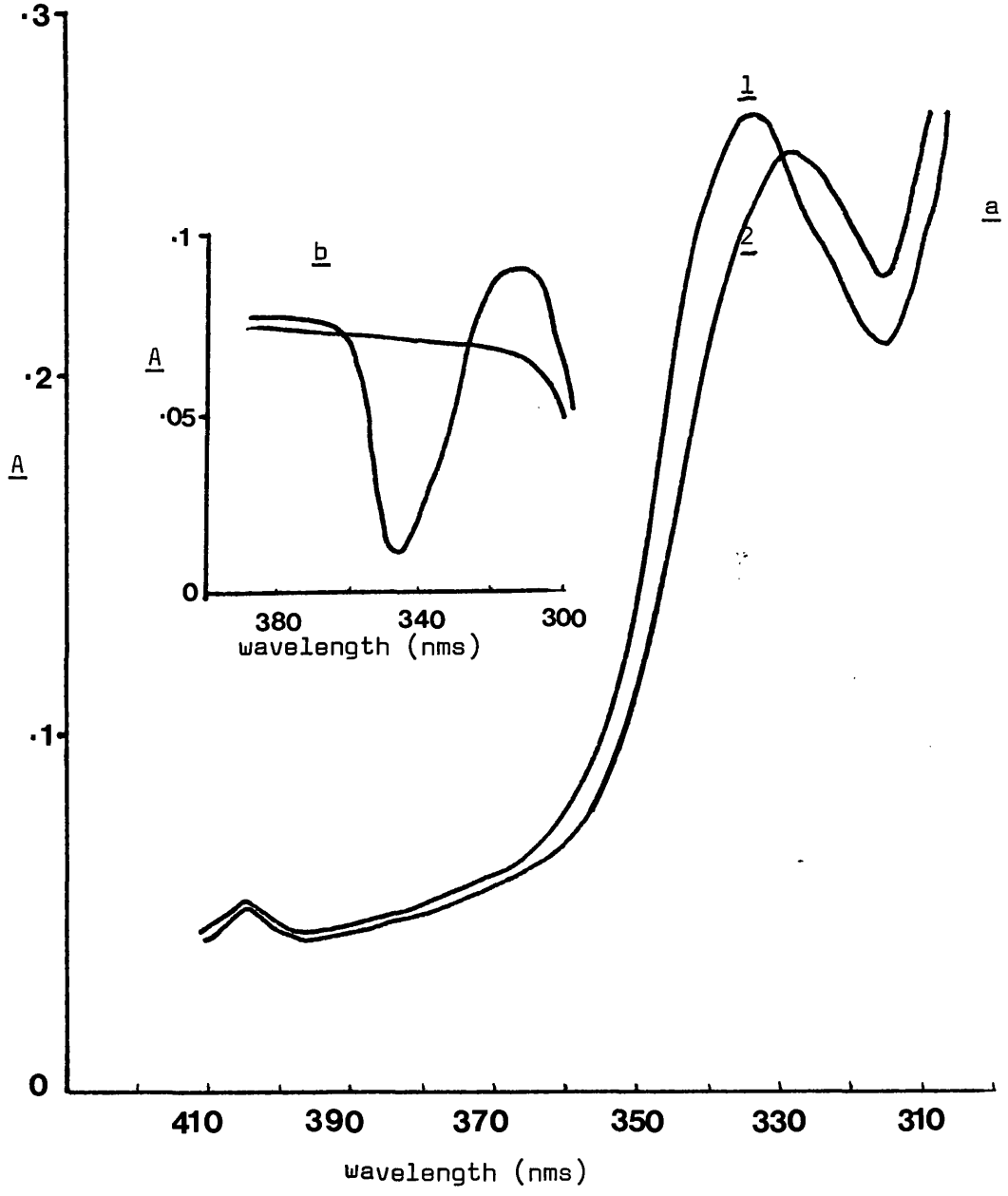

Fig. 27. Absorption spectra of aspartate transaminase in the presence of excess difluoro-oxaloacetate and cysteine sulphinate. (a) Curve 1, aspartate transaminase (21 μM) and cysteine sulphinate (2 mM) in 20 mM sodium pyrophosphate buffer, pH 7.4. Curve 2, as for 1, but with the addition of difluoro-oxaloacetate (0.2 mM). (b), difference spectrum between (2) (sample) and (1) reference.

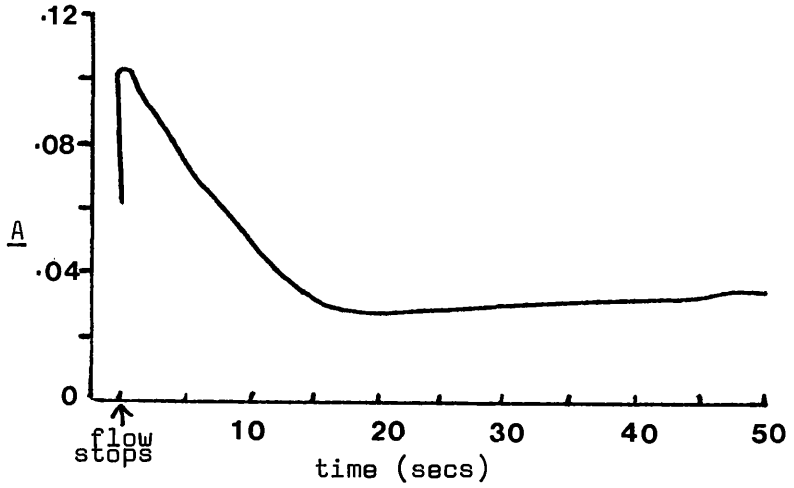

Fig. 28. Variation of $\underline{A}_{345}$ on addition of difluoro-oxaloacetate to the aminic form of aspartate transaminase. The reaction mixture contained the aminic form of aspartate transaminase (final conc. 23.1 μM) from one syringe and difluoro-oxaloacetate (final conc. 80 μM) from the other.

Extent of reaction

Making the assumption that the reaction giving rise to the previously discussed slow spectral change is very much slower than the process giving rise to the species with λ_{max} 328 nm, then the situation at the completion of the fast reaction may be represented as the metastable equilibrium shown below (Equation 12)

$$E' + I \underset{}{\overset{K_D}{\rightleftharpoons}} A \qquad (12)$$

where E' is aminic AAT, I is difluorooxaloacetate and A is the species with λ_{max} 328 nm.

and $$K_D = \frac{[E'][I]}{[A]} \qquad (13)$$

The optical density (OD) of the solution at equilibrium is given by Equation (14)

$$OD = \varepsilon_1 [E'] + \varepsilon_2 [A] \qquad (14)$$

where ε_1 and ε_2 are the extinction coefficients at 345 nm of E' and A respectively. From the conservation equation $[E'] = [E_t] - [A]$

$$\therefore \quad OD = \varepsilon_1 [E_t] + [A] (\varepsilon_2 - \varepsilon_1)$$

As the initial $OD = \varepsilon_1 [E_t]$, then the change in optical density

$$\Delta OD = [A] (\varepsilon_1 - \varepsilon_2) \qquad (15)$$

A plot of Δ OD versus $[A]$ should be a straight line of slope $(\varepsilon_2 - \varepsilon_1)$, passing through the origin.

From equation (13)

$$[A] = \frac{[E'][I]}{K_D}$$

or $K_D[A] = \left([E_t]-[A]\right)\left([I_t]-[A]\right)$ where $[I_t]$ is initial concentration of difluorooxaloacetate

or $K_D[A] = [E_t][I_t] - [E_t][A] - [I_t][A] + [A]^2$

rearranging

$$[A]^2 - [A]\left([I_t] + [E_t] + K_D\right) + [E_t][I_t] = 0 \qquad (16)$$

By assigning a value to K_D, equation 16 may be solved with respect to $[A]$.

The analysis of data from the extent of the reaction was carried out in the same manner as for the analysis of the data from initial rates of the slow spectral change. An arbitrary value was assigned to K_D and equation (16) solved for $[A]$ for each concentration of difluorooxaloacetate. The error variance of the best straight line through the origin of a plot of Δ OD versus $[A]$ was then computed (Bliss 1967). The value assigned to K_D was then varied iteratively until a value

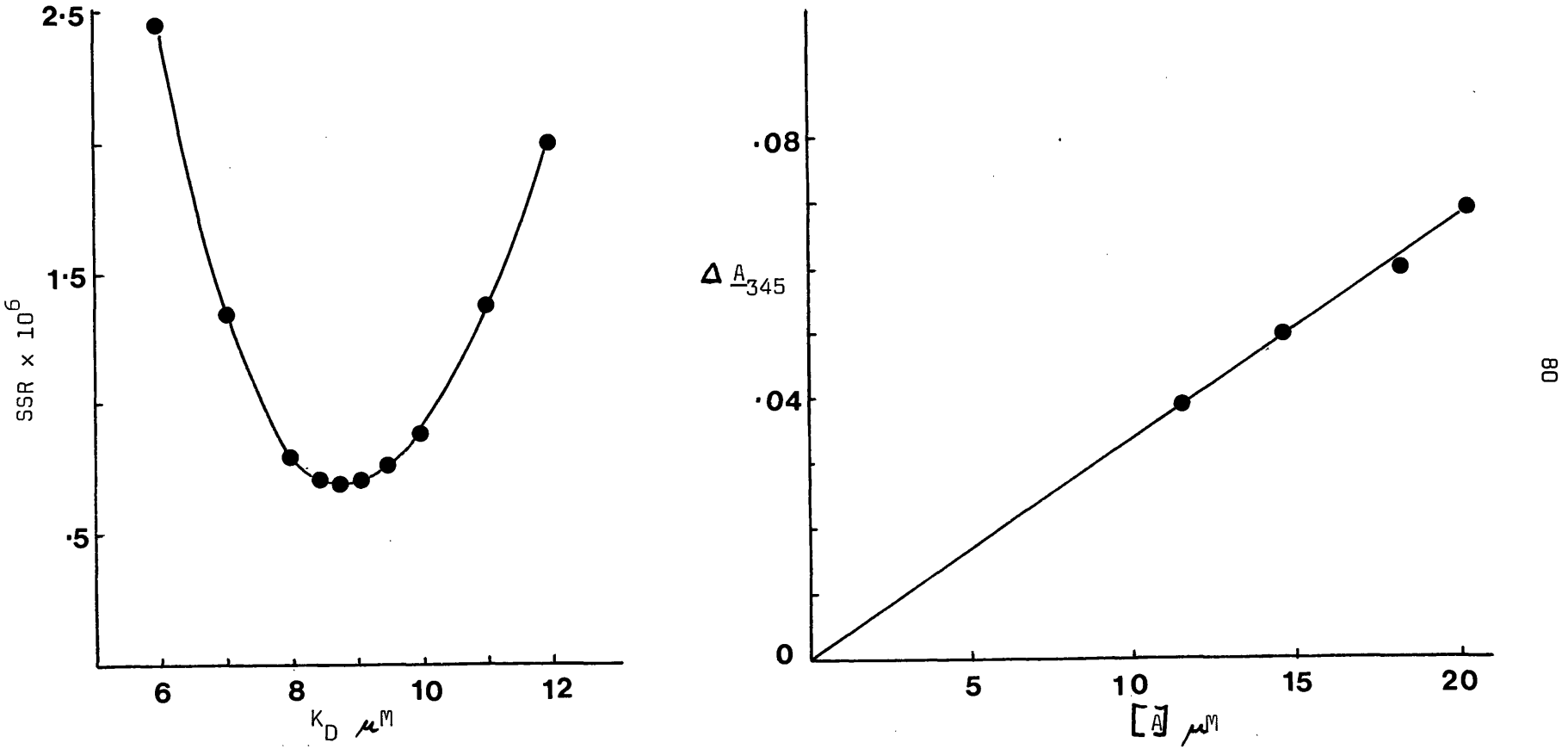

Fig. 29. Iterative solution for K_d from the extent of the 332 - 328 nm spectral change. a) Variation in the sum of square of residuals (SSR) as K_d was varied. b) Plot of ΔA_{345} versus [A] at the value of K_d (8.75 M) giving the minimum SSR.

of K_D was found that gave a minimum value to the error variance. The results of these iterations are shown in Fig.29, together with the plot of OD versus [A] with minimum error variance. This minimum occurred at K_D = 8.75 μ Molar and gives a value of $(\varepsilon_1 - \varepsilon_2) = 3.33 \times 10^3$ $1.M^{-1}cm^{-1}$. As $\varepsilon_1 = 6.08 \times 10^3$ $1.M^{-1}cm^{-1}$ (measured directly), then $\varepsilon_2 = 2.67 \times 10^3$ $1.M^{-1}cm^{-1}$ in good agreement with the ε_{345} for A (3.1×10^3 $1.M^{-1}cm^{-1}$) estimated from the spectrum (Fig.27a) obtained from AAT in the presence of high concentrations of difluorooxaloacetate and cysteine sulphinate.

Rates of fast spectral change

Attempts were made to fit the progress curves obtained from the stopped flow experiments to first and second order kinetics. These plots are shown in Fig.30. Systematic deviations from linearity are apparent in both the first and second order cases, and the system cannot be adequately described in these terms. However a log-log plot of the initial velocity (v) of the fast spectral change versus the initial substrate concentration (Fig.31) is a straight line with a slope of unity indicating that the reaction is first order with respect to [I]. The apparent second order rate constant for the reaction may be obtained from the ordinate intercept ($k = 1.74 \times 10^3$ $1.M^{-1}cm^{-1}$).

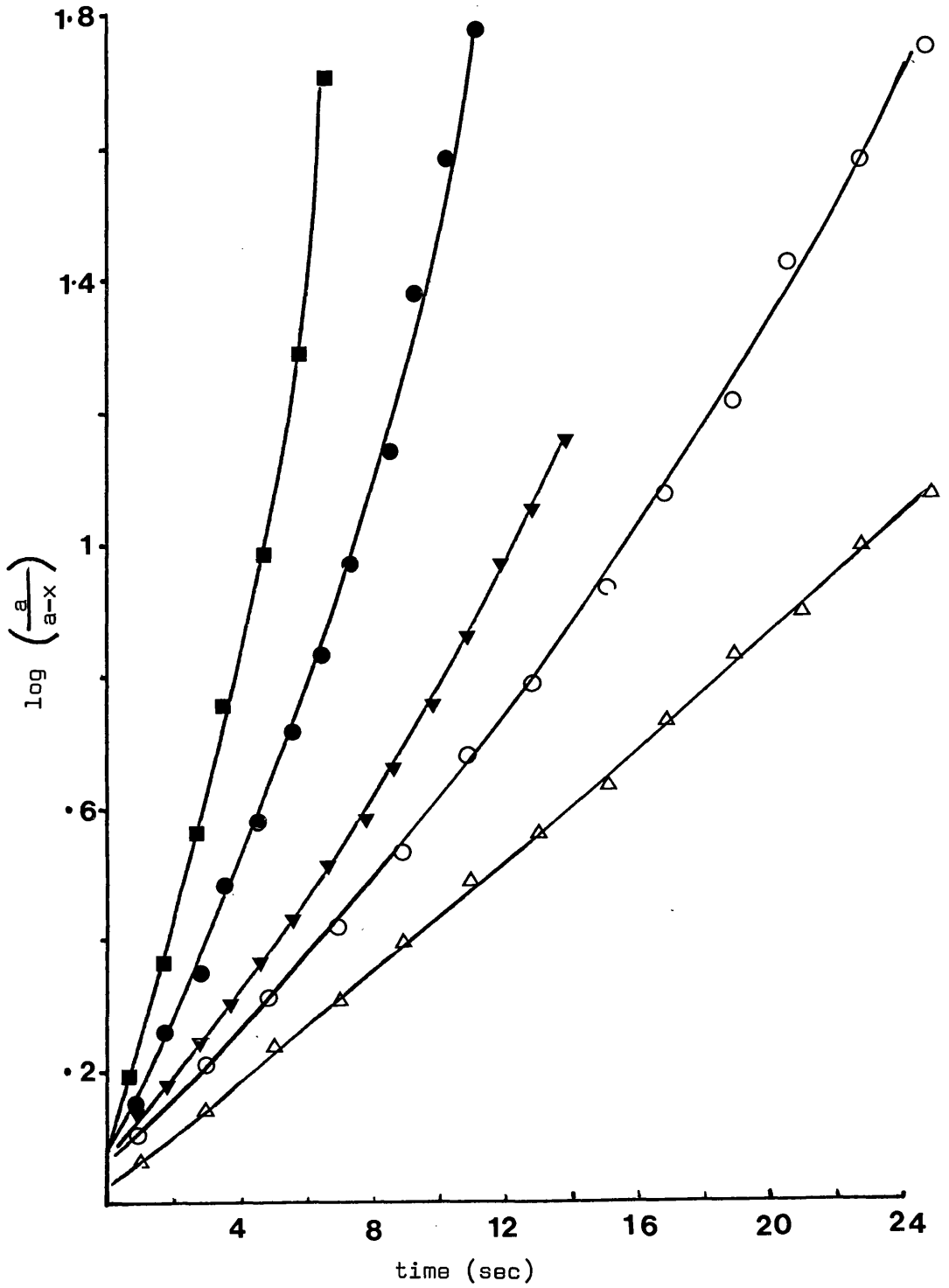

Fig. 30a. Progress curves of the 332 to 328 nm spectral change plotted according to the first order empirical rate equation. Log $\left(\frac{a}{a-x}\right)$ was plotted against time, where a is the initial concentration of enzyme and x is the concentration of enzyme remaining at time t. a and x were determined using the extinction coefficients obtained from the extent of the reaction. Difluoro-oxaloacetate concentrations: (△) 20 μM, (○) 30 μM, (▲) 50 μM, (●) 80 μM, (■) 120 μM.

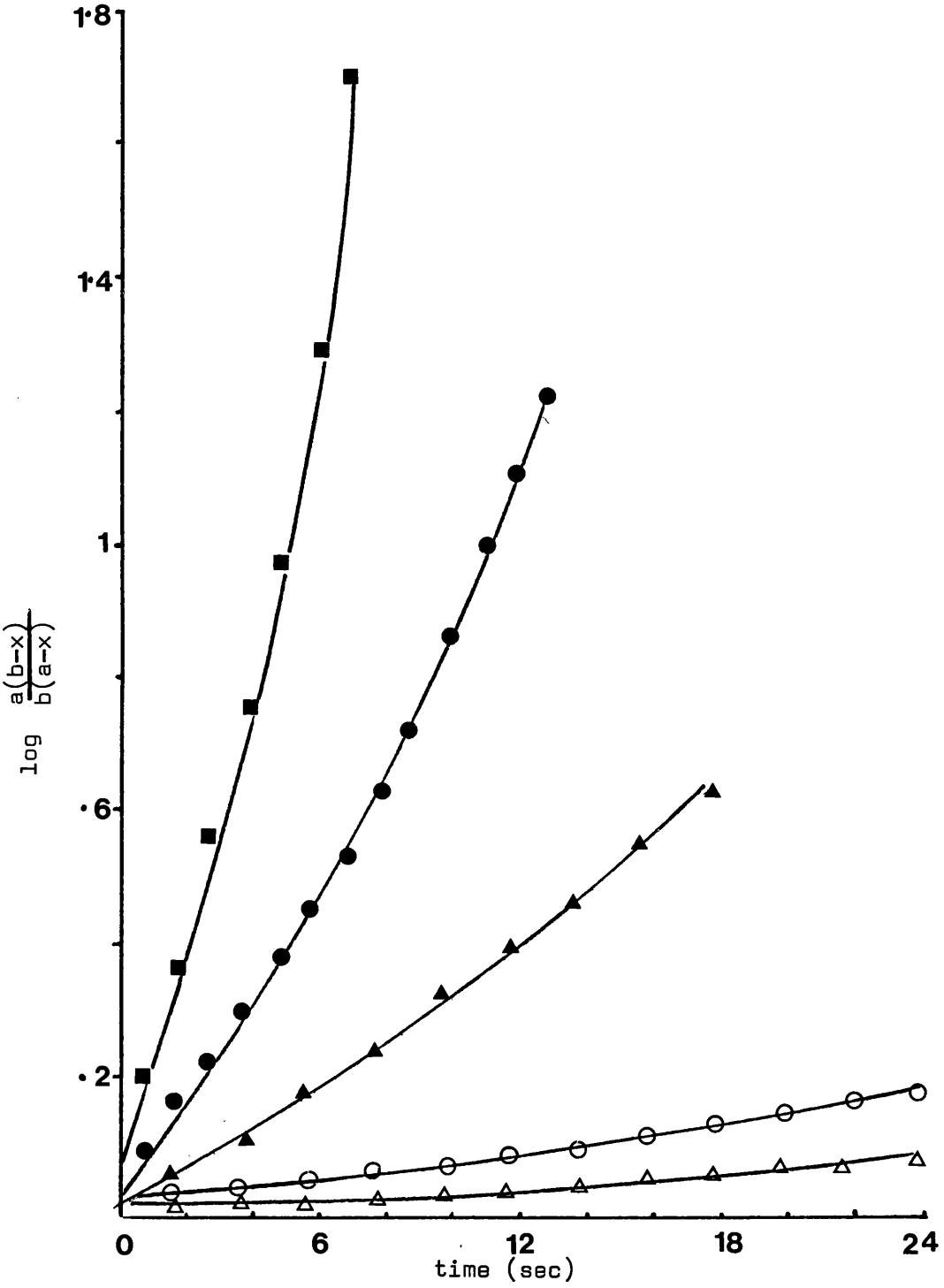

Fig. 30b. Progress curves for the 332 - 328 nm spectral change plotted according to the 2nd order empirical rate equation. Log $\frac{a(b-x)}{b(a-x)}$ was plotted against time. a and x have the same meaning as before and b is the initial concentration of difluoro-oxaloacetate. Difluoro-oxaloacetate concentrations: (△) 20 μM, (○) 30 μM, (▲) 50 μM, (●) 80 μM, (■) 120 μM.

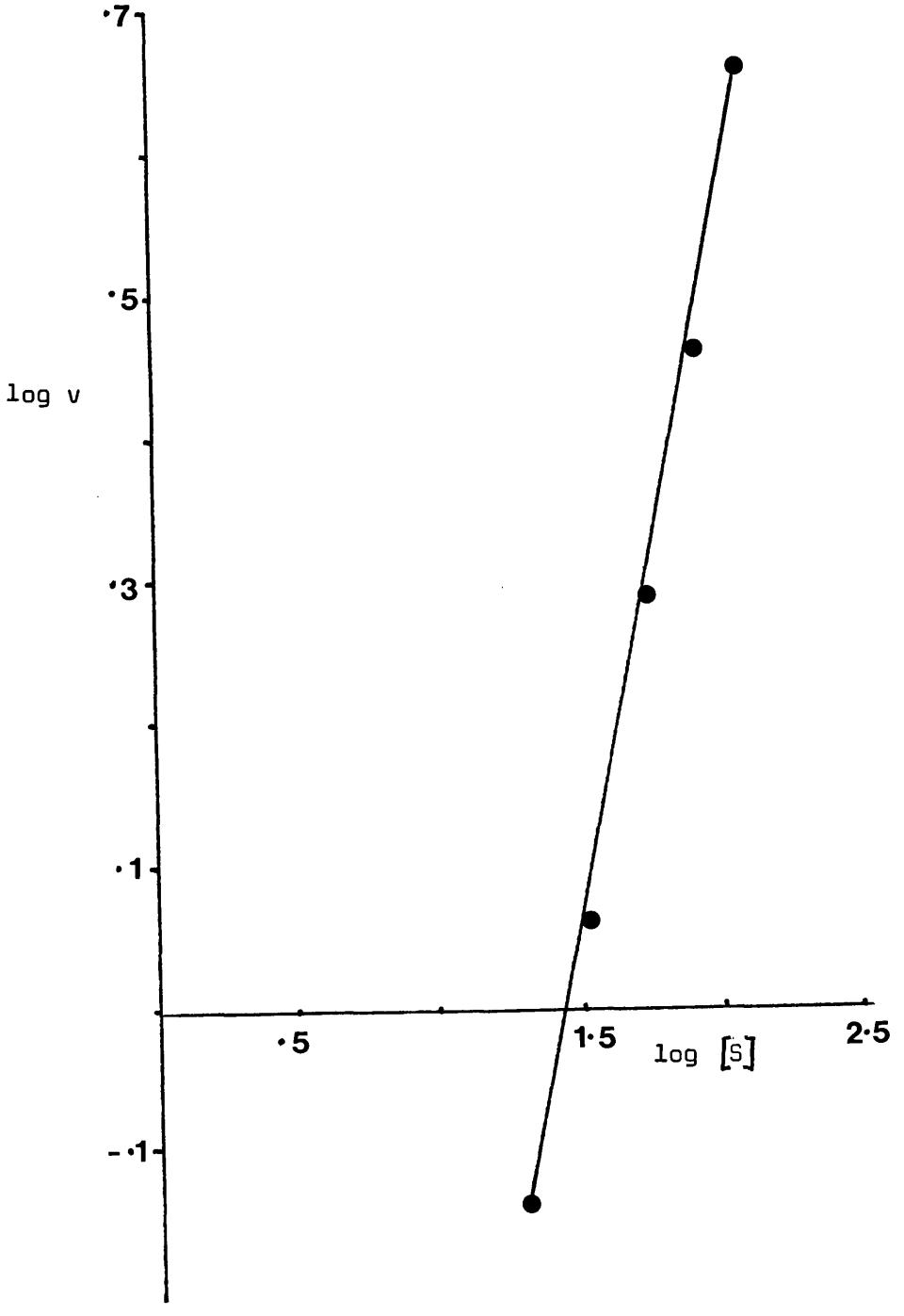

Fig. 31. Initial rates of reaction of difluoro-oxaloacetate with the aminic form of aspartate transaminase as a function of initial difluoro-oxaloacetate concentration. Plot of log initial rate of $\underline{A}_{345}$ versus log difluoro-oxaloacetate concentration. Estimates of initial rates were obtained from the progress curves by the method of Cornish-Bowden (1975).

As the progress curves cannot be described in terms of empirical first or second order rate equations, a more complex mechanism must accordingly be proposed. The mechanism outlined in equation 12 (page 78) can be expanded to include a further complex (X), spectrally indistinquishable from aminic AAT, that precedes the formation of the species with λ_{max} 328 nm (Equation 17)

$$\underset{\lambda_{max}}{E} + \underset{332\ nm}{I} \underset{k_2}{\overset{k_1}{\rightleftharpoons}} \underset{332\ nm}{X} \overset{k_3}{\rightleftharpoons} \underset{328\ nm}{A} \qquad (17)$$

If $[I] \ll \frac{k_2 + k_3}{k_1}$, then the progress curve describing the production of A will give neither first or second order kinetics, but there will be an approximately linear relationship between the initial velocity (v) and $[I]$.

It is not possible to obtain an integrated rate equation for this mechanism, but the system may be analysed in terms of initial rates. The initial rates of the reaction were obtained from the progress curves by the method of Cornish-Bowden (1975), and expressed in terms of μM^{-1}l sec, using the ε_{345} for A previously obtained (2.8×10^3 l $M^{-1}cm^{-1}$). As $[I_t]$ is of the same order as $[E_t]$, then $[I] \neq [I_t]$, and the data must be treated by an interative procedure. The method used is identical to that derived for the analysis of the initial rates of the slow spectral change (page 60). The initial rate data are presented in Table 4 and the results of the iterative procedure shown in Fig.32.

$[I_t]$ μ Molar	Initial rate $\mu M \cdot s^{-1}$
20	0.596
30	1.45
50	1.91
80	2.81
120	4.70

Table 4

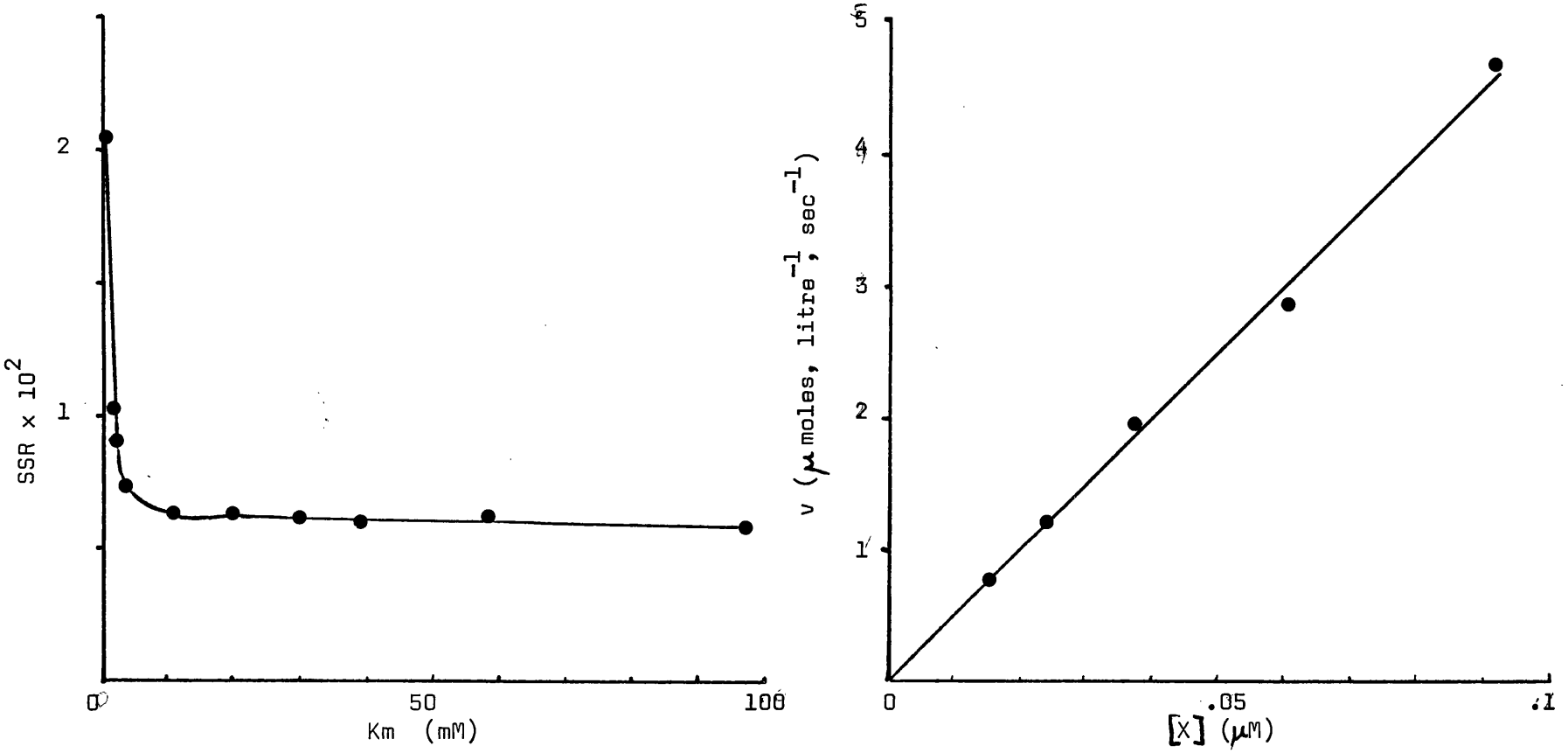

Fig. 32. Iterative solution for Km for the initial rates of the 332 - 328 nm spectral change. a) Variation of the sum of squares of residuals (SSR) as Km was varied. b) Plot of initial rate versus [X] (equation 17) at the value of Km (30mM) after which there is no further decrease in the value of SSR.

The error variance of the slope decreases on increasing the value of K_m up to a value of approximately 30 mM; further increases in the K_m did not significantly alter the goodness of fit. Although this analysis does not precisely determine the parameters involved, it does give estimates of the lower limits of K_m ($>$ 30 mM) and $k_3 \rangle (50\ sec^{-1})$.

An alternative approach to the analysis of the progress curves obtained from the stopped flow experiments, is to assume a mechanism for the reaction and so generate a computor simulation of the progress curves. The computor simulation may then be compared with the experimental progress curves.

A suitable computor program for this analysis is the programme CHEKMAT of Curtis and Chance (1974). Given a mechanism and initial estimates of the constants pertaining to the mechanism, the programme will adjust the values of specified parameters (usually rate constants) to give the best fit between the results of a simulation run and observed time courses. The simulation runs are executed as a subprocess.

The mechanism chosen for the simulation is given in Equation 18

$$E + I \underset{k_2}{\overset{k_1}{\rightleftharpoons}} X \underset{k_4}{\overset{k_3}{\rightleftharpoons}} A \xrightarrow{k_5} B \qquad (18)$$

λ_{max}	332 nm	332 nm	328 nm	360 nm

This is the simplest mechanism taking into account all the complexes suggested by the previous experimental evidence. Although the breakdown of complex A to complex B is very much slower than the formation of A, the relative values of k_5 and k_4 are not known and therefore the slow step must be included in the mechanism. The

value of k_5 was known from the initial rate studies of the slow spectral change and was therefore included in the programme as a fixed constraint on the simulation.

The observed progress curves are in terms of optical density changes and a small subroutine was therefore written into the programme to allow the concentration flux of the various species to be expressed in terms of optical density in the simulation runs.

Initially the simulation was performed allowing the programme to vary the four rate constants, $k_1 - k_4$ and the extinction coefficients of complexes A and B. However the best fits of the data under these conditions occurred at values for ε_{345} of complexes A and B significantly different from the estimates of these two constants obtained from separate experiments.

The simulation was therefore further constrained by fixing the values of these constants to the experimentally obtained values. The value of ε_{345} of A was 2.8×10^3 l $M^{-1}cm^{-1}$ (from extent of the fast spectral change) and the ε_{345} of B was 6.4×10^3 l $M^{-1}cm^{-1}$ (as the slow reaction appears to go to completion the ε_{345} was estimated directly from the spectrum obtained after reacting aminic AAT with a slight excess of difluorooxaloacetate). The best fit was then obtained varying constants $k_1 - k_4$. A copy of the output is shown in Fig.33 and the values of the four rate constants giving this fit, in Table 5.

Rate constant	value
k_1	2.613×10^6 litres $mole^{-1}sec^{-1}$
k_2	1.024×10^5 sec^{-1}
k_3	5.566×10^1 sec^{-1}
k_4	$1.047 \times 10^{-2}sec^{-1}$

Table 5

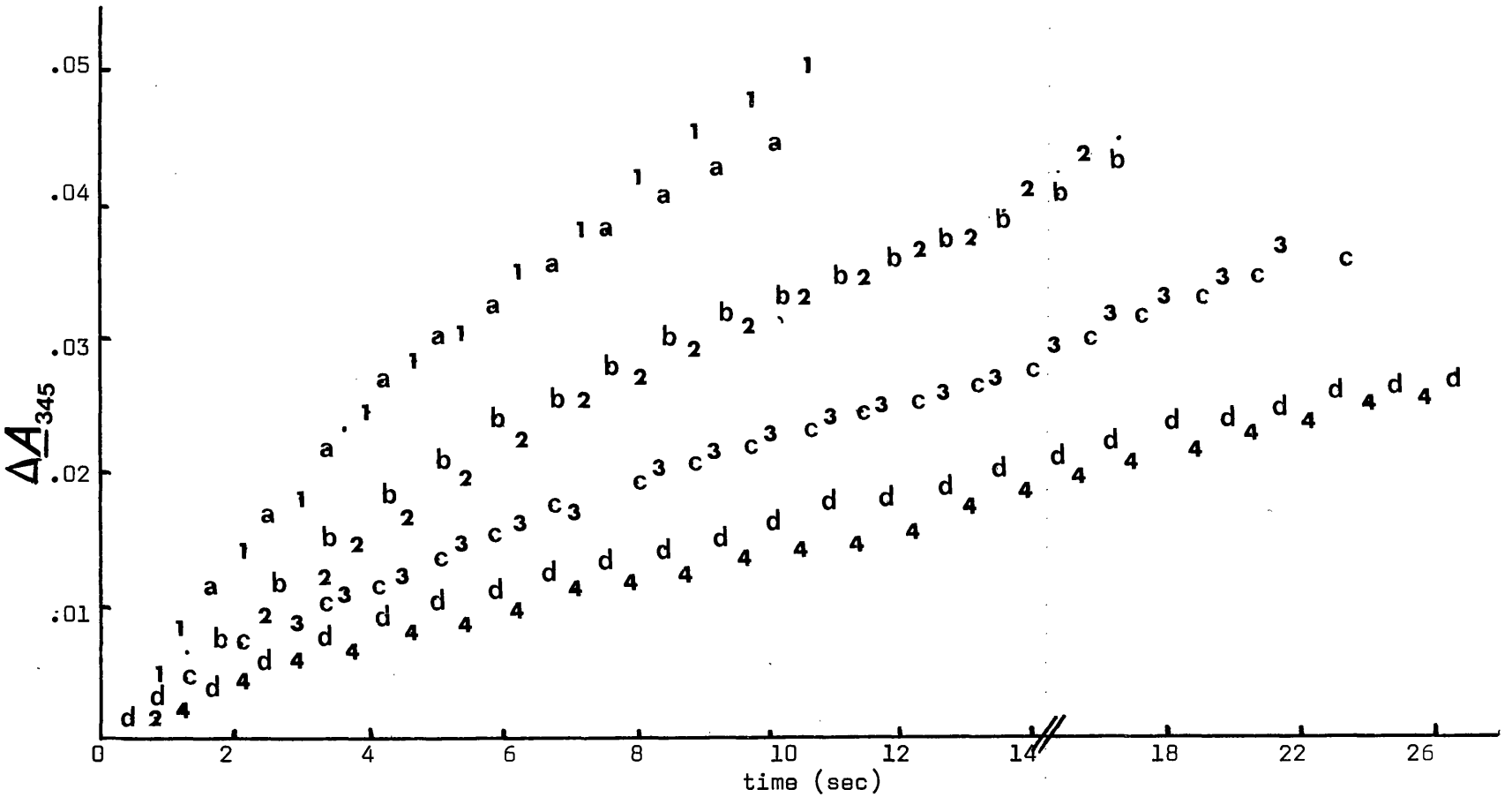

Fig. 33. Computor simulation of the progress curves of formation of the species with λ_{max} 328 nm. The progress curves are plotted as changes in absorbance (ΔA_{345}) from the absorbance of the free aminic enzyme. The experimental points are indicated by numbers, the simulated points by letters. 1,a, 80 μM; 2,b, 50 μM; 3,c, 30 μM; 4,d, 20 μM difluoro-oxaloacetate. Note the change in time scale after 14 secs.

A comparison of various kinetic parameters obtained in separate experiments, with those derivable from the rate constants produced in the simulation/fitting procedure, is given in Table 6.

Search for further spectroscopically distinct intermediates

Observations carried out 3-500 msec after mixing AAT and difluorooxaloacetate in the stopped-flow apparatus, showed that the 332-328 nm spectral change was the fastest event that could be seen at 345 nm. To investigate the possibility that faster optical density changes were taking place in other spectral regions, experiments were carried out using a rapid-scanning stopped-flow device (Methods). Equal volumes of 100 μM aminic AAT and 1 mM difluorooxaloacetate in 20 mM pyrophosphate buffer, pH 7.4, were rapidly mixed (3msec) and the resulting solution scanned from 300-490 nm. Thirty-one spectra were recorded for each experiment. The rate at which spectra were recorded was varied from 1 every 1.25 msec to 1 every 125.0 msec. The temperature was kept constant at 25°C. Throughout this time range the only spectral change observed was the shift in λ_{max} from 332 to 328 nm (Fig.34).

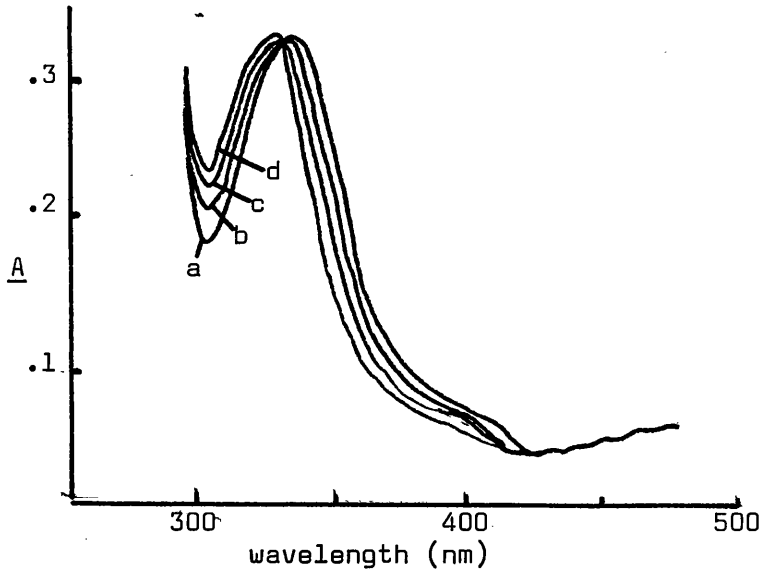

Fig. 34. Rapid spectrophotometric scans of the reaction mixture after addition of difluoro-oxaloacetate to the aminic form of aspartate transaminase. The absorption spectra were scanned at a rate of 200nm/sec after the various time intervals as indicated. a) 0.125s; b) 0.625s; c) 1.25s; d) 2.625s.

Parameter	Experiment	Experimental value	Relationship of rate constants	CHEKMAT value
Kinetic K_i	Steady-state inhibition kinetics	8.24 μ M	$\frac{k_2 k_4}{k_1(k_3 + k_4)}$	7.37 μ M
Overall dissociation constant $K = \frac{[E'][I]}{[A]}$	Magnitude of 332-328 nM spectral change	8.75 μ M	$\frac{k_2 k_4}{k_1 k_3}$	7.37 μ M
Michaelis constant for 332-328 nm spectral change	Initial rates from stopped-flow experiment	$\gg$ 30 mM	$\frac{k_2 + k_3}{k_1}$	39.2 mM
k_3	Initial rates from stopped-flow experiment	$\gg$ 50 sec^{-1}	k_3	55.7 sec^{-1}
Michaelis constant for 328-360 nm spectral change	Initial rates of slow spectral change	7.0 μ M	$\frac{k_2(k_4 + k_5)}{k_1(k_3 + k_4 + k_5)}$	7.43 μ M
Apparent 2nd order rate constant for 332-328 nm spectral change	Initial rates from stopped-flow experiment	1.74×10^3 $M^{-1} \cdot s^{-1}$	$\frac{k_1 k_3}{k_2}$	1.42×10^3 $M^{-1} \cdot s^{-1}$

Table 6

In the previous section, the interaction of difluorooxaloacetate with the aminic form of AAT was studied. It is however well known that many dicarboxylic acids can form abortive complexes with aldimine AAT. The following section is concerned with interactions of ligands with the aldimine form of AAT.

Difluorooxaloacetate-aldimine enzyme complex

Spectrophotometric determination of dissociation constant

Incremental addition of difluorooxaloacetate to a solution of aldimine AAT results in a decrease in absorbance at 360 nm with a concomittant increase in absorbance at 435 nm.

Assuming the ligand (I) interacts with the enzyme (E) to give a complex (EI), then the optical density $\underline{A}$ of the system $E + I \rightleftharpoons EI$ at any wavelength is given by equation (1)

$$\underline{A} = \varepsilon_E [E] + \varepsilon_{EI} [EI] \qquad (1)$$

Where ε_E and ε_{EI} are the extinction coefficients of E and EI respectively. The optical density change $\Delta \underline{A}$, brought about by increasing the total concentration of $[I]$ from $[I_1]$ to $[I_2]$ is related to the dissociation constant K_s of the EI complex by the relationship (Jenkins and Taylor, 1965):-

$$\frac{[I_2]-[I_1]}{\Delta \underline{A}} = \frac{(K_s + [I_1])(K_s + [I_2])}{K_s(\varepsilon_E - \varepsilon_{EI})[I_t]} \qquad (2)$$

where $E_t = [E]+[EI]$, $K_s = \frac{[E][I]}{[EI]}$ and it is assumed that $[I_t] \gg E_t$.

When $[I_1] = 0$, then equation (2) simplifies to:

$$\frac{[I_t]}{\Delta \underline{A}} = \frac{K_s + [I_t]}{K_s(\varepsilon_E - \varepsilon_{EI})\, E_t} \qquad (3)$$

where $\Delta \underline{A}$ is the absorbance change brought about by the presence of ligand (I). A plot of $\frac{[I_t]}{\Delta \underline{A}}$ versus $[I_t]$ then gives a straight line

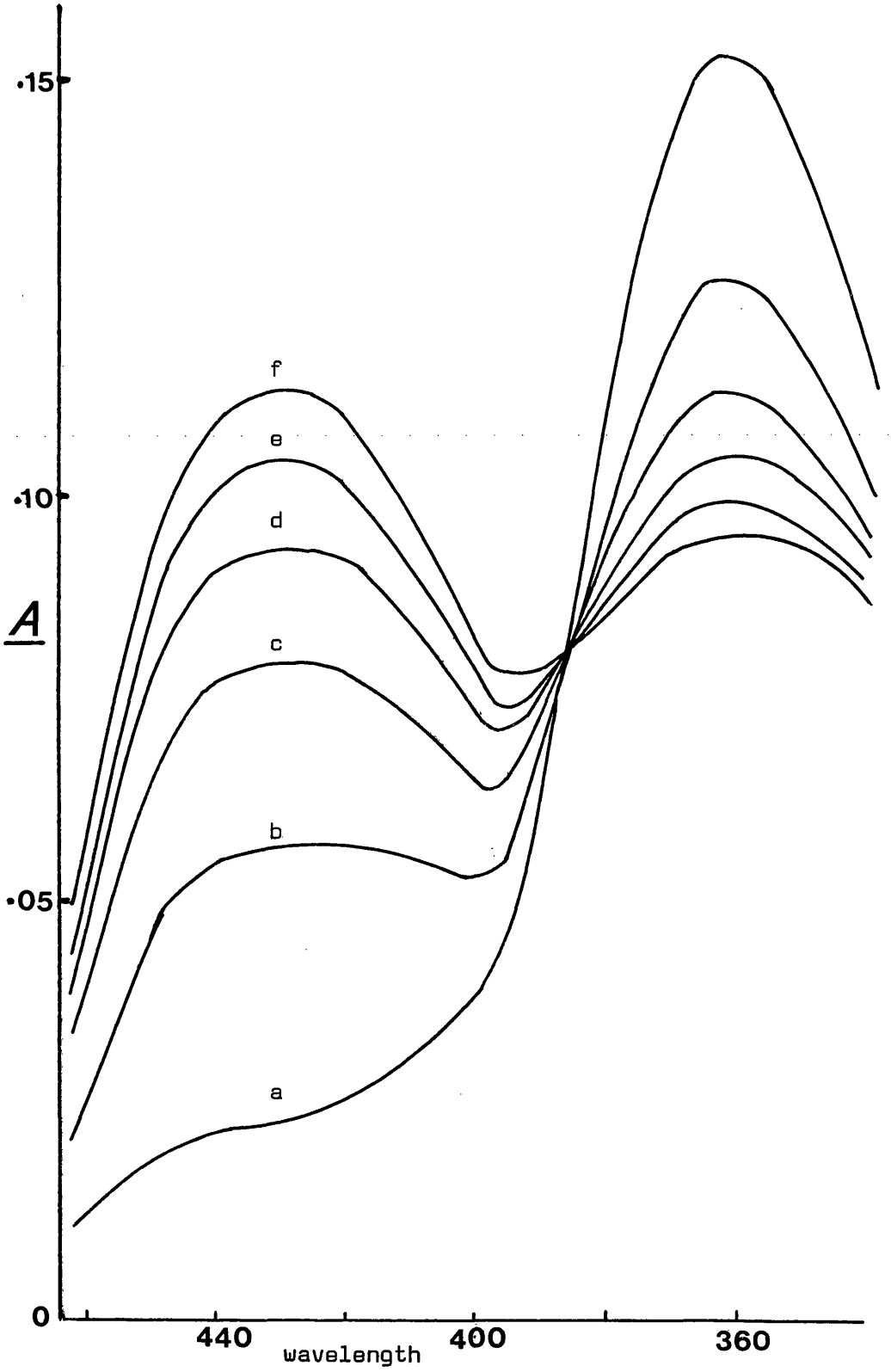

Fig. 35. Spectrophotometric titration of difluoro-oxaloacetate with the aldimine form of aspartate transaminase. The absorption spectra were obtained from successive scans (0.5 nm/s) after addition of aliquots of difluoro-oxaloacetate to give the indicated concentrations. (a) 0; (b) 0.83 mM; (c) 1.65 mM; (d) 2.46 mM; (e) 3.28 mM; (f) 4.08 mM.

from which K_s may be obtained as the negative intercept on the $[I_t]$ axis.

Difluorooxaloacetate was added incrementally to a solution of aldimine AAT (26 μM in sites) in 20 mM pyrophosphate buffer, pH 7.4, at 25°C giving concentrations from 1 to 4 mM, and the spectral changes were monitored by scanning the UV spectrum of the reaction mixture from 300 to 460 nm after each addition of difluorooxaloacetate. The spectral changes are shown in Fig.35. A plot of $\frac{[I]}{\Delta A_{435}}$ versus $[I]$ gave a straight line (Fig.36) from which the dissociation constant K_s was determined (= 2.76 $\pm$ 0.8 mM), together with the value (7.6×10^3 l $M^{-1} cm^{-1}$) of ε_{EI} at 435 nm.

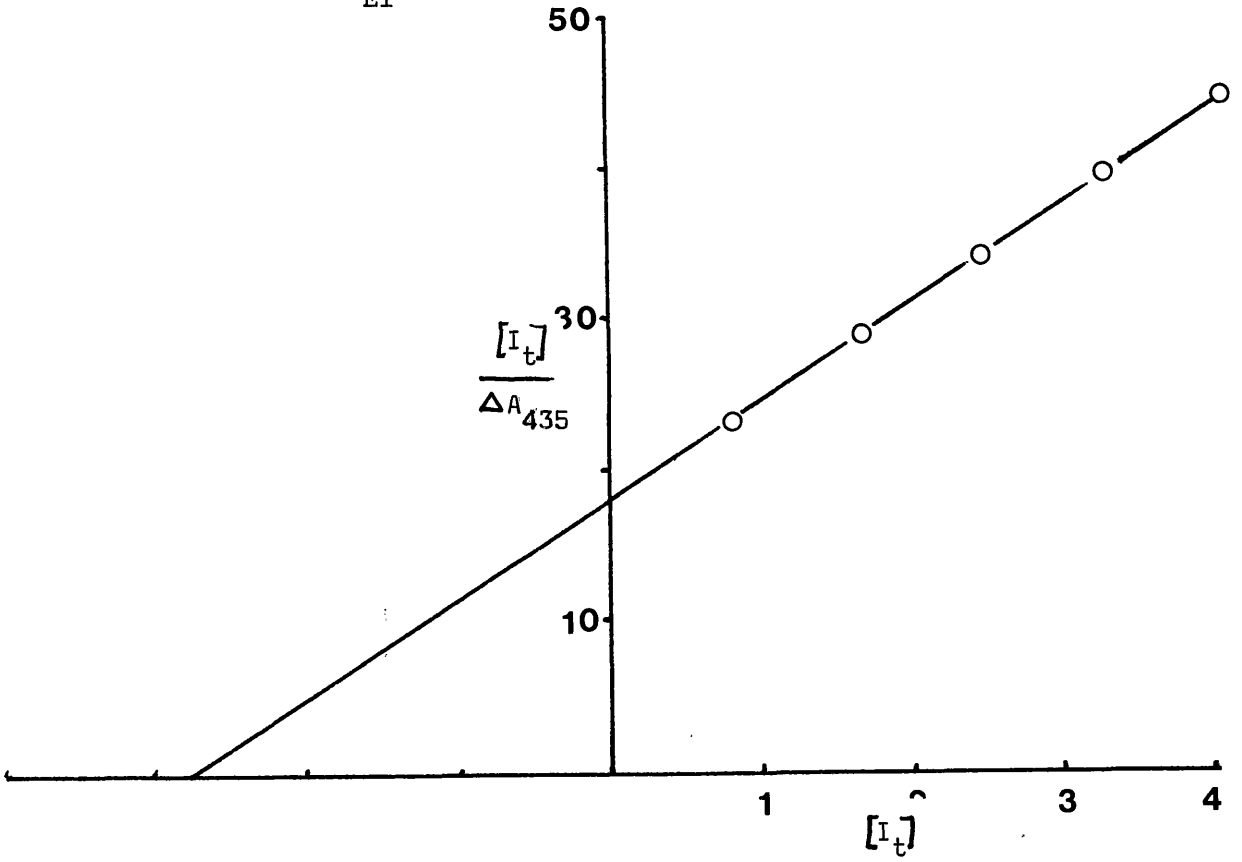

Fig. 36. Plot of $[I_t]/\Delta A_{435}$ against $[I_t]$ for addition of difluoro-oxaloacetate to aldimine enzyme. The absorbance changes at 435 nm relative to free aldimine enzyme were taken from the data shown in Fig.35.

^{19}F nmr determination of dissociation constant and chemical shift (Δ)

The ^{19}F nmr signal of difluorooxaloacetate was found to broaden and move upfield on addition of the aldimine form of AAT. The effect on a single nmr peak of a ligand (I) of adding enzyme (E) which forms a rapidly equilibrating enzyme-ligand complex (EI)

$$E + I \rightleftharpoons EI$$

is to shift the signal by an amount δ_{obs} relative to that of the free ligand in buffer, where

$$\delta_{obs} = \frac{[EI]}{I_t}\Delta + \delta_I \qquad (4)$$

I_t is total ligand, Δ is the corresponding chemical shift of toally bound ligand and δ_I is that of the free ligand in the presence of enzyme.

When the concentrations of I_t and total enzyme (E_t) are comparable, the dissociation constant (K_s) if the EI complex is given by:-

$$K_s = \frac{(E_t - [EI])([I_t] - [EI])}{EI} \qquad (5)$$

and EI is related to K_s by the quadratic solution

$$[EI] = \frac{(E_t + [I_t] + K_s) \pm \sqrt{(E_t + [I_t] + K_s)^2 - 4\,E_t\,I_t}}{2} \qquad (6)$$

subject to the restriction $o < \frac{EI}{E_t}$

Observation of δ_{obs} at a series of $[I_t]$ values at constant E_t allows determination of K_s and Δ by the iterative procedure of Groves et al. (1967). According to this procedure, an arbitrary value is assigned to K_s; equation (6) can then be solved in terms of $[EI]$ knowing E_t and $[I_t]$. These values of $[EI]$ are then used to plot δ_{obs} versus $[EI]/I_t$ which, according to equation (4) should be a straight line. The least mean squares straight line is fitted to the experimental points and the standard deviation of the points from the line obtained. The process is repeated

using different assumed values for K_s until a value is obtained which minimises the deviation of the points from the fitted line. The slope of this fitted line gives Δ (equation 4).

Difluorooxaloacetate was added incrementally to a solution of aldimine AAT (0.46 mM in sites) in 20 mM pyrophosphate buffer at 28 $\pm$ 1°C pH 7.4, in an nmr tube, to give final concentrations in the range 5-16 mM, and the chemical shift of the ^{19}F nmr recorded after each addition of difluorooxaloacetate.

The iterative procedure described above was applied to the data obtained; the results of the iterations are shown in Fig.37. The maximum deviation of the points from the straight line was obtained at K_s = 2.9 mM, this gives Δ 137.2 $\pm$ 1.9 H_z.

pH dependance of nmr parameters

Difluorooxaloacetate acid, neutralised to pH 4.9 with KOH, was added to a solution of extensively-dialysed aldimine AAT (0.75 mM in sites) in double-distilled water, to give a final concentration of 6 mM acid. The ^{19}F nmr chemical shift and line width (relative to free difluorooxaloacetate at pH 7.4) were measured as the pH of the medium was increased by the addition of 10 mM KOH. Plots of both parameters versus pH (Fig.38) show inflexion points in the pH 5.4 and 8.2 regions.

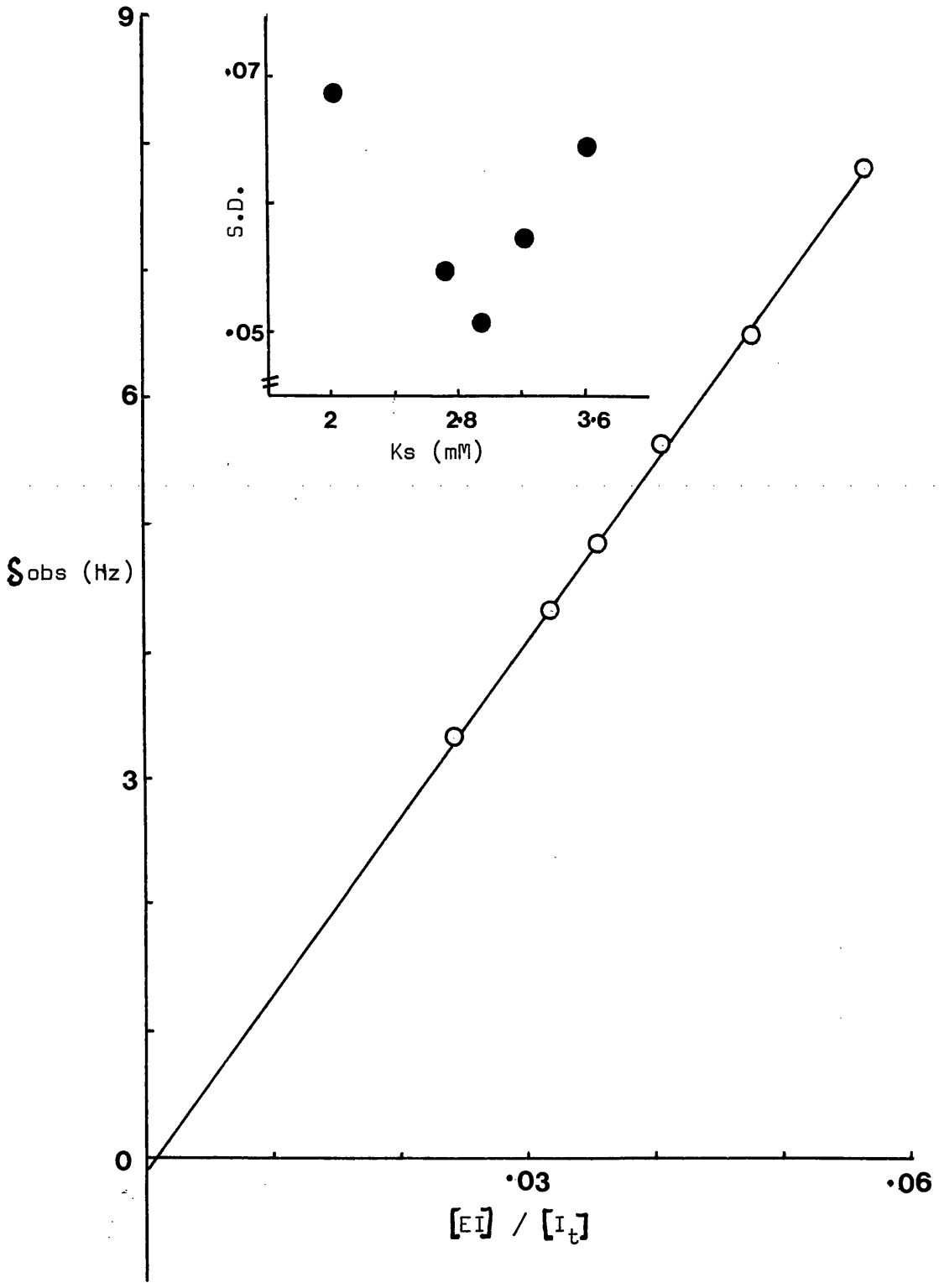

Figure 37. Plot of δ_{obs} against $[EI] / [I_t]$ for the difluoro-oxaloacetate aldimine enzyme. The plot represents the best fit of the experimental points to a straight line according to equation (4), and was obtained at K_s = 2.9 mM. The inset shows the variation in the standard deviation of the points about the line as the value of K_s was varied. Experimental details are given in the text.

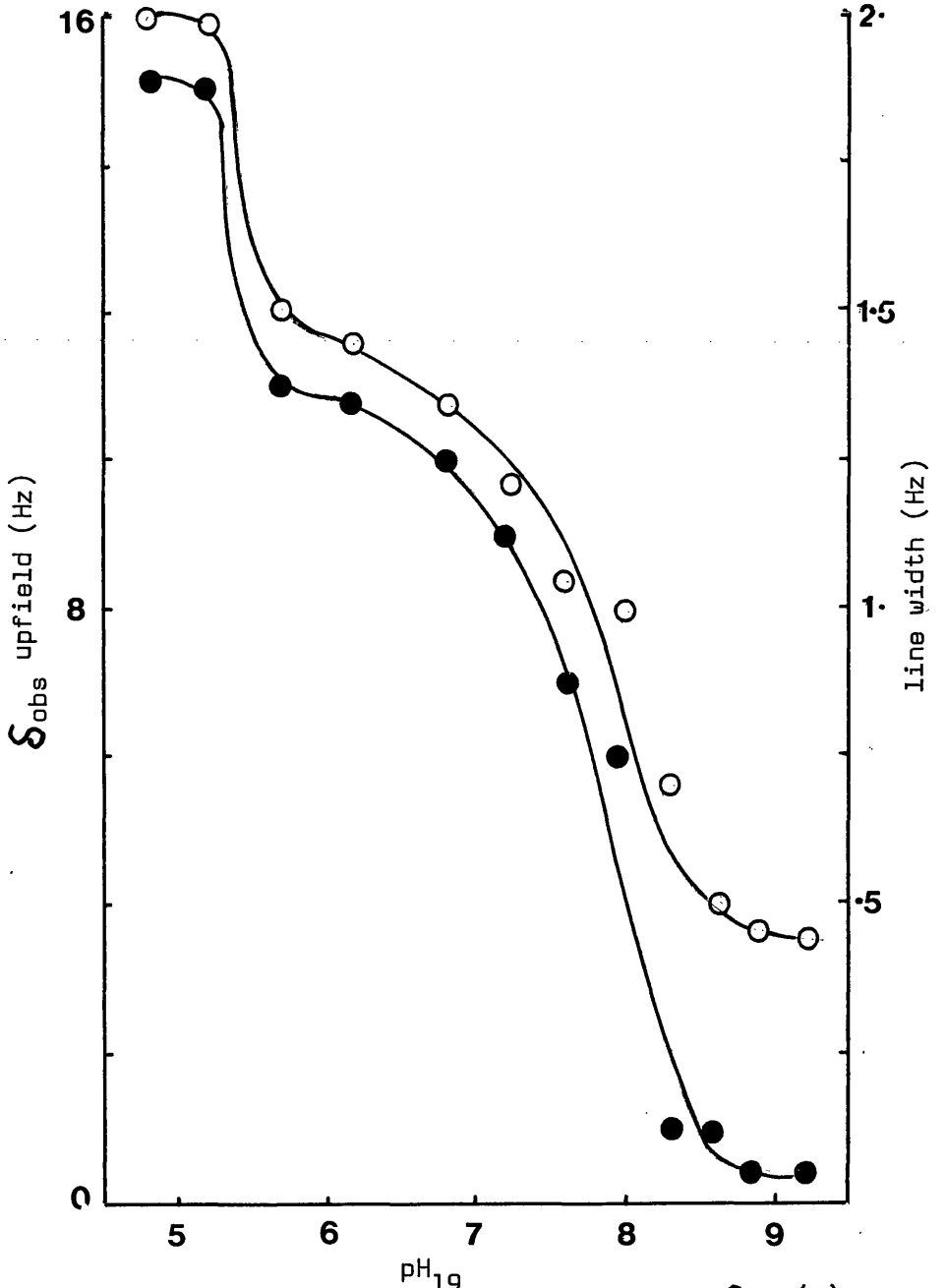

Fig. 38. pH variation of the ^{19}F chemical shift δ_{obs} (●) and line width (○) of difluoro-oxaloacetate in the presence of aldimine enzyme. Experimental details are given in the text.

Interaction of aminic AAT with elevated concentrations of difluorooxaloacetate

Difluorooxaloacetate was added to a solution of aminic AAT (0.5 mM in sites) in 20 mM pyrophosphate buffer, pH 7.4, to give a final concentration of 5 mM. The ^{19}F nmr signal of difluorooxaloacetate was observed to broaden and shift upfield over a 30 min. period before attaining an equilibrium value (Fig.39).

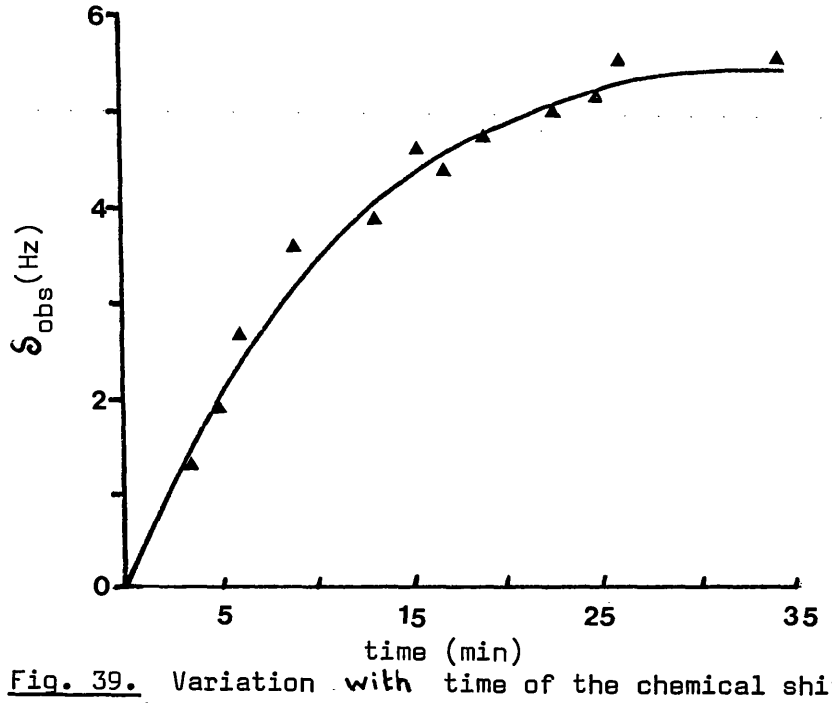

Fig. 39. Variation with time of the chemical shift (δ) of the ^{19}F n.m.r. signal of difluoro-oxaloacetate on addition of difluoro-oxaloacetate to the aminic form of aspartate transaminase. ▲ represents the upfield chemical shift of the ^{19}F n.m.r. signal relative to that in buffer alone. — represents the time course of the chemical shift variation calculated using the first order rate constant ($1.54 \times 10^{-3} s^{-1}$) obtained from a Kezdy-Swinbourne plot (1960) of the data.

The process followed first-order kinetics having first-order rate constant $k = 1.54 \times 10^{-3} sec^{-1}$ at $28^{\circ}C$ (Swinbourne, 1960)

Addition of 5 mM cysteine sulphinate to the equilibrium mixture rapidly cause the ^{19}F nmr peak to sharpen and return to the chemical shift of the free difluorooxaloacetate in buffer (Fig.40).

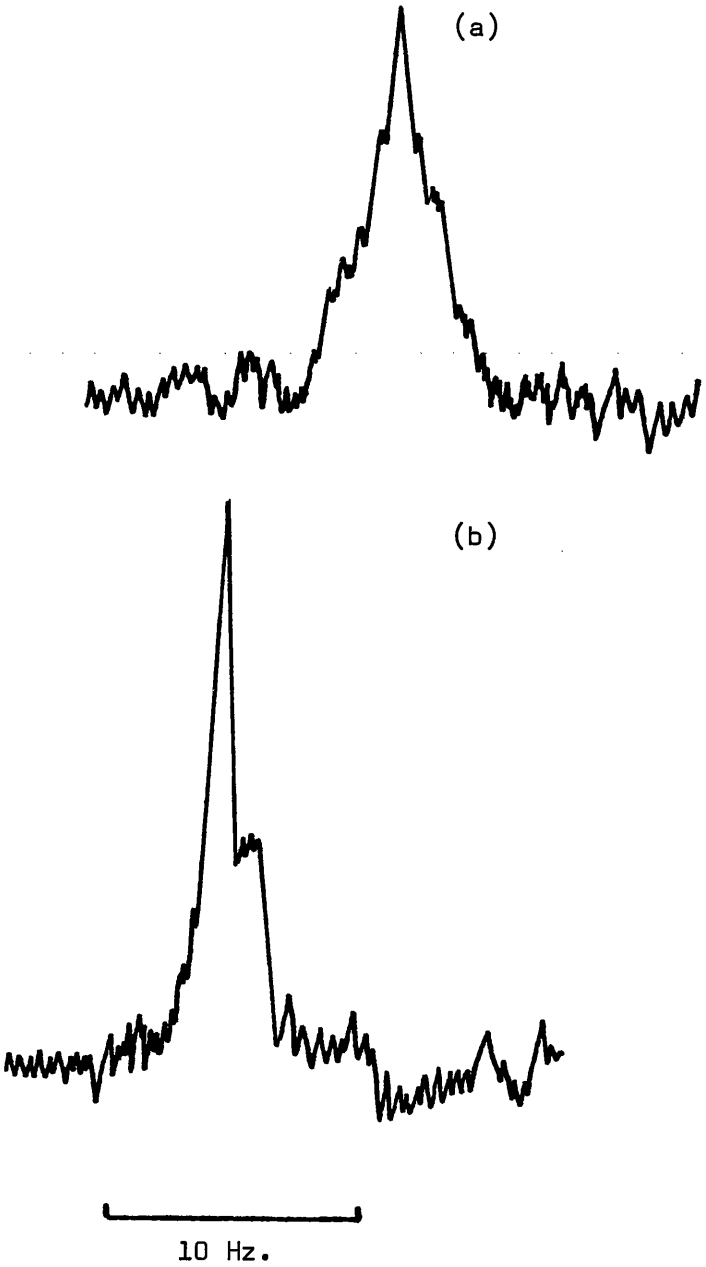

Fig. 40. ^{19}F n.m.r. spectra of a) 5mM difluoro-oxaloacetate in the presence of 0.5 mM (sites) aminic form of aspartate transaminase, 45 min. after the addition of the fluoro-acid. b) as for (a) but with the addition of 0.5 mM (final conc.) cysteine sulphinate. The spectra are the average of 8 scans, recorded with reference to a lock signal of 2 M difluoro-oxaloacetate, pH 3.7, contained in a co-axial capillary.

The experiment was repeated in a spectrophotometer. Spectral changes were recorded following the addition of difluorooxaloacetate (final concentration 5mM) to 0.4 ml aminic AAT (0.75 mM in sites) in 20 mM pyrophosphate buffer, pH 7.4 contained in a 0.2 cm pathlength quartz cuvette. The resultant spectra are shown in Fig.41. The addition of this concentration of difluorooxaloacetate to aminic AAT resulted in a decrease in the absorbance in the 300 nm region with concomittant increase, over a 30 min period, of two absorbance peaks centred in the 360 and 435 nm regions. Both increases in absorbance followed first-order kinetics with first-order rate constants $k = 1.78 \times 10^{-3} sec^{-1}$ $k = 1.81 \times 10^{-3} sec^{-1}$ respectively at $28^{o}C$, (Swinbourne, 1960).

Previous experiments have shown that aminic AAT slowly transaminates difluorooxaloacetate to give an aldimine species absorbing at 362 nm. The simultaneous appearance of a species absorbing at 430 nm suggests that at elevated concentrations difluorooxaloacetate appreciably reacts with aldimine enzyme formed in the transamination reaction, giving rise to an equilibrium mixture of aldimine enzyme and its abortive complex with difluorooxaloacetate. Comparison of the first-order rate constants for the increase in A_{435} with that for the slow ^{19}F nmr shift, suggests that in both cases the process being observed is the build up of the difluorooxaloacetate-aldimine enzyme complex.

Addition of 5 mM cystein sulphinate to the reaction mixture after attainment of equilibrium, resulted in an immediate disappearance of the spectral peaks at 360 and 435 nm and the appearance of a peak with λ_{max} 328 nm, characteristic of the difluorooxaloacetate-aminic enzyme complex. As the ^{19}F nmr signal of the difluorooxaloacetate under these conditions is identical with that of the free compound in buffer, it is

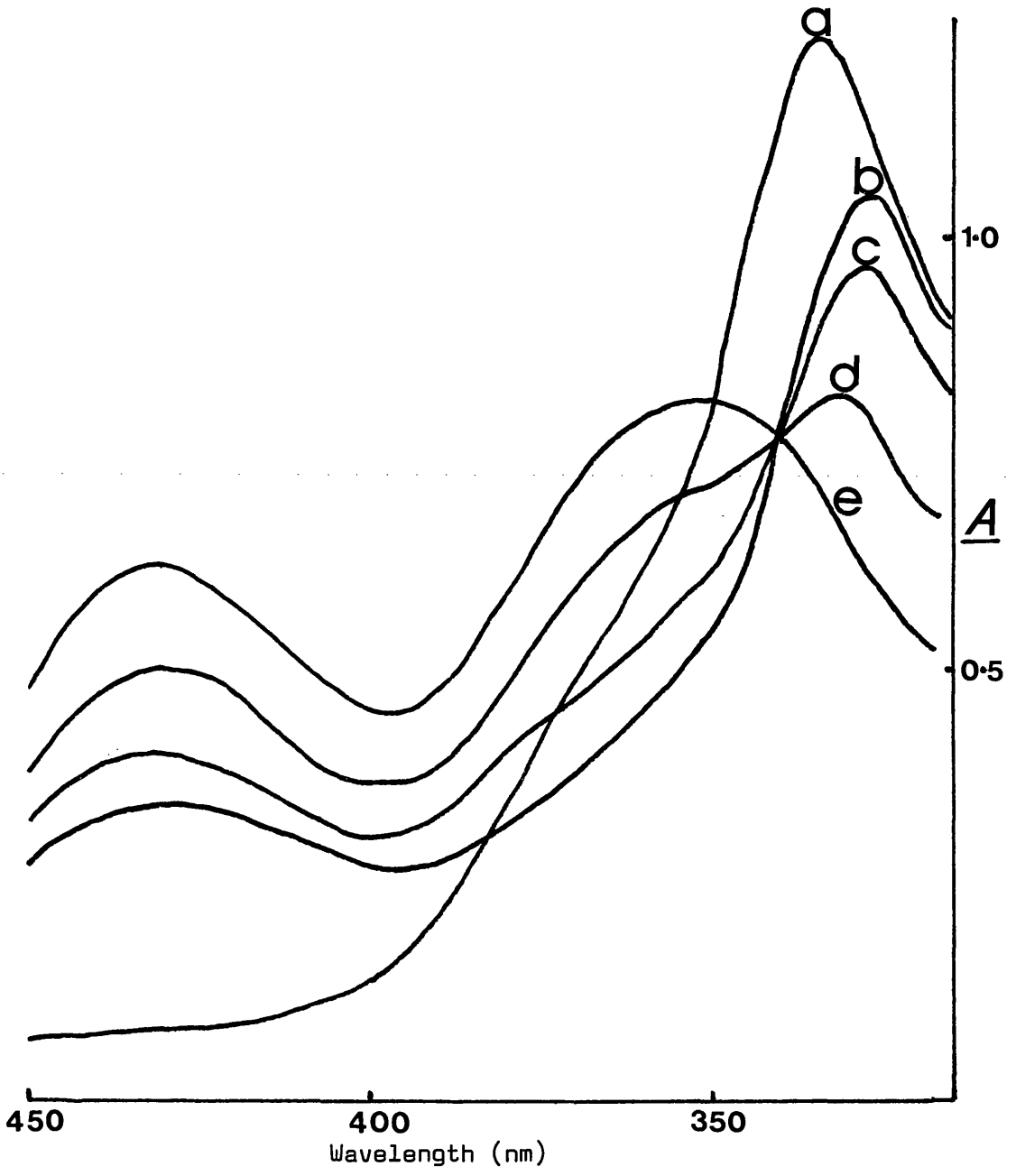

Fig. 41. Spectral changes following the addition of difluoro-oxaloacetate to the aminic form of aspartate transaminase. Spectra were recorded (scan speed 1 nm/sec) before (a), and at the specified time intervals after addition of difluoro-oxaloacetate; (b),0.5 min; (c), 4.5 min; (d), 12.5 min; (e), 29.5 min. Other conditions are stated in the text.

apparent that complex formation with aminic enzyme is not reflected in the chemical shift of difluorooxaloacetate in the nmr experiment.

If it is assumed that the equilibrium situation following the time dependent ^{19}F nmr and spectrophotometric changes represents essentially complete conversion of aminic enzyme to free and complexed aldimine enzyme (see "burst" experiments) then the equilibrium mixture will contain a total concentration of difluoroaspartate (A_t) equal to the total concentration of the enzyme (E_t). The difluoroaspartate produced will act as a competitive inhibitor of difluoroxaloacetate with respect to the formation of the difluorooxaloacetate-aldimine enzyme complex.

A modification of the method used to calculate the dissociation constant (K_s) of the difluorooxaloacetate-aldimine complex (EI) can be made to obtain an estimate of the dissociation constant (K_A) for the difluoroaspartate-aldimine enzyme complex (EA).

If difluorooxaloacetate (I) is incrementally added to aldimine enzyme (E) in the presence of a constant total concentration of difluoroaspartate (A_t), the K_s is now given by the expression

$$K_s = \frac{(E_t - [EI] - [EA])([I_t] - [EI])}{EI} \qquad (7)$$

when $[I_t] \gg E_t$ equation (21) simplifies to

$$K_s = \frac{(E_t - [EI] - [EA]) \cdot [I_t]}{EI} \qquad (8)$$

$$\therefore [EI] = \frac{[I_t](E_t - [EA])}{K_s + [I_t]} \qquad (9)$$

K_A is given by

$$K_A = \frac{(E_t - [EI] - [EA])(A_t - [EA])}{[EA]} \qquad (10$$

Substitution of the expression for [EI] from equation (9) into equation (24), leads to the following quadratic in EA .

$$[EA]^2 - [EA]\left(E_t + A_t + K_A\left(1 + \frac{[I_t]}{K_s}\right)\right) + E_t A_t = o \qquad (11)$$

E_t and A_t are known and K_s has been previously determined, therefore assigning an arbitrary value to K_A, [EA] may be determined for a series of $[I_t]$ values. Substitution of [EA] into equation (9) gives [EI] for each $[I_t]$ value and, as before, δ_{obs} may be plotted versus $\frac{[EI]}{I_t}$ and K_A chosen to minimise the standard deviation of the points from the least mean squares straight line. The slope of the final line again gives Δ for totally bound(I).

5 mM difluorooxaloacetate was allowed to react with 0.5 mM aminic AAT in 20 mM-pyrophosphate buffer, pH 7.4 until the chemical shift of the ^{19}F nmr signal of difluorooxaloacetate reached a constant value (approximately 30 min). Aliquots of difluoroxaloacetate were then added to give concentrations in the range 10-16 mM. The chemical shift of the ^{19}F nmr signal relative to free difluorooxaloacetate in buffer, was measured after each addition.

The iterative procedure described above was applied to the data. The result is shown in Fig.42. Minimum deviation of the points from a straight line was obtained at K_A = 0.7 mM, which leads to a value of $\Delta = 127 \pm 3.5$ H_z for the difluorooxaloacetate-aldimine enzyme complex, consistent with that obtained directly (137.2 ± 1.9 H_z.

Difluorooxaloacetate-apoenzyme complex

Dissociation constant and chemical shift

Spectrophotometric determination of the dissociation constant of ligand-apo-AAT complexes is not possible as the chromophore reporter

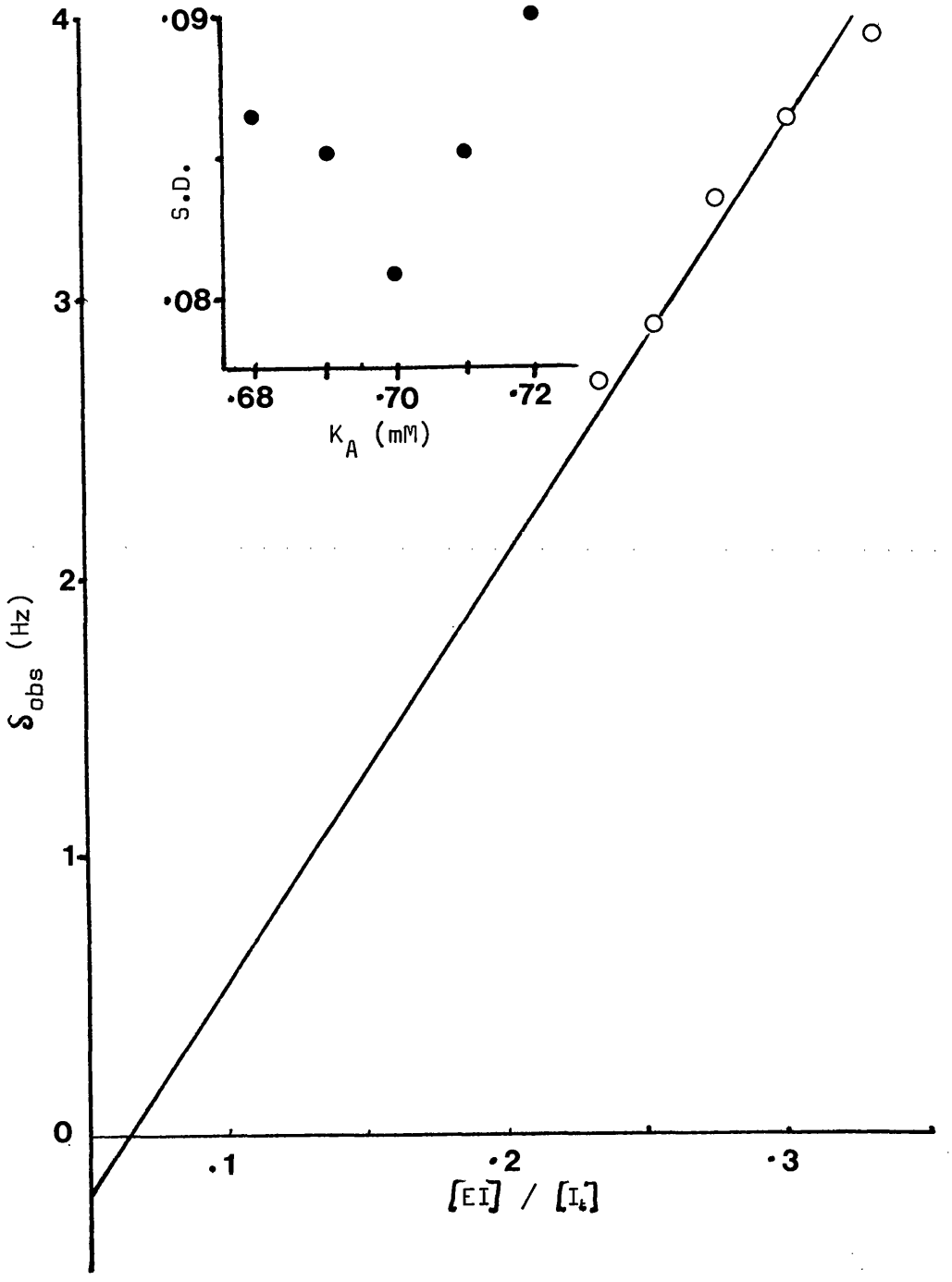

Fig. 42. Plot of δ_{obs} against [EĪ] / [I_t] for difluoro-oxaloacetate (I) in the presence of difluoroaspartate (A) and the aldimine form of aspartate transaminase (E). The plot represents the best fit of the points to a straight line and was obtained at K_A = 0.7 mM. The inset shows the standard deviation of the points from the line as K_A was varied.

group is no longer present. It is however possible to obtain the dissociation constant by means of nmr measurements. Apoenzyme was prepared as described in the Methods section and the restorable activity measured. Addition of 5 mM difluorooxaloacetate to 0.39 mM apoenzyme (restorable activity), in 20 mM pyrophosphate buffer at pH 7.4 gave a ^{19}F nmr signal which was shifted upfield and broadened relative to that of difluorooxaloacetate alone. Incremental addition of further difluorooxaloacetate caused the signal to shift downfield and sharpen as in the case of the aldimine enzyme. The chemical shift values were measured after each addition of difluorooxaloacetate, and the data obtained treated in the same manner as for the aldimine enzyme giving values for the dissociation constant, K_s and the chemical shift of the apoenzyme-difluorooxaloacetate complex. The results of the iterations are shown in Fig.(43). Minimum deviation of the points from a straight line occurred at K_s= 3.4 mM, leading to a value of Δ = 99.2 $\pm$ 6.3 H_z.

pH dependence of nmr parameters

The pH variation of the ^{19}F chemical shift and line width of difluorooxaloacetate was determined as in the case of the aldimine enzyme. Apoenzyme was prepared as before and extensively dialysed against double-distilled water. It was then concentrated by vacuum dialysis and the restorable activity estimated. Difluorooxaloacetic acid was neutralised to pH 4.9 and added to the apoenzyme solution (0.41 mM) to give a final concentration of 6 mM difluorooxaloacetate. The ^{19}F nmr chemical shift and line width (relative to free difluorooxaloacetate at pH 7.4) were measured as the pH of the medium was increased by addition of 10 mM KOH. Aliquots of the solution were removed at various pH, suitable diluted and tested for restorable activity. No decrease in restorable activity was observable during the course of the

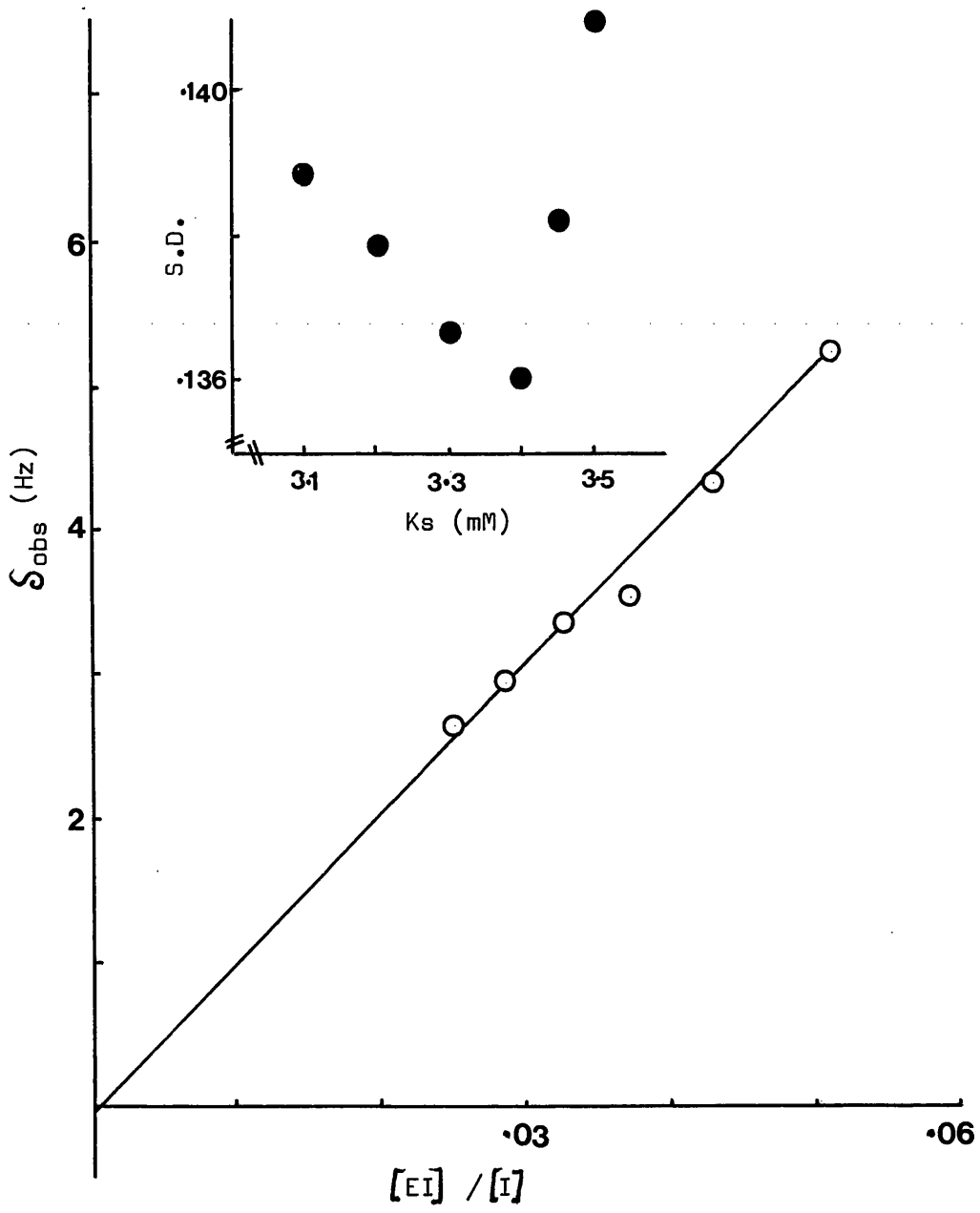

Fig. 43. plot of δ_{obs} against [EI] / [I] for difluoro-oxaloacetate in the presence of the apoenzyme form of aspartate transaminase. The plot represents the best fit of the points to a straight line and was obtained at K_s = 3.4 mM. The inset shows the standard deviation of the points from the line as K_s was varied.

experiment. Plots of both parameters (Fig.44) showed an inflection point in the pH 8.5 region but not at lower pH.

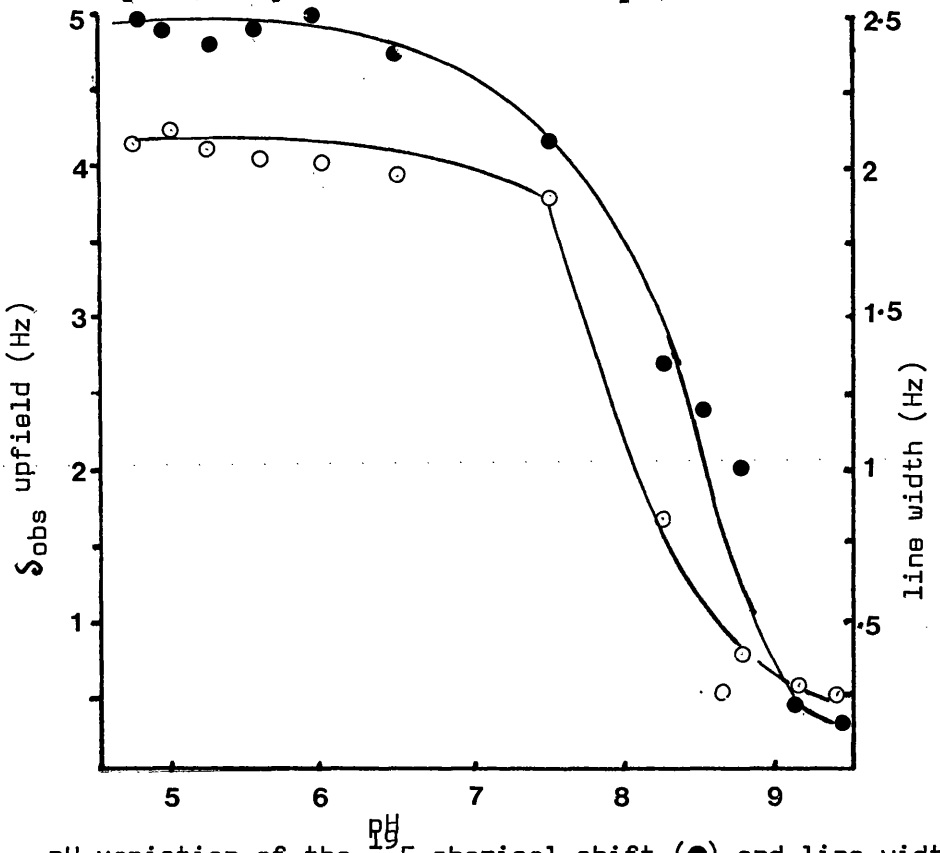

Fig. 44. pH variation of the ^{19}F chemical shift (●) and line width (○) of difluoro-oxaloacetate in the presence of the apoenzyme. The experimental details are given in the text.

Perfluorosuccinate-aldimine enzyme complex

Dissociation constant and chemical shift

The dicarboxylic acid, perfluorosuccinate, like difluorooxaloacetate, binds to the aldimine form of AAT, forming an abortive complex. The ^{19}F nmr spectrum of perfluorosuccinate consists of a single strong peak, thus, as in the case of difluoroxaloacetate, determination of the binding parameters to aldimine AAT is relatively simple using nmr. It was of interest to study the binding of perfluorosuccinate to aldimine AAT under the same experimental conditions as those used for difluorooxaloacetate, as it had previously been reported (Martinez-Carrion et al., 1973) that interaction of perfluorosuccinate with the

enzyme results in a downfield shift of the ^{19}F nmr signal, in contrast to the upfield shift observed with difluorooxaloacetate.

Addition of 10 mM perfluorosuccinate to a solution of aldimine AAT (0.66 mM) in 20 mM pyrophosphate buffer, pH 7.4, gave a single ^{19}F nmr signal which was shifted downfield and broadened relative to that of free perfluorosuccinate alone. Incremental addition of further perfluorosuccinate caused the signal to move upfield and sharpen. The chemical shift of the ^{19}F nmr signal relative to that of free perfluorosuccinate at pH 7.4, was measured after each addition of ligand, and the data treated by the iterative procedure previously described (page 95). The results of the iterations are shown in Fig.45. Minimum deviation of the points from a straight line occurred at K_s= 3 mM which leads to a value of Δ = 92.7 $\pm$ 0.3 Hz for the perfluorosuccinate-aldimine enzyme complex. A comparison of the dissociation constants and chemical shifts of the ligand-enzyme complexes is given in Table 7.

	Enzyme Form			
	Aldimine		Apoenzyme	
ligand	K_s (mM)	Δ (Hz)	K_s (mM)	Δ (Hz)
difluorooxaloacetate	2.9	+137.2$\pm$1.9	3.4	+99.2$\pm$6.3
perfluorosuccinate	3.0	-92.7$\pm$.3	-	-

Table 7 Comparison of dissociation constant and chemical shift of the enzyme ligand complexes, + indicates an upfield shift from the free ligand, - indicates a downfield shift from the free ligand.

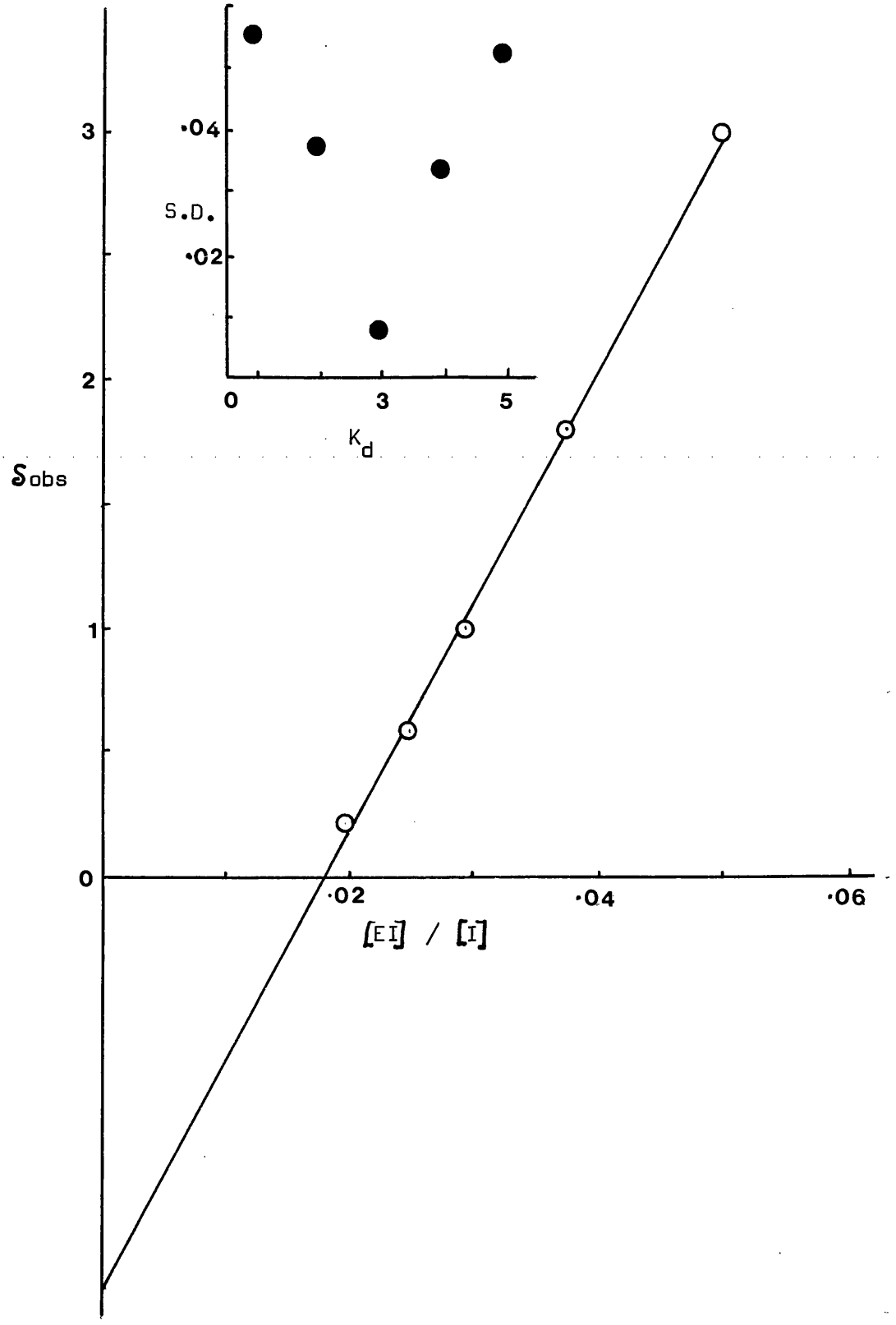

Fig. 45. Plot of the S_{obs} against [EI] /[I] for perfluoro-succinate (I) in the presence of the aldimine form of the enzyme. The plot represents the best fit of the experimental points to a straight line and was obtained at K_s = 3.0 mM. The inset shows the standard deviation of the points from the line as K_s was varied.

Chemical shifts of ^{19}F nmr signals of difluorooxaloacetate and perfluorosuccinate in the absence of enzyme

The difference in the chemical shifts of the free and bound ligand is caused by changes in its microenvironment. If the environment of the free ligand is externally manipulated then observation of the magnitude and direction of any induced chemical shift may provide information as to the nature of the microenvironment of the ligand in the enzyme-bound state.

pH Dependence

A 20 mM solution of free difluorooxaloacetic acid in double-distilled water was titrated in the nmr tube with 200 mM KOH and the chemical shift changes relative to the initial value were observed. The experiment was repeated using 20 mM perfluorosuccinic acid. The chemical shift-pH profiles are shown in Fig.46.

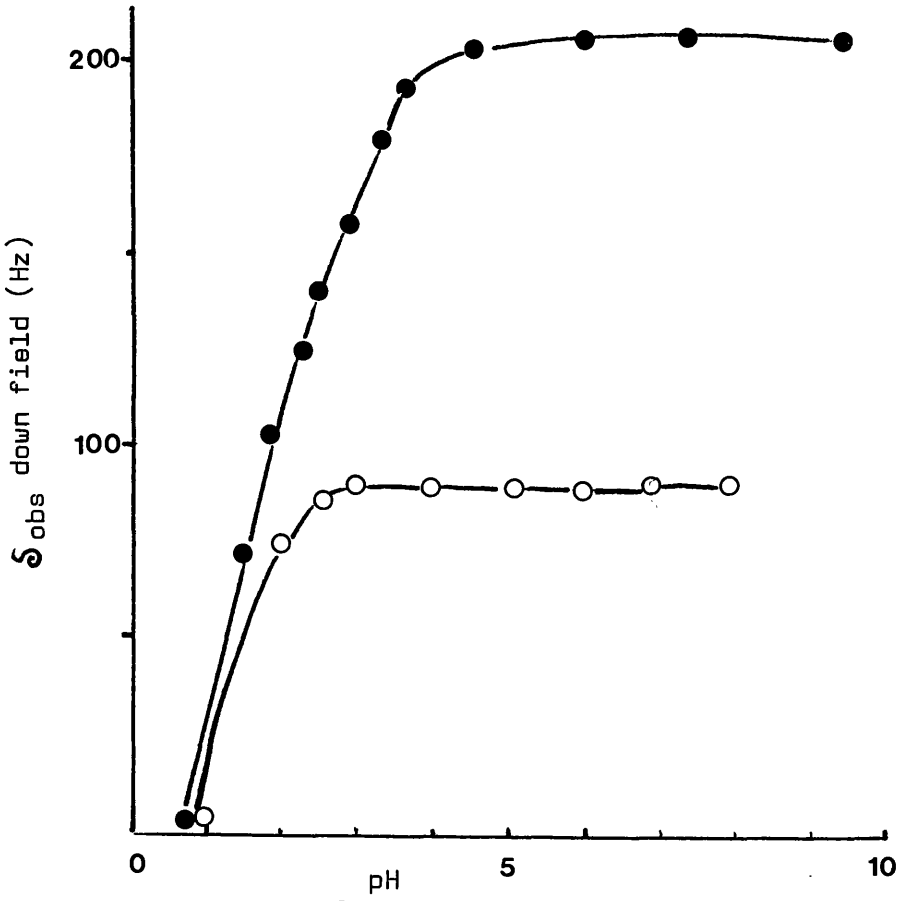

Fig. 46. pH variation of the ^{19}F chemical shift of difluoro-oxaloacetate (●) and perfluorosuccinate (○). Experimental details are given in the text.

The ^{19}F nmr signal of difluorooxaloacetate shows a progressive downfield shift with increasing pH up to pH 5. No further shift was observed between pH 5 and 9. Comparison of the chemical shift pH profile (Fig.46) with the acid base titration curve (Fig.47) for difluorooxaloacetate indicates that the increase in chemical shift corresponds to the ionisation of the second carboxyl group of difluorooxaloacetate, which is complete at pH 5.

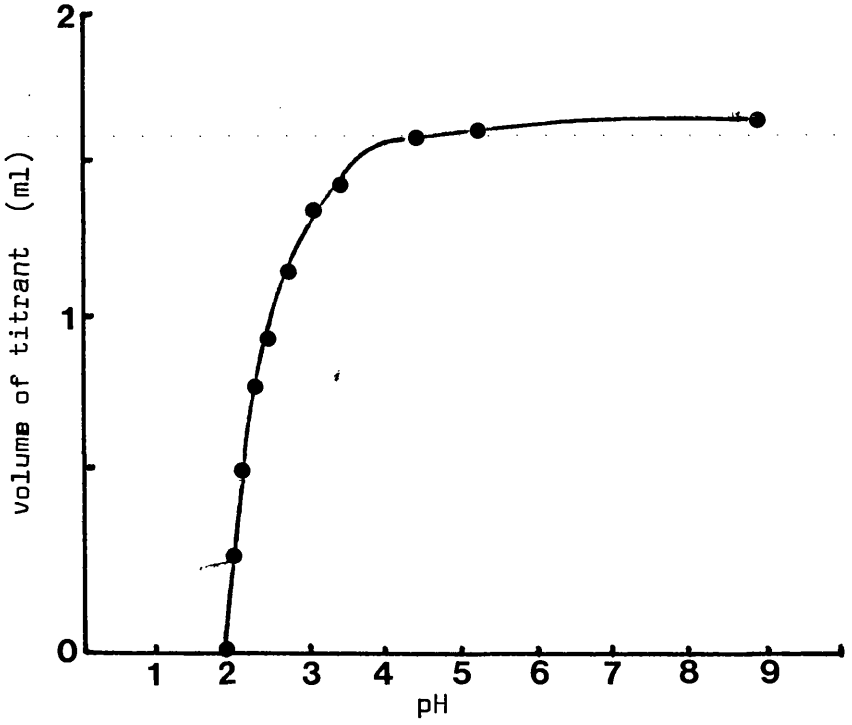

Fig. 47. Variation of pH on titration of difluoro-oxaloacetate with base. The pH of the mixture was followed as 0.2 M difluoro-oxaloacetate (0.5 ml) was titrated with 0.107 M tetramethylammonium hydroxide. (Courtesy of R. Eisenthal, unpublished results).

Similarly the ^{19}F nmr signals of perfluorosuccinate shows a progressive downfield shift with increasing pH up to pH 3.0 after which no further changes in chemical shift were observed. The extent of the downfield shift is less than that of difluorooxaloacetate.

Variation with polarity of the medium

The polarity of a 20 mM solution of difluorooxaloacetate in 20 mM pyrophosphate buffer, pH 7.4, was varied by the incremental addition of either t-butanol or 1-4 dioxan, and the chemical shift of the ^{19}F nmr signal of difluorooxaloacetate measured relative to difluorooxaloacetate in buffer. The experiment was then repeated using 20 mM perfluorosuccinate. Plots of chemical shift versus the dielectric constant of the medium are shown in Fig.48. The dielectric constant (D') of the medium was calculated using the expression

$$\log D' = \phi_1 \log D_1 + \phi_2 \log D_2$$

where D_1 and D_2 are the dielectric constants of the individual solvents and ϕ_1 and ϕ_2 are their respective fractional volumes.

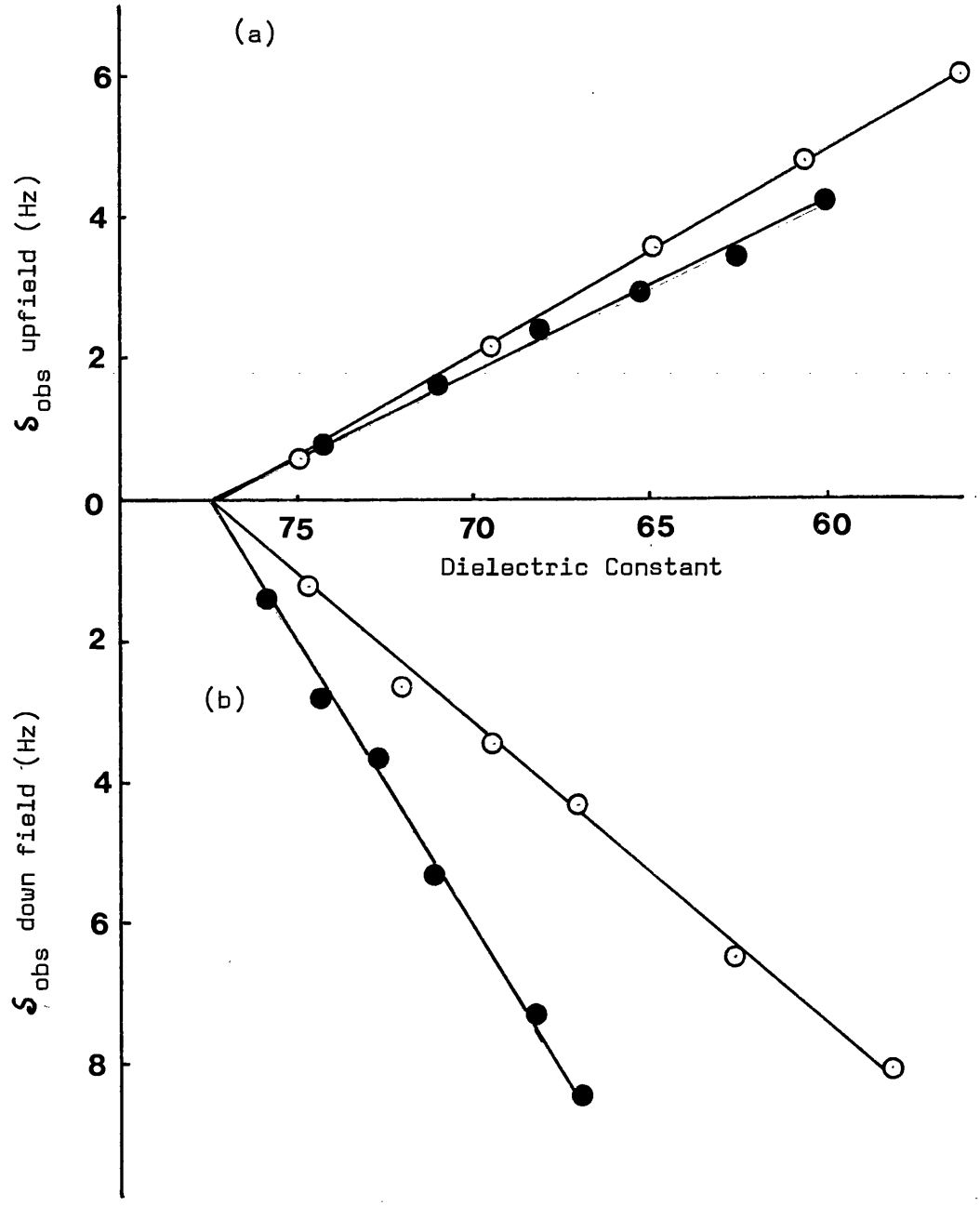

Fig. 48. Variation of the ^{19}F chemical shifts of difluoro-oxaloacetate and perfluorosuccinate with the dielectric constant of the medium. 2-methyl propan-2-ol (●) and dioxan (○) were added incrementally to a solution containing pre-neutralised fluoro acid (20 mM) (a, difluoro-oxaloacetate; b, perfluorosuccinate) in 20 mM pyrophosphate buffer, pH 7.4. The dielectric constant of the medium was calculated as described by von Hippel (1954).

Increasing the content of organic solvent in the t-butanol–water and in the dioxan–water mixture caused the ^{19}F n.m.r. signal of difluoro-oxaloacetate to move progressively upfield whereas the ^{19}F n.m.r. peak of perfluorosuccinate moved downfield.

Variation in ionic strength of the medium

Difluorooxaloacetic acid was added to a series of potassium chloride solutions (0.5 – 2.5 M) in distilled water to give a final concentration of 20 mM acid. The pH of each solution was adjusted to 7.4 with KOH solution and the chemical shift of the ^{19}F n.m.r. signal of difluoro-oxaloacetate measured relative to difluorooxaloacetate in distilled water at pH 7.4. The experiment was repeated using 20 mM perfluorosuccinic acid. In each case the effect of increasing ionic strength was to shift the ^{19}F n.m.r. signal slightly upfield. The maximum shift obtained for both difluoro-oxaloacetate and perfluorosuccinate in the presence of 2.5 M KCl was ~1.0 Hz.

DISCUSSION

In an earlier study on the inhibitory effect of difluoro-oxaloacetate on the activity of rat-liver aspartate transaminase (AAT), Kun et al., (1963), found that inhibition was competitive with respect to the keto acid substrate and non-competitive with respect to the amino acid substrate. In the more detailed study carried out here, the inhibition was also found to be competitive with respect to the keto acid substrate but uncompetitive with respect to the amino acid. An examination of the equations relevant to inhibition in the ping-pong mechanism (equations 2-6), predicts mixed inhibition patterns if the inhibitor reacts with both enzymic forms. If the inhibitor reacts only with the aminic form of the enzyme, the inhibition will be competitive with respect to the keto acid substrate and uncompetitive with respect of the amino acid substrate. The results show that the latter mode of inhibition is indeed the case. Although difluoro-oxaloacetate does in fact form a complex with the aldimine form of aspartate transaminase, the dissociation constant for this complex is~5-fold higher than the inhibitor concentration range employed in these experiments. Thus any effect caused by this complex will be small compared with experimental error.

The value obtained for Ki (5.85 μM) is very much smaller than the values obtained for interaction of other dicarboxylic acid substrate analogues with the aminic form of aspartate transaminase (Haarhoff, 1969). It is however of the same order of magnitude as the Ki obtained for

inhibition of rat-liver AAT (Kun et al, 1963) and is also very similar to the value obtained for the dissociation constant (3 μM) of the oxaloacetate-aminic transaminase complex obtained in temperature jump studies (Hammes & Fasella, 1962). This similarity of dissociation constants suggests that difluoro-oxaloacetate is a better substrate analogue than previously used dicarboxylic acids.

The possibility that substrate activity of difluoro-oxaloacetate might affect the steady state kinetics was considered. Such activity should result in non-hyperbolic variation of initial rates with variation of inhibitor or 2-oxoglutarate concentrations. This was not found (Figs. 13 & 14). However experiments carried out specifically to detect transamination between difluoro-oxaloacetate and aspartate by monitoring the 260 nm absorption of oxaloacetate, showed that a very slow steady-state production of oxaloacetate occurred. Comparison of the turnover numbers for the asparate-oxaloacetate reaction (Fasella and Hammes, 1967) with the aspartate-difluoro-oxaloacetate reaction showed that the reaction with the fluoro analogue is more than five orders of magnitude slower. Under these circumstances the substrate activity of the inhibitor would not be detectable in the steady-state inhibition studies. Although the turnover of difluoro-oxaloacetate is very much less than that of natural substrates, the observed reaction rate was three orders of magnitude faster than that seen in non-enzymic imidazole catalysed model systems using pyridoxal phosphate (Banks et al, 1968).

Substitution of cysteine sulphinic acid for aspartic acid as the amino group donor did not alter the turnover number. The amino acid product of the transamination reaction between cysteine sulphinic acid and difluoro-oxaloacetate was isolated in sufficiently large quantities to obtain an ^{19}F n.m.r. spectrum. Although a sample of synthetically prepared difluoro-aspartate was not available for the purposes of comparison, the n.m.r. splitting pattern is exactly that predicted for difluoro-aspartate.

A reaction mixture of the aminic form of aspartate transaminase and difluoro-oxaloacetate did not contain any detectable free fluoride ion. This indicates that the reaction of the enzyme with difluoro-oxaloacetate does not proceed via β-elimination of fluoride as suggested in Fig. 23.

Examination of the UV spectrum of a mixture of aminic transaminase and difluoro-oxaloacetate showed that two spectral changes took place. On initial mixing, a fairly rapid ($\sim$ 7 s) shift in the spectral maximum from 332 to 328 nm occurred, followed by a much slower change from 328 to 360 nm.

The 332 nm-360 nm spectral change*

The progress curve of the slow spectral change followed apparent first order kinetics. The rate constant increased non-linearly with

*See note on page 128

increasing analogue concentration, reaching a limiting value at approximately 100 μM difluoro-oxaloacetate. This behaviour suggests that the observed spectral change reflects the first-order breakdown of an enzyme-analogue complex, the upper limit occurring when all of the enzyme is in the form of the complex. Further evidence for this assumption is the initial rapid shift in the absorption maximum (332 nm-328 nm), which may be taken as representing the formation of the enzyme-analogue complex prior to the slow spectral change.

Comparison of the limiting value of the first-order rate constant for the 332 → 360 nm spectral change ($1.22 \times 10^{-3} s^{-1}$) with the turnover number of the enzyme-catalysed reaction of difluoro-oxaloacetate with either asparate or cysteinesulphinate ($1.20 \times 10^{-3} s^{-1}$) shows that the spectral change reflects the rate limiting step in the reaction of aminic enzyme with the fluoro-compound.

Analysis of the initial rates of the spectral change allowed the determination of the Km and the first-order rate constant for the breakdown of the enzyme-analogue complex (λmax 328 nm). The value obtained for the latter ($1.30 \times 10^{-3} s^{-1}$) is in good agreement with the limiting value obtained using the empirical first-order rate equation. If the assumption is made that $k_2 << k_{-1}$ (equation 9b), then the Km is approximately equal to the dissociation constant for the complex with λmax 328 nm. The similarity between Km (7 μM) and the kinetic Ki (8.25 μM) suggest that the species with the λmax 328 nm

is the species responsible for the strong inhibiton found in the steady-state studies.

The extent of the absorbance change at 360 nm, on completion of the slow spectral change, suggests that this reaction goes to completion. The "burst" experiments confirm this assumption and also demonstrate the fact that if any enzyme-analogue complexes are present, then they are in rapid equilibrium with free aldimine enzyme.

Burst techniqes are commonly used to measure the total amount of enzyme present in a system. They have not previously been used to measure concentration of enzyme intermediates on either side of a system at equilibrium since enzyme equilibria normally respond very rapidly to alteration in the level of intermediates. In this case however the rate limiting step is very much slower than other steps in the reaction sequence. Preliminary experiments using α-ketoglutarate and excess cysteine sulphinic acid and similar concentration of asparatate transaminase showed that the reaction was too fast to be followed using conventional spectrophotometry. The reaction of cysteine sulphinic acid with the aldimine form of asparate transaminase has been reported to be faster than that of aspartic acid with the enzyme (Meister, 1955). This data forms the basis for the central assumption of the method, i.e. that the reaction which regenerates aminic enzyme is very much faster than the rate of adjustment of the equilibrium situation.

Spectral change from 332 nm to 328 nm

Addition of difluoro-oxaloacetate to aminic AAT resulted in a fast ($t_{\frac{1}{2}} \sim 7s$) change in the λmax of the solution from 332 to 328 nm. The peak at 328 nm is fugacious, changing slowly to a spectral maximum at 360 nm as described above. However in the presence of cysteine sulphinate, the system reaches a dynamic equilibrium, in which the predominant enzyme species is the complex λmax 328 nm. This equilibrium situation allowed estimates of the extinction coefficients of the complex to be made at various wavelengths. The difference spectrum between the complex and free aminic enzyme showed the spectral region in which the maximal optical density changes occurred (345 nm) and this wavelength was used in more detailed studies of the kinetics of the rapid reaciton.

Where cysteine sulphinate was used as an amino group donor for the transamination of difluoro-oxaloacetate, no inactivation of AAT was observed. This is contrary to the studies of Cavallini et al (1973), who found progressive inactivation of aspartate transaminase on incubation with cysteine sulphinate, the inactivation being accelerated by addition of the keto acid α-oxoglutarate. The inactivation was found to be caused by aminoacrylic acid, produced from cysteine sulphinate by β-elimination. This β-elimination is catalysed only be the aldimine form of AAT. However where difluoro-oxaloacetate is the keto acid substrate, the dynamic equilibrium appears to lie on the side of the aminic enzyme, thus β-elimination is greatly reduced because of the low steady-state concentration of aldimine enzyme.

Observation of both the rate and the extent of the 332 to 328 nm spectral change by stopped-flow spectrophotometry, gave information about the kinetics of formation and removal of the species with λmax 328 nm. The iterative procedure used to analyse the variation of amplitude of this spectral change with difluoro-oxaloacetate concentration leads to an estimate of 2.8×10^3 $M^{-1} \cdot cm^{-1}$ for the extinction coefficient at 345 nm (ε_{345}), in good agreement with that obtained under pseudo equilibrium conditions ($\varepsilon_{345} = 3.1 \times 10^3$ $M^{-1} \cdot cm^{-1}$). Comparison of the K_d obtained for the complex from this analysis (8.75 μM), with the Km (7 μM) from the initial rates of the slow spectral change, confirms the assumption that Km ≃ Kd and that it is the formation of this complex that is responsible for the strong inhibition of transaminase activity shown by difluoro-oxaloacetate.

The kinetics of the formation of the λmax 328 nm species suggest the presence of a complex of aspartate transaminase and difluoro-oxaloacetate prior to the formation of the complex absorbing at 328 nm. However use of the rapid-scanning stopped-flow apparatus did not reveal the presence of any spectrally distinct intermediates. Two reasons might account for this. The complex may have an identical UV spectrum to that of free aminic enzyme; or the kinetic constants of its formation and removal may be such that under the experimental conditions the complex is present in negligibly low concentrations.

Assuming that a spectrally non-detectable complex exists, the linear

relationship between the initial rate of the fast spectral change and the total difluoro-oxaloacetate concentration suggests that the Km for this reaction is much greater than the substrate concentration substration used i.e. Km >> 120 μM. Analysis of the initial rate data by the iterative procedure did not provide precise values for the kinetic parameters because the error variance of the points about a straight line did not show a definite minimum as the Km was varied. The procedure did however allow lower limits to be fixed for these constants, (Km > 30 mM and $k_3 \geq 50\ s^{-1}$).

Estimates of the four rate constants, k_1 - k_4 (equation 18), were obtained by using the simulation fitting procedure CHEKMAT. In view of the agreement in values of the rate constant for the slow step (k_5, equation 18), obtained from four independent experiments, this constant was supplied to the program as a fixed value. The irreversibility of a slow step is justified by the results of the "burst" experiments.

The CHEKMAT program is an iterative procedure, and adjusts the constants to give the best fit to the experimental data. The rate constants so obtained may be compared with kinetic parameters obtained in other experiments. The kinetic parameters contain the individual rate constants in various combinations and thus the degree of similarity between the derived and the observed parameters is a good measure of the accuracy of the iterative solution. These values are compared in Table 6 and it can be seen that in each case good agreement exists between the values. The reaction sequence given below (Scheme 3) together with the appropriate rate constants would therefore seem to

be an accurate description of the reaction.

$$E + I \underset{1.02 \times 10^{5}\ s^{-1}}{\overset{2.6 \times 10^{6}\ l/mol/s}{\rightleftharpoons}} X \underset{1.05 \times 10^{-2}\ s^{-1}}{\overset{5.5 \times 10^{1}\ s^{-1}}{\rightleftharpoons}} A \xrightarrow{1.25 \times 10^{-3}\ s^{-1}} B$$

λmax 332 nm 332 nm 328 nm 360 nm

Scheme 3

The molecular nature of the intermediates shown in Scheme 3 may be deduced in part from their absorption maxima and by analogy with the generally accepted mechanism of transamination. Complex B, (Scheme 3) lies to the right of the rate limiting step of the reaction. The result of the "burst" experiment indicates that this species is either free aldimine enzyme or difluoro-aspartate-aldimine enzyme complexes in rapid equilibrium with free aldimine enzyme. With the natural substrates, L-glutamate and L-aspartate (Banks et al, 1968) and with threo-β-chloroglutamate (Antonini et al, 1970), the rate limiting step is believed to be the loss of a proton from the aldimine Schiff base initiating the prototropic shift to a ketimine Schiff base. Furthermore, the prototropic shift is thought to occur via a quinoid type intermediate (Jenkins, 1964). This intermediate has a strong absorbance at 490 nm and has been observed with the natural substrates (Jenkins and D'Ari, 1966a) and with the substrate analogue erythro-β-hydroxy aspartate. However no spectral change in the 490 nm region was observed with difluoro-oxaloacetate as the substrate. If addition of a proton to the quinoid intermediate were rate limiting, a build up of this intermediate would be expected, with a concomitant increase in the optical density at 490 nm. The fact that this was not

observed indicates that the rate-limiting step is the removal of a proton from the ketimine Schiff base to form the quinoid intermediate.

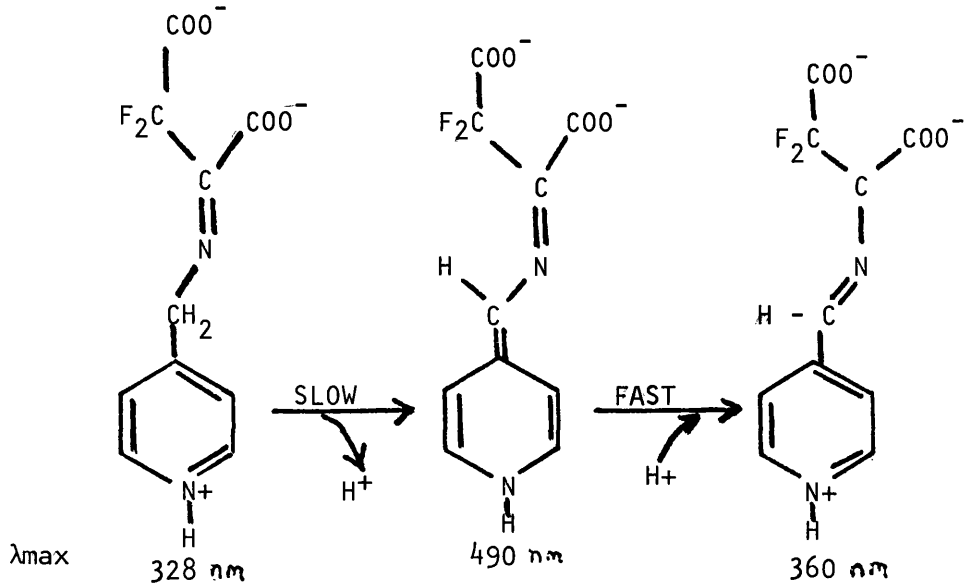

Scheme 4: Prototropic shift in the transamination of difluoro-oxaloacetate, illustrating the rate limiting step and the probable absorption maxima of the intermediates.

From the above discussion it follows that A, the species absorbing at 328 nm is either the ketimine Schiff base or its precursor, a tetrahedral intermediate (Fig. 49).

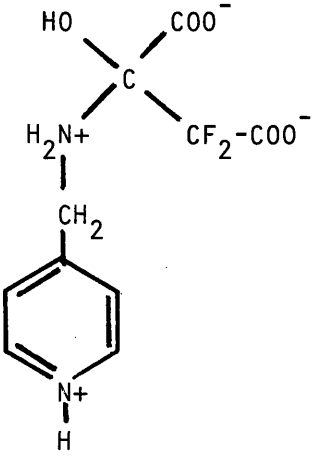

Fig. 49: Tetrahedral addition product between pyridoxamine and F_2OA

Jenkins (1963) has briefly noted the occurrence of a derivative with absorbance maximum at 325 nm on reaction of difluoro-oxaloacetate with the aminic form of aspartate transaminase. Hammes and Haslam (1969), using temperature-jump techniques, obtained evidence for a ketimine species absorbing in the 330 nm region in the reaction of erythro-β-hydroxyaspartate with the aldimine form of the enzyme. However no spectrally-distinct species corresponding to that with λmax 328 nm has been reported with the natural substrates of aspartate transaminase.

Although no further spectrally distinct intermediates could be detected before formation of A, the kinetics of its formation indicated the presence of at least one intermediate with λmax 332, designated X in Scheme 3. It is likely that X represents a non-covalent Michaelis complex; this is consistent with an absorbance maximum at 332 nm.

The value obtained for the second-order rate constant (2.6×10^6 litre.mol^{-1},s^{-1}) describing the rate of formation of X, is smaller than the lower limits obtained for the natural substrates ($> 10^8$ litres.mol^{-1}.s^{-1}). However in solution, difluoro-oxaloacetate probably exists as the hydrate, β,β-dihydroxydifluorosuccinate (Kun and Dummel, 1969), which would decrease the effective concentration of the reactive keto form.

The question also arises as to why transamination of difluoro-oxalo-acetate is slow, the turnover number being some five orders of magnitude

smaller than for the natural substrates (Fasella and Turano, 1970). As discussed earlier, the spectral evidence indicates that the rate limiting step in the transamination of difluoro-oxaloacetate is the removal of the proton from the coenzyme 4'-carbon to give the semi-quinoid carbanion intermediate. According to Dunathan's hypothesis (1966), the labilisation of this proton requires that the bond be orientated perpendicular to the π-electron system conjugated to the coenzyme pyridine ring. Molecular models show that achievement of the correct orientation is severely restricted by steric interactions between the fluorine atoms and the benzylic protons in a difluoro-oxaloacetate moiety aligned relative to the cofactor ring as described by Ivanov and Karpeisky (1969). Such steric hindrance, absent with the natural substrates, would serve to account for the very much slower reaction of the fluoro-analogue.

An additional factor that may contribute to the slowness of difluoro-oxaloacetate transamination is suggested by the fact that aspartate transaminase catalysed transamination of monocarboxylic acids such as L-alanine is also very slow (Jenkins, 1961). It is suggested that binding by only one carboxylate, allows flexibility of orientation of the coenzyme-substrate with respect to essential protein groups. The substitution of fluorine for hydrogen on the β-carbon restricts rotation of the two carboxylate groups with respect to each other. Therefore binding of the analogue to the active site may be by only one carboxylate group, giving rise to a situation analogous to that described for alanine.

It may be possible to obtain further information on the nature of the reaction by the use of borohydride and borotritiide to reduce intermediates at various steps in the reaction sequence. Isolation of the reduced coenzyme-substrate products may allow characterisation by n.m.r. spectroscopy.

*Note: After the completion of the work reported in this thesis, Boettcher and Martinez-Carrion (1976) have reported a slow spectral change from 332 to 360 nm, on the addition of difluoro-oxaloacetate to the aminic form of aspartate transaminase. However, these workers have not investigated the 332 to 360 nm spectral change in any detail, but have used this phenomenon as a tool to demonstrate lack of subunit interactions in aspartate transaminase and to investigate the non-specific anion binding site.

Difluoro-oxaloacetate as a ^{19}n.m.r. active site probe

Difluoro-oxaloacetate interacts with the aldimine form of aspartate transaminase to give an 'abortive complex' absorbing in the 430 nm region. The change in absorbance at 435 nm, on titrating the fluoro-analogue with aldimine enzyme enabled the dissociation constant of the 'abortive complex' to be determined (2.8 mM). This is close in value to that determined for the 'abortive complex' of oxaloacetate with aldimine aspartate transaminase (1.8 mM; Michuda and Martinez-Carrion, 1970). When the titration of difluoro-oxaloacetate with enzyme was monitored by following the ^{19}F n.m.r. shift of the fluoro-compound, a dissociation constant of 2.9 mM was obtained. This is in very good agreement with result of the spectrophotometric titration and indicates that the two techniques are measuring the same phenomenon and thus validates the use of the ^{19}F n.m.r. signal to further probe the binding of the ligand.

Micro-environment of enzyme bound difluoro-oxaloacetate

Decreasing the pH of a solution containing the aldimine form of aspartate transaminase and difluoro-oxaloacetate cause the ^{19}F n.m.r. signal of the fluoro-analogue to broaden and shift upfield. The pH profiles of both the line width and chemical shift show inflexion points at pH 5.4 and 8.0, (Fig. 38). The chemical shift of difluoro-oxaloacetate alone does not vary at pH values greater than 5 (Fig. 46), it is therefore probable that the two inflexion points result from

ionisation of groups associated with the enzyme. The pH profiles may be explained in terms of a model in which each of the two carboxyl groups of difluoro-oxaloacetate binds to a specific group on the enzyme as that group is protonated. As the pH of the medium is decreased, the groups on the enzyme will become successively protonated and the difluoro-oxaloacetate becomes progressively more tightly bound. The resulting increase in correlation time is reflected in the increase in the line widths of the ^{19}F n.m.r. signal. Binding of the carboxyl groups of the fluoro-analogue to protonated enzyme groups would result in effective charge neutraliation. Thus the ^{19}F n.m.r. signal of the enzyme bound ligand would be expected to shift in the same direction as when the ligand is protonated in the absence of enzyme, i.e. upfield, which is indeed the case.

However, other factors apart from charge-neutralisation effects may contribute to the overall chemical shift of the bound ligand. In this context it is of interest to consider the effect of aldimine enzyme on the ^{19}F n.m.r. signal of perfluoro-succinate. The ^{19}F n.m.r. line-width-pH profile for perfluoro-succinate in the presence of aldimine enzyme (Martinez-Carrion et al, 1973) is very similar to that obtained for difluoro-oxaloacetate. This suggests that binding of both dicarboxylic acids is dependent on the protonation of the same two enzyme groups. For perfluoro-succinate, however, the effect of the enzyme is to shift the ^{19}F n.m.r. signal downfield, whereas that of difluoro-oxaloacetate is shifted upfield. In the absence of enzyme, perfluoro-succinate behaves like difluoro-oxaloacetate in that

protonation shifts the ^{19}F n.m.r. signal upfield (Fig. 46). The net downfield shift on addition of enzyme cannot therefore be attributed to effective protonation of perfluoro-succinate on binding to the enzyme.

A possible explanation is suggested by the effect on the ^{19}F n.m.r. signal of perfluoro-succinate and difluoro-oxaloacetate of non-polar solvents. As the dielectric constant of dioxan/water and 2 methyl-propan-2-ol systems is decreased, the ^{19}F signal of perfluoro-succinate shifts downfield and that of difluoro-oxaloacetate shifts upfield (Fig. 48). Thus in both cases, transfer of the fluoro-acids to a less polar environment effects a shift in the ^{19}F n.m.r. signal in the same direction as when the fluoro-acids bind to the enzyme.

The enzyme binding data can be qualitatively explained if the dominant effect on the chemical shift is associated with binding in an apolar environment on the enzyme. In the case of difluoro-oxaloacetate, the upfield shift arising from binding to the apolar enzyme site, is reinforced by the upfield shift arising from charge neutralisation of the carboxyl groups. With perfluoro-succinate, however, the shifts arising from the two effects would be in opposite directions. Thus the downfield shift caused by the apolar environment may be partially negated by upfield shift caused by charge neutralisation resulting in lower overall shifts.

An apolar environment at the binding site of aspartate transaminase has previously been suggested (Metzler et al, 1973) on the basis of spectrophotometric evidence. It is however possible that other factors such as hydrogen bonding or ring-current effects may be important in influencing the chemical shifts of the fluorine atoms of the enzyme bound fluoro-acids.

Enzyme groups responsible for substrate binding

The chemical-shift-pH and line-width-pH profiles of difluoro-oxaloacetate in the presence of the aldimine form of asparatate transaminase showed inflexion points at pH 5.4 and 8.0. In corresponding pH profiles of difluoro-oxaloacetate obtained in the presence of the apoenzyme, the inflexion at pH 5.4 was absent. This suggests that the low pH inflexion point in the profiles of the aldimine enzyme results from the ionisation of a group associated with the cofactor. The enamine group linking pyridoxal phosphate to a lysine residue in the aldimine enzyme is known (Cheng et al, 1971) to be protonated with a pK 5.4 in the absence of buffer ions. The available data therefore suggest that a carboxylate group of difluoro-oxaloacetate binds to the protonated form of the internal Schiff base (Fig. 51).

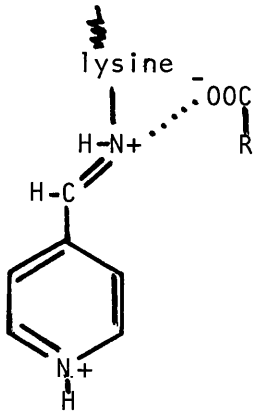

Fig. 5 Schematic representation of carboxylate binding by protonated internal Schiff base.

This grouping has been previously suggested as the low-pH carboxylate binding site for glutarate to the aldimine enzyme (Jenkins and D'Ari, 1966).

The n.m.r. parameter-pH profiles of difluoro-oxaloacetate in the presence of both holoenzyme and apoenzyme, show an inflexion point at pH 8.0. This indicates that binding at high pH is by ionisation of an enzyme grouping that is not associated with cofactor. The protonated form of an enzyme histidyl residue has been suggested (Martinez-Carrion, et al, 1973), as the high pH binding site for other dicarboxylic acids. However, a pK of 8.0 is rather higher than that normally associated with histidine residues. Further experiments, involving the determination of n.m.r. parameter-pH profiles of difluoro-oxaloacetate in the presence of photo-inactivated holoenzyme, may enable a definite assignment to be made.

Changes in the ^{19}F n.m.r. chemical shift of difluoro-oxaloacetate on titration of the ligand with the apoenzyme allowed the determination of K_D (3.4 mM) and Δ (99.2 h_3) for the ligand-apoenzyme complex. The K_D value is not far removed from that obtained for the difluoro-oxaloacetate-aldimine enzyme complex (2.9 mM). This is in agreement with the pH-profile data since the internal Schiff base will not be appreciably protonated at pH 7.4. The Δ is rather smaller than that obtained in the case of the holoenzyme. This may be a direct result of the absence of the coenzyme or an indirect result such as caused by an induced conformational change in enzyme on removal of the cofactor.

The model of ligand binding presented in this thesis, where binding is directly influenced by protonation of enzyme groups, fits the available data. It is possible however that protonation of enzyme groups may affect ligand binding indirectly, such as via conformational changes of the enzyme. It must also be borne in mind that these studies have examined binding characteristics of the formation of an "abortive complex". Binding of substrates in the productive mode may occur by alternative mechanisms.

Reaction of aminic aspartate transaminase with high concentrations of difluoro-oxaloacetate

The ^{19}F n.m.r. signal obtained on admixture of difluoro-oxaloacetate and aminic aspartate transaminase shifted upfield and broadened over a period of one hour. Repetition of the experiment in a scanning spectrophotometer, showed that during this time, the peak at 332 nm decreased and was replaced by peaks at 360 and 435 nm. The λmax 360 is characteristic of the aldimine enzyme and that at 435 nm characteristic of the abortive complex between aldimine enzyme and difluoro-oxaloacetate. The first order rate constants for the slow n.m.r. shift ($1.54 \times 10^{-3} s^{-1}$) and for the slow spectral changes ($1.795 \times 10^{-3} s^{-1}$) are very similar. This suggests that the slow ^{19}F n.m.r. shift reflects a slow conversion of the aminic form of aspartate transaminase to the aldimine form which then establishes a rapid equilibrium with a difluoro-oxaloacetate-aldimine enzyme complex. It is the build up of the abortive complex that results in a shift in the ^{19}F n.m.r. signal of

difluoro-oxaloacetate.

$$E' + F_2OA \rightleftharpoons A \xrightarrow{\text{slow}} B \rightleftharpoons E + F_2Asp$$

$$E + F_2OA \rightleftharpoons E.F_2OA$$

λmax 360 nm $\qquad\qquad$ λmax 435 nm

Scheme 5: Suggested mechanism for the slow ^{19}F n.m.r. shift. E' and F represent aminic and aldimine enzyme respectively. A and B are intermediate enzyme complexes; F_2OA and F_2Asp represent difluoro-oxaloacetate and difluoro-aspartate respectively.

This interpretation is supported by the fact that addition of cysteine sulphinate to completed reaction mixtures resulted in the immediate disappearance of the 360 and 435 nm peaks and the appearance of a maximum at 328 nm, previously attributed to formation of an aminic-enzyme difluoro-oxaloacetate complex. Concurrent with these changes the chemical shift of the ^{19}F n.m.r. signal reverted to that characteristic of free difluoro-oxaloacetate in buffer alone with a concomittant sharpening of the signal. Therefore the presence of a complex between difluoro-oxaloacetate and aminic enzyme is not reflected in the chemical-shift and line-width of the ^{19}F n.m.r. signal of difluoro-oxaloacetate. This can be explained if there is a slow exchange situation between the free ligand and the complex with λmax 328 nm. In this case two n.m.r. signals will be present corresponding to difluoro-oxaloacetate in its free and complexed states respectively. It is probable that the signal of the complexed ligand would be too broad to observe under the conditions of the experiment,

leaving the signal of the unbound ligand as the only visible peak. The complex with λmax 328 nm has been shown in this thesis to have a dissociation constant of ~7 μM. Such a tight complex can easily give rise to the slow exchange situation.

Measurement of the ^{19}F n.m.r. on titration of a completed reaction mixture with aliquots of difluoro-oxaloacetate, allowed the estimation of the dissociation constant of an aldimine-enzyme-difluoro-aspartate complex. The presence of this complex was suggested when treatment of the data by the iterative routine previously used to determine the dissociation constant of the aldimine-enzyme-difluoro-oxaloacetate complex, gave value for K_D = 7.5 mM and Δ = 187 h_3, incompatible with the values obtained directly (K_D = 2.9 mM; Δ = 137 h_3). The modified iterative routine gave a value of K_D = 0.7, for the difluoro-aspartate-enzyme complex, and Δ = 127 h_3 for the difluoro-oxaloacetate-enzyme complex, the latter result in good agreement with that obtained directly. Enzymic synthesis of difluoro-aspartate should allow confirmation of this indirect determination.

Study on Malate Dehydrogenase

Introduction

In most living organisms, oxidation of L-malate is catalysed by two distinct types of enzyme. One class utilises NADP as a coenzyme, producing pyruvate and carbon dioxide, and is therefore known as decarboxylating dehydrogenases. The other type uses NAD as a coenzyme; in this case oxaloacetate is the product. NAD-dependent malate dehydrogenase occurs in virtually all eukaryotic cells in two major forms, a soluble or cytoplasmic form (c-MDH) and a mitochondrial form (m-MDH). This distribution of the enzyme provides a means by which NADH equivalents, in the form of malate, may be transported across the mitochondrial membrane. In addition, m-MDH is a necessary component of the tricarboxylic acid cycle.

Mitochondrial L-malate:NAD oxidoreductase (E.C. 1.1.1.37)

Molecular weight: Initially, estimates of the molecular weight of m-MDH from various mammalian sources showed a great deal of variation (15,000 - 74,000). However, recent investigations using gel-filtration techniques, indicate that the molecular weight is in the region of 60,000 - 70,000 (Murphy et al., 1967). Compositional analysis (Noyes et al., 1974) of pig heart m-MDH suggests a molecular weight of 68,000. Pig heart mitochondria have also been shown (Consiglio et al., 1970) to contain a larger malate dehydrogenase, of molecular weight approximately 138,000. Although this protein can be dissociated into two separate

proteins of approximately equal molecular weight by the action of thyroxine (Covelli et al., 1969), only one shows malate dehydrogenase activity. The biochemical or physiological significance of this heavy form is unknown.

Subunit structure: Mitochondrial MDH is composed of two identical subunits of molecular weight 34,000. The sequence of the first 28 amino acid residues has been determined (Banaszak and Bradshaw, 1970). Although the structure of the subunits is very similar in both c- and m-MDH (Devenyi et al., 1966), the terminal amino group of the cytoplasmic form is blocked, whereas it is free in the mitochondrial form. There is no evidence that association of the subunits is by disulphide bonds.

Subforms: Electrophoretic studies have shown that the enzyme can exist as multiple subforms (Thorne et al., 1963; Kitto et al., 1966a), and that these subforms possess similar catalytic properties, resistance to thermal inactivation and indistinguishable amino acid compositions. The origin of the subforms has been attributed to such factors as conformational differences (Kitto et al., 1966b), combinations of non-identical but similar polypeptide chains (Kulick and Barnes, 1968) and proteolytic degradation (Cassman and King, 1972). However, more recent investigations (Glatthaar et al., 1974) indicate that the subforms arise as artifacts of the preparation procedures, probably through deamidation of asparaginyl and/or glutaminyl residues.

Essential amino acid residues: A number of amino acid residues have been examined as candidates for the role of active site residues. Mitochondrial MDH combines with low concentrations of mercurials to produce activation and with high concentrations of mercurials producing inactivation (Kuramitsu, 1968; Devenyi et al., 1966b). Using p-mercuribenzoate Silverstein and Sulebele (1970a,b) found that maximum inactivation occurred after modification of 3-4 cysteinyl residues, but reaction of 7-8 cysteine residues produced greater but transient inactivation followed by a proportional inactivation. The enzyme is protected against inactivation by NAD or NADH but not by L-malate or oxaloacetate. The activation shown by Kuramitsu (1968) was however dependent on the presence of L-malate.

N-ethyl maleimide (NEM) has also been shown (Gregory et al., 1971a) to effect the modification of two essential thiol groups per enzyme molecule resulting in a loss of enzyme activity. The modification was inhibited by NAD and NADH. However, further studies (Bleile et al., 1977) indicated that the modification with NEM resulted in the formation of inactive monomeric units, the coenzymes affording protection against inactivation by shifting the monomer-dimer equilibrium in favour of the dimeric structure.

Involvement of a histidine residue at the active site has been demonstrated by Anderton (1970) and Gregory and Harrison (1970) using iodoacetamide. The reaction was accompanied by complete

inactivation; upon hydrolysis of the inactivated enzyme, 3-carboxamidohistidine was found. This modification can be wholly prevented by the presence of NADH, and the rate of inactivation reduced in the presence of L-malate or oxaloacetate. Amino acid analysis of a pronase digest of enzyme labelled with ^{14}C iodoacetamide (Gregory et al., 1971; Foster and Harrison, 1974), revealed a peptide sequence containing the labelled histidine that is homologous with a region of lactate dehydrogenase containing its active site histidine (Taylor et al., 1973).

A lysine residue has also been implicated as being present at the active site because of the irreversible inhibition of the enzyme by pyridoxal-5'-phosphate (Yost and Harrison, 1971). However, Schiff's base formation between the ε-amino group of lysine and pyridoxal-5'-phosphate is usually reversible, and therefore a secondary reaction is probably occurring.

Interaction with the coenzyme: Utilising the fact that the fluorescence of NADH is enhanced on binding to the enzyme, it has been shown (Holbrook and Wolfe, 1972) that there are two equivalent binding sites for NADH per enzyme molecule. Similarly, by studying the competition of NAD for NADH binding sites, two equivalent sites for NAD were deduced. It was also found that the dissociation constant for NADH from the E-NADH complex markedly decreased with decreasing pH. No evidence was found in this study for co-operative binding of the coenzyme; this differs from

results obtained using beefheart c-MDH, for which the data indicate co-operative binding of NADH in the presence of fructose 1,6-diphosphate (Cassman, 1973; Cassman and King, 1973).

Enzyme Reaction Mechanism

The mechanism of a reaction such as that catalysed by malate dehydrogenase is complex, involving as it does three substrates, namely a dinucleotide coenzyme, a dicarboxylic acid and a proton. However, detailed kinetic and equilibrium studies using m-MDH have been carried out, and have allowed the determination of the type of mechanism and of individual velocity and dissociation constants for some of the discrete steps involved.

Initial rate studies: Measurement of initial rates of the reaction in both directions (Raval and Wolfe, 1962a) showed that the reaction most probably obeyed a compulsory binding order mechanism and allowed the determination of the Michaelis constants for the appropriate substrates. The data obtained did not indicate the presence of a ternary complex and it was therefore suggested that the mechanism was a Theorell-Chance type involving a kinetically insignificant ternary complex (Theorell and Chance, 1951).

Further investigation, using the technique of product inhibition (Raval and Wolfe, 1962b), was carried out to ascertain the presence or absence of a ternary complex. Product inhibition

by all four substrates, NAD, L-malate, NADH and oxaloacetate, was demonstrated, and the data obtained were shown to support a compulsory binding order (coenzyme binding first), and a kinetically insignificant ternary complex. No evidence was obtained for the formation of an abortive ternary complex, inhibition by malate or oxaloacetate being consistent with a mass law effect only. However, relatively low concentrations of product inhibitor were used in this study.

Equilibrium measurements: The mechanism of an enzyme-catalysed reaction may also be studied by the isotopic exchange of substrate at equilibrium. If the only binary complexes that are formed are E-NAD or E-NADH, then increasing levels of oxaloacetate and malate should depress the NAD $\rightleftharpoons$ NADH isotopic exchange rate, but not the isotopic exchange rate of malate $\rightleftharpoons$ oxaloacetate. This is because dissociation of E-NAD and E-NADH would increasingly be prevented by binding of substrate to reform the ternary complexes from which NAD and NADH cannot dissociate.

Such experiments (Silverstein and Sulebele, 1969) strongly supported an ordered mechanism for m-MDH at pH 8.0, with the coenzyme binding first. At pH 9.0, the results indicated a change in mechanism to a partially compulsory pathway, in which dissociation of coenzyme from the ternary complex may occur but at a slower rate than from the enzyme-coenzyme complex. The

data also supported the formation of the abortive complex, E-NADH-malate, but no evidence was found for the corresponding complex, E-NAD-oxaloacetate.

At pH 9.0, the oxaloacetate $\rightleftharpoons$ malate exchange rate decreased and then plateaued with increasing concentrations of malate and oxaloacetate. It was suggested that this may result from binding of malate, oxaloacetate or both at a non-catalytic modifier site, resulting in a decrease in the rate constant of the slow step.

Thus both initial rate and equilibrium studies give rise to the same general mechanism for catalysis by m-MDH, as illustrated in Scheme 1.

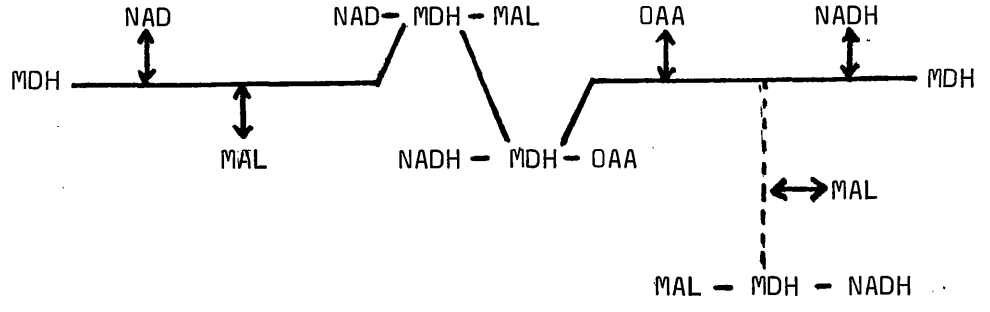

Scheme 1. Catalytic pathway for the ordered reaction mechanism for m-MDH. The ternary complexes are not kinetically significant. An abortive ternary complex is included, shown by the dotted line.

Effect of pH of the mechanism: The effect of pH on an enzyme catalysed reaction in which a proton is a reactant may be complex, since changes in the rate of the reaction can be brought about by availability of substrate (H^+) or by changes in the ionic state of functional groups. Detailed kinetic studies have been carried out by Raval and Wolfe (1962c), who found that the kinetic behaviour of the system can be explained through a model in which groups on the enzyme surface having pk's of approximately 7 and 10 are involved in the catalytic function.

The proton generated during the oxidation of malate is taken up by the enzyme and not released into the medium. The results obtained suggest that a compulsory substrate binding order is followed at all pH values studied (pH 5.5 - 10.5), in disagreement with the equilibrium experiments of Silverstein and Sulebele (1969) which suggest a change in mechanism at pH $>$ 9.0.

Substrate inhibition and activation: As is the case with many enzymes, mitochondrial malate dehydrogenase shows initial rate kinetics that deviate from Michaelis-Menten theory at high substrate concentrations. It has been shown (Raval and Wolfe, 1962a) that substrate inhibition of m-MDH is produced by NAD, NADH and oxaloacetate. A more detailed study (Raval and Wolfe, 1963) on inhibition at high concentrations of oxaloacetate

showed that the inhibition was of the mixed type with respect to NADH. Analysis of the data allowed the determination of the two inhibition constants for the competitive and uncompetitive components of the inhibition. The values obtained for these two constants are nearly identical, suggesting a similar binding mechanism in both inhibition modes. The authors propose that the competitive part of the inhibition may occur through oxaloacetate binding reversibly at the NADH binding site or through an enzyme conformational change when combined at some locus adjacent to the NADH binding site. The uncompetitive inhibition was suggested to result from formation of the abortive ternary complex, E-NAD-oxaloacetate.

Mitochondrial malate dehydrogenase also shows the phenomenon of substrate activation at malate concentrations greater than 30 mM (Telegdi et al., 1973). Product inhibition experiments under normal and activating conditions suggest that the mechanism of activation apparently involves malate binding at a site distinct from the catalytic site, with the induction of a 10-fold decrease in the Michaelis constant for NAD. This mechanism will give activation through increased prevailing velocity without altering the basic compulsory order mechanism or the maximum velocity. Assuming a compulsory order mechanism under normal and activating conditions, it was shown that the ON constant for binding of NAD to the enzyme is increased 10-fold, implying that

NAD binding is facilitated by activation, possibly by a conformational change in the enzyme. Activating concentrations of malate do not however influence NADH binding.

Experiments utilising the enhancement of fluorescence of NADH on binding to the enzyme (Theorell and Langan, 1960; Thorne and Kaplan, 1963) confirmed the observation that L-malate does not influence NADH binding. D-malate however forms a ternary complex with the enzyme and reduced coenzyme, resulting in a large increase in the fluorescence.

Hydroxymalonate inhibition: Kinetic studies using the natural substrates provide data that fit a simple compulsory order mechanism. However, a more complicated mechanism is required to account for the anomalous kinetics shown when the substrate analogues keto-malonate and hydroxymalonate are used.

Ketomalonate is reduced by m-MDH with half the turnover number observed with oxaloacetate, but no appreciable oxidation of hydroxymalonate is observed (Harada and Wolfe, 1968a). Hydroxymalonate uncompetitively inhibits the oxidation of malate catalysed by m-MDH but acts as a competitive inhibitor in the reduction of oxaloacetate. This paradoxical inhibition, coupled with the fact that in a compulsory ordered mechanism with the coenzyme leaving last, no alteration in Vmax should occur when the keto-substrate is changed, led Harada and Wolfe (1968b) to

propose as a working hypothesis a reciprocating compulsory order mechanism (Scheme 2).

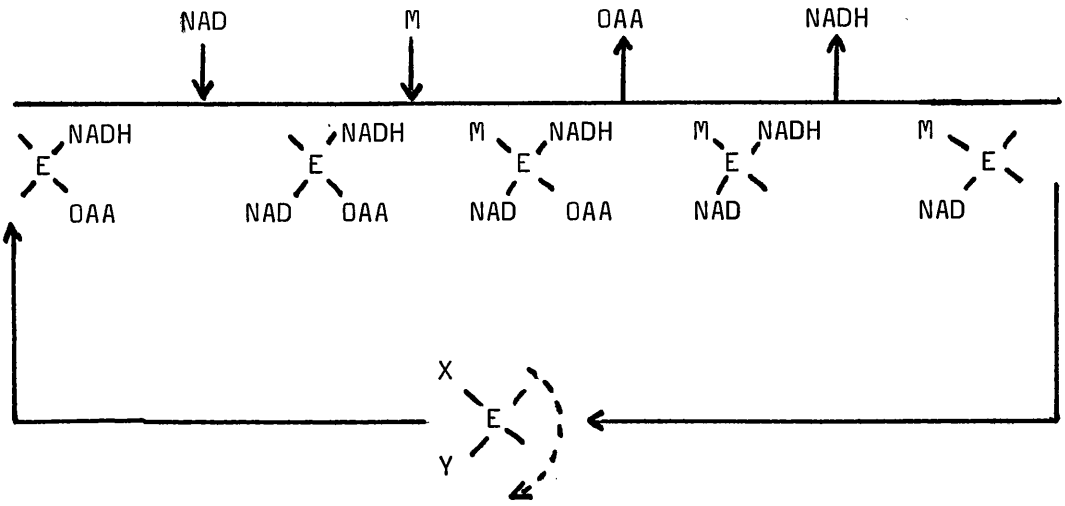

Scheme 2. Reciprocating compulsory mechanism for m-MDH. (Harada and Wolfe, 1968b).

In this mechanism, subunit interactions occur, such that although substrate and coenzyme may bind and react on one subunit, release of the products of the reaction does not occur until another substrate-coenzyme pair is bound on the other subunit. After one set of products has been released, the enzymic reaction can take place on the other subunit and what was a substrate binding site becomes a product leaving site. Although this mechanism can be used to explain the observed inhibition patterns produced by hydroxymalonate and substrate

inhibition by oxaloacetate as well as the product inhibition patterns accountable for by the compulsory ordered mechanism, there are two points which mitigate against its usefulness. The obligatory presence of a pentenary intermediate in the reciprocal mechanism does not agree with the results obtained by measuring the isotopic exchange rates in the equilibrium situation (Silverstein and Sulebele, 1969). At high concentrations of malate and oxaloacetate the concentration of the pentenary complex would be maximised, and this would result in a decrease in the oxaloacetate $\rightleftharpoons$ malate exchange, since the chemical transformation cannot take place in this complex. This effect was not observed.

Furthermore the reciprocating mechanism predicts that the monomeric form of m-MDH should be enzymically inactive. Recent studies (Shore and Chakrabarti, 1976) have been carried out using fluorescent polarisation techniques as an indicator of the rotational correlation time and hence dissociation state of m-MDH. These experiments indicated that dissociation of the enzyme into enzymically active monomers takes place on dilution of the enzyme. Thus it would seem likely that this model is not completely satisfactory, and that the anomalous kinetics may be due to the presence of a modifier site distinct from the active site.

MATERIALS

The ion-exchange resins, DE-52 and CM-52 were purchased from Whatman Biochemicals Ltd., Maidstone, Kent, and AG-50 cation exchange resin from Bio-Rad Laboratories, Bromley, Kent. NAD and NADH were from The Boehringer Corporation (London) Ltd. All other reagents were purchased from BDH Chemicals, Poole, Dorset, and were of Analar grade, except for iodoacetamide which was recrystallised twice from ethyl-acetate/benzene before use.

METHODS

Purification of Mitochondrial Malate Dehydrogenase

Purification of the pig heart mitochondrial malate dehydrogenase was initially attempted using the method of Gregory et al (1971a). However, the preparation of the acetone powder preliminary to extraction of the enzyme is time consuming and the fractionation on a Bio-Rex ion exchange column gave an inconsistent yield of the enzyme. The method was therefore modified by using the freeze-thawing and ion-exchange procedures described by Anderton (1970). The modified preparation, described in detail in Scheme 3, consists of freeze-thawing the heart mince to disrupt the mitochondria, extracting into phosphate buffer and precipitating with ammonium sulphate. This is followed by column chromatography on DE-52 and CM-52 celluloses. A typical preparation, starting with 2 kg of pig heart, yielded 250 mg of malate dehydrogenase with a specific activity of 1140 U/mg as assayed under the standard assay conditions. The preparation of Anderton (1970) assayed under the same conditions had a specific activity of 1050 U/mg protein.

2kg minced ventricles

↓ Frozen overnight, thawed, homogenised with 5 litres of Buffer A.

Homogenate

↓ Centrifuged at 2,500 x g for 30 min. Precipitate discarded.

Supernatant

↓ Taken to 52.5% saturation with respect to $(NH_4)_2SO_4$, stirred for 12 h, then centrifuged at 2,500 x g for 30 min, the precipitate discarded.

Supernatant

↓ Taken to 75% saturation with respect to $(NH_4)_2SO_4$, stirred for 12 h, then centrifuged at 2,500 x g for 30 min. Supernatant discarded.

Precipitate

↓ 100 ml of Buffer B added and the suspension dialysed against 5 x 2 litres of the same buffer over 24 h.

Non-diffusible material

↓ Dialysed against 2 litres of 75% PEG 8000 solution for 6 h.

Concentrate

↓ Applied to a DE-52 ion exchange column (30 x 2.5 cm) and eluted with 500 ml of Buffer B. m-MDH is unretarded.

Active fractions

↓ Dialysed against 3 l of saturated ammonium sulphate solution, precipitate collected and dialysed against 3 x 2 l of Buffer C.

Non-diffusible material

↓ Applied to a CM-52 ion exchange column (30 x 2.5 cm) and eluted with a linear gradient of 500 ml of Buffer C and 500 ml of Buffer D.

Active fractions

↓ Dialysed against 3 l of saturated $(NH_4)_2SO_4$ solution, the precipitate collected and stored under saturated $(NH_4)_2SO_4$ solution.

Purified enzyme

Buffer A. 20 mM potassium hydrogen phosphate, pH 7.0.

Buffer B. 25 mM TRIS-HCl, pH 8.2.

Buffer C. 5 mM potassium hydrogen phosphate, pH 6.56.

Buffer D. 500 mM potassium hydrogen phosphate, pH 6.56.

In addition, all buffers contained 1 mM EDTA and 1 mM β-mercaptoethanol.

Scheme 3. Flow diagram illustrating the purification procedure used to prepare mitochondrial malate dehydrogenase from pig heart ventricles. All operations were performed at $5^{\circ}C$.

Purification Table

Step	Volume (ml)	Total Activity	Total Protein (gms)	Specific Activity (U/mg)	Purification yield (%)	
Supernatant from homogenate	5050	1,650,000	559.3	2.95	1	100
Supernatant from 1st $(NH_4)_2SO_4$ ppt	5200	1,042,000	230.5	4.52	1.53	63.1
Concentrate of 2nd $(NH_4)_2SO_4$ ppt	25	865,700	38.8	22.3	7.56	52.4
DE-52 column eluate	175	328,000	2.102	156	52.9	19.8
Dialysate from $(NH_4)_2SO_4$ ppt	12	329,500	1.781	185	62.7	19.9
CM-52 column eluate	192	292,000	0.257	1135	384.7	17.6
Final product	20	286,000	0.250	1140	386.4	17.3

Standard Enzyme Assay

Suitably diluted enzyme solution (10 µl) was added to 1 ml of 0.1 M phosphate buffer, pH 7.4, containing 0.25 µMoles oxaloacetate and 0.12 µMoles NADH, in a quartz cuvette (pathlength 1 cm), maintained at 25°C in a thermostated cell holder. The reaction was monitored by following the decrease in absorbance at 340 nm. One unit of enzyme activity is defined as that amount of enzyme causing the disappearance of 1 µMole NADH per minute.

Protein Estimation

The protein content of crude samples was estimated using a modified Lowry method (Hartree, 1972), and that of purified samples by using the absorbance difference at 215 and 225 nm and a conversion factor of 144 (Layne, 1957).

Purification of NAD

Commercial samples of NAD were purified by chromatography on a DEAE-52 ion-exchange column. 200 mg of NAD in 2 ml of ammonium bicarbonate buffer (0.03 M, pH 7.5) were applied to a column (1.1 x 15 cm) of DEAE-52 cellulose equilibrated with the same buffer. The column was developed with 200 ml of buffer then eluted with a linear gradient consisting of 500 ml 0.03 M and 500 ml 0.5 M ammonium bicarbonate solution, pH 7.5. The eluant was monitored at 254 nm and assayed for NAD content (Klingenberg, 1974). Fractions containing NAD were pooled and freeze dried. Average recovery was 78% of the applied NAD. The product was stored *in vacuo* at -10°C.

Preparation of Difluoromalate

DL-difluoromalate was prepared by borohydride reduction of difluorooxaloacetate using the method of Bentley and Bhate (1960) for the synthesis of ^{3}H-malate from oxaloacetate. 500 Mg of difluoro-oxaloacetate, prepared as previously described,

were dissolved in 10 ml of distilled water. The pH of the solution was then adjusted to 7.0 by the addition of 2 M NaOH solution, monitoring the pH with a pH electrode. 2mMoles of KBH_4 in 2 ml of distilled water were then added in small aliquots ($\sim 100\ \mu l$) and the pH adjusted back to 7.0 after each aliquot by the addition of 1 N H_2SO_4 from a microburette. After all the potassium borohydride had been added, the pH of the solution was adjusted to 5.5 with 1 N H_2SO_4 and left to stand at room temperature for 10 min. The total volume of H_2SO_4 added was noted and an equivalent amount of barium acetate added. The precipitated barium sulphate was removed by centrifugation.

The supernatant solution was passed down a column (1.5 x 20 cm) containing Bio-Rad AG-50 resin in the H^+ form to remove cations, eluting with distilled water until the pH of the eluant was 6.0. Borate and acetate were then removed from the eluant by repeated additions of methanol (10 x 50 ml), the solution being taken to low bulk after each addition in a rotary film evaporator under reduced pressure (1 mmHg ; 35^oC). After the final addition the solution was taken to dryness, 30 ml of 10% aqueous HCl added and refluxed over a boiling water bath for 1 h. The HCl was then removed with repeated additions of distilled water in a rotary film evaporator. The product on evaporating to dryness was a white hygroscopic powder.

Elemental analysis of the product gave the following results.

	C	H	F
Calculated	28.23%	2.35%	22.36%
Found	27.97%	2.39%	22.60%

The calculated values were obtained assuming an empirical formula of $C_4H_4O_5F_2$ (molecular weight 170.1). Titration of a known amount of product with standardised NaOH solution gave an equivalent weight of 85.15. The ^{19}F n.m.r. spectrum of the product in distilled water was an octet, typical of the AB-X system expected from difluoromalate, the spectrum having the following coupling constants at 94.1 MH_z.
J_{AX}, 14.92 hz; J_{BX}, 11.08 hz; J_{AB}, 268 hz; V_A-V_B, 225.4 hz.
No peak corresponding to difluoro-oxaloacetate was detected in the ^{19}F n.m.r. spectrum.

^{19}F n.m.r. Measurements

^{19}F nuclear magnetic resonance spectra were recorded on a Jeol PS100 nuclear magnetic spectrometer at 94.1 MH_z in the field sweep mode. Where necessary the spectrum was enhanced by repeated scans using a Jeol JNM SB-3 signal to noise booster. All measurements were made at 28 $\pm$ 1°C.

Kinetic Measurements

Kinetic measurements following the production or removal of NADH were performed on a Pye Unicam SP1800 spectrophotometer.

Unless otherwise stated, all assays were carried out at $27 \pm 1^{o}C$, using a thermostated cell holder. Kinetic constants were obtained by direct linear plots (Eisenthal and Cornish-Bowden, 1974) of the initial rates of reaction against substrate concentration. The data are presented as $[S]/v$ against $[S]$ plots, the lines being fitted to the points using the parameters calculated from the direct linear plots.

Substrate Activity of Difluoro-oxaloacetate

Difluoro-oxaloacetate has been shown to be a substrate for malate dehydrogenase (Kun et al, 1963). However, only approximate values for the Km's of difluoro-oxaloacetate and NADH were determined and therefore a more detailed study was carried out to ascertain the relevant kinetic constants and to establish the mechanism.

The kinetics with the natural substrate pair, oxaloacetate and malate have been shown to obey a Theorell-Chance type mechanism, i.e. having a kinetically insignificant ternary complex in the absence of product (Raval & Wolfe, 1962b).

The general equation for a two substrate mechanism can be expressed in the following form (Dalziel, 1957).

$$\frac{[E_t]}{v} = \phi_o + \frac{\phi_1}{[A]} + \frac{\phi_2}{[B]} + \frac{\phi_{12}}{[A][B]} \qquad (1)$$

where $[A]$ $[B]$ represents the concentration of the two substrates, $[E_t]$ is the total concentration of enzyme. v, is the initial velocity of the reaction and ϕ_o, ϕ_1, ϕ_2 and ϕ_{12} are kinetic coefficients.

A pair of primary plots may then be constructed corresponding to the following two equations.

$$\frac{Et[A]}{v} = \left(\phi_o + \frac{\phi_2}{[B]}\right)[A] + \left(\phi_1 + \frac{\phi_{12}}{[B]}\right) \quad (2)$$

$$\frac{Et[B]}{v} = \left(\phi_o + \frac{\phi_1}{[A]}\right)[B] + \left(\phi_2 + \frac{\phi_{12}}{[A]}\right) \quad (3)$$

Secondary plots of the slopes and ordinate intercepts of these primary plots against the "constant" substrate, allows determination of the coefficients.

The experiment was carried out by measuring the initial rate of NADH oxidation while systematically varying the concentration of difluoro-oxaloacetate and NADH. NADH (0.01 to 0.10 mM) and difluoro-oxaloacetate (0.5 to 5.0 mM) in 50 mM TEA buffer, pH 7.4, were placed in a 1 cm path-length quartz cuvette, thermostatted to 27°. The reaction was started by the addition of .09 µg MDH and the initial rate of the decrease in absorbance at 340 nm was measured. Total volume in the cuvette was 3.0 mls.

Primary plots of the data obtained are shown in Figs. 1 and 2. The rates are expressed as molecular activity (MA), the number of moles of product produced per min per mole of enzyme.

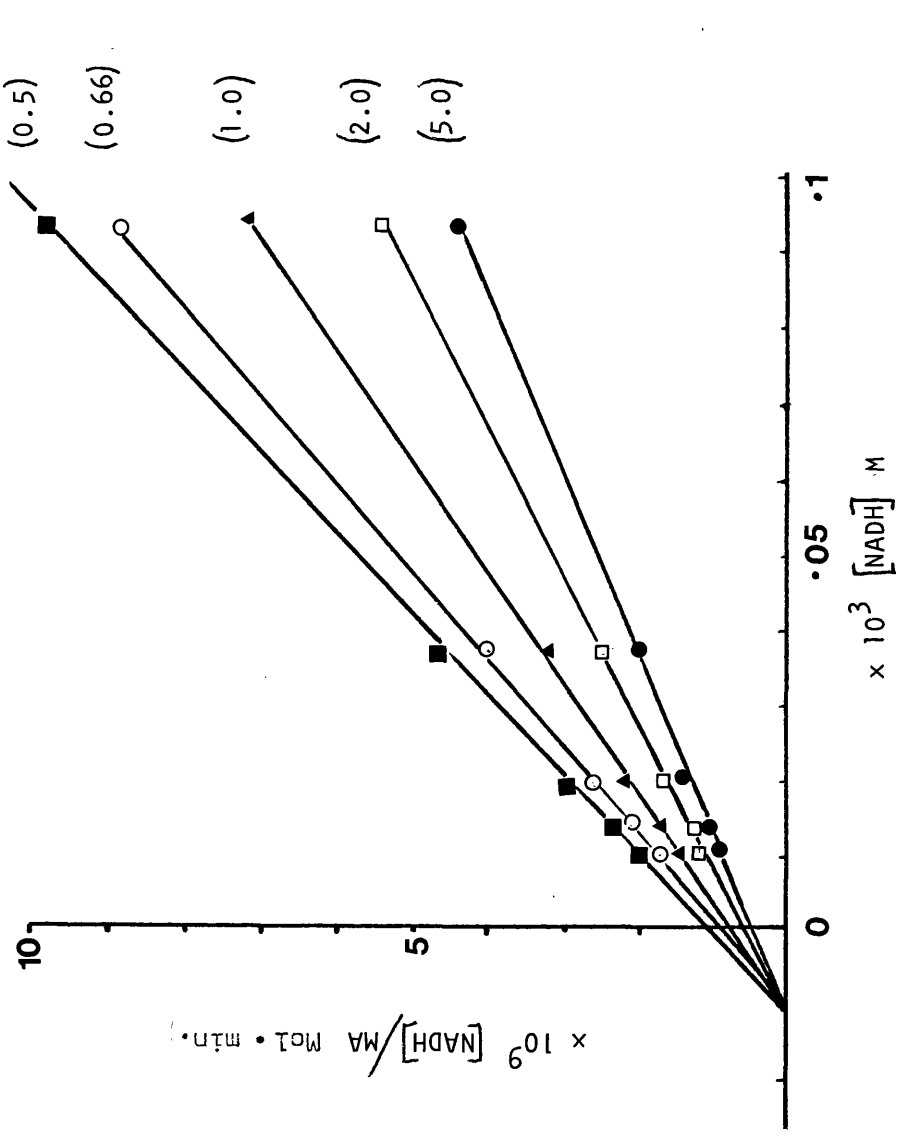

Fig. 1: Variation of initial veolocity of m.MDH catalysed reduction of difluoro-oxaloacetate with [NADH] at different fixed difluoro-oxaloacetate concentrations. The velocity is expressed in terms of Molecular Activity (MA) (see legend to table 1). The concentration of difluoro-oxaloacetate used is given in parentheses at the end of each line.

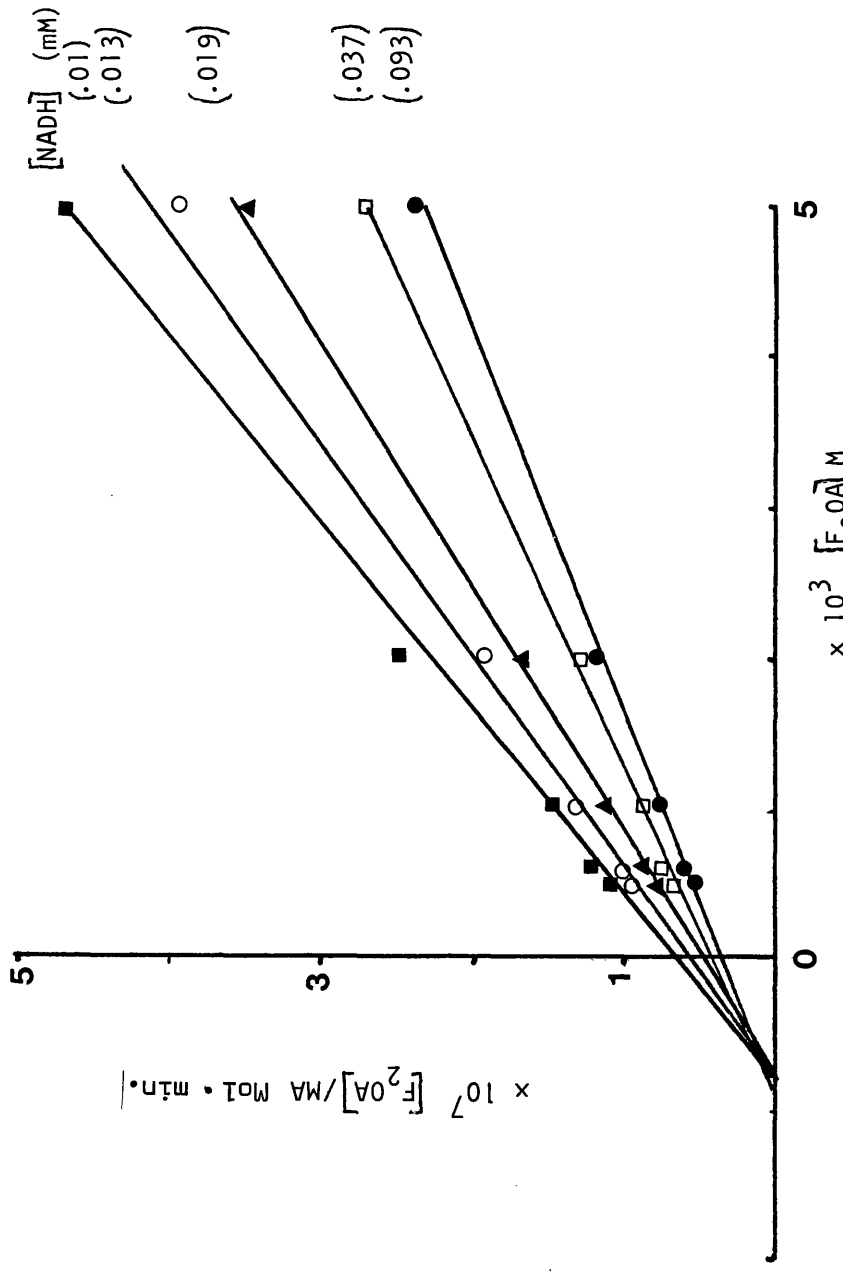

Fig. 2: Variation of initial velocity of m.MDH catalysed reduction of difluoro-oxaloacetate with difluoro-oxaloacetate concentration at different fixed NADH concentrations. Other conditions are as for Fig. 1.

Replots of the slopes and intercepts from Fig. 1 and 2 are shown in Figs. 3 a,b,c,d.

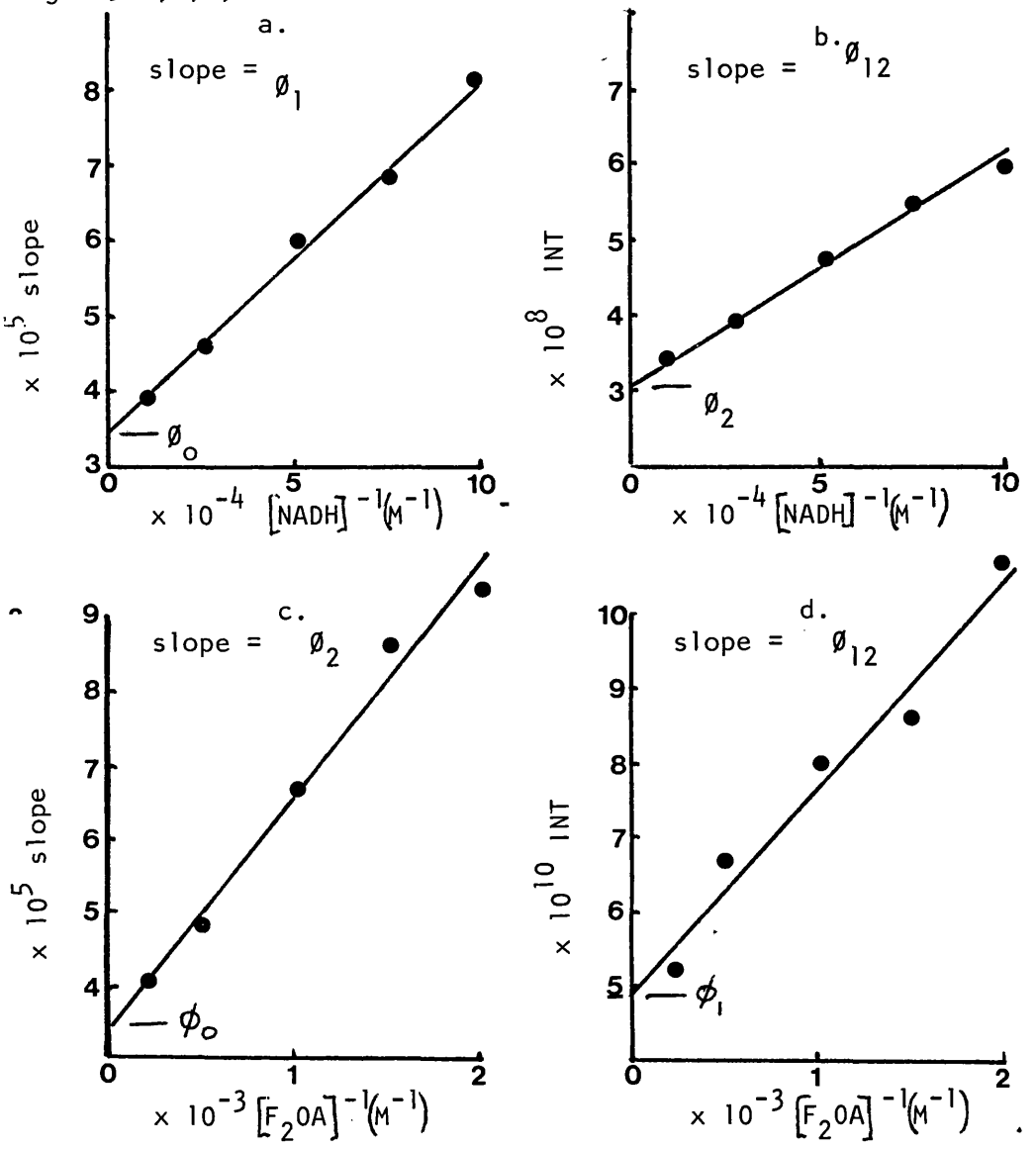

Fig. 3: Secondary plots of parameters obtained from primary plots shown in Fig. 1 and 2. a) slopes from Fig. 2 versus reciprocal [NADH] b) ordinate intercepts from Fig. 2 versus reciprocal [NADH]. c) slopes from Fig. 1 versus reciprocal [$F_2$0A]. d) ordinate intercepts from Fig. 1 versus reciprocal [$F_2$0A]. The coefficients obtained are indicated on the appropriate plots.

The values of the coefficients obtained from the plots shown in Fig. 3 are displayed in Table 1.

Coefficient	Value	
$\emptyset_o$	3.43×10^{-5}	MA^{-1}
$\emptyset_1$	4.75×10^{-10}	MA^{-1}.Moles/litre
$\emptyset_2$	3.12×10^{-8}	MA^{-1}.Moles/litre
$\emptyset_{12}$	2.93×10^{-13}	MA^{-1}.(Moles/litre)^2
$\emptyset_{12}/\emptyset_2$	9.39×10^{-6}	Moles/litre
$\emptyset_1\emptyset_2/\emptyset_{12}$	5.05×10^{-5}	MA^{-1}

Table 1: Values of the kinetic coefficients determined in the preceding experiment. MA represents the molecular activity expressed as the moles of product produced per min per mole of enzyme, calculated using 70,000 as the molecular weight of the enzyme.

Protection Studies

Iodoacetamide inactivates pig-heart mitochondrial malate dehydrogenase by reacting specifically with two histidine residues per mole of enzyme (Anderton, 1970). The presence of substrates or substrate analogues protects the enzyme, either fully or partially, against inactivation (Anderton and Rabin, 1970).

If a ligand fully protects the enzyme against inactivation, the data may be fitted to the model

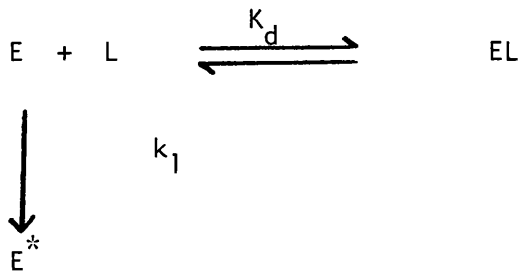

where E, L, EL and E^* represent enzyme, ligand, enzyme-ligand complex and inactivated enzyme respectively. K_d is the dissociation constant of the enzyme-ligand complex and k_1 is the first order rate constant for inactivation of free enzyme in the presence of a large excess of iodoacetamide.

$$\text{Since } K_d = \frac{[E][L]}{[EL]}$$

$$\text{then } [E] = \frac{K_d[EL]}{[L]}$$

$$\text{Since } E_t = [EL] + [E] + [E^*]$$

$$\text{then } [E] = K_d\frac{(E_t - [E] - [E^*])}{[L]}$$

where E_t represents total enzyme.

$$\therefore [E]([L] + K_d) = K_d(E_t - [E^*])$$

$$\therefore [E] = \frac{K_d(E_t - [E^*])}{[L] + K_d}$$

If the rate of inactivation is v,

$$\text{then } v = k_1[E]$$

$$\text{or } v = \frac{k_1K_d(E_t - [E^*])}{[L] + K_d}$$

$$\text{then} \qquad k_1^o = \frac{k_1 K_d}{[L] + K_d}$$

where k_1^o is the observed first order rate constant at that concentration of ligand $[L]$.

$$\therefore \qquad \frac{1}{k_1^o} = \frac{[L]}{k_1 K_d} + \frac{1}{k_1} \qquad (4)$$

Therefore the dissociation constant, K_d, may be obtained from a plot of $\frac{1}{k_1^o}$ versus $[L]$.

If however, the protection is only partial, then the model must be altered to

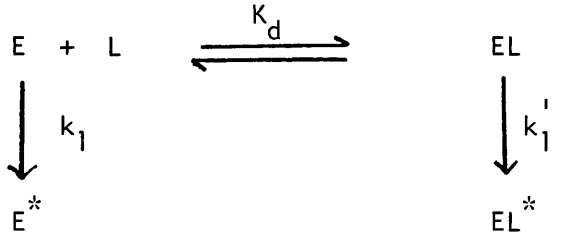

where k_1' is the first order rate constant for inactivation of the EL complex and the other terms have the same meaning as before.

The expression for the rate of inactivation (v) now is

$$v = k_1 [E] + k_1' [EL]$$

$[E]$ and $[EL]$ may be obtained in terms of E_t and $[E^*]$ as before to give:

$$v = \frac{(E_t - [E^*])[k_1 K_d + k_1' [L]]}{K_d + [L]}$$

$$\text{then } k_1^o = \frac{k_1 K_d + k_1' [L]}{K_d + [L]}$$

where k_1^o is the observed first order rate constant at that concentration of ligand, $[L]$.

$$\therefore \quad k_1^o - k_1 = \frac{(k_1' - k_1)[L]}{K_d + [L]}$$

$$\text{and} \quad \frac{1}{k_1^o - k_1} = \frac{K_d}{[L](k_1' - k_1)} + \frac{1}{(k_1' - k_1)} \qquad (5)$$

Thus a plot of the reciprocal of the difference between the rate constant in presence and absence of protecting ligand versus the reciprocal of the ligand concentration should give a straight line from which K_d may be determined.

The enzyme (30 µg/ml) was incubated at 27° in 50 mM TEA buffer, pH 7.4, containing iodoacetamide (2.1 mM) and varying concentration of difluoro-oxaloacetate (0-8 mM). Aliquots (10 µl) of the incubation mixtures were removed at intervals throughout the experiment, diluted in 10 mls of TEA buffer (50 mM, pH 7.4) and assayed for malate dehydrogenase using the standard assay.

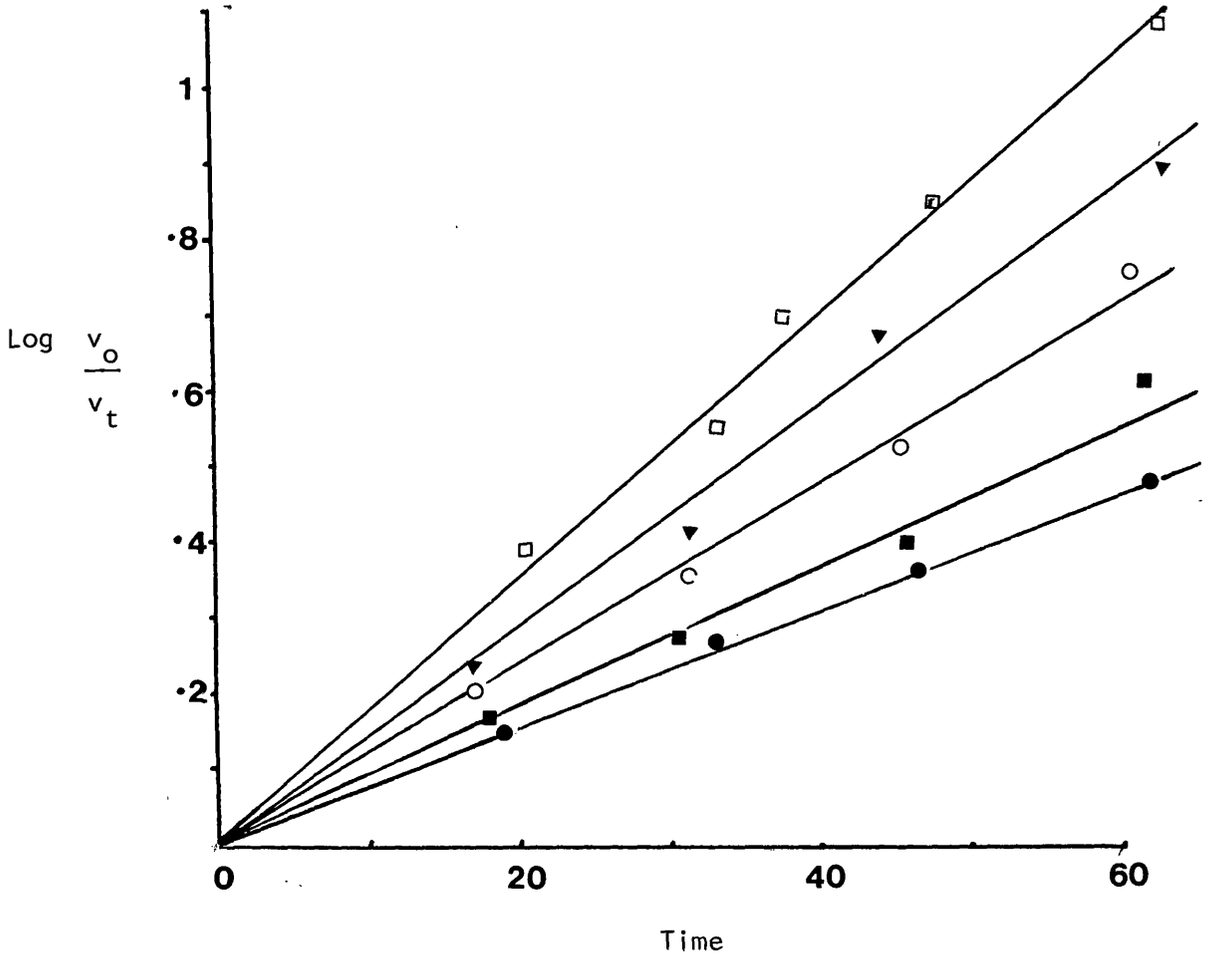

Fig. 4: Semi-logarithmic plot of log ($^{Vo}/Vt$) against time, where V_o is the enzyme activity at time zero, and V_t is the activity at time t. Enzyme activity was assayed as described in the text. The lines were fitted to the points by linear regression analysis. The rate constant for inactivation was calculated from the slopes of the graphs, difluoro-oxaloacetate concentrations: (□), 0; (▼), 2 mM; (0), 4 mM); (■), 6 mM; (●), 8 mM.

The apparent first order rate constants for inactivation were calculated from plots of log V_o/V_t against time where v_o is the enzyme activity at time zero and v_t is the activity at time t. The semi-log plot is shown in Fig. 4.

Preliminary experiments using high concentrations of difluoro-oxaloacetate (0.1 M) indicated that only partial protection against inactivation was afforded to the enzyme and the data were treated according to equation (5). The results are shown in Fig. 5.

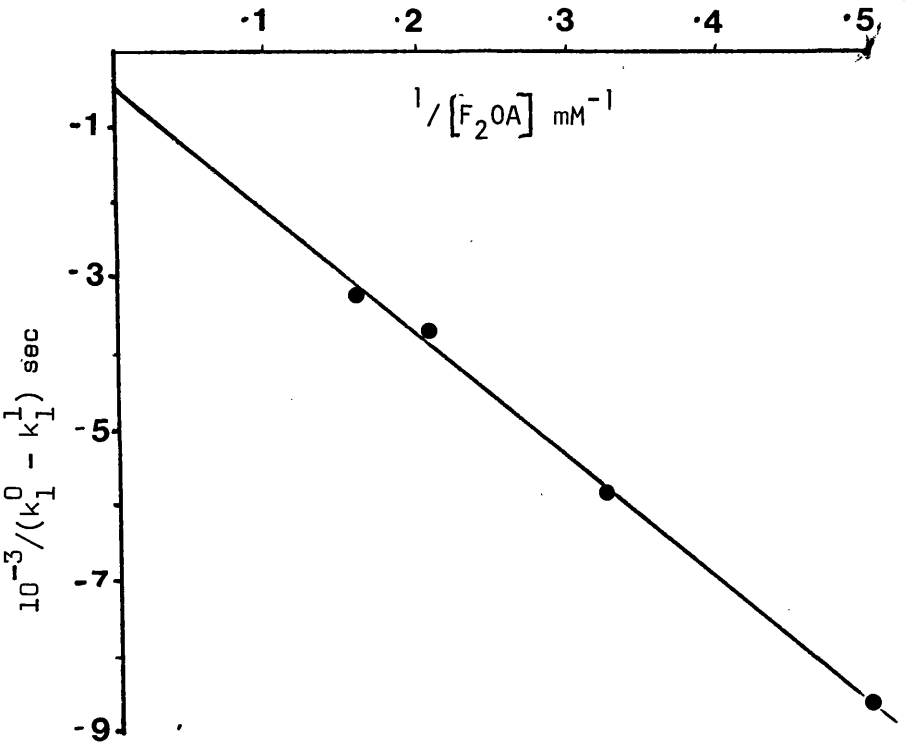

Fig. 5: Double reciprocal plot of the difference between the rate constant for inactivation in the presence and absence of difluoro-oxaloacetate versus difluoro-oxaloacetate concentration.

From the graph shown in Fig. 5, the dissociation constant (K_d) for the enzyme-difluoro-oxaloacetate complex was calculated as 27.7 mM.

A similar experiment was performed to demonstrate the formation of the abortive ternary complex between enzyme NAD and difluorooxaloacetate. Preliminary experiments using 0.1 M difluoro-oxaloacetate and 10 mM NAD showed that this combination fully protected the enzyme; to simplify analysis the experiment was performed at saturating levels of NAD. Conditions were the same as for the previous experiment except that the incubation mixtures contained NAD (10 mM). The first order rate constants for inactivation at each difluoro-oxaloacetate concentration were determined as before and the data analysed according to equation (4) The results are shown in Fig. 6.

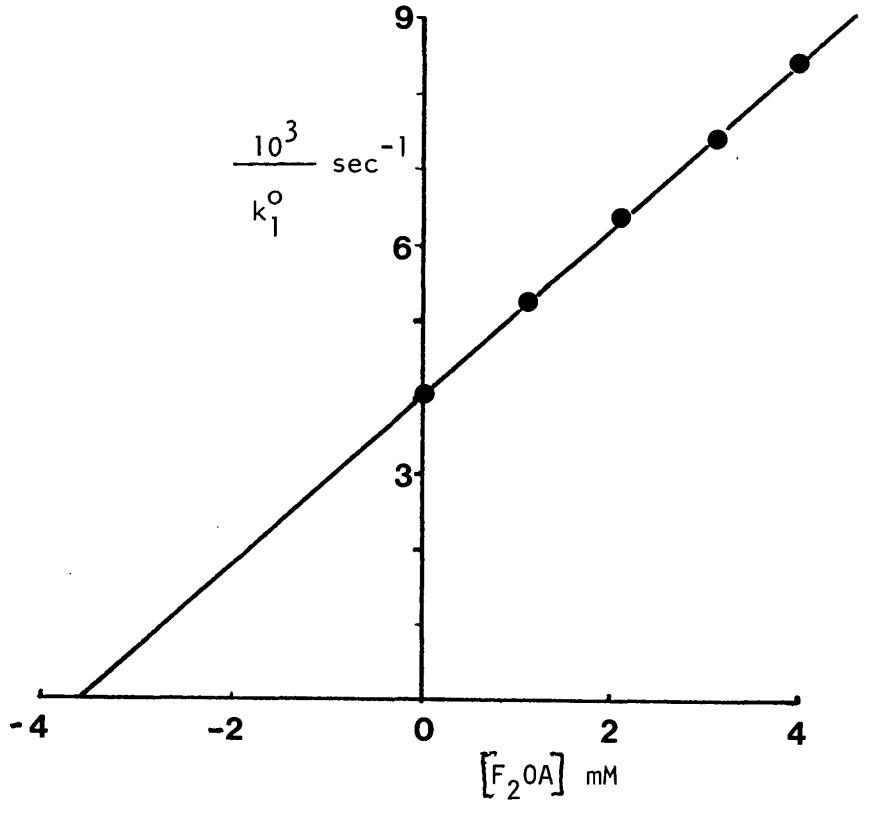

Fig. 6: Variation of the reciprocal of the apparent first order rate constant for inactivation of m.MDH with difluoro-oxaloacetate concentrations, in the presence of 10 mM NAD.

The dissociation constant for difluoro-oxaloacetate from MDH-NAD complex was calculated from the data shown in Fig. 6, and found to be 3.2 mM.

The observation that difluoro-oxaloacetate alone partially protected the enzyme against inactivation by iodoacetamide may appear to conflict with the results of Anderton and Rabin (1970) who found that 5 mM oxaloacetate afforded no protection against inactivation. Since the dissociation constant for the binary complex of enzyme and difluoro-oxaloacetate was found to be quite high (27.7 mM), a protection experiment was carried out using oxaloacetate at higher levels than in the previous study.

Experimental conditions were the same as for the study with difluoro-oxaloacetate alone, except that oxaloacetate was the protecting agent. The resulting data were treated according to equation (5), assuming that protection by oxaloacetate would only be partial. The appropriate plot is shown in Fig. 7.

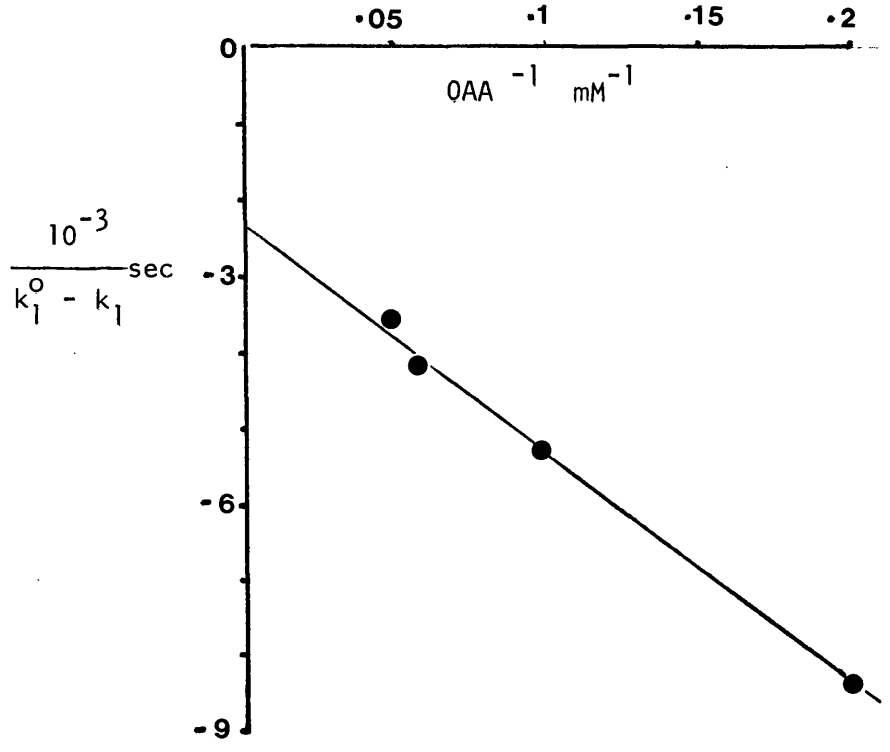

Fig. 7: Protection by oxaloacetate against inactivation by iodoacetate The reciprocal of the difference between the observed first order rate constant and the rate constant in the absence of oxaloacetate plotted against the reciprocal oxaloacetate concentration. Oxaloacetate was varied between 0 and 20 mM and the apparent rate constants for inactivation determined as before.

The dissociation constant of oxaloacetate from the enzyme-oxaloacetate complex was calculated from the data shown in Fig. 7 , and found to be 14.4 mM. Thus oxaloacetate is also shown to form a binary complex with malate dehydrogenase. The results from this set of experiments are presented in Table 2.

Ligand	K_d mM	K_d in presence of saturating [NAD]
Oxaloacetate	14.4	*0.8
Difluoro-oxalo-acetate	27.7	3.2

Table 2: Dissociation constants of oxaloacetate and difluoro-oxaloacetate-MDH complexes with and without NAD. * taken from Anderton and Rabin (1970).

The protection experiments indicate that the binding of difluoro-oxaloacetate to malate dehydrogenase is enhanced in the presence of NAD (K_d decreased 8.7 fold). This finding was confirmed by examining the n.m.r. chemical shift of difluoro-oxaloacetate in the presence of malate dehydrogenase, with and without added NAD.

Difluoro-oxaloacetate (final concentration 6 mM) was added to 0.4 ml of 0.7 mM MDH in 50 mM TEA buffer, pH 7.4, contained in a 5 mm diameter n.m.r. tube. The ^{19}F chemical shift of the ligand was measured relative to that 2 M difluoro-oxaloacetate (pH 3.7) contained in a co-axial capillary tube. The chemical shifts of difluoro-oxaloacetate in buffer alone and in the presence of malate dehydrogenase were found to be identical. Addition of NAD (final concentration 10 mM) caused the ^{19}F n.m.r. signal to broaden and shift downfield. Addition of successive aliquots of difluoro-oxaloacetate, cause the signal to sharpen and move upfield. The chemical shift after each addition was measured and the data analysed by the iterative procedure used in the n.m.r. investigation of the difluoro-oxaloacetate-aspartate transaminase abortive complex. The minimum error variance of a plot of S_{ob} versus $[EI]/[I]$ occurred at a K_d of 4.1 mM. This plot is shown in Fig. 8, the slope of which gives a Δ value of 37.2 hz downfield from free difluoro-oxaloacetate in 50 mM TEA buffer, pH 7.4.

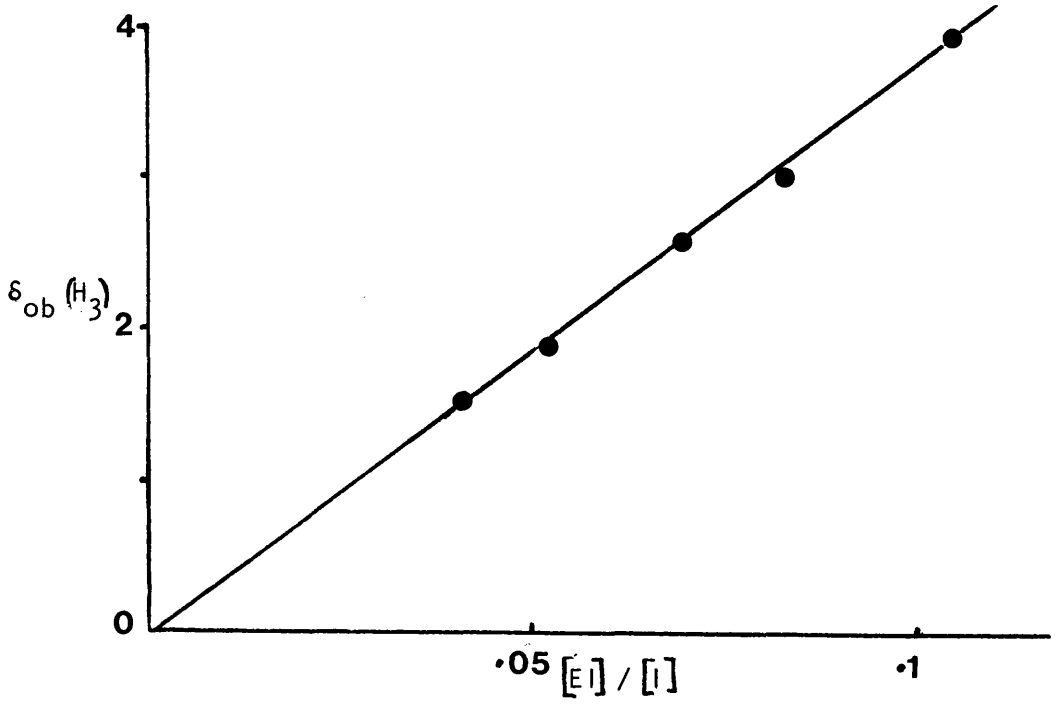

Fig. 8: Plot of δ_{ob} versus $[EI]/[I]$ at K_D = 4.1 mM. Experimental conditions are given in the text. $[I]$ represents the concentration of ligand and $[EI]$ the concentration of the enzyme ligand complex.

Addition of oxaloacetate (final concentration 20 mM) to a solution of 1 mM MDH in TEA buffer (50 mM pH 7.6) containing 8 mM difluoro-oxaloacetate and 1 mM NAD, caused the ^{19}F n.m.r. signal of the fluoro compound to shift upfield to a position identical to that of difluoro-oxaloacetate in buffer alone.

Difluoro-oxaloacetate as an inhibitor of the MDH catalysed oxidation of L-malate by NAD

It has been shown (Kun et al, 1963) that difluoro-oxaloacetate is an effective inhibitor of malate dehydrogenase. In order to establish the mode of inhibition, the effect of different fixed levels of difluoro-oxaloacetate on the initial velocity as both [NAD] and [L-malate] were systematically varied, was studied. Inhibition may occur by any of the following mechanisms either singly or in combination:

1) Formation of an abortive binary complex between inhibitor and enzyme
2) Formation of an abortive ternary complex between inhibitor, coenzyme and enzyme
3) Since the inhibitor is a good substrate for the enzyme, it may act as an alternate product inhibitor, affecting the rate by the law of mass action.

The exact type of inhibition may be determined from the nature of the primary and secondary plots of the data.

Difluoro-oxaloacetate (0 to 8 mM) was added to a cuvette (5 cm pathlength) containing L-malate (0.1 to 1.0 mM) and NAD (0.16 to 1.0 mM) in 6 ml of 0.1 M TEA buffer, pH 8.0, maintained at 27°C. The reaction was initiated by the addition of 0.15 µg of enzyme. The results of the experiment are shown as plots of [S]/v versus [S]

in Figs. 9 and 10. Secondary plots of the ordinate intercepts and slopes of the primary plots versus [I], the concentration of difluoro-oxaloacetate, are shown in Figs. 11a and b.

The primary plots are linear and in each case both slope and ordinate intercept vary as the concentration of difluoro-oxaloacetate is varied, indicating mixed type inhibition. The replots of the ordinate intercepts of primary plots versus [I] show upward curvature (parabolic inhibition) as [I] is increased, as does the replot of slope versus [I] from Fig. 9, ([Malate] constant, [NAD] varying). The other replot of slope ([NAD]constant, [Malate] varying) versus [I] is apparently linear, with an abscissa intercept of -3.68 mM.

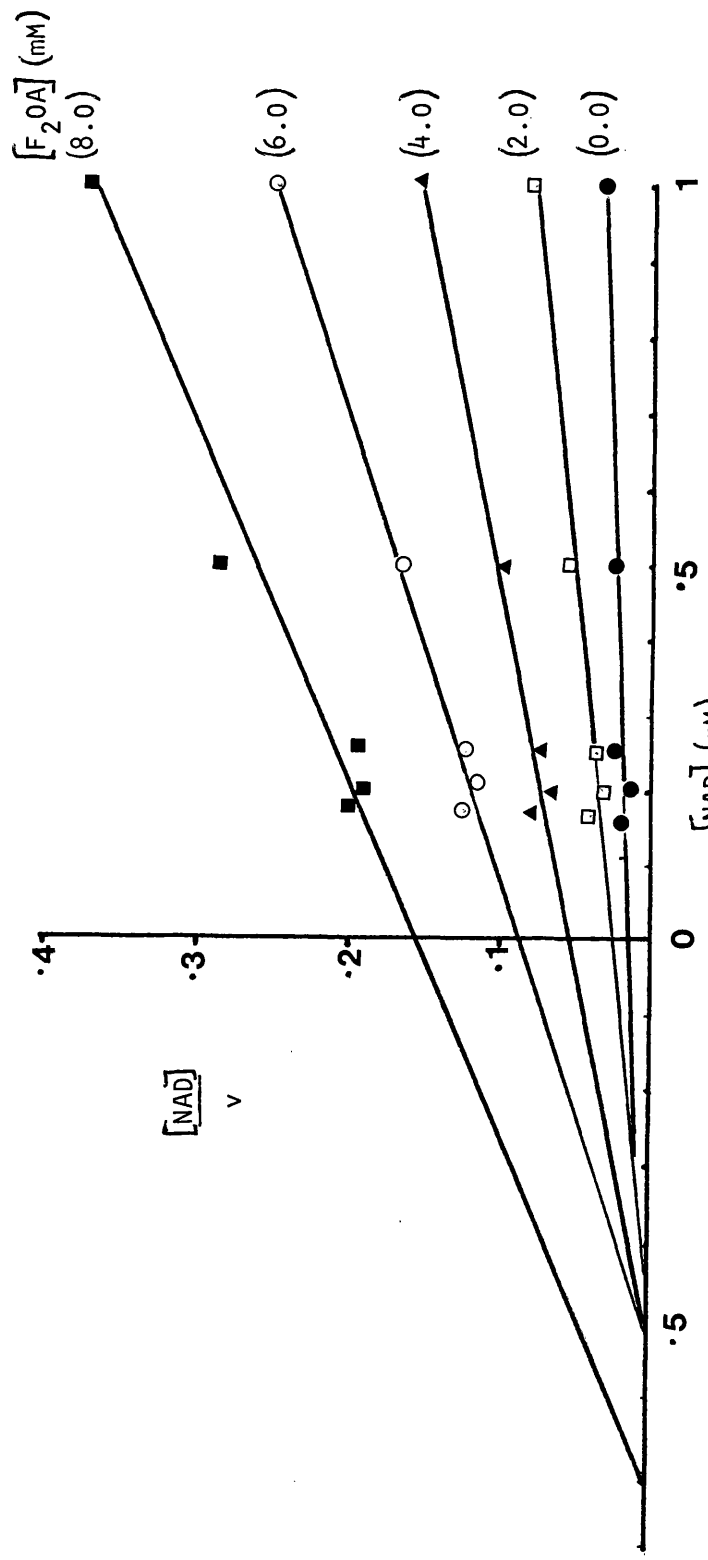

Fig. 9: Plot of NAD /v versus NAD at constant Malate (1.0 mM) and various difluoro-oxaloacetate (F_2OA). The concentration of F_2OA is indicated in parentheses at the end of each curve. All other conditions are as stated in the text. The lines were fitted to the points as described in Methods. The velocity is given in arbitrary units.

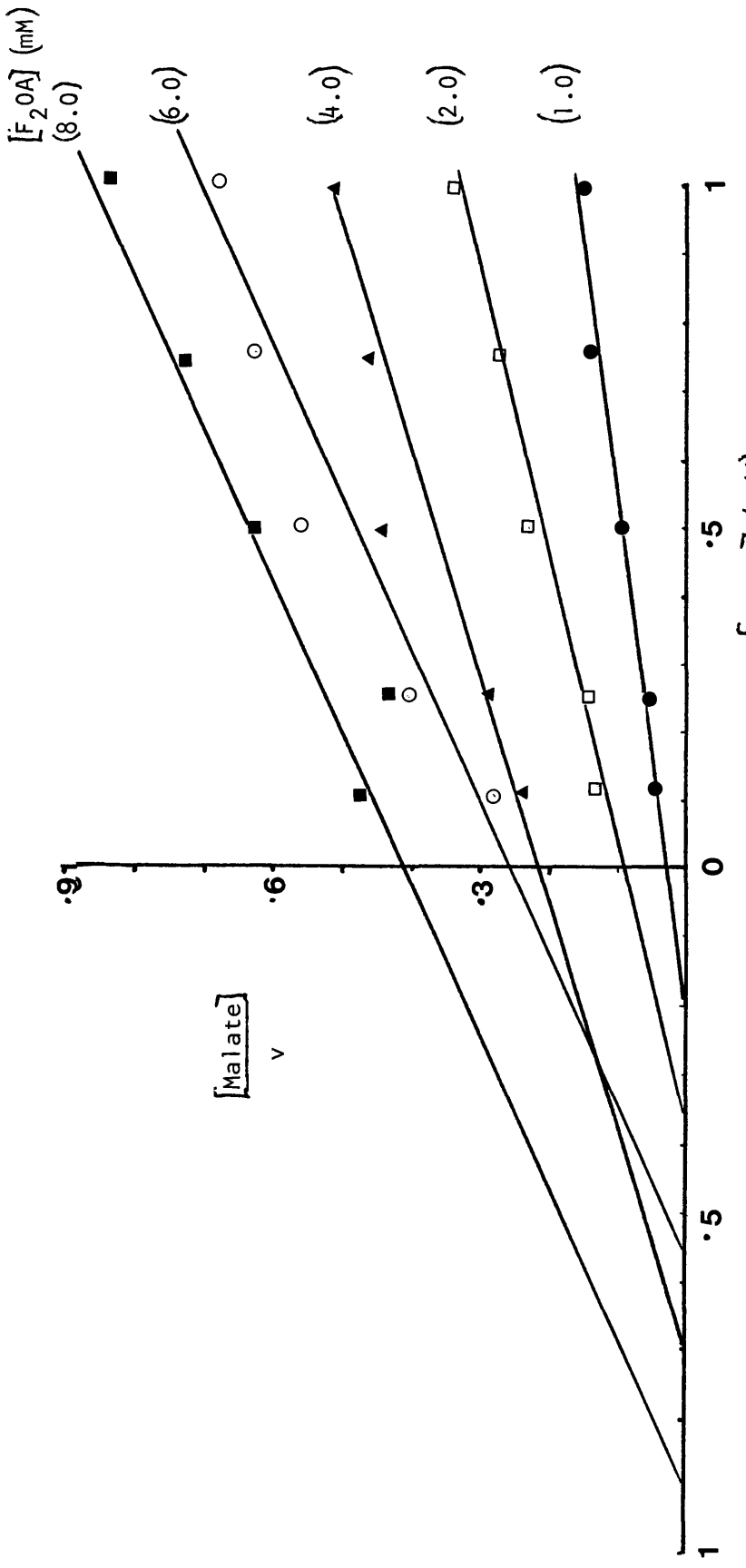

Fig. 10: Plot of Malate /v versus Malate at constant NAD (0.8 mM) and various F_2OA. The F_2OA is indicated in parentheses at the end of each curve. All conditions are the same as for fig.9.

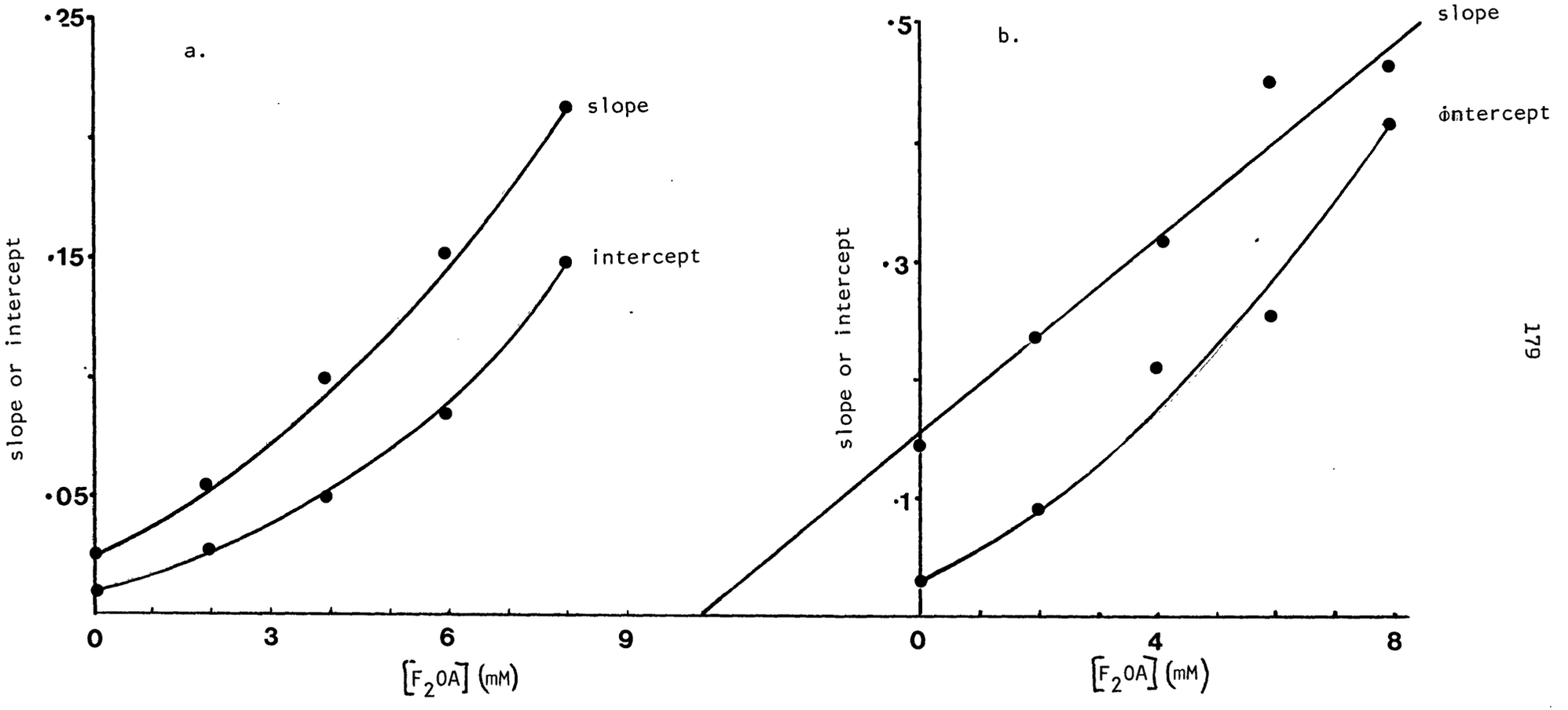

Fig. 11: Secondary plots of slopes and ordinate intercepts from the data in Figs. 9 & 10. versus F_2OA a) Replots from Fig. 9, [NAD] varying, [Malate] constant; b) Replot from Fig. 10, [Malate] varying, [NAD] constant.

Inhibition of difluoro-oxaloacetate reduction by DL-difluoro-malate

Although difluoro-malate is not a substrate for malate dehydrogenase, it has been shown (Kun et al, 1963) to be an inhibitor of MDH-catalysed reduction of oxaloacetate. Experiments were therefore carried out to determine the mode of action of difluoro-malate as a product inhibitor of MDH catalysed reduction of difluoro-oxaloacetate.

Two parallel experiments were performed; in the first, difluoro-oxaloacetate and difluoro-malate concentrations were systematically varied while the NADH concentration was held constant. In the second, NADH and difluoro-malate concentrations were varied and the concentration of difluoro-oxaloacetate was held constant.

Difluoromalate (final concentration 0-8 mM) and the varied substrate (final concentration, F_2OA 0.5-5.0 mM or NADH 0.01-0.10 mM) were added to 50 mM TEA buffer, pH 7.4, containing the substrate held constant ([NADH], 0.1 mM or [F_2OA], 8.0 mM). The experiments were performed in a 1 cm pathlength quartz cuvette, thermostatted to 27°. The final volume was 1.0 ml. The reaction was initiated by the addition of 0.1 µg of malate dehydrogenase, followed by the decrease in absorbance at 340 nm. The results of the experiments are shown in Figs. 12 and 13.

Figs. 12 and 13 show that inhibiton of difluoro-oxaloacetate reduction by difluoro-malate is of the pure non-competitive type, i.e. binding of the ligand decreases the Vmax for the reaction but does not effect the Michaelis constants for either NADH or difluoro-oxaloacetate. Secondary plots of the ordinate intercept and slope from the primary plots versus the concentration of difluoro-malate are shown in Fig. 14a-d. Each plot shares a common interecept on the abscissa axis. The value of the abscissa intercept determined from these four plots is 3.86 ± .08mM.

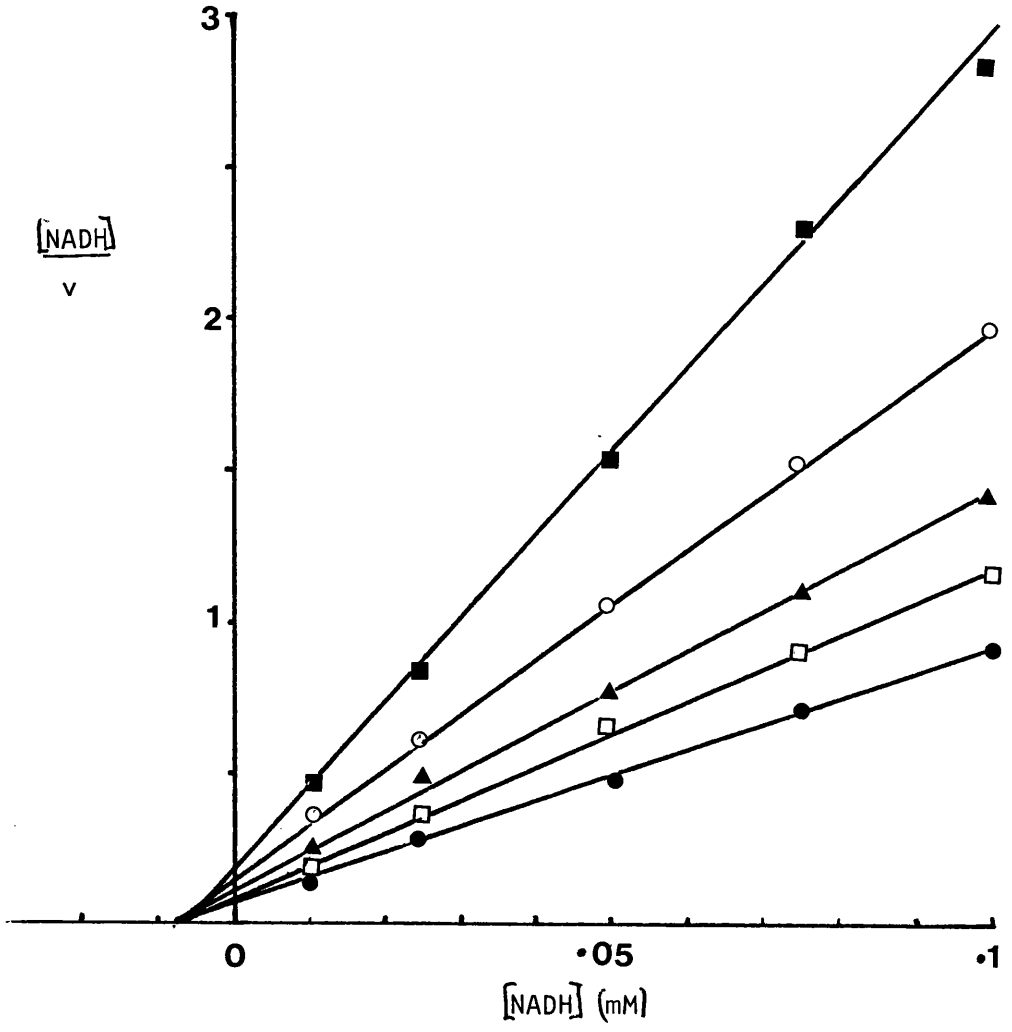

Fig. 12: Plot of [NADH]/v versus [NADH], showing inhibiton of reaction by Difluoromalate. Difluorooxaloacetate was held constant at 8.0 mM. The straight lines were fitted to the points using parameters calculated from direct linear plots of $^{v}/_{s}$ versus $^{1}/_{s}$. Difluoromalate concentrations: (●), zero; (□), 1 mM; (▲), 2 mM; (o), 4 mM; (■) 8 mM.

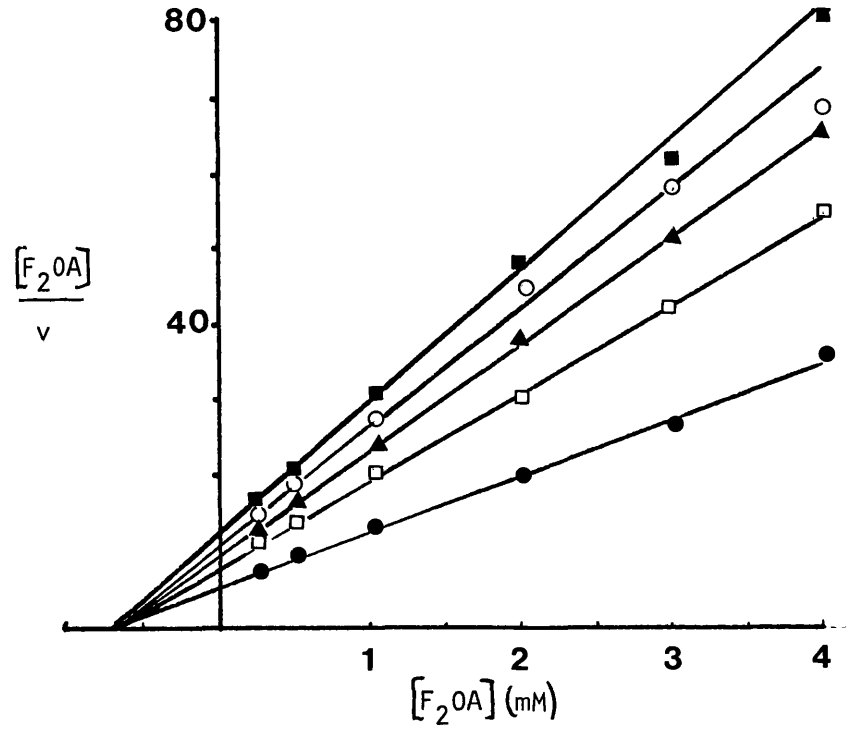

Fig. 13: Plot of F_2OA /v versus F_2OA, at various levels of difluoromalate. [NADH] was held constant at 0.1 mM. The initial velocity (v) was given as Δ OD_{340}/min. Difluoromalate concentrations: (●), zero; (□), 2 mM; (▲), 3 mM; (o), 4 mM; (■), 5 mM.

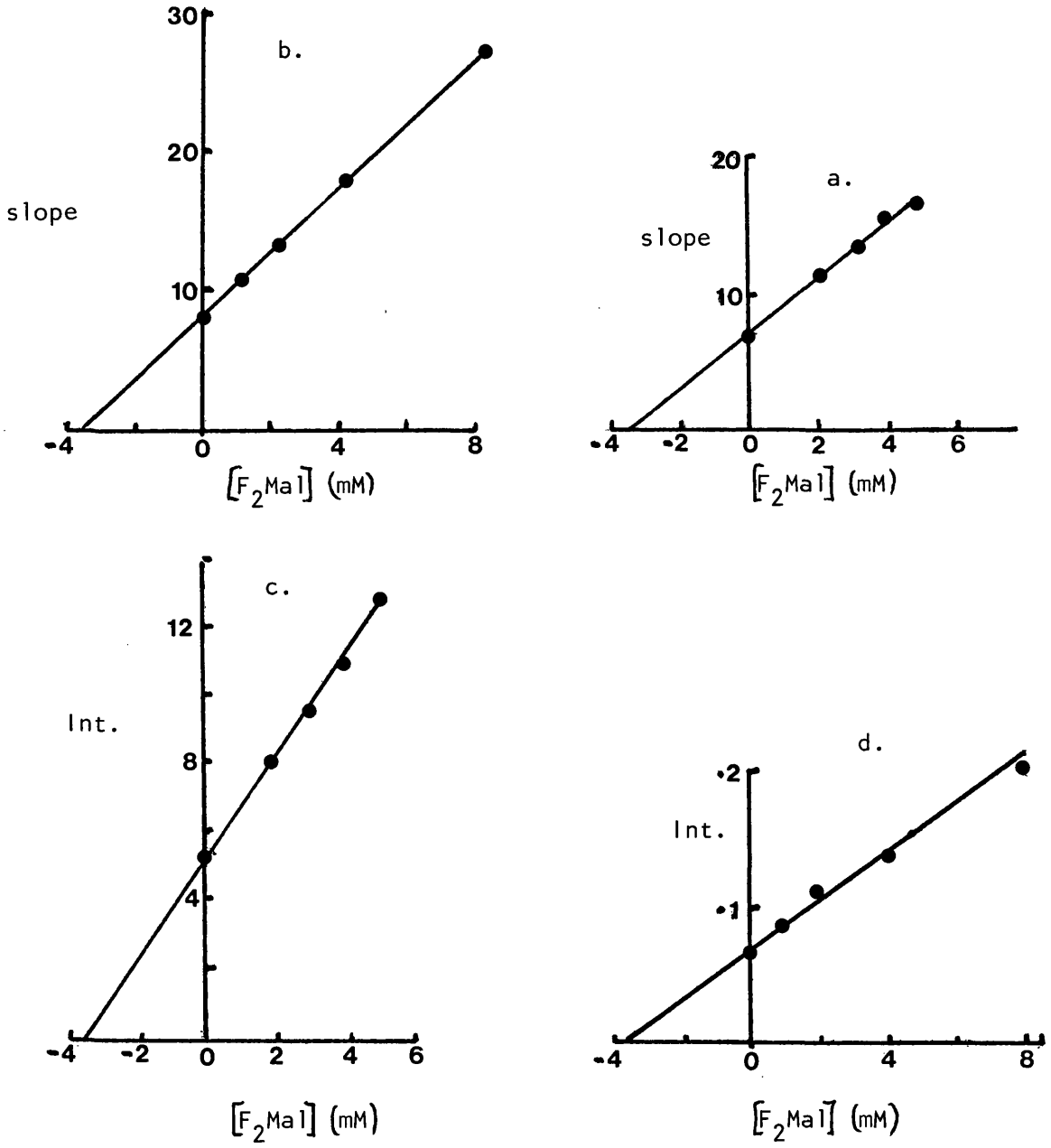

Fig. 14: Secondary plots of the parameters obtained from Figs. 12 & 13 a) Slopes (Fig 12) versus [F2Mal]; b) Slopes (Fig. 13) versus [F2Mal]; c) ordinate intercept (Fig.12) versus [F2Mal]; d) ordinate intercept (Fig.13) versus [F2Mal]

DISCUSSION

Non-productive binding of difluoro-oxaloacetate to malate dehydrogenase

Difluoro-oxaloacetate was shown to protect malate dehydrogenase against inactivation by iodoacetamide, affording partial protection in the absence of NAD and complete protection in the presence of the coenzyme. This demonstrates that difluoro-oxaloacetate binds to malate dehydrogenase and must bind in such a way so as to prevent alkylation of the active site histidine by iodoacetamide. The fact that the ternary abortive complex gives complete protection indicates either that the presence of the co-enzyme alters the binding of the fluoro compound so that the substrate analogue completely restricts access to the histidine or that both binding sites are close together and the combination of both molecules blocks access. The latter hypothesis is the more reasonable since NAD alone affords partial protection against inactivation by iodoacetamide (Anderton and Rabin, 1970).

The protection experiments show that the presence of the coenzyme (NAD) markedly lowers the dissociation constant of difluoro-oxaloacetate from the enzyme from 27.7 mM to 3.2 mM. Oxaloacetate has been reported not to bind to malate dehydrogenase in the absence of coenzyme (Anderton and Rabin, 1970). However in the present study oxaloacetate alone was shown to protect the enzyme against alkylation by iodoacetamide. The enzyme-oxaloacetate dissociation constant was 14.4 mM; in the presence of NAD, the dissociation constant was 0.8 mM. Thus under the conditions of these experiments, difluoro-oxaloacetate behaves in a similar manner

to the natural keto acid.

It is difficult however, to understand why in the similar protection study of Anderton and Rabin (1970), no protection by oxaloacetate against inactivation by iodoacetamide was observed at 5 mM keto acid. The experiments reported in this thesis were carried out in triethanolamine buffer at pH 7.4; those of Anderton and Rabin in phosphate buffer, pH 7.8. The histidine that is alkylated has a pK of 7.1 (Anderton and Rabin, 1970). Therefore at pH 7.4, 33.4% of this group exists in the protonated form, but at pH 7.8 only 16.6% is protonated. If the protonated histidine is involved in binding the keto-acid via a negatively charged carboxylate group, then the difference in pH may account for the apparent discrepancy.

The marked lowering of the dissociation constants for both oxaloacetate and difluoro-oxaloacetate from their respective complexes with the enzyme in the presence of NAD, suggests that binding of the coenzyme induces a change, conformational or electrostatic, which greatly enhances the affinity of the enzyme for these keto acids.

The n.m.r. binding experiment confirms the results obtained from the protection study. Although n.m.r. spectroscopy is not sensitive enough to detect binding of ligand by the enzyme alone, in the presence of coenzyme, formation of a complex was detected by the shift and broadening in the ^{19}F n.m.r. signal. The value of 4.1 mM calculated for the dissociation constant of difluoro-oxaloacetate from the enzyme. NAD.ligand complex is in good agreement with that calculated from the protection studies (3.2 mM).

Addition of 20 mM oxaloacetate to the enzyme, coenzyme, difluoro-oxaloacetate mixture, caused the ^{19}F n.m.r. signal of the fluoro compound to shift to a position identical with that of that ligand in buffer alone. This indicates that excess oxaloacetate displaces difluoro-oxaloacetate from the enzyme, and that both keto acids are binding at the same site on the enzyme in this non-productive binding mode.

Δ, the chemical shift of the ^{19}F n.m.r. signal of difluoro-oxaloacetate in the enzyme-coenzyme-ligand complex is 36 hz downfield from that of free ligand in buffer. This chemical shift is in the opposite direction to that found for the difluoro-oxaloacetate-aspartate aminotransferase complex, (Δ = 137 hz, upfield from free ligand). Decreasing the polarity or increasing the pH or ionic strength of the medium also causes an upfield shift in the ^{19}n.m.r. signal of difluoro-oxaloacetate, (see Section 2, n.m.r. studies on aspartate aminotransferase), and therefore the chemical shift of difluoro-oxaloacetate bound to malate dehydrogenase cannot be accounted for by micro-environmental changes of this nature. However, deshielding of the ^{19}F-nuclei may result from the close proximity of the coenzyme aromatic ring structure.

Difluoro-oxaloacetate as a substrate for malate dehydrogenase

Difluoro-oxaloacetate was shown to be a substrate for mitochondrial malate dehydrogenase, and a number of kinetic coefficients obtained from the variation of initial rate with changes in the initial concentrations of substrates (Table 1).

The following mechanisms can be excluded on the basis of theoretically required values of the various coefficients (Dalziel, 1957).

1) No binary enzyme substrate complexes, but a single ternary complex is formed. This requires that $\emptyset_1$ and $\emptyset_2$ be zero.
2) A binary complex mechanism in which the enzyme is itself reversibly oxidised and reduced. This mechanism requires that $\emptyset_{12}$ be zero.
3) Reversible oxidation and reduction of the enzyme without the formation of an enzyme substrate complex. This requires that $\emptyset_o$ and $\emptyset_{12}$ be zero.

Although equation (1) is applicable to a number of mechanisms, the coefficients will contain different combinations of rate constants depending on the particular mechanisms. Thus the mechanism involved may be distinguished on the basis of the relationships between the coefficients. The derivation of the relationships for the mechanisms listed below is given in Appendix (2).

1a) Compulsory order mechanism, involving no kinetically discernable ternary complex (Theorell-Chance).

$$\frac{\emptyset_1\emptyset_2}{\emptyset_{12}} = \emptyset_o' \quad \text{(where primed coefficients indicate the reverse action)}$$

and $\emptyset_{12}/\emptyset_2 = {}^{k}{}_{-1}/k_1 = \overline{K}a$ (the dissociation constant for (EA) complex)

1b) Compulsory order mechanism involving at least one kinetically discernable ternary complex.

$$\frac{\emptyset_1\emptyset_2}{\emptyset_{12}} < \emptyset_o' \quad \text{and } \emptyset_{12}/\emptyset_2 = \overline{K}a$$

2a) Random order mechanism, where the binding of one substrate does not affect the affinity of the enzyme for the second substrate. All equilibria are rapidly adjusted except for the interconversion of two kinetically important ternary complexes.

$$\frac{\emptyset_1\emptyset_2}{\emptyset_{12}} = \emptyset_o \text{ and } \emptyset_{12}/\emptyset_2 = \overline{K}a$$

2b) Random order mechanism as for 2a), without the restrictions on the dissociation constants.

$$\emptyset_{12}/\emptyset_1 = \overline{K}a$$

Mechanism (2a) may be rejected because $\emptyset_1.\emptyset_2/\emptyset_{12} \neq \emptyset_o$. As the dissociation constant ($\overline{K}a$) for the enzyme-NADH complex is 0.01 mM (Anderton and Rabin, 1970), mechanism (2b) may be rejected because this gives a value to $\overline{K}a$ of .6 mM whereas mechanisms (1a) and (1b) give $\overline{K}a$ = .0094 mM, a much closer agreement.

Mechanism (1a) and (1b) may theorteically be distinguished by the relationship of $\emptyset_1.\emptyset_2/\emptyset_{12}$ to $\emptyset_o'$. This however requires a knowledge of the reverse reaction, and at concentrations of difluoromalate up to 0.1M, no substrate activity, in terms of reduction of NAD, could be demonstrated.

The Michaelis constants for difluoro-oxaloacetate and NADH may be obtained from the secodnary plots of Fig. 3a and c. Equation (1) is

a general equation which covers both mechanisms (1a) and (1b), therefore

$$\text{Slope (Fig.3a)} = \left[\frac{\phi_o + \phi_1}{[A]}\right] = \left[1 + \frac{K_A}{[A]}\right] \frac{Et}{Vmax}$$

$$\text{Slope (Fig.3c)} = \left[\frac{\phi_o + \phi_2}{[B]}\right] = \left[1 + \frac{K_B}{[B]}\right] \frac{Et}{Vmax}$$

Therefore $K_A = \phi_1/\phi_o$ and $K_B = \phi_2/\phi_o$, which gives $K_A = 1.38 \times 10^{-5}$M and $K_B = 9.09 \times 10^{-4}$M.

Thus the Michaelis constant for NADH is not significantly different from that found with oxaloacetate, the natural substrate (1.8×10^{-5}M, Raval and Wolfe, 1962). The Km for difluoro-oxaloacetate is considerably higher than that of oxaloacetate (3.0×10^{-5}M, Raval and Wolfe, 1962). Assuming the simplest mechanism, that is one containing a kinetically insignificant ternary complex (Theorell-Chance mechanism), several rate constants may be evaluated from the kinetic coefficients since in a Theorell-Chance mechanism $\phi_o = {}^1/k_3$; $\phi_1 = {}^1/k_1$; $\phi_2 = {}^1/k_2$; $\phi_{12} = {}^{k_{-1}}/k_1.k_2$. The mechanism together with the calculated rate constants is shown in Scheme 4.

$$E + NADH \underset{k_{-1}=1.5 \times 10^2\ s^{-1}}{\overset{k_1=2.48 \times 10^7 M^{-1}s^{-1}}{\rightleftharpoons}} E.NADH$$

$$ENADH + F_2OA \underset{k_{-2}}{\overset{k_2=2.55 \times 10^5 M^{-1}s^{-1}}{\rightleftharpoons}} E.NAD + F_2Mal$$

$$E.NAD \underset{k_{-3}=7.76 \times 10^5\ M^{-1}s^{-1}}{\overset{k_3=3.96 \times 10^2\ s^{-1}}{\rightleftharpoons}} E + NAD$$

Scheme 4: Theorell-Chance mechanism for malate dehydrogenase catalysed reduction of difluoro-oxaloacetate (F_2OA) by NADH. The kinetic constants k_1, k_{-1}, k_2 and k_3 were calculated from the kinetic coefficients. The dissociation constant of NAD from the E.NAD complex was determined from protection experiments and was found to be 0.51 mM. The kinetic constant k_{-3} could therefore be calculated.

Incubation of 0.1M NAD with .05M difluoromalate in the presence of malate dehydrogenase did not produce a change in the absorbance of the system at 340 nm. If the failure to show substrate activity is solely due to the position of the equilibrium, then a lower limit may be assigned to k_{-2}. Under the experimental conditions the smallest observable change in absorbance was 0.01 units. Therefore, the concentration of NADH (and also difluoro-oxaloacetate) formed was $< 1.6 \times 10^{-6}$. Using the equilibrium expression:

$$\frac{[F_2OA][NADH]}{[F_2Mal][NAD]} = \frac{k_{-1}k_{-2}k_{-3}}{k_1k_2k_3} = Keq$$

a value of $k_{-2} \leq 2.4 \times 10^{-17} s^{-1}$ may be obtained. Although the data have been fitted to a model with a kinetically significant ternary complex, a mechanism containing a kinetically significant ternary complex is also possible. In this case the values of k_1 and k_{-1} remain the same, but it is not possible to assign specific values to the remaining rate constants from the available data.

Inhibition of m-MDH catalysed oxidation of L-malate by difluoro-oxaloacetate

Difluoro-oxaloacetate was shown to be an effective inhibitor of m-MDH

catalysed oxidation of L-malate. When [malate] was varied and [NAD] held constant, or [NAD] varied and [malate] held constant, at different fixed levels of difluoro-oxaloacetate, then plots of [S]/v versus (S) were families of straight lines in which both slope and ordinate intercept varied. A replot of the slopes of Fig. 10, ([NAD] constant, [malate]varying) versus [I] (difluoro-oxaloacetate) was linear with an abscissa intercept of -3.68 mM. Replots of the slope from Fig. 9 and ordinate intercepts from Figs. 9 and 10 against [I] were non-linear, curving upward with increasing [I].

Consideration of the ways in which the inhibitor can interact with the enzyme to cause inhibition, enables prediction of expected inhibition patterns from the way in which the initial rate expression is modified as a result of these interactions.

Given that malate dehydrogenase follows a Theorell chance mechanism involving a kinetically insignificant ternary complex (Ravel & Wolfe, 1962b) (Scheme 5)

$$E + A \underset{k_{-1}}{\overset{k_1}{\rightleftharpoons}} EA$$

$$EA + B \underset{k_{-2}}{\overset{k_2}{\rightleftharpoons}} ED + C$$

$$ED \underset{k_{-3}}{\overset{k_3}{\rightleftharpoons}} E + D$$

Scheme 5

where E represents malate dehydrogenase, A, B, C and D represent NAD,

malate, oxaloacetate and NADH and EA and ED are binary complexes of the enzyme with NAD and NADH respectively.

The expression relating the initial velocity (v_f) to the substrate concentrations is then:

$$v_f = \frac{Vmax}{1 + \frac{K_A}{[A]} + \frac{K_B}{[B]} + \frac{K_{AB}}{[A][B]}} \qquad 6$$

where $[A]$ and $[B]$ are as defined previously, and

$K_A = \frac{k_3}{k_1}$, $K_B = \frac{k_3}{k_2}$, $K_{AB} = \frac{k_{-1}k_3}{k_1 k_2}$ and $Vmax = [E_t]\ k_3$.

Difluoro-oxaloacetate (I), may act as an inhibitor by forming an abortive binary complex with free enzyme (Scheme 6).

$$E + I \underset{}{\overset{k_i}{\rightleftharpoons}} EI \qquad \underline{\text{Scheme 6}}$$

where $k_i = [E][I]/[EI]$

This mechanism gives the following rate equation:

$$v_f = \frac{Vmax}{1 + \frac{K_A}{[A]} + \frac{K_B}{[B]} + \frac{K_{AB}}{[AB]} + \frac{[I]K_A}{Ki[A]} + \frac{[I]K_{AB}}{Ki[A][B]}} \qquad 7$$

which may be rearranged to give equations (8) and (9):

$$\frac{[A]}{v_f} = \frac{[A]}{Vm}\left(1 + \frac{K_B}{[B]}\right) + \left(K_A + \frac{K_{AB}}{[B]} + \frac{[I]K_{AB}}{Ki\,[B]} + \frac{[I]K_A}{Ki}\right)\frac{1}{Vm} \qquad (8)$$

$$\frac{[B]}{v_f} = \frac{[B]}{Vm}\left(1 + \frac{K_A}{[A]} + \frac{[I]\,K_A}{Ki\,[A]}\right) + \frac{1}{Vm}\left(\frac{K_{AB}}{[A]} + K_B + \frac{[I]K_{AB}}{Ki\,[A]}\right) \qquad (9)$$

If the data are plotted according to equation (8) and (9), then if the mechanism of inhibition is that suggested by equation (7), plots of $\frac{[A]}{v}$ versus $[A]$ at various levels of $[I]$ should be a family of parallel straight lines; similar plots of $\frac{[B]}{v}$ versus $[B]$ should be a family of straight lines with a common interaction point in the 2nd or 3rd quadrant.

However, inhibition may also result from formation of an abortive ternary complex of difluoro-oxaloacetate with the binary complex (EA, Scheme 5) of enzyme and NAD^+, (Scheme 7)

$$EA + I \underset{}{\overset{Ki'}{\rightleftharpoons}} EAI \qquad \text{(Scheme 7)}$$

where $Ki' = \dfrac{[EA]\,[I]}{[EAI]}$

In this case the appropriate initial rate expression is:

$$v_f = \frac{Vmax}{\left(1 + \frac{K_A}{[A]} + \frac{K_B}{[B]} + \frac{K_{AB}}{[A][B]} + \frac{[I]\,K_B}{[B]\,Ki'}\right)} \qquad (10)$$

leading to equations (8) and (9)

$$\frac{[A]}{v_f} = \frac{[A]}{Vm}\left(1 + \frac{K_B}{[B]} + \frac{[I]K_B}{[B]K_i'}\right) + \frac{1}{Vm}\left(\frac{K_{AB}}{[B]} + K_A\right) \quad (11)$$

$$\frac{[B]}{v_f} = \frac{[B]}{Vm}\left(1 + \frac{K_A}{[A]}\right) + \frac{1}{Vm}\left(\frac{K_{AB}}{[A]} + K_B + \frac{[I]K_B}{K_i'}\right) \quad (12)$$

Thus if the mechanism of inhibition is that resulting from Scheme 7, a plot of $\frac{[A]}{v}$ verus $[A]$ at various levels of $[I]$ will be a family of straight lines having a common ordinate intercept, and a plot of $\frac{[B]}{v}$ versus $[B]$ will be a series of parallel lines.

Finally, inhibition may be due to a combination of both mechanisms, in which case the initial rate expression is:

$$v_f = \frac{Vmax}{\left(1 + \frac{K_A}{[A]} + \frac{K_B}{[B]} + \frac{K_{AB}}{[A][B]} + \frac{[I]K_{AB}}{[A][B]Ki} + \frac{[I]K_A}{[A]Ki} + \frac{[I]K_B}{[B]Ki'}\right)} \quad (13)$$

which may be rearranged to give equations (11) and (12):

$$\frac{[A]}{v_f} = \frac{[A]}{Vm}\left(1 + \frac{K_B}{[B]} + \frac{[I]K_B}{[B]Ki'}\right) + \frac{1}{Vm}\left(K_A + \frac{K_{AB}}{[B]} + \frac{[I]K_{AB}}{[B]Ki} + \frac{[I]K_A}{Ki}\right) \quad (14)$$

$$\frac{[B]}{v_f} = \frac{[B]}{Vm}\left(1 + \frac{K_A}{[A]} + \frac{[I]K_A}{[A]Ki}\right) + \frac{1}{Vm}\left(K_B + \frac{K_{AB}}{[A]} + \frac{[I]K_{AB}}{[A]Ki} + \frac{[I]K_B}{ki'}\right) \quad (15)$$

The appropriate $\frac{[S]}{v}$ versus S plots in this case will each give a series of straight lines in which both slope and ordinate intercept will vary.

From the above equations it can be seen that if inhibition is attributable to any of the suggested mechanisms, it should be possible to distinguish the particular mechanism on the basis of the primary plots. The observed pattern of inhibition being different in each case (Table 3).

Inhibitory complex	[A]/v versus [A]		[B]/v versus [B]	
	slope	intercept	slope	intercept
EI	constant	varying	varying	varying
EAI	varying	constant	constant	varying
EI + EAI	varying	varying	varying	varying

Table 3: Inhibition patterns expected for each of the previously discussed models of inhibitory modes.

The third model, in which inhibition is by the formation of both abortive binary and ternary complexes, appears to fit the data shown in Figs. 9 and 10. However equation (13), reveals that for this model the slope and ordinate intercepts should be a linear function of [I]. Figs. 11a & b, show that this is not the case. There is however another mode of inhibition which can give rise to parabaloid secondary plots. It has been shown that difluoro-oxaloacetate is a good substrate for malate dehydrogenase. This compound may be acting as an alternate product inhibitor and affecting the rate by the law of mass action, Scheme 8.

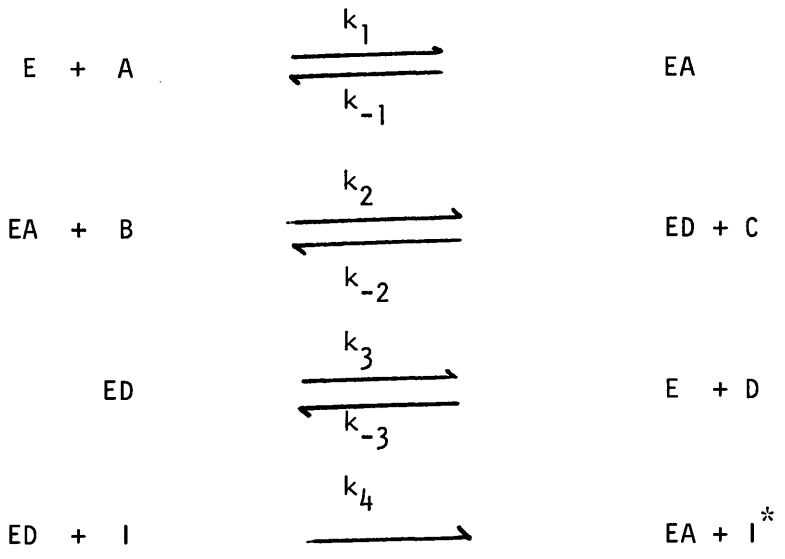

Scheme 8: Reaction sequence for alternate product inhibition by difluoro-oxaloacetate. (I) and (I^*) represent difluoro-oxaloacetate and difluoromalate respectively. All other terms are as previously defined.

The mechanism shown in scheme gives rise to the velocity expression below, (equation 16):

$$v_f = \frac{Vmax}{1 + \frac{K_B}{[B]} + \frac{K_A}{[A]} + \frac{K_{AB}}{[A][B]} + \frac{[I]k_4}{[B]k_2} + \frac{[I]k_{-1}k_4}{[A][B]k_1k_2}} \qquad (16)$$

where Michaelis constants K_A, K_B and K_{AB} are as previously defined. When A (NAD) is the varied substrate, primary plots of $[S]/v$ against $[S]$ at various $[I]$ will show mixed inhibition. When $[B]$ is varied, the primary plots will show competitive inhibition. Secondary plots of slope or ordinate intercept versus $[I]$ will be linear. This mechanism alone cannot account for the observed inhibition.

If in addition to alternate product inhibtion, the possibility of an abortive ternary complex is considered (Scheme, 7), the velocity equation becomes (equation 17).

$$v_f = \frac{Vmax}{\left(1 + \frac{K_A}{[A]} + \frac{K_B}{[B]} + \frac{K_{AB}}{[A][B]} + \frac{[I]k_4}{[B]k_2} + \frac{[I]k_4k_{-1}}{[A][B]k_1k_2} + \frac{[I]K_B}{Ki'[B]} + \frac{[I]^2k_4}{Ki'[B]k_2}\right)} \quad (17)$$

In equation 17, $[I]^2$ terms appear in the rate expression, consistent with the curved secondary plots. However a plot of $[B]/v$ against $[B]$ at various $[I]$, will show competitive inhibition which was not observed.

Alternate product inhibition together with formation of an abortive binary complex of enzyme and inhibitor (Scheme 6) gives rise to the velocity expression shown in equation (18).

$$v_f = \frac{Vmax}{\left(1 + \frac{K_A}{[A]} + \frac{K_B}{[B]} + \frac{K_{AB}}{[A][B]} + \frac{I\ K_A}{[A]Ki} + \frac{[I]K_{AB}}{[A][B]Ki} + \frac{[I]k_4}{[B]k_2} + \frac{[I]k_4k_{-1}}{[A][B]k_1k_2} + \frac{[I]^2k_{-1}k_4}{[A][B]Kik_1k_2}\right)} \quad (18)$$

Equation (18) predicts that plots of $[A]/v$ versus $[A]$ and $[B]/v$ verus $[B]$ at various $[I]$ will be parabolas, but replots of the slopes of the primary plots against $[I]$ will be linear.

Combination of all three modes of inhibition, i.e. alternate product inhibition, abortive binary complex and abortive ternary complex, gives equation (19).

$$v_f = \frac{Vmax}{1 + \frac{K_A}{[A]} + \frac{K_B}{[B]} + \frac{K_{AB}}{[A][B]} + \frac{[I]K_A}{[A]Ki} + \frac{[I]K_{AB}}{[A][B]Ki} + \frac{[I]^2 k_{-1}k_4}{[A][B]k_1k_2Ki} + \frac{[I]k_4}{B\ k_2} \cdots}$$

$$\cdots\cdots + \frac{[I]k_{-1}k_4}{[A][B]k_1k_2} + \frac{[I]K_B}{[B]K_i'} + \frac{[I]^2k_4}{[B]k_2K_i'} \qquad (19)$$

where $Ki = \frac{[E][I]}{[EI]}$ and $K_i' = \frac{[EA][I]}{[EAI]}$

Equation 19 predicts that plots of $[S]/v$ against $[S]$ (where $[S]$ is $[A]$ or $[B]$) at various $[I]$ will show mixed inhibition, and three of the four secondary plots will be parabolic with respect to $[I]$. However the replot of slope ($[B]$ varying, $[A]$ constant) versus $[I]$ will be linear. This situation is the case obtained in the present study.

It may be possible to obtain inhibition parameters from the parabolic replots by iterative curve fitting procedures. In the case of the linear slope replot, the equation corresponding to the graph in Fig. 11b is

$$(slope) = \frac{1}{Vm}\left(1 + \frac{K_A}{[A]} + \frac{[I]K_A}{[A]Ki}\right) \qquad (20)$$

when the value of (slope) is zero then,

$$-\frac{1}{Vm}\left(1 + \frac{K_A}{[A]}\right) = \frac{[I]}{Vm}\left(\frac{K_A}{[A]\ Ki}\right)$$

$$\text{or} \quad -[I] = Ki\left(\frac{[A] + K_A}{K_A}\right) = \text{abscissa intercept.}$$

$[NAD]([A])$ was held constant at 0.8 mM and K_A at pH 8.0 is 0.20 mM (Raval and Wolfe, 1962)

$$\therefore \quad Ki = \frac{3.68 \times .20}{1}$$

$$Ki = 0.74 \text{ mM}$$

This Ki represents the dissociation constant of the binary complex of enzyme and difluoro-oxaloacetate. This Ki is much smaller than the dissociation constant for the binary complex obtained from the protection studies (27.7 mM). It is however in the same order of magnitude as the dissociation constant for difluoro-oxaloacetate from ternary complex of difluoro-oxaloacetate. NAD-enzyme (3.2 mM), also obtained from protection studies.

This discrepancy between values for the dissociation constant of the binary complex, means that either the model chosen for inhibition is incorrect or that binding of ligands to the enzyme when it is in the catalytic mode is different to the binding of ligands when binding is non productive as in the protection and n.m.r. experiments. Although the proposed inhibitory mechanism is the simplest model that accounts for the results, it also uses all the combinations of single site inhibitor-enzyme interactions. The possibility also exists that inhibition may occur via binding of difluoro-oxaloacetate at more than one site per enzyme subunit. This mode of inhibition will also give rise to upward curving secondary plots.

It has been suggested (Harada and Wolfe, 1968b) that binding of ligands to one sub-unit causes conformational changes in the other sub-unit. The conformational changes alter the binding of ligands to that sub-unit. Such sub-unit interactions could be operating in this case, binding of NAD on one sub-unit increasing the affinity of the binding site on the other sub-unit for difluoro-oxaloacetate.

Inhibition by difluoro-malate of m-MDH catalysed reduction of difluoro-oxaloacetate

Difluoro-malate (F_2Mal) was shown to be an inhibitor of m-MDH catalysed reduction of difluoro-oxaloacetate (F_2OA). Plots of $[F_2OA]/v$ versus $[F_2OA]$ at constant [NAD] and varying $[F_2Mal]$ and $[NADH]/v$ versus [NAD] at constant $[F_2OA]$ and varying $[F_2Mal]$ were families of straight lines, each family of lines having a common abscissa intercept, characteristic of pure non-competitive inhibition. Replots of slope or ordinate intercepts of the primary plots versus $[F_2Mal]$ were straight lines having a common abscissa intercept of -3.86 mM.

If a ternary complex is lacking in the mechanism for reduction of difluoro-oxaloacetate (Scheme 9)

$$E + A \underset{k_{-1}}{\overset{k_1}{\rightleftharpoons}} EA$$

$$EA + B \underset{k_{-2}}{\overset{k_2}{\rightleftharpoons}} ED + C$$

$$ED \xrightarrow{k_3} E + D$$

Scheme 9: E, A, B, C, and D represent enzyme, NADH, difluoro-oxaloacetate, difluoro-malate and NAD respectively. EA and ED represent the binary complexes.

Then the rate expression becomes.

$$v_f = \frac{[E_t]\, k_3}{1 + \frac{k_3}{[A]k_1} + \frac{k_3}{[B]k_2} + \frac{k_{-1}k_3}{[A][B]k_1k_2} + \frac{[C]k_{-2}}{[B]k_2} + \frac{[C]k_{-1}k_{-2}}{[A][B]k_1k_2}} \qquad (21)$$

From equation (22) it can be seen that a plot of $[B]/v$ versus $[B]$ at various $[I]$ will show competitive inhibition, and a plot of $[A]/v$ versus $[A]$ at various $[I]$ will show mixed inhibition.

If a ternary complex is included in the reaction mechanism (Scheme 10),

$$E + A \underset{k_{-1}}{\overset{k_1}{\rightleftharpoons}} EA$$

$$EA + B \xrightarrow{k_2} EX$$

$$EX \underset{k_{-3}}{\overset{k_3}{\rightleftharpoons}} ED + C$$

$$ED \xrightarrow{k_4} E + D$$

Scheme 10: [EX] represents the ternary complex. All other terms are as defined for scheme 2. The step governed by k_{-2} is made irreversible to account for the lack of substrate activity shown by difluoromalate

then the rate equation is:

$$v_f = \frac{\dfrac{[Et]\ k_3k_4}{k_3 + k_4}}{1 + \dfrac{k_3k_4}{[A]k_1(k_3 + k_4)} + \dfrac{k_3k_4}{[B]k_2(k_3 + k_4)} + \dfrac{k_3k_4k_{-1}}{[A][B]k_2k_1(k_3+k_4)} + \dfrac{[C]k_{-3}}{(k_3+k_4)}} \quad (22)$$

Equation (22) predicts that a plot of [B]/v versus [B] at constant [A] and various [I] will show uncompetitive inhibition, as will the alternate plot of [A]/v versus [A] at constant [B]. Where the step EA + B ⟶ EX (Scheme 10) is reversible, then both the above plots will show mixed inhibition.

The observed results are therefore not explicable in terms of product inhibition, and this coupled with the fact that difluoro-malate is not an effective substrate for malate dehydrogenase, suggests that inhibition by difluoro-malate occurs at a site removed from the normal substrate binding site. It is therefore postulated that difluoro-malate binds equally to all forms of the enzyme at a separate binding site to give catalytically inert complexes (Scheme 11).

				Inhibitory complexes	
	$E + A \underset{k_{-1}}{\overset{k_1}{\rightleftharpoons}} EA$			$E + C \overset{K_i}{\rightleftharpoons} EC^*$	
	$B + EA \underset{k_{-2}}{\overset{k_2}{\rightleftharpoons}} EX$			$EA + C \overset{K_i}{\rightleftharpoons} EAC^*$	
G	$EX \xrightarrow{k_3} ED + C$			$EX + C \overset{K_i}{\rightleftharpoons} EXC^*$	
	$ED \xrightarrow{k_4} E + D$			$ED + C \overset{K_i}{\rightleftharpoons} EDC^*$	

Scheme 11: Proposed reaction scheme for difluoro-malate inhibition of reduction of difluoro-oxaloacetate by malate dehydrogenase. The symbols are as defined for scheme 2. * complexes are catalytically inert.

The rate equation corresponding to scheme 4 is given by equation (23).

$$v_f = \frac{\frac{Etk_3k_4}{k_3 + k_4}}{(1 + \frac{[C]}{Ki}) + \frac{k_4k_3}{[A]k_1(k_3+k_4)}(1 + \frac{[C]}{Ki}) + \frac{k_4(k_{-2}+k_3)}{[B]k_2(k_3+k_4)}(1 + \frac{[C]}{Ki}) + \frac{k_4k_{-1}(k_{-2}+k_3)}{[A][B]k_1k_2(k_3+k_4)} \ldots \ldots (1 + \frac{[C]}{Ki})} \quad (23)$$

Equation (23) predicts that plots of $[A]/v$ versus $[A]$ at constant $[B]$ and varying $[C]$ and the alternate plot at constant $[A]$, will shown non-competitive inhibition patterns. If $[C]$ does not combine with all forms of the enzyme or if all the dissociation constants (Ki) are not equal, then an inhibition pattern different to non-competitive will result. Equation (24) also predicts that secondary plots of the slopes and ordinate intercepts of the plots in Figs. 12 and 13, versus the inhibitor concentration will be straight lines and should all intercept the abscissa axis at the same point, i.e. Ki. As can

be seen from Fig. 14a-d, this situation is obtained, and give a Ki of 3.86 mM for difluoro-malate. It should be noted however that this experiment was performed using DL-difluoro-malate. The experiment should be repeated using enzymically synthesised L-difluoro-malate, to determine whether the D-difluoro-malate is responsible for the inhibition. Steady state product inhibition studies (Telegdi et al, 1973) have indicated that substrate activation of malate dehydrogenase by L-malate involves the binding of L-malate at a site distinct from the active site.

If this proposal is true, then DL-difluoro-malate might be expected to inhibit the reduction of oxaloacetate (and presumably the oxidation of malate) catalysed by malate dehydrogenase, by the same mechanism and with the same Ki. The value of Ki for difluoro-malate might also be derived from protection studies, and these represent promising directions for future work.

SUMMARY

Difluoro-oxaloacetate is a substrate for mitochondrial malate dehydrogenase, and appears to obey an ordered mechanism with the coenzymes binding first. It was not possible to determine whether the mechanism is a Theorell-Chance type (ternary complex is kinetically insignificant in the absence of product), since the product, difluoro-malate is not an effective substrate for the reverse reaction.

Difluoro-oxaloacetate forms a weak complex with mitochondrial malate dehydrogenase alone, the complex having a dissociation constant of 27.7 mM. In the presence of the coenzyme NAD, a much tighter complex is formed, having a dissociation constant of 3.2 mM.

Difluoro-oxaloacetate inhibits the MDH catalysed oxidation of L-malate, the inhibition is of the mixed type. Inhibition occurs via the formation of abortive binary and ternary complexes of the fluoro-analogue with enzyme and enzyme plus coenzyme respectively. In addition difluoro-oxaloacetate acts as an alternate product inhibitor, reducing the rate by the mass law effect. The value of the dissociation constant of the inhibitor binary complex, difluoro-oxaloacetate + enzyme, was found to be 0.74 mM, considerably lower than the value for the dissociation constant of same complex determined under non-catalytic conditions. It is suggested that this disparity may result from sub-unit interactions, coenzyme binding to one sub-unit, resulting in an increase in the affinity for the inhibitor of the hydroxy-acid

binding site on the other sub-unit.

Difluoro-malate was found not to be a substrate for malate-dehydrogenase, under the conditions of this study. It is however an effective inhibitor of difluoro-oxaloacetate reduction, showing pure non-competitive inhibition. The data suggest that inhibition occurs at site removed from the active site.

APPENDIX 1

Estimation of aldimine enzyme species by "burst" titration

A number of enzymes (E') react with one of their substrates (A) to yield a product (B) and a different catalytically active form of the enzyme (E), (substituted enzyme mechanism, equation 1).

$$E' + A \underset{k_r}{\overset{k_f}{\rightleftharpoons}} E + B \qquad (1)$$

If conditions are such that the exchange rates between the two enzyme species in equilibrium (1) are very much slower than the rate of reaction of E with a species C, to regenerate E' thus,

$$E + C \xrightarrow{k_1} E' + D \qquad (2)$$

then the amount of E present in the equilibrium (1) can be determined from the kinetics of the production D.

In the present thesis, difluoro-oxaloacetate (A) was preincubated with the aminic form of aspartate transaminase (E') in order to establish an equilibrium corresponding to equation (1). Addition of cysteine sulphinate (C) to the equilibrium system led to the formation of pyruvate (D) which was monitored by observation of the rate of oxidation of NADH in the presence of excess lactate dehydrogenase. Sufficient cysteine sulphinate was added to ensure zero order kinetics with respect to cysteine sulphinate and to ensure $[E][C]k_1 \gg [E][B]k_r$, in which

case the overall system can be represented as in Scheme 1.

$$E \xrightarrow{k_1} E' + D$$

$$E' + A \underset{k_{-2}}{\overset{k_2}{\rightleftharpoons}} X \longrightarrow E + B$$

Scheme 1: X represents all intermediate complexes of E' and A to the left of the rate limiting step.

The observed rate $$\frac{d[D]}{dt} = [E].k_1 \qquad (3)$$

and $$\frac{d[E]}{dt} = [X]k_3 - [E]k_1 \qquad (4)$$

Assuming rapid pre-equilibrium,

$$[X] = \frac{[E'][A]}{K} \quad \text{where } K = k_{-2}/k_2 \qquad (5)$$

If E_t = total enzyme then

$$E_t = [E'] + [E] + [X]$$

and from equations 4, 5 and 6 we can obtain equation 7.

$$\frac{d[E]}{dt} = a - [E]\,b \qquad (7)$$

where $a = \frac{Et\,[A]k_3}{K + [A]}$ and $b = \frac{[A]\,k_3}{K + [A]} + k_1$

Integration of equation (7) from t = 0 give:-

$$[E] = \frac{a}{b} (1 - e^{-bt}) + [E_{eq}] e^{-bt} \qquad (8)$$

where $[E_{eq}]$ is the concentration of E present in the initial equilibrium described be equation (1). Substituting for $[E]$ in equation (3)

$$\frac{d[D]}{dt} = \frac{k_1 a}{b} - \frac{k_1 a.e^{-bt}}{b} + k_1 [E_{eq}] e^{-bt} \qquad (9)$$

which on integration yields

$$[D] = \frac{k_1 a.t}{b} + \frac{[E_{eq}] k_1}{b} (1 - e^{-bt}) - \frac{k_1 a}{b^2} (1 - e^{-bt}) \qquad (10)$$

When t becomes large, the exponential terms vanish and the equation reduces to the form

$$[D] = \alpha.t + \beta \qquad (11)$$

representing a linear steady-state production of D following an initial burst. Evaluation of α and β is simplified if $[A] >> K$ for then

$$a = k_3 [Et] \text{ and } b = k_3 + k_1$$

Under these conditions the slope term $\alpha = \frac{k_1 k_3 [E_t]}{k_3 + k_1}$

The system is however designed so that $k_1 >> k_3$ whence

$\alpha = k_3 [E_t]$

Similarly the intercept term $\beta = \frac{k_1}{k_1+k_3}\left([E_{eq}] - \frac{k_3 E_t}{k_1+k_3}\right)$

which simplifies to $\beta = [E_{eq}] - \frac{k_3 Et}{k_1} \simeq [E_{eq}]$, the concentration of E present in the initial equilibrium (1). If the maximum rate of approach to equilibrium has been previously determined then the slope of the linear portion can be used to calculate E_t; producing a useful check. It should be noted that E_{eq} includes not only free E but also all complexes of E which equilibrate rapidly enough to be kinetically equivalent to free E.

APPENDIX 2

Derivation of relationships between kinetic coefficients in different mechanisms for the reaction of malate dehydrogenase

1. Ordered mechanism lacking a ternary complex.

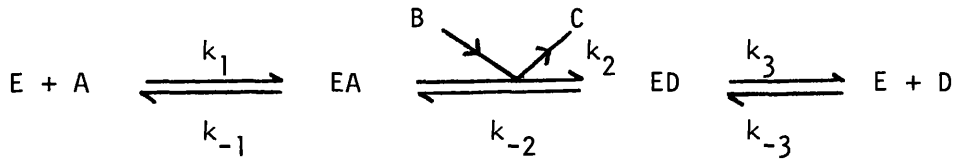

$$\frac{E_t}{v_f} = \frac{1}{k_3} + \frac{1}{[A]\ k_1} + \frac{1}{[B]\ k_2} + \frac{k_{-1}}{[A]\ [B]\ k_1 k_2}$$

$$\emptyset_0 = {}^{1}/_{k_3} : \emptyset_1 = {}^{1}/_{k_1} : \emptyset_2 = {}^{1}/_{k_2} : \emptyset_{12} = {}^{k_{-1}}/_{k_1 k_2}$$

$$\emptyset_{12}/\emptyset_2 = {}^{k_{-1}}/_{k_1} = \overline{K}_a \quad \text{(dissociation constant of EA)}$$

2. Ordered mechanism with a ternary complex

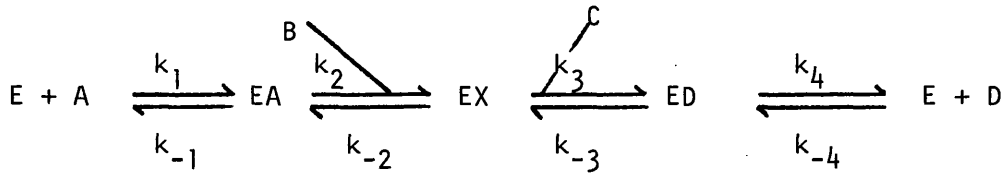

$$\frac{E_t}{v_f} = \frac{k_4 + k_3}{k_3 k_4} + \frac{1}{[A]\ k_1} + \frac{k_{-2} + k_3}{[B] k_2 k_3} + \frac{k_{-1}(k_{-2} + k_3)}{[A][B]\ k_1 k_2 k_3}$$

$$\phi_o = \frac{k_4 + k_3}{k_3 k_4} : \phi_1 = {}^1/k_1 : \phi_2 = \frac{k_{-2} + k_3}{k_2 k_3} : \phi_{12} = \frac{k_{-1}(k_{-2} + k_3)}{k_1 k_2 k_3}$$

$$\phi_{12}/\phi_2 = {}^{k_{-1}}/k_1 = \overline{K}_a$$

If the ternary complex is kinetically insignificant, i.e. $k_3 >> k_4$ and $k_3 >> k_{-2}$, then the equation degenerates to give case (1).

3. Random mechanism (all binary complexes formed rapidly and reversibly. The magnitude of any dissociation constant is unaffected by the prior attachment of any other reactant to the enzyme) and slow step is interconversion of ternary complexes.

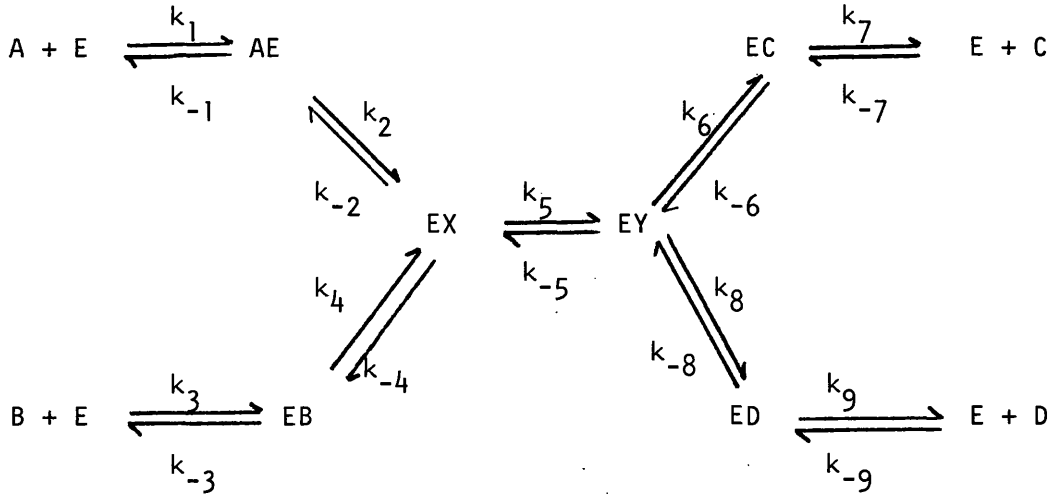

$$\frac{E_t}{v_f} = \frac{1}{k_5} + \frac{k_{-1}}{k_1 k_5 [A]} + \frac{k_{-3}}{k_3 k_5 [B]} + \frac{k_{-1}\, k_{-3}}{k_1 k_3 k_5 [A]\,[B]}$$

$$\phi_o = {}^{1}/_{k_5} \; ; \; \phi_1 = {}^{k_{-1}}/_{k_1 k_5} \; ; \; \phi_2 = {}^{k_{-3}}/_{k_3 k_5} \; ; \; \phi_{12} = {}^{k_{-1} k_{-3}}/_{k_1 k_3 k_5}$$

$$\phi_{12}/\phi_2 = {}^{k_{-1}}/_{k_1} = \overline{K}_a$$

but $\phi_1 \phi_2 / \phi_{12} = \phi_o$

4. Random mechanism, but the restriction in the various $\overline{K}$'s do not hold.

$$\frac{E_t}{v_f} = \frac{1}{k_5} + \frac{k_{-4}}{k_4 k_5 [A]} + \frac{k_{-2}}{k_2 k_5 [B]} + \frac{k_{-4} k_{-1}}{k_4 k_1 k_5 [A][B]}$$

$$\phi_o = {}^{1}/_{k_5} \; ; \; \phi_1 = {}^{k_{-4}}/_{k_4 k_5} \; ; \; \phi_2 = {}^{k_{-2}}/_{k_2 k_5} \; ; \; \phi_{12} = {}^{k_{-4} k_{-1}}/_{k_4 k_1 k_5}$$

$$\phi_{12}/\phi_1 = {}^{k_{-1}}/_{k_1} = \overline{K}_a$$

REFERENCE LIST

Alberty, R A and Hammes, G G (1958) J. Phys. Chem. 62, 154-159

Anderton, B H (1970) Eur. J. Biochem., 15, 562-567

Anderton, B H and Rabin, B R (1970) Eur. J. Biochem., 15, 568-573

Antonini, E, Brunori, M, Fasella, P, Khomutor, R, Manning, J M and Severin, E S (1970) Biochemistry, 9, 1211-1216

Arrio-Dupont, M (1972) Eur. J. Biochem., 30, 307-312

Auld, D S and Bruice, T C (1967) J. Am. Chem. Soc., 89, 2098-2106

Ayling, J E, Dunathon, H C and Snell, E E (1968) Biochemistry, 7, 4537-4542

Banaszak, L J and Bradshaw, R A (1970) The Enzymes, 3rd Edition, II, pp. 369-396. Ed. P D Boyer.

Banks, B E C, Lawrence, A J, Thain, E M and Vernon, C A (1963) J. Chem. Soc., 5799-5806

Banks, B E C, Lawrence, A J, Vernon, C A and Wootton, J F (1963) In Chemical and Biological Aspects of Pyridoxal Catalysis. (E E Snell et al, eds). p. 197. Pergamon Press, Oxford.

Banks, B E C, Doonan, S, Lawrence, A J and Vernon, C A (1968) Eur. J. Biochem., 5, 528-539.

Bentley, R and Bhate, D S (1960) J. Biol. Chem., 235, 1225-1233

Banks, B.E.C., Bell,M.P., Lawrence,A.J., and Vernon,C.A. (1968a) Pyridoxal Catalysis: Enzymes and Model Systems (Snell,E.E. et al, eds) p. 191, Interscience, Lomdon.

Besmer, P and Arigoni, D (1969) Chimia, 23, 190-197

Birchmeier, W, Zaoralek, P E and Christen, P (1973)
Biochemistry, 12, 2874-2879

Blank, I, Mager, J and Bergmann, E D (1955) J. Chem. Soc., 2190-2193

Bliss, C I (1967) Statistics in Biology, Vol. 1., pp. 438-439,
McGraw-Hill, New York.

Bleile, D M, Schulz, R A, Harrison, J H and Gregory, E M (1977)
J. Biol. Chem., 252, 755-758

Bocharov, A L, Ivanov, V I, Karpeisky, M.Ya., Mamaeva, O K and
Florentiev, V L (1968) Biochem. Biophys. Res. Commun., 30, 459-464

Boettcher, B and Martinez-Carmon, M (1976) Biochemistry, 15, 5657-5663

Bradbury, J H and Wilairat, P (1967) Biochem. Biophys. Res. Commun.,
29, 84-89

Braunstein, A E (1960) In. The Enzymes, 2nd edition, Vol. 2, pp. 113
(P D Boyer, et al, eds) Academic Press, N.Y.

Braunstein, A E (1964) Vitam, Horm., (N.Y), 22, 451-484

Braunstein, A E (1970) FEBS Symposium, 18, 123-131

Braunstein, A E and Kritzmann, M G (1937) Nature, 140, 503-504

Brewer, S D and Herbst, R M (1941) J. Org. Chem., 6, 867-871

Briley, P A, Eisenthal, R and Harrison, R (1973)
Biochem. Soc. Trans, 1, 1276-1277

Bruice, T C and Topping, R M (1962) J. Am. Chem. Soc., 84, 2448-2450

Bruice, T C and Topping, R M (1963) J. Am. Chem. Soc., 85, 1480-1496

Cammarata, P S and Cohen, P P (1950) J. Biol. Chem., 187, 439-452

Cassman, M (1973) Biochem. Biophys. Res. Commun., 53, 666-672

Cassman, M and King, R (1972) Biochem. Biophys. Acta, 257, 143-149

Cassman, M and King, R (1973) Biochemistry, 11, 4937-4941

Cheng, S and Martinez-Carrion, M (1972) J. Biol. Chem., 247, 6597-6602

Cheng, S, Michuda-Kozak, C and Martinez-Carrion, M (1971)
J. Biol. Chem., 246, 3263-3630

Ciba Foundation Symposium (1972) Carbon-Fluorine Compounds. Chem.
Biochem. Biol. Activities,Ciba Found. Symp., Elsevier, Amsterdam.

Cohen, J S and Jardetzky, D (1968) Proc. Natl. Acad. Sci. US.,
60, 92-99

Consiglio, E, Varrone, S and Covelli, I (1970) Eur. J. Biochem.,
17, 408-414

Cornish-Bowden, A (1975) Biochem. J., 149, 305-312

Cournil, I and Arrio-Dupont, M (1973) Biochimie, 55, 103-109

Covelli, I, Consiglio, F and Varrone (1969) Biochim. Biophys. Acta,
184, 678-681.

Cavallini, D., Giorgio, F., Bossa,F., and Granata, F. (1973) Eur. J. Biochem.
39 301-304.

Cram, D J and Guthrie, R D (1965) J. Am. Chem. Soc., 397-398

Curtis, A R and Chance, E M (1972) FEBS Meet. Proc. 7th, 25, 39-57

Czerlinski, G and Malkewitz, J (1965) Biochemistry, 4, 1127-1137

Dahlquist, F W and Raftery, M A (1968) Biochemistry, 7, 3269-3276

Dalziel, K (1957) Acta. Chem. Scand., 11, 1706-1723

Devenyi, T, Rogers, S J and Wolfe, R G (1966)
Biochem. Biophys. Res. Commun., 23, 496-501

Doonan, S, Vernon, C A and Banks, B E C (1970) Prog. Biophys.
Mol. Biol., 20, 307-313

Dunathan, H C (1966) Proc. Natl. Acad. Sci.US, 55, 712-716

Dunathan, H C, Davis, L and Kaplan, M (1968a) Pyridoxal Catalysis:
Enzymes and Model Systems (Snell, E E et al, eds) p. 325, Interscience,
London.

Dunathan, H C, Davis, L, Kury, P G and Kaplan, M (1968b)
Biochemistry, 7, 4532-4537

Eisenthal, R and Cornish-Bowden, A (1974) Biochem. J., 139, 715-720

Emsley, J W, Feeney, J and Sutcliffe, L H (1965) High Resolution
Nuclear Magnetic Spectroscopy, 1, p.357. Pergamon Press, Oxford.

Emsley, J W and Philips, L (1971) Progress in Nuclear Magnetic
Resonance Spectroscopy, 7, 3-36

Fasella, P, Giartosio, A, Hammes, G G (1966) Biochemistry, 5, 197-202

Fasella, P and Hammes, G G (1964) Biochemistry, 3, 530-535

Fasella, P and Hammes, G G (1965) Biochemistry, 4, 801-805

Fasella, P and Hammes, G G (1967) Biochemistry, 6, 1798-1804

Fasella, P and Turano, C (1970) Vitamins and Hormones, 28, 157-194

Feldman, L I and Gunsalus, I C (1950) J. Biol. Chem., 187, 821-830

Fonda, M L and Johnson, R J (1970). J. Biol. Chem., 245, 2709-2716

Foster, M and Harrison, J H (1974) Biochem. Biophys. Acta., 351, 295-300

Frieden, C and Alberty, R A (1955) J. Biol. Chem., 212, 859-868

Glatthaar, B E, Barbarash, G R, Noyes, B E, Banaszak, L J and Bradshaw, R A (1974) Analytical Biochem., 57, 432-451

Gerig, J T (1968) J. Am. Chem. Soc., 90, 2681-2686

Gregory, E M and Harrison, J H (1970) Biochem. Biophys. Res. Commun., 40, 995-1001

Gregory, E M, Rohrbach, M S and Harrison, J H (1971) Biochim. Biophys. Acta, 243, 489-497

Gregory, E M, Yost, F J, Rohrbach, M S and Harrison, J H (1971) J. Biol. Chem., 246, 5491-5497

Groves, P D, Huck, P J and Homer, J (1967) Chemistry and Industry, 915-917

Guirard, B M and Snell, E E (1964) Comp. Biochem., 15, 138-196

Gutfreund, H, Ebner, K E and Mendiola, L (1961) Nature, 192, 820-823

Haarhoff, K N (1969) J. Theor. Biol., 22, 117-150

Hammes, G G and Fasella, P (1962) J. Am. Chem. Soc., 84, 4644-4648

Hammes, G G and Fasella, P (1963) J. Am. Chem. Soc., 85, 3929-3935

Hammes, G G and Haslam, J L (1968) Biochemistry, 7, 1515-1525

Hammes, G G and Haslam, J L (1969) Biochemistry, 8, 1591-1598

Hammes, G G and Tancredi, J (1967) Biochim. Biophys. Acta, 146, 312-313

Harada, K and Wolfe, R G (1968a) J. Biol. Chem., 243, 4123-4130

Harada, K and Wolfe, R G (1968b) J. Biol. Chem., 243, 4131-4137

Hartree, E F (1972) Analytical Biochem., 48, 422-427

Harris, H E and Bayley, P M (1975) Biochem. J., 145, 125-128

Healy, M J and Christen, P (1973) Biochemistry, 12, 35-41

Heinert, D and Martell, A E (1963) J. Am. Chem. Soc., 85, 183-194

Henson, C P and Cleland, W W (1964) Biochemistry, 3, 338-345

Herbst, R M and Engel, L L (1934) J. Biol. Chem., 107, 505-512

von Hippel, A R (1954) Dielectrics and Waves, p. 231. John Wiley & Son, New York.

Holbrook, J J and Wolfe, R G (1972) Biochemistry, 11, 2499-2502

Holloway, M R and White, H A (1975) Biochem. J., 149, 221-231

Hollis, D P (1967) Biochemistry, 6, 2080-2087

Hollis, D P, Bolen, J L and Kellum, J M (1966) Biochem. Biophys. Res. Commun., 22, 135-140

Huestis, W H and Raftery, M A (1971) Biochemistry, 10, 1181-1186

Hughes, R C, Jenkins, W T and Fischer, E H (1962) Proc. Natl., Acad. Sci., US, 48, 1615-1618

Ivanov, V I and Karpeisky, M Ya (1969) Adv. Enzymology, 32, 21-53

Jencks, W P (1969) Catalysis in Chemistry and Enzymology, pp. 572-574 McGraw-Hill, New York.

Jenkins, W T (1961a) J. Biol. Chem., 236, 474-478

Jenkins, W T (1961b) J. Biol. Chem., 236, 1121-1125

Jenkins, W T (1964) J. Biol. Chem., 239, 1742-1747

Jenkins, W T and D'Ari, L (1966a) J. Biol. Chem., 241, 2845-2854

Jenkins, W T and D'Ari, L (1966b) Biochemistry, 5, 2900-2905

Jenkins, W T and D'Ari, L (1966c) J. Biol. Chem., 241, 5667-5674

Jenkins, W T and D'Ari, L (1966d) Biochem. Biophys. Res. Commun., 22, 376-382

Jenkins, W T and D'Ari, L (1968) in Pyridoxal Catalysis: Enzymes and Model Systems (Snell, E E et al, eds). Interscience, London. pp. 317-324.

Jenkins, W T, Orlowski, S and Sizer, I W (1959b) J. Biol. Chem., 234, 2657-2660

Jenkins, W T and Sizer, I W (1957) J. Am. Chem. Soc., 79, 2655-2656

Jenkins, W T and Sizer, I W (1960) J. Biol. Chem., 235, 620-624

Jenkins, W T and Taylor, R T (1965) J. Biol. Chem., 240, 2907-2913

Jenkins, W T, Yphantis, D A and Sizer, I W (1959a) J. Biol. Chem., 234, 51-57

John, R and Jones, R (1974) Biochem. J., 141 401-406

Johnston , C C, Brooks, H G, Albert, J D and Metzler, D E (1963) In: Chemical and Biological Aspects of Pyridoxal Catalysis (Snell, E E et al, eds) Pergamon Press, Oxford, pp. 69

Kearney, E B and Singer, T P (1953) Biochim. Biophys. Acta. 11, 276-289

Kitto,G B, Wasserman, P M, Michjeda, J and Kaplan, N O (1966a) Biochem. Biophys. Res. Commun., 22, 75-81

Kitto, G B, Wasserman, P M and Kaplan, N O (1966b) Proc. Natl. Acad. Sci. US, 56, 578-585

Klingenberg, M (1974) In: Methods of Enzymatic Analysis, 2nd Edition (Bergmeyer, H V ed) Academic Press, N.Y., p.429

Kritzmann, M G and Samarina, O (1946) Nature, 158, 104

Kulick, R J and Barnes, S (1968) Biochim. Biophys. Acta, 167, 1-8

Kun, E and Dummel, R J (1969) Methods in Enzymology, 13, 623-672

Kun, E? Grassetti, D R, Fanshier, D W and Featherstone, R M (1959) Biochem. Pharm., 1, 207-212

Kun, E, Fanshier, D W and Grassetti, D R (1960) J. Biol. Chem., 235, 416-419

Kun, E, Gotwald, L K, Fanshier, D W and Ayling, J E (1963) J. Biol. Chem., 238, 1456-1463

Kuramitsu, H K (1968) J. Biol. Chem., 243, 1016-1021

Layne, E (1957) Methods in Enzymology, 3, 447-454

Lichstein, H C, Gunsalus, I C and Umbreit, W W (1946) J. Biol. Chem., 161, 311-320

Lis, H, Fasella, P, Turano, C and Vecchini, P (1960) Biochim. Biophys. Acta, 45, 529-536

Malakhova, E A and Torchinskii, Yu M (1965) Dokl. Akad. Nauk, SSSR, 161, 1224-1226

Manning, J M, Khomutov, R M, Fasella, P (1968) Eur. J. Biochem., 5, 199-208

Martell, A E (1963) In: Chemical and Biological Aspects of Pyridoxal Catalysis (Snell, E E et al, eds) Pergamon Press, Oxford, p. 13

Martinez-Carrion, M, Riva, F, Turano, C and Fasella, P (1965) Biochem. Biophys. Res. Commun., 20, 206-211

Martinez-Carrion, M, Turano, C, Chiancone, E, Bossa, F, Giartosi, A Riva, F and Fasella, P (1967) J. Biol. Chem., 242, 2397-2409

Martinez-Carrion, M, Cheng, S and Relimpio, A M (1973) J. Biol. Chem., 248 2153-2160

Matsushima, Y and Martell, A E (1967) J. Am. Chem. Soc., 89, 1331-1335

Meister, A and Tice, S V (1950) J. Biol. Chem., 187, 173-189

Metzler, D E (1957) J. Am. Chem. Soc., 79, 485-490

Metzler, D E, Harris, G M, Johnson, R J, Siano, D B and Thompson, J A (1973) Biochemistry, 12, 5377-5392

Metzler, D, Ikawa, M and Snell, E E (1954) J. Am. Chem. Soc., 76, 648-652

Metzler, D and Snell, E E (1952) J. Am. Chem. Soc., 74, 979-983

Michuda, C and Martinez-Carrion, M (1969) Biochemistry, 8, 1095-1104

Morino, Y and Okamoto, M (1973) Biochem. Biophys. Res. Commun., 50, 1061-1067

Morino, Y, Osman, A M and Okamoto, M (1974) J. Biol. Chem., 249, 6684-6692

Murphey, W H, Barnby, C, Lin, F J and Kaplan, N O (1967) J. Biol. Chem., 242, 1548-1559

MacDonald, A M (1971) In: Encyclopedia of Industrial Chemical Analysis (Snell, F D and Ellre, L S, eds) 13, 6-36

Nisselbaum, J S and Bodanski, O (1964) J. Biol. Chem., 239, 4232-4236

Nisselbaum, J S and Bodanski, O (1966) J. Biol. Chem., 241, 2661-2664

Novogrodsky, A and Meister, A (1964) Biochim. Biophys. Acta, 81, 605-608

Noyes, B E, Glatthaar, B E, Garavelli, J S and Bradshaw, E (1974) Proc. Natl. Acad. Sci. US, 71, 1334-1338

Ovelhinnikov, Yu. A, Egorov, C A, Aldanova, N A, Feigina, M. Yu., Lipkin, V M, Abdulaev, N G, Grishin, E G, Kiselev, A P, Modyanov, N N Braunstein, A E, Polyanovsky, O L and Nosikov, V V (1973) FEBS Letts., 29, 31-34

Peterson, D L and Martinez-Carrion, M (1970) J. Biol. Chem., 245, 806-813

Raftery, M A, Dahlquist, F W, Chan, S I and Parsons, S M (1968) J. Biol. Chem., 243 4175-4180

Raftery, M, Huestis, W H and Millet, F (1971) Cold Spring Harbor Symp. Quant. Biol., 36, 541-550

Raval, D N and Wolfe, R G (1962a) Biochemistry, 1, 263-269

Raval, D N and Wolfe, R G (1962b) Biochemistry, 1, 1112-1117

Raval, D N and Wolfe, R G (1962c) Biochemistry, 1, 1118-1123

Raval, D N and Wolfe, R G (1963) Biochemistry, 2, 220-224

Riva, F, Vecchini, P, Turano, C and Fasella, P (1964) Proc. 6th Int. Cong. Biochem. Abstr. Section IV. N.Y. p. 329

Scardi, V, Scotto, P, Iaccarino, M and Scarano, E (1963) Biochem. J. 88, 172-175

Schirch, L and Slotter, R A (1966) Biochemistry, 5, 3175-3181

Schlenk, F and Fisher, A (1945) Arch. Biochem. 8, 337-338

Schlenk, F and Snell, E E (1945) J. Biol. Chem., 157, 425-426

Shlyapnikov, S V and Karpeisky, M. Ya (1969) Eur. J. Biochem., 11 424-426

Shore, J D and Chakrabarti, S K (1976) Biochemistry, 15, 875-879

Silverstein, E and Sulebele, G (1969) Biochemistry, 8, 2543-2550

Silverstein, E and Sulebele, G (1970) Biochemistry, 9, 274-282

Sizer, I W and Jenkins, W T (1963) In: Chemical and Biological Aspects of Pyridoxal Catalysis (Snell, E E et al, eds) Pergamon Press, Oxford. pp. 123-137

Snell, E E (1944) J. Biol. Chem., 154, 313-314

Snell, E E (1945) J. Am. Chem. Soc., 67, 194-197

Spotswood, T, Evans, J and Richards, J H (1967) J. Am. Chem. Soc., 89, 5052-5054

Sulebele, G and Silverstein, E (1970) Biochemistry, 9, 283-290

S winbourne, E S (1960) J. Chem. Soc., 2371-2372

Sykes, B D (1969) J. Am. Chem. Soc. 91, 949-955

Tate, S S and Meister, A (1969) Biochemistry, 8, 1056-1065

Taylor, S S, Oxley, S S, Allison, W S and Kaplan, N O (1973) Proc. Natl. Acad. Sci. US, 70, 1790-1794

Telegdi, M, Wolfe, D V and Wolfe, R G (1973) J. Biol. Chem., 248, 6484-6489

Theorell, H and Chance, B (1951) Acta. Chem. Scand., 5, 1127-1144

Theorell, H and Langan, T A (1960) Acta. Chem. Scand., 14, 933

Thorne, C J R and Kaplan, N O (1963) J. Biol. Chem., 238, 1861-1868

Thorne, C J R, Grossman, L I and Kaplan, N O (1963) Biochim. Biophys. Acta, 73, 193-203

Torchinsky, Yu. M, and Koreneva, L G (1973) Biokhimiya, 28, 1087-1092

Torchinsky, Yu. M, Malakhova, E A, Livanova, N B and Pikhelgas, V. Ya (1968) In: Pyridoxal Catalysis: Enzymes and Model Systems, pp. 269-290 (Snell, E E et al, eds) Interscience, London

Turano, C, Giarstosio, A, Riva, F and Fasella, P (1964) Biochem. Biophys. Res. Commun., 16, 221-226

Turano, C, Giartosio, A, Riva, F, Baroncelli, J and Bossa, F (1966) Arch. Biochem. Biophys., 117, 678-680

Velick, S F and Vavra, J (1962a) J. Biol. Chem. 237, 2109-2122

Velick, S F and Vavra, J (1962b) in The Enzymes, 6 (Boyer, P., et al., eds) p219. Academic Press. N.Y.

Wada, H and Morino, Y (1964) Vit. Horm. 22, 411-444

Wada, H and Snell, E E (1962a) J. Biol. Chem. 237, 133-137

Wada, H and Snell, E E (1962b) J. Biol. Chem. 237, 127-132

Yost, F J and Harrison, J H (1971) Biochem. Biophys. Res. Commun. 42, 516-522

Zefren, E and Reavill, R E (1968) Biochem. Biophys. Res.Commun. 32, 73-80

Acknowledgments

I wish to thank the Enzyme Chemistry and Technology Committee of the Science Research Council for a research studentship, Robert Eisenthal and Roger Harrison for their guidance and patience, and Gill, for much help in writing this thesis.

ANALYTICAL BIOCHEMISTRY 79, 643–647 (1977)

Determination of Dissociation and Michaelis Constants at Near-Equal Enzyme-Substrate Concentrations

It is occasionally necessary to determine dissociation or Michaelis constants under experimental conditions in which the concentrations of protein and ligand are of the same order of magnitude. In such cases, approximations commonly used in the calculation of the constants are no longer valid. This communication describes an iterative procedure which allows calculation of the constants in such cases.

Where a 1:1 molecular complex exists between a protein E and a ligand S,

$$E + S \rightleftharpoons ES; \qquad [1]$$

the dissociation constant ($K = [E]\,[S]/[ES]$) of ES may be determined by observation of some physical property of the system that depends upon [ES]. For example, the change in absorbance (E) of the system upon addition of S to E is given by:

$$E = [ES](\epsilon_E - \epsilon_{ES}), \qquad [2]$$

if the ligand S does not absorb at the observed wavelength, at which ϵ_E and ϵ_{ES} are the extinction coefficients of E and ES, respectively. Similarly, in cases in which S shows a nuclear magnetic resonance signal, the observed chemical shift (δ_{obs}) of the system relative to that of free S is related to the corresponding shift of bound S (Δ) by the expression:

$$\delta_{obs} = [ES]\Delta/[S_t], \qquad [3]$$

provided that the exchange of S between free and bound forms is sufficiently rapid (1). S_t is the total ligand.

The relationship between [ES] and K in systems described by Eq. [1] may be expressed as:

$$K = ([E_t] - [ES])([S]_t] - [ES])/[ES], \qquad [4]$$

where S_t is total ligand and E_t the total protein. This leads to a quadratic equation in [ES]:

$$[ES]^2 - [ES]([E_t] + [S_t] + K) + [E_t][S_t] = 0. \qquad [5]$$

Determination of K is simplified if conditions are chosen such that $[S_t] \gg [E_t]$ when Eq. [4] can be written as:

$$[ES] = [E_t][S_t]/(K + [S_t]), \qquad [6a]$$

ISSN 0003-2697

or such that $[E_t] \gg [S_t]$ when

$$[ES] = ([E_t][S_t])/(K + [E_t]). \quad [6b]$$

In practice, it is usual to arrange conditions so that $[S_t] \gg [E_t]$. In this case, Eq. [6] applies, and substitution in Eq. [2] and [3] leads, in each case, to a relationship containing the observed parameter (E or δ_{obs}), together with $[E_t]$ and $[S_t]$, in a form such that K can be obtained from a linear plot (1,2). K may be similarly derived when $[E_t] \gg [S_t]$.

A similar situation arises in systems obeying Michaelis–Menten kinetics where:

$$E + S \underset{k_{-1}}{\overset{k_{+1}}{\rightleftharpoons}} ES \xrightarrow{k_2} E + P \quad [7]$$

If a steady state for ES is assumed, we have equations exactly analagous to Eq. [4] and [5] in which K is replaced by the Michaelis constant (K_m). In steady-state kinetics, it is usual that $[S_t] \gg [E_t]$; then, [ES] is given by:

$$[ES] = ([ES][S_t])/(K_m + [S_t]), \quad [8]$$

analagous to Eq. [6a]. The rate of reaction is given by:

$$v = k_2[ES], \quad [9]$$

and substitution of Eq. [8] in Eq. [9] leads to the familiar Michaelis–Menten equation and to a number of linear plots containing v, $[S_t]$, and $[E_t]$ from which K_m and $k_2[E_t]$ may be determined (3).

These methods depend upon the conditions that $[S_t] \gg [E_t]$ or $[E_t] \gg [S_t]$ which are not always practicable. For example, if $[E_t]$ approaches or is greater than K (or K_m), under the condition $[S_t] \gg [E_t]$, the observed parameter (E, δ_{obs}, v etc.) is relatively insensitive to changes in the variable $[S_t]$, and experimental error is high. This can be seen from Eq. [6a] and [8] for, if $[E_t] \gtrsim K$ (or K_m), then $[S_t] \gg K$ (or K_m), and changes in $[S_t]$ lead to only small variation in [ES] and, hence, in the observed parameter. Such situations arise when S has a high affinity for E (i.e., K is small) or when relatively high concentrations of E are necessary (e.g., the absorbance of E is being used to monitor the system or E is an enzyme catalysing a slow reaction). Similar difficulties can arise under the alternative conditions $[E_t] \gg [S_t]$ when $[E_t] \approx K$ (or K_m) implies K (or K_m) $\gg [S_t]$ (4).

Accordingly, there is a need for a method of calculation of dissociation or Michaelis constants in cases of protein–ligand binding, where neither protein nor ligand is in great excess. The present paper describes such a method which is applicable to all cases in which a relationship between [ES] and a measurable parameter can be represented as a straight line through the origin as in the examples above.

METHOD

The method involves an iterative procedure in which the quadratic Eq. [5] is solved for [ES] at each of a series of values of $[S_t]$, using an assumed value of K (or K_m) and subjected to the restriction that $[S_t] > [ES] < [E_t]$. The observed parameter is then plotted against that function of [ES] that predicts a straight line through the origin (e.g., E versus [ES] from Eq. [2] or δ_{obs} versus $[ES]/[S_t]$ from Eq. [3]). The best fit to such a straight line (5) will be obtained when the correct value of K (or K_m) has been assumed. The criterion for best fit is the sum of squares of the residuals (differences between experimental and calculated values); values of K (or K_m) are incremented or decremented, and the process is repeated until the sum of squares of the residuals (SSR) reaches a minimum; the value of K (or K_m) giving this condition is taken as the true value. The slope of the best straight line so obtained may be used to determine further constants (eg., $\epsilon_E - \epsilon_{ES}$, Δ, and k_2 in the aforementioned examples).

EXAMPLE

An example of the application of the method to the determination of K_m is provided in the case of the slow reaction of the aminic form of asparate transaminase (L-aspartate: 2-oxoglutarate aminotransferase, EC 2.6.1.1.) with the substrate analog, difluoro-oxaloacetate (6):

Aminic enzyme	+ difluoro-oxaloacetate	$\rightleftharpoons$ Enzyme–difluoro-oxaloacetate complex	$\xrightarrow{\text{slow}}$ aldimine enzyme.
λ_{max} ca. 330 nm		λ_{max} ca. 330 nm	λ_{max} 360 nm

The reaction is followed by observing either the decrease in E_{330} or the increase in E_{360} which necessitates relatively high concentration of enzyme, a condition also required by the slowness of the reaction. For these reasons, it is experimentally desirable that $[E_t] \approx K_m$ and, as explained before, the simplifying conditions, $[S_t] \gg [E_t]$ or $[E_t] \gg [S_t]$, are precluded accordingly.

The plot of SSR versus assumed values of K_m is shown in Fig. 1, in which the curve can be seen to reach a well-defined minimum at $K_m = 7.0$ μM; the corresponding best straight line through the origin of v versus [ES] is shown in Fig. 2. The calculated value of K_m is in good agreement with the values of 9.2 and 5.85 μM obtained from different experiments (7) in which difluoro-oxaloacetate was used as an inhibitor of the transamination of oxaloacetate. Moreover, the slope of the line in Fig. 2 gives a value for k_2 (Eq. [9]) of 1.25×10^{-3} sec^{-1}; this may be compared

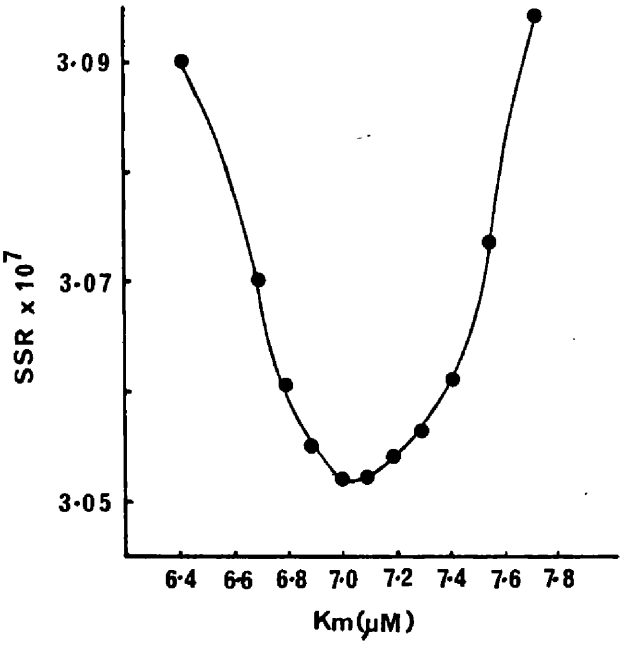

FIG. 1. Plot of the sum of the squares of the residuals (SSR) versus the assumed values of K_m for initial rates of the slow reaction of difluoro-oxaloacetate with the aminic form of aspartate transaminase.

with the limiting first-order rate constant, 1.22×10^{-3} sec^{-1}, obtained from the progress curve of the reaction (6).

The iterative process may be done using a programmable desk calculator. The enzyme and substrate concentrations, an initial estimate of K (or K_m), and the values of the observed parameter are supplied to the

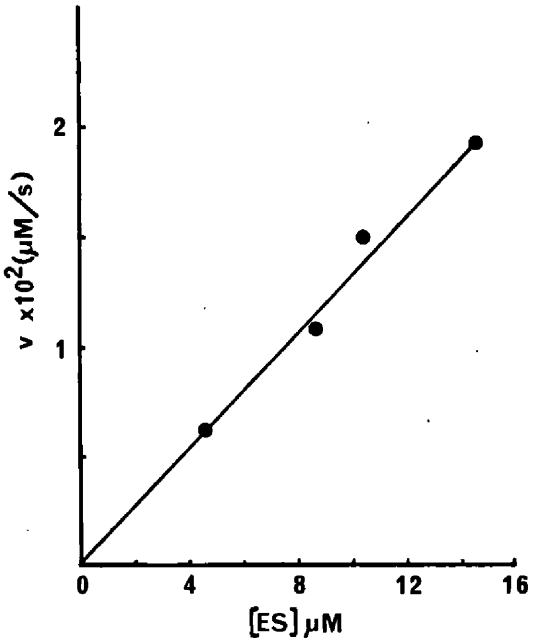

FIG. 2. Plot of initial velocity (v) versus concentration of enzyme–substrate complex [ES], using that value of K_m giving the minimum SSR (Fig. 1).

program which solves the quadratic Eq. [5] for each concentration of substrate. This gives a set of values for [ES] which are used to calculate the SSR of the values to the best straight line through the origin. The program then increments K (or K_m) by a preset amount and repeats the overall process. If the SSR is thereby diminished, a further incremental change in K (or K_m) is made in the same direction as the first. The process is repeated until the SSR begins to increase. At this stage, smaller incremental changes are made in the opposite direction, and the entire process is repeated until K (or K_m) is defined to the required accuracy.

Copies of the program are available from the authors.

The method can be extended to cases in which the observed parameter is a linear function of, rather than directly proportional to, [ES]. In this case, the data are fitted to the best straight line which is not constrained to pass through the origin, and further information is obtainable from the ordinate intercept of such a line. The convergence to a minimum value of SSR, as SSR is plotted against K, is, however, likely to be less sharp in such a case.

ACKNOWLEDGMENT

We wish to thank the Enzyme Chemistry and Technology Committee of the Science Research Council for a research grant (to RE and RH) and a research fellowship (to GDS).

REFERENCES

1. Dwek, R. A. (1973) Nuclear Magnetic Resonance in Biochemistry, pp. 136–137, Claredon Press, Oxford.
2. Jenkins, W. T., and Taylor, R. T. (1965) *J. Biol. Chem.* **240,** 2907–2913.
3. Cornish-Bowden, A. (1976) Principles of Enzyme Kinetics, pp. 23–28, Butterworths, London.
4. Segel, I. H. (1975) Enzyme Kinetics: Behaviour and Analysis of Rapid Equilibrium and Steady State Systems, pp. 46–48. John Wiley, New York.
5. Bliss, C. I. (1967) Statistics in Biology, Vol. 1, pp. 444–451, McGraw–Hill, New York.
6. Briley, P. A., Eisenthal, R., Harrison, R., and Smith, G. D., unpublished results.
7. Briley, P. A., Eisenthal, R., Harrison, R., and Smith, G. D. (1977) *Biochem. J.* **161,** 383–387.

GEOFFREY D. SMITH
ROBERT EISENTHAL
ROGER HARRISON

Biochemistry Group
School of Biological Sciences
Bath University
Claverton Down, Bath BA2 7AY
Received November 8, 1976; accepted January 6, 1977

Biochem. J. (1977) **167**, 193–200
Printed in Great Britain

Reaction of the Aminic Form of Aspartate Transaminase with Difluoro-oxaloacetate

By PATRICIA A. BRILEY, ROBERT EISENTHAL, ROGER HARRISON and GEOFFREY D. SMITH
Biochemistry Group, School of Biological Sciences, University of Bath, Claverton Down, Bath BA2 7AY, U.K.

(*Received* 10 *February* 1977)

Addition of difluoro-oxaloacetate to the aminic form of aspartate transaminase causes a rapid shift of absorbance maximum of the enzyme from 332nm to 328nm, followed by a much slower shift to 360nm corresponding to complete conversion of the aminic form of the enzyme into the aldimine form or a species with similar spectral parameters in rapid equilibrium with it. Kinetic analysis of both the initial fast reaction and the overall slow reaction by using repeated spectral scanning and stopped-flow techniques allows formulation of a basic reaction mechanism involving at least two intermediate enzyme complexes. Computer simulation of the progress curves of the initial fast reaction based on the suggested reaction mechanism gives kinetic parameters that are consistent with all the data obtained by other methods. A molecular reaction scheme involving a ketimine Schiff-base intermediate is proposed.

Difluoro-oxaloacetate, an isosteric substrate analogue of oxaloacetate in which the CH_2 grouping of oxaloacetate is replaced by CF_2, has been shown to be a competitive inhibitor of the oxo acid substrate in the transamination reaction catalysed by aspartate transaminase (Briley *et al.*, 1977a). Difluoro-oxaloacetate itself was shown to undergo enzyme-catalysed transamination with aspartate, but this reaction occurred on a time scale that was too slow to affect the inhibition kinetics. Further evidence for transamination was provided by the demonstration of a ^{19}F n.m.r. (nuclear-magnetic-resonance) spectrum corresponding to that expected from difluoroaspartate after incubation of difluoro-oxaloacetate with the enzyme and an amino acid substrate. Moreover, addition of difluoro-oxaloacetate to the aminic (pyridoxamine) form of aspartate transaminase was reported to cause a slow shift in absorbance maximum from 332nm to 360nm characteristic of the aldimine (pyridoxal) form of the enzyme. This slow reaction of difluoro-oxaloacetate suggested the use of the fluoro analogue to help clarify the reactions of the aminic form of aspartate transaminase, which have been less studied than those of the aldimine form.

Materials and Methods

Difluoro-oxaloacetate was prepared as described by Briley *et al.* (1977*a*); aqueous solutions were adjusted to pH7.4 with KOH before use. Cysteinesulphinate was from Sigma (London) Chemical Co., London S.W.6, U.K., and all other reagents were from BDH Chemicals, Poole, Dorset, U.K.

The aminic form of cytoplasmic aspartate transaminase (L-aspartate–2-oxoglutarate aminotransferase, EC 2.6.1.1) was prepared as described by Briley *et al.* (1977*a*). Concentrations of enzyme are quoted in terms of active sites, assuming a dimer of mol.wt. 93000 (Ovchinnikov *et al.*, 1973). Active sites were determined from A_{332} by using extinction coefficients determined as described by Torchinsky *et al.* (1968).

All spectrophotometric measurements were done on a Unicam SP.1800 instrument unless otherwise stated.

Results

Spectral shift from 332*nm to* 360*nm*

Addition of difluoro-oxaloacetate to the aminic form of aspartate transaminase resulted in a time-dependent shift of $\lambda_{max.}$ of the absorption spectrum from 332nm to 360nm. This change was sufficiently slow to follow the progress of the reaction by repeated spectral scans (Fig. 1). After 75min the reaction was complete as judged by the disappearance of the absorbance maximum in the 330nm region and by the fact that addition of 0.5mM-oxaloacetate (or 2-oxoglutarate) to the completed reaction mixture elicited no further spectral change.

Pseudo-first-order rate constants were calculated from semilogarithmic plots of $A^{\infty}_{360}-A^{t}_{360}$ against time, obtained from reaction mixtures containing difluoro-oxaloacetate (5–500μM) and the aminic form of aspartate transaminase (25μM) in 20mM-sodium pyrophosphate buffer, pH7.4 at 25°C. Although the time-dependence of the increase in A_{360} appeared to follow first-order kinetics at all concentrations of

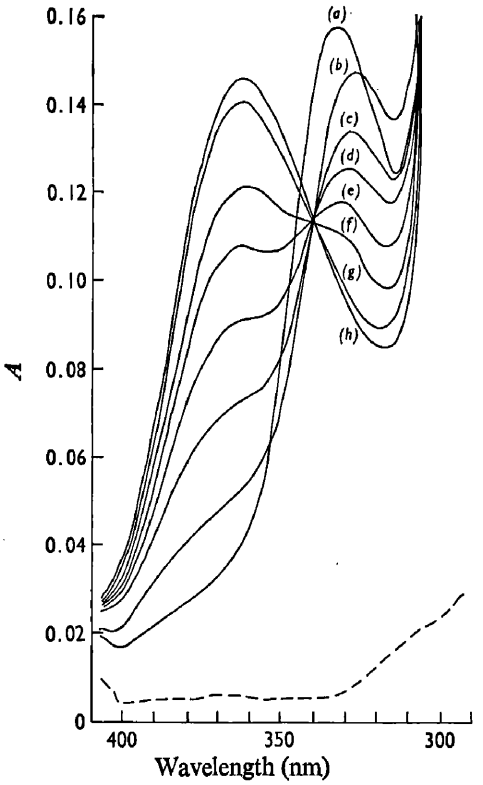

Fig. 1. *Spectral changes on addition of difluoro-oxaloacetate to the aminic form of aspartate transaminase*

Difluoro-oxaloacetate (25 μM) was added to a solution of the aminic form of aspartate transaminase (19 μM) in 20mM-sodium pyrophosphate buffer, pH7.4, at 25°C. The absorption spectra were obtained from successive scans (scan rate 0.5nm/s) before (*a*) and after (*b–h*) addition of difluoro-oxaloacetate after the time intervals indicated: (*b*) 0.5min; (*c*) 5min; (*d*) 9min; (*e*) 16min; (*f*) 25min; (*g*) 45min; (*h*) 75min. ----, Baseline.

$$\underset{(\lambda_{max.}\ 332\text{nm})}{E'} + S \underset{k'_{-1}}{\overset{k'_{+1}}{\rightleftharpoons}} X \xrightarrow{k'_{+2}} \underset{(\lambda_{max.}\ 360\text{nm})}{Y}$$

Scheme 1. *Mechanism consistent with the kinetics of the slow spectral change in the reaction of difluoro-oxaloacetate (S) with the aminic form of aspartate transaminase (E')*

X, enzyme species absorbing in the 330nm region.

difluoro-oxaloacetate, the apparent first-order rate constant increased with the concentration of difluoro-oxaloacetate becoming independent of the latter at concentrations of difluoro-oxaloacetate greater than 150 μM when the constant reached a limiting value of $1.18\times10^{-3}s^{-1}$ at 25°C. This behaviour is consistent with a mechanism involving a bimolecular step followed by at least one unimolecular step (Jencks, 1969) as shown in Scheme 1. The occurrence of an intermediate X (Scheme 1) is also indicated by a rapid initial shift of $\lambda_{max.}$ from 332nm to 328nm on addition of difluoro-oxaloacetate to the aminic form of the enzyme. This rapid shift has been noted previously (Briley *et al.*, 1977*a*) and is observable in the spectra of Fig. 1. Further evidence for such an intermediate is provided by the absence of an isosbestic point between the species with $\lambda_{max.}$ 332nm and that with $\lambda_{max.}$ 360nm (Fig. 1), although an isosbestic point does exist between the 328nm peak and that at 360nm.

Initial rates of the above spectral change were determined at constant enzyme (19 μM) and varying difluoro-oxaloacetate concentrations (7–40 μM) in 20mM-sodium pyrophosphate buffer, pH7.4, by following the increase in A_{360} at 25°C. The data were analysed by the mechanism of Scheme 1 assuming a steady state for X. By using the iterative procedure described by Smith *et al.* (1977) values of $K'_m = (k'_{-1}+k'_{+2})/k'_{+1} = 7.0\,\mu$M and $k'_{+2} = 1.25\times10^{-3}s^{-1}$ were obtained.

Changes in absorption maxima of pyridoxal phosphate-dependent enzymes from the 330nm region to that at 360nm are known (Fasella & Turano, 1970) to be associated with the conversion of aminic (ketimine) forms of such enzymes into aldimine species. Addition of excess of asparate or glutamate (100mM) to a mixture of difluoro-oxaloacetate (13 μM) and the aminic form of the enzyme (12 μM) in 20mM-sodium pyrophosphate buffer, pH7.4, which had been left to react to completion at 25°C, resulted in rapid disappearance of the 360nm absorption maximum and reappearance of a peak at approx. 330nm. This indicates the presence of free aldimine enzyme in the reaction mixture at completion.

Spectral shift from 332nm to 328nm

It is reasonable to assume that the kinetically predicted intermediate X of Scheme 1 represents the spectrally observable species with $\lambda_{max.}$ 328nm, although further intermediates are not precluded. Direct observation of the pre-equilibrium of Scheme 1 is complicated by the ensuing slow shift of the absorbance maximum from 328nm to 360nm (X → Y). A close approximation to the pre-equilibrium was obtained in practice, however, in the presence of cysteinesulphinate, a substrate analogue that reacts rapidly and irreversibly with the aldimine form of aspartate transaminase giving pyruvate and the aminic form of the enzyme (Jenkins & D'Ari, 1966). As shown in Scheme 2, cysteinesulphinate can be used to recycle the aldimine form of the enzyme to the aminic species. Because the formation of X (Scheme 2) from E' is very much faster than the conversion of X into E virtually all the enzyme will be represented by the pre-equilibrium of Scheme 2, provided that the concentration of cysteinesulphinate is sufficient to ensure that the recycling of the aldimine species (Scheme 2, step 3) is not rate-limiting. The spectrum

$$\underset{(\lambda_{max.}\ 332\,nm)}{E'} + S \rightleftharpoons \underset{(\lambda_{max.}\ 328\,nm)}{X} \quad (1)$$

$$X \xrightarrow{\text{Slow}} E + A \quad (2)$$

$$E + \text{cysteinesulphinate} \longrightarrow E' + \text{pyruvate} + SO_2 \quad (3)$$

Scheme 2. *Reaction sequence used to observe the 328 nm spectral peak*

S, difluoro-oxaloacetate; A, difluoroaspartate; E' and E, aminic and aldimine forms respectively of aspartate transaminase; K_D, dissociation constant of X (step 1).

obtained under these conditions is shown in Fig. 2 which shows that the 328 nm absorption maximum is a well-defined peak with no shoulder at 332 nm, indicating that the pre-equilibrium of the aminic form of the enzyme with difluoro-oxaloacetate (Scheme 2, step 1) lies well to the right-hand side. This is consistent with the kinetic parameters derived from initial-rate data for the intermediate X and so further supports the identification of the latter with the species having $\lambda_{max.}$ 328 nm. Direct determination of the absorption coefficient at 328 nm gave a value of 7.7×10^3 litre·mol^{-1}·cm^{-1}.

The kinetics of the spectral change from 332 nm to 328 nm were studied by recording the time course of the change in A_{345} after rapid mixing of the aminic form of aspartate transaminase and difluoro-oxaloacetate in a stopped-flow spectrophotometer. The choice of 345 nm was based on the difference spectrum between aminic enzyme and the species with $\lambda_{max.}$ 328 nm (Fig. 2 inset) from which it was found that maximum differences in extinction coefficient occur at 310 nm and 345 nm. Progress curves were recorded at five different initial concentrations of difluoro-oxaloacetate; the ratio of concentrations of difluoro-oxaloacetate to enzyme varied from approx. 1:1 to approx. 6:1. The progress curve of a typical experiment (Fig. 3) shows a rapid initial decrease in A_{345} followed by a much slower increase (associated with the slow shift from 328 nm to 360 nm). No transient lag or burst was detected. Observation of the spectral region from 300 nm to 500 nm during the first 3 s of the reaction (at concentrations similar to those used in the stopped-flow experiments) by using a rapid-scanning spectrophotometer (Hollaway & White, 1975) confirmed the absence of a spectrally distinct intermediate between the aminic enzyme and the species with $\lambda_{max.}$ 328 nm on a time scale down to 50 ms (Fig. 4).

The amplitude of the initial absorbance change at 345 nm was dependent on the difluoro-oxaloacetate concentration (Fig. 5, inset). The data were analysed by assuming that the amplitude can be taken as a measure of a metastable equilibrium between the species with $\lambda_{max.}$ 332 nm and that with $\lambda_{max.}$ 328 nm.

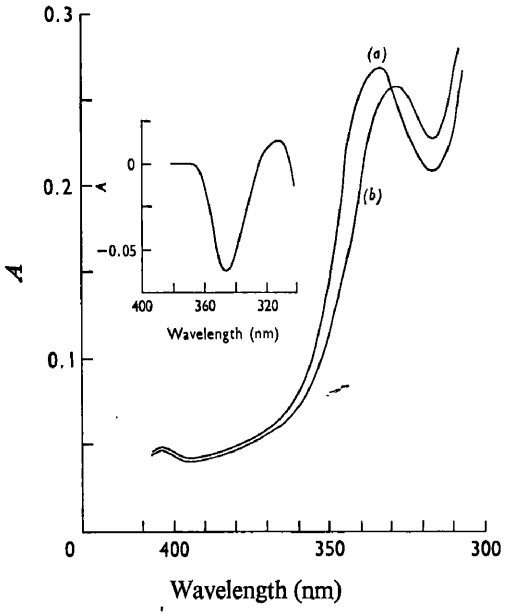

Fig. 2. *Absorption spectra of aspartate transaminase in the presence of excess of difluoro-oxaloacetate and cysteinesulphinate*

(*a*) Aspartate transaminase (21 μM) and cysteinesulphinate (2 mM) in 20 mM-sodium pyrophosphate buffer, pH 7.4, at 25°C. (*b*) As for (*a*) with the addition of difluoro-oxaloacetate (0.2 mM final concn.). Inset: difference spectrum between (*b*) (sample) and (*a*) (reference).

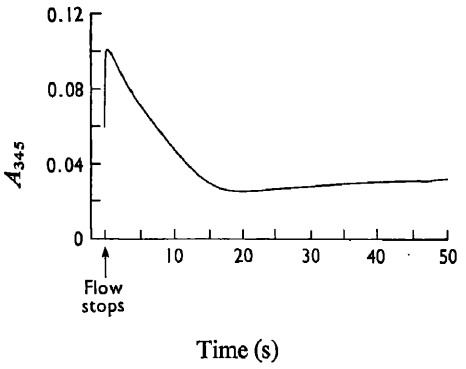

Fig. 3. *Variation of A_{345} on addition of difluoro-oxaloacetate to the aminic form of aspartate transaminase*

The reaction mixture contained the aminic form of aspartate transaminase (final concn. 23.1 μM) from one syringe and difluoro-oxaloacetate (final concn. 80 μM) from the other in 20 mM-sodium pyrophosphate buffer, pH 7.4, at 25°C in a Durrum–Gibson stopped-flow spectrophotometer (light-path 2 cm) coupled to a Tectronix storage oscilloscope. Permanent records of the traces were made on Polaroid film.

Application of the iterative procedure described by Smith *et al.* (1977) gave a final plot (Fig. 5) from which a value (8.75 μM) for the dissociation constant K_D of

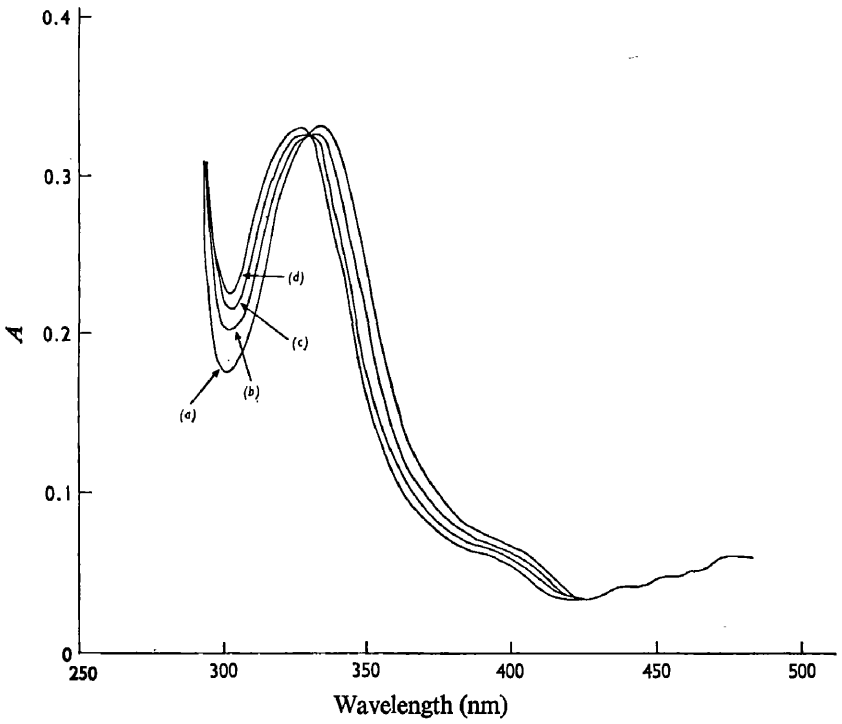

Fig. 4. *Rapid spectrophotometric scans of the reaction mixture after addition of difluoro-oxaloacetate to the aminic form of aspartate transaminase*

The aminic form of aspartate transaminase (final concn. 100μM) and difluoro-oxaloacetate (final concn. 1mM) in 20mM-sodium pyrophosphate buffer, pH7.4, were rapidly mixed (3ms) and the absorption spectrum was scanned (200nm/ms) after various time intervals as indicated by using the spectrophotometer described by Hollaway & White (1975). (*a*) 0.125s; (*b*) 0.625s; (*c*) 1.25s; (*d*) 2.625s.

$$\underset{(\lambda_{max.}\ 332nm)}{E'} + S \underset{k_{-1}}{\overset{k_{+1}}{\rightleftharpoons}} \underset{(\lambda_{max.}\ 332nm)}{X_1} \underset{k_{-2}}{\overset{k_{+2}}{\rightleftharpoons}} \underset{(\lambda_{max.}\ 328nm)}{X_2} \xrightarrow{k_{+3}} \underset{(\lambda_{max.}\ 360nm)}{Y}$$

Scheme 3. *Mechanism used as the basis for computer simulation of the fast spectral change in the reaction of difluoro-oxaloacetate (S) with the aminic form of aspartate transaminase (E')*

the species with $\lambda_{max.}$ 328nm and a value for the absorption coefficient at 345nm (2.8×10^3 litre·mol^{-1}·cm^{-1}) of the same species were derived. The latter value is in good agreement with that (3.1×10^3 litre·mol^{-1}·cm^{-1}) obtained directly from the spectrum of a mixture of difluoro-oxaloacetate, the aminic form of the enzyme and cysteinesulphinate (Fig. 2).

A double-logarithmic plot of the initial rates [obtained from the progress curves by the method of Cornish-Bowden (1975)] of the decrease in A_{345} against initial difluoro-oxaloacetate concentration was linear, with a slope of unity, indicating first-order kinetics with respect to difluoro-oxaloacetate. The apparent second-order rate constant calculated from the intercept was 1.74×10^3 litre·mol^{-1}·s^{-1}. However, analysis of the total progress curves by using integrated empirical rate equations showed that the data could not be analysed in terms of simple first- or second-order kinetics and suggested a mechanism for the formation of the species with $\lambda_{max.}$ 328nm involving a bimolecular reaction followed by a unimolecular step. The progress curves were analysed by digital simulation with the program CHEKMAT of Curtis & Chance (1972). This program adjusts the values of specified parameters (usually rate constants) of a reaction mechanism to give the best fit between simulated and experimentally observed time courses. The mechanism (Scheme 3) chosen for simulation was an expanded version of Scheme 1 in which a further intermediate X_1, spectrally indistinguishable from aminic enzyme, is included before the species with $\lambda_{max.}$ 328nm (redesignated X_2). Because the progress

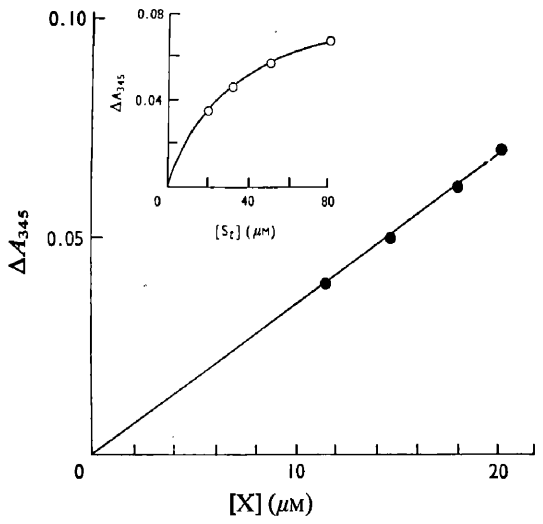

Fig. 5. *Determination of the dissociation constant (K_D) and absorption coefficient ε_{345} of the species with $\lambda_{max.}$ 328 nm (X)*

Addition of difluoro-oxaloacetate (S) to the aminic form of aspartate transaminase (E′) resulted in an initial rapid decrease in A_{345} (Fig. 3), the amplitude (ΔA_{345}) of which varied with [S_t] (concn. of S at time t) (see inset). By using the procedure of Smith *et al.* (1977), assumed values of K_D ([E′]. [S]/[X]) were varied until the best fit to a straight line through the origin was obtained when ΔA_{345} was plotted against [X] at different values of [S_t]. The above plot represents the best-fit line and corresponds to a value for K_D 8.75 μM. The gradient of the line is $\varepsilon'_{345}-\varepsilon_{345}$ where ε'_{345} is the absorption coefficient of the aminic form of aspartate. Conditions are as described in the legend to Fig. 3 except that difluoro-oxaloacetate concentrations varied from 20 μM to 80 μM.

curves were recorded in absorbance units, the absorption coefficients of the reactants and intermediates at 345 nm were supplied to the program to enable the concentration flux of the various species to be expressed in terms of absorption in the simulation runs.

The absorption coefficient of E′ (and hence of X_1) was obtained from direct measurement of the spectrum of aminic enzyme, and that of X_2 from the variation with difluoro-oxaloacetate concentration of the amplitude of the initial decrease in A_{345} as described above. The absorption coefficient for Y was obtained directly from the spectrum of a completed reaction mixture of the aminic form of aspartate transaminase and a small excess of difluoro-oxaloacetate. The value of the first-order rate constant k'_{+2} (Scheme 1) was known both as the limiting first-order rate constant derived from the progress curves of the slow spectral change (332 nm → 360 nm) and from analysis of the initial rates of that spectral shift. This value was accordingly assigned to k_{+3} (Scheme 3) as a fixed parameter. The irreversibility of the step X → Y is justified by the total absence of absorbance in the 330 nm region of mixtures of the aminic form of aspartate transaminase and difluoro-oxaloacetate, which had been left to react to completion.

The computer program simulated the progress of the reaction, varying k_{+1}, k_{-1}, k_{+2} and k_{-2} to give the best fit to the experimental progress curves (Fig. 6). The values of the rate constants so obtained are: k_{+1}, 2.61×10^6 litre·mol^{-1}·s^{-1}; k_{-1}, 1.02×10^5 s^{-1}; k_{+2}, 5.57×10^1 s^{-1}; k_{-2}, 1.05×10^{-2} s^{-1}. The form of output of the program CHEKMAT does not allow the definition of precise confidence limits for the rate constants. It does, however, give an indication of the relative precision of these values; from these it can be stated that values for k_{-2} and k_{-1} are more highly defined than those of k_{+1} and k_{+2}.

Although the fit between experiment and theory in Fig. 6 is reasonable, it can be seen that at the highest substrate concentration the fit becomes progressively worse as the reaction proceeds. A possible explanation for this may be the formation of a difluoro-oxaloacetate–aldimine enzyme complex ($\lambda_{max.}$ 430 nm) which is known to absorb only weakly at 345 nm (Briley *et al.*, 1977*b*). As the reaction is followed as a decrease in A_{345}, the conversion of enzyme into this complex would increase the apparent rate of reaction. This effect would be more pronounced at high concentrations of difluoro-oxaloacetate.

Discussion

The results show that addition of difluoro-oxaloacetate to the aminic form of aspartate transaminase leads to complete conversion of the enzyme into its aldimine form or into a species in rapid equilibrium with it. Simulation of the progress curves of the fast initial spectral change (332 nm → 328 nm) based on the mechanism shown in Scheme 3 led to a derivation of rate constants k_{+1}, k_{-1}, k_{+2}, k_{-2} which correlate well with independent determinations of related kinetic parameters as follows.

(1) The Michaelis constant $[(k'_{-1}+k'_{+2})/k'_{+1}$; Scheme 1] derived from the initial rates of the overall slow spectral change (332 nm → 360 nm) gave a value of 7.0 μM. In terms of the rate constants of Scheme 3, the Michaelis constant is $(k_{-1}k_{-2}+k_{+2}k_{+3}+k_{-1}k_{+3})/k_{+1}(k_{+2}+k_{-2}+k_{+3})$ giving a predicted value of 7.4 μM.

(2) The dissociation constant of the species with $\lambda_{max.}$ 328 nm ([E′] [S]/[X]; Scheme 2, step 1) obtained from analysis of the amplitudes of the fast spectral change had a value of 8.75 μM, compared with 7.4 μM predicted from the rate constants of Scheme 3 $(k_{-1}k_{-2}/k_{+1}k_{+2})$.

(3) The apparent second-order rate constant derived from the initial rates of the fast spectral change is 1.74×10^3 litre·mol^{-1}·s^{-1} compared with a

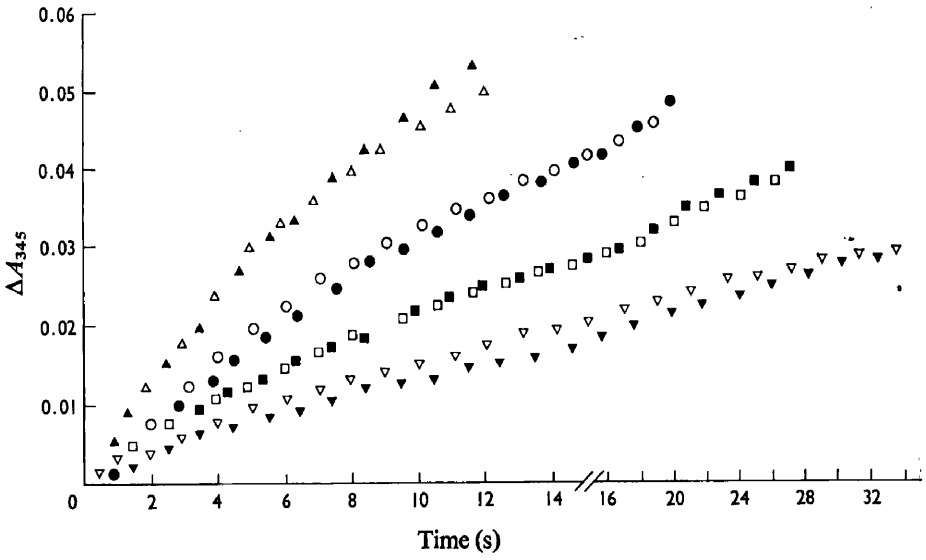

Fig. 6. *Computer simulation of the progress curves of formation of the species with* $\lambda_{max.}$ *328 nm*

The experimental curves (▲, ●, ■, ▼) are plotted as changes in absorbance (ΔA_{345}) from the absorbance of the free aminic enzyme and were obtained under the conditions described in the legend to Fig. 3, except that the final concentrations of difluoro-oxaloacetate were: ▲, 80 μM; ●, 50 μM; ■, 30 μM; ▼, 20 μM. The simulated curves (△, ○, □, ▽) corresponding to curves ▲, ●, ■, ▼ respectively represent the best fit to the experimental curves which were obtained as the rate constants $k_{+1}, k_{-1}, k_{+2}, k_{-2}$ were varied by using the computer program CHEKMAT of Curtis & Chance (1972) run on an IBM 360 computer at University College, London. Note the change of time scale after 15 s.

predicted value of 1.42×10^3 litre·mol^{-1}·s^{-1} ($k_{+1}k_{+2}/k_{-1}$).

The internal consistency of the kinetic parameters justifies the mechanism of Scheme 3 as a basis for the reaction of the aminic form of the enzyme with difluoro-oxaloacetate, although further intermediates are not precluded.

The question arises as to the significance in molecular terms of the species in Scheme 3. By analogy with the generally accepted mechanism of transamination (Fasella & Turano, 1970), interaction of difluoro-oxaloacetate and the aminic form of the enzyme might be expected to lead, via a tetrahedral intermediate (I) to a ketimine Schiff base (II) which would undergo a prototropic shift to the aldimine Schiff base (III) (Scheme 4). On the assumption that Y (Scheme 3) is either the aldimine form of the enzyme or a complex in rapid equilibrium with it, then k_{+3} represents the slow step in the interconversion of aminic and aldimine species. With the natural substrates L-glutamate and L-aspartate (Banks *et al.*, 1968) and with *threo*-β-chloroglutamate (Antonini *et al.*, 1970) the rate-limiting step in transamination is believed to coincide with the loss of a proton from the aldimine Schiff base initiating the prototropic shift to a ketimine complex (corresponding to the interconversion III → II in Scheme 4). For difluoro-oxaloacetate the evidence presented here is consistent with a similar assignment of the slow step to abstraction of a proton from the Schiff base (II) leading to the aldimine species (III). However, it is also possible that the rate-determining step could reflect a conformational change of the ketimine Schiff base (II) or even a dehydration of its tetrahedral precursor (I) (cf. Hammes & Haslam, 1969).

On the basis of the above discussion X_2, the species absorbing at 328 nm (Scheme 3), could represent the ketimine Schiff base (II) or possibly its precursor (I) (Scheme 4). Jenkins (1963) has briefly noted the occurrence of a derivative with absorbance maximum 325 nm on reaction of difluoro-oxaloacetate with the aminic form of aspartate transaminase, and Hammes & Haslam (1969), using temperature-jump techniques, obtained evidence for a ketimine species absorbing in the 330 nm region in the reaction of *erythro*-β-hydroxyaspartate with the aldimine form of the enzyme. However, no spectrally distinct species corresponding to that with $\lambda_{max.}$ 328 nm has been reported with the natural substrates of aspartate transaminase.

It is probable that X_2 is the aminic enzyme–difluoro-oxaloacetate complex responsible for competitive inhibition of transamination of 2-oxoglutarate by aspartate transaminase in the the presence of difluoro-oxaloacetate (Briley *et al.*, 1977*a*). The K_i value kinetically derived for the inhibitory complex was 9.2 μM or 5.9 μM, depending on the experimental approach. These values are compatible with that of 7.4 μM calculated from the rate constants of Scheme 3 [$K_i = k_{-1}k_{-2}/k_{-1}(k_{+2}+k_{-2})$].

Although no further spectrally distinct intermediates could be detected before formation of X_2,

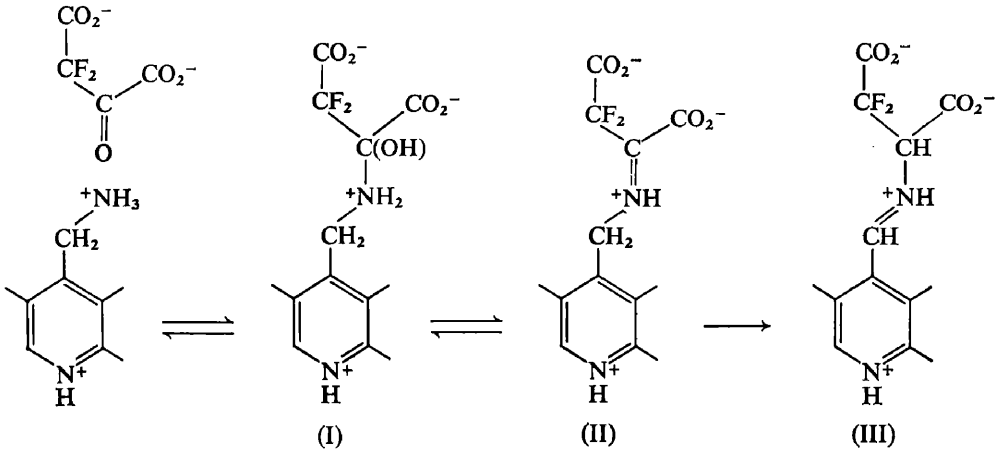

Scheme 4. *Possible molecular species involved in the reaction of difluoro-oxaloacetate with the aminic form of aspartate transaminase*

kinetic evidence indicated the presence of at least one intermediate with $\lambda_{max.}$ 332nm, which was accordingly included (X_1) in the mechanism of Scheme 3 and in the computer simulation. It is likely that X_1 represents a non-covalent Michaelis complex; this is consistent with an absorbance maximum at 332nm, as for the aminic enzyme and with a dissociation constant of 39mM (k_{-1}/k_{+1}).

The second-order rate constant (k_{+1}) describing the rate of formation of X_1 is smaller than the lower limits obtained for the natural substrates (>10^8 litre·mol^{-1}·s^{-1}). A possible explanation for this could lie in a tendency for difluoro-oxaloacetate to exist in solution as its hydrate (Kun & Dummel, 1969), which would decrease the effective concentration of the reactive keto form.

Whereas the first-order rate constant for the slowest step in the transformation of difluoro-oxaloacetate (k_{+3}) is three orders of magnitude greater than that seen in non-enzymic imidazole-catalysed model systems involving pyridoxal phosphate (Banks *et al.*, 1969), k_{+3} is some five orders of magnitude less than that for the corresponding step in the enzymic transamination of the natural substrates (Fasella & Turano, 1970). There are clearly a number of possible explanations for this discrepancy, depending on the assignment of the rate-determining step. If this is assumed to be the abstraction of a benzylic proton from the ketimine Schiff base (II) as suggested above, then the reaction might be expected on steric grounds to be considerably slower than with oxaloacetate. According to the hypothesis of Dunathan (1966), conversion of aldimine into ketimine Schiff bases is initiated by labilization of the substrate α C–H bond, which must be oriented perpendicular to the π-electron system conjugated to the coenzyme pyridine ring. Attainment of a corresponding orientation of the benzylic proton labilized in the ketimine–aldimine tautomerization would, according to molecular models, be severely restricted by steric interactions between the fluorine atoms and the benzylic protons in a difluoro-oxaloacetate moiety aligned relative to the cofactor ring as described by Ivanov & Karpeisky (1969). Such steric hindrance, absent with the natural substrate, would serve to account for the very much slower reaction of the fluoro analogue.

The general paucity of knowledge about the reaction of the aminic form of aspartate transaminase has been attributed to the lack of a suitable substrate analogue (Fasella & Turano, 1970). Difluoro-oxaloacetate, which is a stable isosteric analogue, appears to go some way toward fulfilling this need insofar as the slowness of its reaction with the aminic enzyme has provided evidence for the presence of two aminic enzyme–analogue complexes without resort to particularly sophisticated techniques. The direct demonstration of the species with $\lambda_{max.}$ 328nm, provisionally attributed to a ketimine Schiff base (II), suggests the possibility of trapping this intermediate by borohydride reduction. Moreover, the apparently complete conversion into aldimine species after the slow step of the reaction further suggests a similar trapping and isolation of the corresponding aldimine complex, again from reactions involving initially difluoro-oxaloacetate.

We thank Dr. E. M. Chance and Dr. C. M. Kemp for help in running the programme CHEKMAT, Dr. M. R. Hollaway and Mr. H. A. White for making available the rapid-scanning stopped-flow spectrophotometer, Dr. C. Wharton for use of the stopped-flow spectrophotometer, and the Enzyme Chemistry and Technology Committee of the Science Research Council for a grant (to R. E. and R. H.) and a studentship (to G. D. S.).

References

Antonini, E., Brunori, M., Fasella, P., Khomutov, R., Manning, J. M. & Severin, E. S. (1970) *Biochemistry* **9**, 1211–1216

Banks, B. E. C., Bell, M. P., Lawrence, A. J. & Vernon, C. A. (1968) in *Pyridoxal Catalysis, Enzymes and Model Systems* (Snell, E. E., Braunstein, A. E., Severin, E. S. & Torchinsky, Yu. M., eds.), pp. 191–202, Wiley–Interscience, London

Briley, P., Eisenthal, R., Harrison, R. & Smith, G. D. (1977*a*) *Biochem. J.* **161**, 383–387

Briley, P., Eisenthal, R., Harrison, R. & Smith, G. D. (1977*b*) *Biochem. J.* **163**, 325–331

Cornish-Bowden, A. (1975) *Biochem. J.* **149**, 305–312

Curtis, A. R. & Chance, E. M. (1972) *Proc. FEBS Meet. 7th* **25**, 39–57

Dunathan, H. C. (1966) *Proc. Natl. Acad. Sci. U.S.A.* **55**, 712–721

Fasella, P. & Turano, C. (1970) *Vitam. Horm. (N.Y.)* **28**, 157–194

Hammes, G. G. & Haslam, J. L. (1969) *Biochemistry* **8**, 1591–1598

Hollaway, M. R. & White, H. A. (1975) *Biochem. J.* **149**, 221–231

Ivanov, V. I. & Karpeisky, M. Ya. (1969) *Adv. Enzymol.* **32**, 22–53

Jencks, W. P. (1969) *Catalysis in Chemistry and Enzymology*, pp. 572–574, McGraw–Hill, New York

Jenkins, W. T. (1963) in *Chemical and Biological Aspects of Pyridoxal Catalysis* (Snell, E. E., Fasella, P. M., Braunstein, A. & Rossi Fanelli, A., eds.), p. 146, Pergamon Press, Oxford

Jenkins, W. T. & D'Ari, L. (1966) *Biochem. Biophys. Res. Commun.* **22**, 376–382

Kun, E. & Dummel, R. J. (1969) *Methods Enzymol.* **13**, 629

Ovchinnikov, Yu. A., Egorov, C. A., Aldanova, V. A., Feigina, M. Yu., Lipkin, V. M., Abdulaev, N. G., Grishin, E. G., Kiselev, A. P., Modyanov, N. N., Braunstein, A. E., Polyanovsky, O. L. & Nosikov, V. V. (1973) *FEBS Lett.* **29**, 31–34

Smith, G. D., Eisenthal, R. & Harrison, R. (1977) *Anal. Biochem.* **79**, 643–647

Torchinsky, Yu. M., Malakhova, E. A., Livanova, N. B. & Pikhelgas, V. Yu. (1968) in *Pyridoxal Catalysis: Enzymes and Model Systems* (Snell, E. E., Braunstein, A. E., Severin, E. S. & Torchinsky, Yu. M., eds.), pp. 269–290, Wiley–Interscience, London

Biochem. J. (1977) **163**, 325–331
Printed in Great Britain

[^{19}F]Fluorine Nuclear-Magnetic-Resonance Study of the Interaction of Difluoro-oxaloacetate with Aspartate Transaminase

By PATRICIA A. BRILEY, ROBERT EISENTHAL, ROGER HARRISON and GEOFFREY D. SMITH
Biochemistry Group, School of Biological Sciences, University of Bath, Bath BA2 7AY, U.K.

(*Received* 12 *October* 1976)

Difluoro-oxaloacetate interacts with the aldimine form of aspartate transaminase to give a complex, the dissociation constant of which has been determined spectrophotometrically and by ^{19}F n.m.r. (nuclear magnetic resonance). The ^{19}F n.m.r. line-width–pH and chemical-shift–pH profiles of difluoro-oxaloacetate in the presence of the aldimine form of the enzyme both show inflexion points in the pH5 and pH8 regions, which may arise from variations in the binding of difluoro-oxaloacetate as specific groups on the enzyme are successively protonated. Difluoro-oxaloacetate also interacts with apoenzyme to form a complex, the dissociation constant of which was determined by ^{19}F n.m.r. The ^{19}F n.m.r. line-width–pH and chemical-shift–pH profiles of difluoro-oxaloacetate in the presence of apoenzyme show a single inflexion point in the region of pH8. The absence, in this case, of an inflexion in the pH5 region indicates that the latter, present in the corresponding profiles for the aldimine form of the enzyme, results from ionization of an enzyme group associated with the pyridoxal phosphate cofactor.

Difluoro-oxaloacetate behaves as an effective analogue of oxaloacetate in being transaminated by the aminic (pyridoxamine) form of aspartate transaminase (Briley *et al.*, 1977). In view of the known binding of oxaloacetate and of a number of other dicarboxylic acids to the aldimine (pyridoxal) form of aspartate transaminase (hereinafter called 'aldimine enzyme') (Haarhoff, 1969), difluoro-oxaloacetate might be expected to act as an analogue of oxaloacetate in this respect also and to form an 'abortive complex' with the aldimine enzyme. Although such a complex was not detected by kinetic analysis of the inhibition of transamination of 2-oxoglutarate and aspartate by difluoro-oxaloacetate (Briley *et al.*, 1977), an abortive complex having a dissociation constant in the millimolar range would not be apparent under the conditions of the experiments.

Like perfluorosuccinate, which has been used to study binding of dicarboxylic acids to the enzyme (Martinez-Carrion *et al.*, 1973), difluoro-oxaloacetate gives rise to a single sharp ^{19}F n.m.r.* signal and so constitutes a convenient probe with which to study binding to both holoenzyme and apoenzyme, particularly so in the case of the apoenzyme, which is not readily susceptible to spectrophotometric study. The present paper describes the use of the ^{19}F n.m.r. signal of difluoro-oxaloacetate to report on the nature of the binding to both forms of aspartate transaminase.

* Abbreviation: n.m.r., nuclear magnetic resonance.

Experimental

Materials

Difluoro-oxaloacetic acid was prepared as described by Briley *et al.* (1977) and perfluorosuccinic acid was purchased from Koch–Light Laboratories Ltd., Colnbrook, Bucks., U.K. Unless otherwise stated, both acids were neutralized to pH7.4 with KOH before use. Cysteinesulphinate was from Sigma (London) Chemical Co., London S.W.6, U.K., and all other reagents were from BDH Chemicals Ltd., Poole, Dorset, U.K.

The aldimine and aminic forms of cytoplasmic aspartate transaminase (L-aspartate–2-oxoglutarate aminotransferase, EC 2.6.1.1) were prepared from pig heart as described by Briley *et al.* (1977). The aldimine enzyme typically showed an A_{280}/A_{362} ratio of 7.25 at pH7.4. The apoenzyme was prepared from the aldimine enzyme via the aminic form as described by Scardi *et al.* (1963), except that cysteinesulphinate was substituted for glutamate. This procedure consistently achieved greater than 95% resolution as determined by residual transaminase activity.

The apoenzyme could be re-activated with excess of pyridoxal phosphate in 50mM-sodium acetate buffer, pH7.4, at 22°C. Throughout experiments using apoenzyme, restorable activity was monitored and was found to be greater than 90% of original activity in experiments at pH7.4 and greater than 70% at lower pH values. Concentrations of apoenzyme are quoted in terms of restorable activity.

Methods

Enzyme activity was assayed by determination of the rate of oxaloacetate production (A_{260}) from 2-oxoglutarate and aspartate. Protein was determined by measuring A_{280} as described by Banks *et al.* (1968). Concentrations of enzyme are quoted in terms of active sites, assuming a dimer of mol.wt. 93000 (Ovchinnikov *et al.*, 1973). Active sites were determined from A_{360} (aldimine) and A_{332} (aminic) by using absorption coefficients determined as described by Torchinsky *et al.* (1968).

N.m.r. determinations. ^{19}F n.m.r. spectra were recorded at 94.1 MHz with a JEOL PS 100 n.m.r. spectrometer in 5mm-diameter sample tubes with co-axial capillary tubes containing either 2M-difluoro-oxaloacetate or 2M-perfluorosuccinate as internal lock signal. Chemical shifts were determined relative to the internal lock signal by using an electronic counter, and line widths were recorded as the peak width at half height. Where necessary, the signal-to-noise ratio was enhanced by using repeated scans with a JEOL JNM SB-3 signal-to-noise booster. Samples were maintained at 28±1°C.

For experiments at constant pH, enzyme (approx. 20mg) was dissolved in a small volume of 20mM-potassium pyrophosphate buffer, pH7.4, dialysed against 2×5 litres of the same buffer and concentrated by vacuum dialysis to 0.4ml. For determinations at varied pH values the enzyme was dialysed against 2×5 litres of double-distilled water.

Spectrophotometric determinations. These were done in a Pye–Unicam SP. 1800 instrument at 25±1°C unless otherwise stated.

Calculation of dissociation constants and absorption coefficients by spectrophotometric titration. The interaction of an enzyme (E) with a ligand (S) to give a complex (ES)

$$E+S \rightleftharpoons ES$$

can conveniently be followed from absorbance changes of the $\lambda_{max.}$ of ES provided that this differs from that of the free enzyme. If $[E_t]$ and $[S_t]$ are the total concentrations of enzyme and ligand respectively and K is the dissociation constant of the complex ES, then it can be shown that:

$$\frac{[S_t]}{\Delta A}=\frac{K+[S_t]}{(\varepsilon_E-\varepsilon_{ES})[E_t]}$$

where ΔA is the difference between the absorbance of the system and that of free enzyme alone, ε_E and ε_{ES} are the molar absorption coefficients of E and ES respectively at the given wavelength, and it is assumed that $[S_t] \gg [E_t]$.

$[S_t]/\Delta A$ was plotted against $[S_t]$ as described by Jenkins & Taylor (1965) to give a straight line, from which K was obtained as the negative intercept on the $[S_t]$ axis. Substitution of ε_E (determined directly from aldimine enzyme alone) in the expressions for the slope and intercept gave ε_{ES}.

Calculation of dissociation constants and chemical shifts (Δ) *by using* ^{19}F *n.m.r.* K and Δ values for difluoro-oxaloacetate and perfluorosuccinate in the presence of aldimine enzyme and for difluoro-oxaloacetate with apoenzyme were determined by the iterative procedure described by Groves *et al.* (1967) and Smith *et al.* (1977). In this procedure, assumed values of K are varied so as to obtain the best fit of the experimental points to a straight line when $\delta_{obs.}$ (chemical-shift value) is plotted against $[ES]/[S_t]$, where [ES] is the concentration of enzyme–ligand complex and $[S_t]$ the total concentration of ligand. The slope of the final line is Δ.

Results

Difluoro-oxaloacetate–aldimine-enzyme complex

Spectrophotometric determination of dissociation constant and absorption coefficient. Incremental addition of difluoro-oxaloacetate (S) to a solution of the aldimine form of aspartate transaminase ($\lambda_{max.}$ = 360nm) in pyrophosphate buffer at pH7.4 gave rise to an absorbance peak with $\lambda_{max.}$ = 435nm, characteristic of the difluoro-oxaloacetate–enzyme complex. A plot of $[S_t]/\Delta A_{435}$ against $[S_t]$ gave a straight line (Fig. 1) from which the dissociation constant K (2.8±0.1mM) and ε_{435} (7600litre·mol^{-1}·cm^{-1}) of the difluoro-oxaloacetate–aldimine-enzyme complex were obtained as described in the Experimental section. An identical value of K was obtained

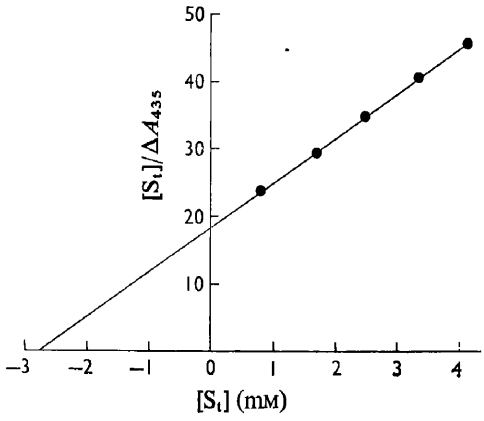

Fig. 1. *Plot of* $[S_t]/\Delta A_{435}$ *against* $[S_t]$ *for addition of difluoro-oxaloacetate to aldimine enzyme*

Difluoro-oxaloacetate was added incrementally to a solution of the aldimine form of aspartate transaminase (26μM) in 20mM-pyrophosphate buffer, pH7.4. $[S_t]$ represents the total concentration of difluoro-oxaloacetate and ΔA_{435} the absorbance difference at 435nm relative to that of free aldimine enzyme.

when the α-form of the aldimine enzyme (Martinez-Carrion *et al.*, 1965) was used.

^{19}F n.m.r. determination of dissociation constant and chemical shift (Δ). Difluoro-oxaloacetate gives a single ^{19}F n.m.r. signal which moved upfield and broadened on addition of the aldimine form of aspartate transaminase. Incremental addition of difluoro-oxaloacetate to a solution of the aldimine enzyme in pyrophosphate buffer gave a series of chemical-shift values ($\delta_{obs.}$) which were used, as described in the Experimental section, to derive values (Table 1) for the dissociation constant K and chemical shift (Δ) of the difluoro-oxaloacetate–enzyme complex. The final plot of $\delta_{obs.}$ against $[ES]/[S_t]$ is shown in Fig. 2.

pH-dependence of n.m.r. parameters. The chemical shifts and peak widths of the ^{19}F n.m.r. signal of difluoro-oxaloacetate were measured at a range of pH values in the presence of aldimine enzyme. Plots of both parameters against pH (Fig. 3) show inflexion points at pH5.4 and pH8.0.

Difluoro-oxaloacetate–apoenzyme complex

Dissociation constant and chemical shift (Δ). Addition of difluoro-oxaloacetate (5mM) to a solution of apoenzyme (0.39mM) in 20mM-pyrophosphate buffer, pH7.4, gave a ^{19}F n.m.r. signal which was shifted upfield and broadened relative to that of difluoro-oxaloacetate in buffer alone. Incremental addition of further difluoro-oxaloacetate caused the signal to shift downfield and sharpen, as with the aldimine enzyme, and chemical-shift values were used in the same way to derive values of the dissociation constant, K, and the chemical shift (Δ) of the difluoro-oxaloacetate–apoenzyme complex (Table 1).

pH-dependence of n.m.r. parameters. The pH variations of the ^{19}F chemical shift and line width of difluoro-oxaloacetate in the presence of the apoenzyme were determined as for the aldimine form of the enzyme. Plots of both parameters versus pH (Fig. 4) showed an inflexion point at pH8.2, but not at lower pH values.

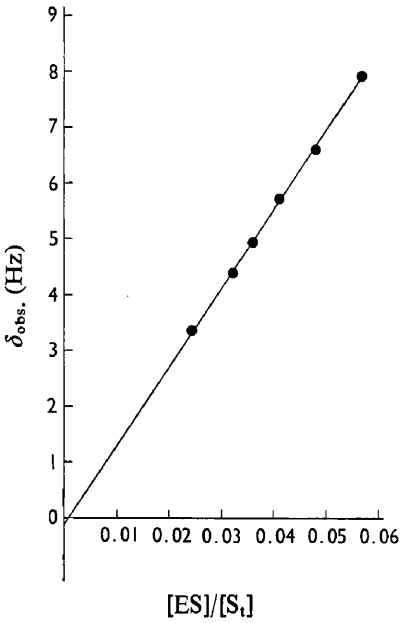

Fig. 2. *Plot of $\delta_{obs.}$ against $[ES]/[S_t]$ for the difluoro-oxaloacetate–aldimine enzyme*

Difluoro-oxaloacetate (total concentration $[S_t]$) was added incrementally (5–16mM) to a solution of the aldimine form of aspartate transaminase (0.46mM) in 20mM-pyrophosphate buffer, pH7.4, and the chemical shift ($\delta_{obs.}$) of the ^{19}F n.m.r. signal of difluoro-oxaloacetate relative to that of difluoro-oxaloacetate in buffer alone was observed. The plot represents the best fit of the experimental points to a straight line for a series of assumed values of K (see the Experimental section). This plot was obtained for $K = 2.9$mM (Table 1).

Table 1. *Dissociation constants and chemical shifts* (Δ) *of enzyme–fluoroacid complexes*

Positive values of Δ indicate an upfield shift relative to that of free ligand in buffer alone. Negative values indicate a corresponding downfield shift. Values for Δ are ±S.E. (Bliss, 1967).

	Aldimine		Apoenzyme	
Ligand	K (mM)	Δ (Hz)	K (mM)	Δ (Hz)
Difluoro-oxalo-acetate	2.9	+137±2	3.4	+99±6
Perfluorosuccinate	3.0	−93±1	—	—

Perfluorosuccinate–aldimine-enzyme complex

Dissociation constant and chemical shift (Δ). Addition of perfluorosuccinate (10mM) to a solution of the aldimine form of aspartate transaminase (0.66mM) in 20mM-pyrophosphate buffer, pH7.4, gave a single ^{19}F n.m.r. signal which was shifted downfield and broadened relative to that of perfluorosuccinate in buffer alone. Incremental addition of further perfluorosuccinate caused the signal to move upfield and sharpen. Chemical-shift values were used as described in the Experimental section to derive values for the dissociation constant and chemical shift (Δ) (Table 1) of the perfluorosuccinate–aldimine-enzyme complex.

Chemical shifts of ^{19}F n.m.r. signals of difluoro-oxaloacetate and perfluorosuccinate in the absence of enzyme

pH-dependence. The ^{19}F n.m.r. signal of difluoro-oxaloacetate showed a progressive downfield shift with increasing pH up to pH5. No further shift was observed between pH5 and 9. Comparison of the

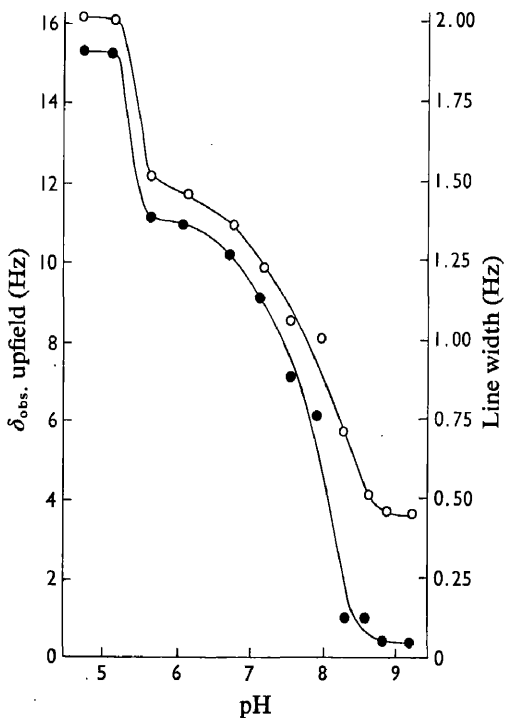

Fig. 3. *pH variation of ^{19}F chemical shift ($\delta_{obs.}$, ●) and line width (○) of difluoro-oxaloacetate in the presence of aldimine enzyme*

Difluoro-oxaloacetate was neutralized to pH4.9 with KOH and added to a solution of extensively dialysed aldimine form of aspartate transaminase (0.75mM) in double-distilled water, giving a final concentration of 6mM-difluoro-oxaloacetate and final pH4.9. The ^{19}F n.m.r. chemical shift ($\delta_{obs.}$) and line width relative to that of free difluoro-oxaloacetate in 20mM-pyrophosphate buffer, pH7.4, were observed as the pH of the system was increased by stepwise addition of 10mM-KOH.

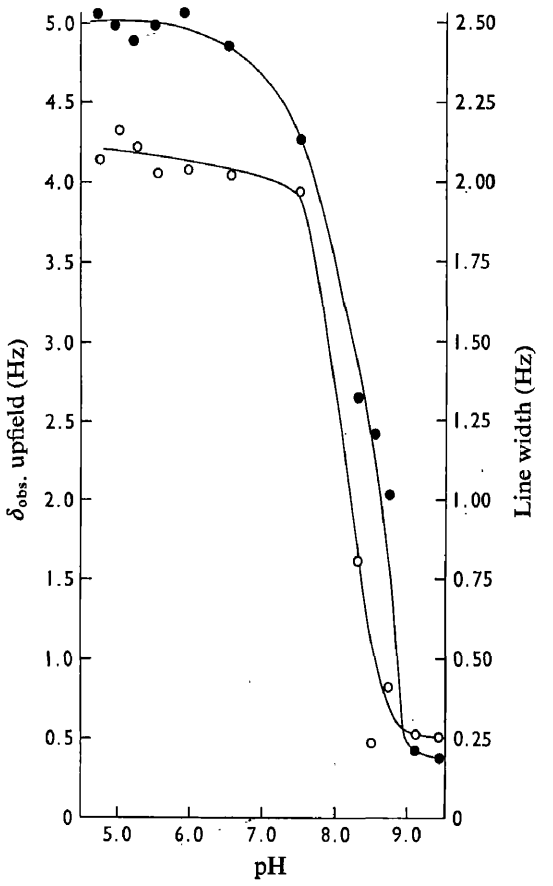

Fig. 4. *pH variation of ^{19}F chemical shift (●) and line width (○) of difluoro-oxaloacetate in the presence of apoenzyme*

Difluoro-oxaloacetic acid was neutralized to pH4.9 with KOH, and added to a solution of extensively dialysed apoenzyme (0.41 M) in double-distilled water to give a final concentration of 6mM-difluoro-oxaloacetate and final pH4.9. The ^{19}F n.m.r. chemical shift, $\delta_{obs.}$, and line width relative to those of difluoro-oxaloacetate in 20mM-pyrophosphate buffer, pH7.4, were observed as the pH of the system was increased by stepwise addition of 10mM-KOH.

chemical-shift–pH profile (Fig. 5) with the acid–base titration curve (Fig. 6) for difluoro-oxaloacetate indicates that the increase in chemical shift corresponds to the ionization of the second carboxyl group of difluoro-oxaloacetate, which is complete at pH5.

The ^{19}F n.m.r. signal of perfluorosuccinate shifted downfield with increasing pH up to pH3. No further shift was observed between pH3 and pH9 (Fig. 5).

Solvent effects. The chemical shifts of the ^{19}F n.m.r. signals of solutions of both difluoro-oxaloacetate and perfluorosuccinate in organic solvent/water mixtures varied with the composition of the mixture. Increasing the content of organic solvent in 2-methylpropan-2-ol/water and in dioxan/water mixtures caused the ^{19}F n.m.r. signal of difluoro-oxaloacetate to move progressively upfield, whereas the signal of perfluorosuccinate moved downfield. Over the range studied, the chemical shifts of both fluorinated compounds showed a linear dependence on the dielectric constant of both media (Fig. 7).

Discussion

Difluoro-oxaloacetate binds to the aldimine form of the enzyme to give an 'abortive complex' absorbing in the 430nm region, and spectrophotometric titration monitoring A_{435} gave a dissociation constant for the difluoro-oxaloacetate–aldimine-enzyme complex (2.8mM) close to that (1.8mM) previously reported for the oxaloacetate complex (Michuda & Martinez-Carrion, 1970). Good agreement with the spectrophotometrically determined dissociation constant was obtained by titration of the enzyme with

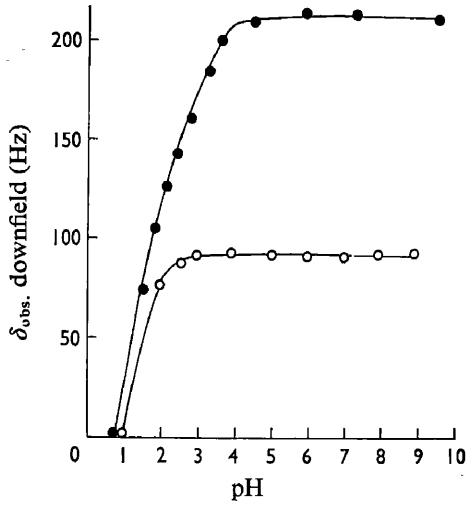

Fig. 5. *pH variation of ^{19}F chemical shift of difluoro-oxaloacetate* (●) *and perfluorosuccinate* (○)
Solutions of the free acids (20mM) in double-distilled water were titrated in the n.m.r. tube with 200mM-KOH and the chemical-shift changes ($\delta_{obs.}$) relative to the initial values observed.

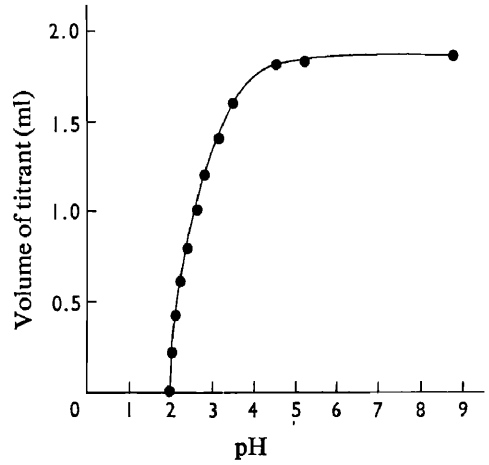

Fig. 6. *Variation of pH on titration of difluoro-oxaloacetate with base*
The pH of the mixture was followed as 0.2M-difluoro-oxaloacetic acid (5ml) was titrated with 0.107M-tetramethylammonium hydroxide.

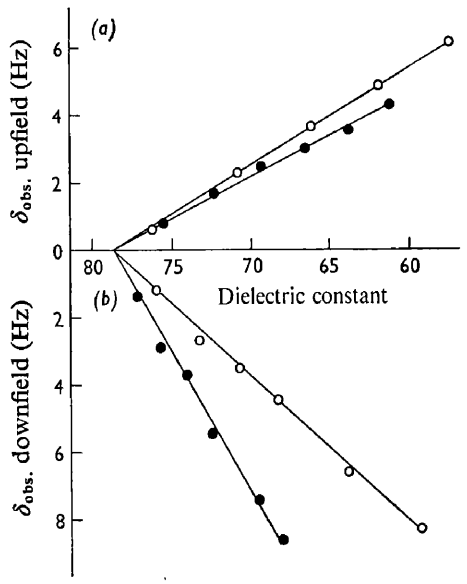

Fig. 7. *Variation of the ^{19}F chemical shifts of difluoro-oxaloacetate and perfluorosuccinate with the dielectric constant of the medium*
2-Methylpropan-2-ol (●) and dioxan (○) were added incrementally to a solution containing pre-neutralized fluoro acid (20mM) (*a*, difluoro-oxaloacetate; *b*, perfluorosuccinate) in 20mM-pyrophosphate buffer, pH7.4, and the ^{19}F chemical shift ($\delta_{obs.}$) was determined relative to that of the acid in buffer alone. Dielectric constants were calculated as described by von Hippel (1954).

difluoro-oxaloacetate, by following the ^{19}F n.m.r. chemical shift of the latter.

The ^{19}F n.m.r. signal of the difluoro-oxaloacetate–aldimine-enzyme system shifts upfield and broadens as the pH of the medium is decreased, and pH profiles of both chemical shift and line width show inflexion points at pH5.4 and 8.0 (Fig. 3). It is probable that the two inflexion points result from ionization of groups associated with the enzyme, as the chemical shift of difluoro-oxaloacetate alone does not vary at pH values greater than 5 (Fig. 5). The pH profiles of both line width and chemical shift can be explained in terms of a model in which each of the two carboxyl groups of difluoro-oxaloacetate binds to a specific group on the enzyme as that group is protonated. As the pH of the medium is lowered, the groups on the enzyme will be successively protonated and the difluoro-oxaloacetate becomes progressively more tightly bound. The resulting increase in correlation time is reflected in the increased line widths of the ^{19}F n.m.r. signal. Tighter binding of the carboxyl groups of difluoro-oxaloacetate to protonated enzyme might be expected to result in shifts of the ^{19}F n.m.r. signal in the same direction as when difluoro-oxaloacetate is protonated in the absence of enzyme, i.e. upfield, which is indeed the case.

It is of course possible that other factors apart from such charge-neutralization effects will contribute to the upfield shift of the ^{19}F n.m.r. signal of difluoro-oxaloacetate on binding to the enzyme. In this context it is of interest to consider the effect of aldimine enzyme on the ^{19}F n.m.r. signal of perfluorosuccinate. The ^{19}F n.m.r. line-width–pH profile for perfluorosuccinate in the presence of

aldimine enzyme (Martinez-Carrion *et al.*, 1973) is very similar to that for difluoro-oxaloacetate, suggesting that binding of both dicarboxylic acids is dependent on protonation of the same two enzyme groups. For perfluorosuccinate, however, the effect of enzyme is to shift the ^{19}F n.m.r. signal downfield, the opposite direction to that for difluoro-oxaloacetate. In the absence of enzyme, perfluorosuccinate behaves like difluoro-oxaloacetate in that protonation shifts the ^{19}F n.m.r. signal upfield (Fig. 5). The net downfield shift on addition of enzyme cannot therefore be attributed to effective protonation of perfluorosuccinate on binding to the enzyme. A possible explanation is suggested by the effect on the ^{19}F n.m.r. chemical shifts of perfluorosuccinate and difluoro-oxaloacetate of increasing the content of organic solvent in the systems dioxan/water and 2-methylpropan-2-ol/water. As the dielectric constant of the medium is decreased, the ^{19}F signal of perfluorosuccinate shifts downfield and that of difluoro-oxaloacetate upfield (Fig. 7). Although a number of factors contribute to the effects of the medium on fluorine chemical shifts (Emsley & Phillips, 1971), it is noteworthy that, in both cases, the effect of transfer to a less polar environment is to shift the ^{19}F n.m.r. signal in the same direction as when the fluorinated acids bind to the enzyme. The data can be qualitatively explained if the dominant effect on the chemical shift is one associated with binding in an apolar environment on the enzyme. With difluoro-oxaloacetate, the upfield shift arising from the apolarity of the enzyme surface would be reinforced by that caused by effective protonation of its carboxyl groups as they bind to protonated groups on the enzyme. With perfluorosuccinate, however, shifts caused by the two effects would be in opposite directions, and it may be significant that Δ for the perfluorosuccinate–aldimine-enzyme complex (95Hz downfield) is some 50% lower than that for the corresponding difluoro-oxaloacetate complex (140Hz upfield). The suggestion of an apolar environment at the binding site of aspartate transaminase is in accord with spectrophotometric data (Metzler *et al.*, 1973). In the absence of detailed three-dimensional structural data for aspartate transaminase, discussion of factors influencing chemical-shift effects in an enzyme complex is necessarily crude, and it is quite possible that further factors such as hydrogen-bonding or ring-current effects may be important in influencing chemical shifts of the fluorine atoms of the fluorinated dicarboxylic acids in their enzyme environment.

The inflexion point at pH5.4, which appears in the chemical-shift–pH and the line-width–pH profiles of difluoro-oxaloacetate in the presence of the aldimine form of the holoenzyme, is absent from the corresponding profiles with apoenzyme. This suggests that the low-pH inflexion point in the profiles of the aldimine enzyme results from ionization of a group associated with cofactor. The enamine group linking pyridoxal phosphate to a lysine residue in the aldimine enzyme is known (Cheng *et al.*, 1971) to be protonated with pK5.4 in the absence of buffer ions, and the data are consistent with binding of a carboxylate group of difluoro-oxaloacetate to the protonated form of this internal Schiff base. This grouping has been previously suggested as the low-pH carboxylate-binding site for glutamate to the aldimine enzyme (Jenkins & D'Ari, 1966).

The n.m.r.-parameter–pH profiles of difluoro-oxaloacetate in the presence of both holoenzyme and apoenzyme show an inflexion point at pH8.0, indicating that binding at high pH is influenced by ionization of an enzyme grouping that is not associated with cofactor. It is possible that this inflexion point reflects binding of a carboxylate group of difluoro-oxaloacetate to the protonated form of a histidine residue on the enzyme, as has been suggested for other dicarboxylic acids (Martinez-Carrion *et al.*, 1973). The pK for protonation of this enzyme group is, however, rather higher than that normally associated with histidine residues, and further evidence is necessary before such an assignment can be made.

Although a model in which binding of carboxylate groupings of difluoro-oxaloacetate to the enzyme is directly influenced by protonation of specific enzyme groups is attractive, it should be borne in mind that ionization of enzyme groupings could affect ligand binding in a less direct manner, such as via conformational changes in the enzyme, and such effects cannot be ruled out. The similarity of the n.m.r.-parameter–pH profiles in the difluoro-oxaloacetate–aldimine-enzyme system with those of perfluorosuccinate (Martinez-Carrion *et al.*, 1973) indicates that the two fluorinated dicarboxylic acids bind in the same manner to the enzyme. Moreover, as difluoro-oxaloacetate and perfluorosuccinate have been shown to mimic oxaloacetate (Briley *et al.*, 1977) and succinate (Martinez-Carrion *et al.*, 1973) respectively in their interactions with aspartate transaminase, it is likely that all four dicarboxylic acids, and possibly all dicarboxylic acids known to form abortive complexes, bind similarly to the aldimine enzyme.

We thank the Enzyme Chemistry and Technology Committee of the Science Research Council for a grant (to R. E. and R. H.) and for a research studentship (to G. D. S.).

References

Banks, B. E. C., Doonan, S., Lawrence, A. J. & Vernon, C. A. (1968) *Eur. J. Biochem.* **5**, 528–539

Bliss, C. I. (1967) *Statistics in Biology*, vol. 1, pp. 438–439, McGraw–Hill, New York
Briley, P. A., Eisenthal, R., Harrison, R. & Smith, G. D. (1977) *Biochem. J.* **161**, 383–387
Cheng, S., Michuda-Kozak, C. & Martinez-Carrion, M. (1971) *J. Biol. Chem.* **246**, 3623–3630
Emsley, J. W. & Phillips, L. (1971) *Prog. Nucl. Magn. Reson. Spectrosc.* **7**, 3–36
Groves, P. D., Huck, P. J. & Homer, J. (1967) *Chem. Ind.* 915–917
Haarhoff, K. N. (1969) *J. Theor. Biol.* **22**, 117–150
Jenkins, W. T. & D'Ari, L. (1966) *J. Biol. Chem.* **241**, 5667–5674
Jenkins, W. T. & Taylor, R. T. (1965) *J. Biol. Chem.* **240**, 2907–2913
Martinez-Carrion, M., Riva, F., Turano, C. & Fasella, P. (1965) *Biochem. Biophys. Res. Commun.* **20**, 206–211
Martinez-Carrion, M., Cheng, S. & Relimpo, A. M. (1973) *J. Biol. Chem.* **248**, 2153–2160
Metzler, D. E., Harris, C. M., Johnson, R. J., Siano, D. B. & Thomson, J. A. (1973) *Biochemistry* **12**, 5377–5392
Michuda, C. M. & Martinez-Carrion, M. (1970) *J. Biol. Chem.* **245**, 262–269
Ovchinnikov, Yu. A., Egorov, C. A., Aldanova, V. A., Feigina, M. Yu., Lipkin, V. M., Abdulaev, N. G., Grishin, E. G., Kiselev, A. P., Modyanov, N. N., Braunstein, A. E., Polyanovsky, O. L. & Nosikov, V. V. (1973) *FEBS Lett.* **29**, 31–34
Scardi, V., Scotto, P., Jaccarino, M. & Scarano, E. (1963) *Biochem. J.* **88**, 172–175
Smith, G. D., Eisenthal, R. & Harrison, R. (1977) *Anal. Biochem.* in the press
Torchinsky, Yu. M., Malakhova, E. A., Livanova, N. B. & Pikhelgas, V. Yu. (1968) in *Pyridoxal Catalysis: Enzymes and Model Systems* (Snell, E. E., Braunstein, A. E., Severin, E. S. & Torchinsky, Yu. M., eds.), pp. 269–290, Interscience, London
von Hippel, A. R. (1954) *Dielectrics and Waves*, p. 231, John Wiley and Sons, New York

Biochem. J. (1977) **161**, 383–387
Printed in Great Britain

Interaction of Difluoro-oxaloacetate with Aspartate Transaminase

By PATRICIA A. BRILEY, ROBERT EISENTHAL, ROGER HARRISON and GEOFFREY D. SMITH
Biochemistry Group, School of Biological Sciences, University of Bath, Claverton Down, Bath BA2 7AY, U.K.

(*Received* 10 *August* 1976)

Difluoro-oxaloacetate behaves as a competitive inhibitor of 2-oxoglutarate and as an uncompetitive inhibitor with respect to aspartate in steady-state kinetic experiments with cytoplasmic aspartate transaminase. In the presence of high concentrations of aspartate transaminase, difluoro-oxaloacetate is slowly transaminated to difluoro-aspartate, suggesting its use as a kinetic probe to study the reactions of the aminic form of the enzyme.

Difluoro-oxaloacetate is an isosteric analogue of oxaloacetate in which the CH_2 grouping of oxaloacetate is replaced by CF_2. Such analogues, containing one or more fluorine atoms in place of corresponding hydrogen atoms of a natural substrate, have been shown in many cases to mimic the biological activity of the latter (Ciba Foundation Symposium, 1972). However, little is known about the interaction of difluoro-oxaloacetate with aspartate transaminase, an enzyme that normally catalyses the transamination of oxaloacetate. The kinetics of aspartate transaminase have been studied in detail by using analogues of the amino acid substrates which give information about the reactions of the aldimine form of the enzyme (Braunstein, 1973). Difluoro-oxaloacetate, which is easily prepared and uncomplicated by enolization, appeared to be a suitable oxo acid analogue with which to examine the lesser-known reactions of the aminic form of the enzyme. The steady-state kinetics of the interaction of difluoro-oxaloacetate with cytoplasmic aspartate transaminase of pig heart are reported in the present paper.

Experimental

Materials

Difluoro-oxaloacetic acid. Difluoro-oxaloacetic acid was prepared by a modification of the method described by Kun *et al.* (1963) in which the geminal hydrogen atoms on the β-carbon of diethyl oxaloacetate are replaced by fluorine by using perchloryl fluoride. NaH was used as a basic catalyst in place of the sodium ethoxide of the earlier method.

A stirred suspension of diethyl oxaloacetate sodium enolate (21g; Kodak Ltd., Kirkby, Liverpool, U.K.) in toluene/dioxan (2:1, v/v; 100ml) was cooled to −10°C in an atmosphere of dry CO_2-free N_2. Perchloryl fluoride was bubbled into the reaction mixture for 25min and the temperature was allowed to rise to between −5° and 0°C. NaH (50% suspension in mineral oil; 4.8g) suspended in toluene/dioxan (2:1, v/v; 10ml) was added dropwise to the reaction mixture without interrupting the flow of perchloryl fluoride, which was continued for a further 30min. After this time gas chromatographic analysis of samples of the reaction mixture showed the content of diethyl difluoro-oxaloacetate to have reached a maximum value. The flow of perchloryl fluoride was stopped and the reaction mixture was purged with CO_2-free N_2. Ether (250ml) and sufficient distilled water to dissolve inorganic salts were added to the reaction mixture followed by saturated aq. NaCl (100ml). The ether phase was shaken, separated and washed successively with water (200ml) and saturated aq. NaCl (100ml). Each aqueous extract was extracted in turn with ether (3×250ml) and benzene (2×100ml). All organic extracts were combined, dried (over $MgSO_4$) and concentrated under diminished pressure giving a brown oil from which an immiscible layer of mineral oil was removed by using a Pasteur pipette. Distillation gave diethyl difluoro-oxaloacetate (9.2g, yield 41%), b.p. 65–66°C/67Pa (0.5mmHg) as a colourless oil, which was homogeneous by g.l.c. Kun *et al.* (1963) quote b.p. 64°C/134Pa (1mmHg).

The diethyl ester was hydrolysed by boiling a solution of it (9.2g) in 3M-HCl (60ml) under reflux for 1h. The hydrolysate was cooled and concentrated under reduced pressure to give a crystalline residue that was recrystallized from trifluoroacetic acid/benzene to give difluoro-oxaloacetic acid as its monohydrate (5.2g, yield 68%), m.p. 116–117°C. Titration of the acid with 1M-NaOH gave mol.wt. 186 consistent with its being a monohydrate. Kun *et al.* (1963) give m.p. 119–120°C.

Aspartate transaminase. Cytoplasmic aspartate transaminase (L-aspartate–2-oxoglutarate aminotransferase, EC 2.6.1.1) was prepared in its aldimine form from fresh pig heart ventricles by the method of

Jenkins *et al.* (1959) as modified by Turano *et al.* (1964). 2-Oxoglutarate was included in all buffers. The final product was extensively dialysed against double-distilled water, freeze-dried and stored under vacuum at 5°C. In a typical preparation 2kg of pig heart ventricles yielded 250mg of aspartate transaminase (specific activity 640units/mg) having A_{280}/A_{362} 7.25 at pH7.4.

The aminic form of the enzyme was prepared from the aldimine form by using cysteine sulphinate as described by Jenkins & D'Ari (1966).

Unless otherwise stated all laboratory reagents were purchased from BDH Chemicals, Poole, Dorset, U.K.

Methods

Enzyme assays. Aspartate transaminase activity was assayed by spectrophotometric determination of oxaloacetic acid at 260nm at 30°C in 100mM-KH_2PO_4 adjusted to pH7.4 with KOH under conditions such that enolization of the oxo form of the acid is not partially rate-limiting (Banks *et al.*, 1963). Standard assay conditions were as described by Banks *et al.* (1968). A cuvette (1cm path-length) contained L-aspartate (64.5mM) and 2-oxoglutarate (6.85mM) in 100mM-triethanolamine/HCl buffer (final pH7.5) in a total volume of 3ml at 25°C. Reactions were initiated by addition of enzyme and were followed by changes in A_{260}. One unit of activity is defined as that amount of enzyme catalysing a change in A_{260} of 0.1/min. Enzyme concentrations are expressed in terms of sites, calculated from protein concentration, determined as described by Banks *et al.* (1968), and a mol.wt. of 46500 (Ovchinnikov *et al.*, 1973).

Gas–liquid chromatography. G.l.c. was done on columns (2m×6mm) of coiled stainless-steel packed with 3% silicone-gum rubber SE-301 on High Performance (H.P.) Chromasorb W (80–100 mesh). Samples were chromatographed isothermally at 100°C in a Perkin–Elmer F11 gas chromatograph equipped with a flame ionization detector.

N.m.r. spectra were recorded on a Jeol PS 100 n.m.r. spectrometer and the signal-to-noise ratio was enhanced by means of repeated scans with a Jeol JNB SB-3 signal-to-noise booster. Spectrophotometric measurements were performed in a Pye–Unicam SP. 1800 spectrophotometer and free F^- was assayed by using a combination fluoride electrode, model 96-09 (Orion Research Inc., Cambridge, MA, U.S.A.). All measurements were done at 30°C unless otherwise stated.

Results and Discussion

In its catalytic role the aminic form of aspartate transaminase interacts with oxo acid substrates and is converted into the aldimine form which reacts with amino acid substrates. The substrate kinetics of the enzyme are known (Braunstein, 1973) to be consistent with a substituted enzyme (Ping Pong) mechanism involving binary complexes. It is also well established (Haarhoff, 1969) that most dicarboxylic acid substrate analogues of aspartate transaminase bind to both forms of the enzyme, as shown for difluoro-oxaloacetate in Scheme 1. The rate equation corresponding to Scheme 1 is:

Scheme 1. *Possible reaction scheme for the interaction of difluoro-oxaloacetate with aspartate transaminase*

E', Aminic transaminase; E, aldimine transaminase; A, oxo acid substrate (2-oxoglutarate); B, amino acid substrate (aspartate); I, inhibitor (difluoro-oxaloacetate); P, amino acid product (glutamate); Q, oxo acid product (oxaloacetate).

$$\begin{aligned} E'+A &\rightleftharpoons E'A \\ E'A &\rightarrow E+P \\ E+B &\rightleftharpoons EB \\ EB &\rightarrow E'+Q \\ E'+I &\rightleftharpoons E'I \\ E+I &\rightleftharpoons EI \end{aligned}$$

$$v=\frac{V[A][B]}{[A][B]+K_b[A](1+[I]/K_i)+K_a[B](1+[I]/K_i')} \quad (1)$$

where A, B and I are as defined in Scheme 1, K_i' is the dissociation constant of the aminic transaminase–inhibitor complex, K_i is that of the aldimine enzyme–inhibitor ('abortive') complex, and K_a and K_b are the Michaelis constants for 2-oxoglutarate and aspartate respectively. Eqn. (1) is of the form:

$$v=\frac{V[A][B]}{[A][B]+K_a^i[B]+K_b^i[A]} \quad (2)$$

where $K_a^i=K_a(1+[I]/K_i')$ and $K_b^i=K_b(1+[I]/K_i)$. The effect of difluoro-oxaloacetate (I) on K_a^i and K_b^i was investigated by kinetic studies in which concentrations of 2-oxoglutarate (A) and aspartate (B) were systematically varied at each of a series of concentrations of I. Eqn. (2) may be written as:

$$v=\frac{\frac{V[B]}{[B]+K_b^i}[A]}{[A]+K_a^{app.}} \quad (3)$$

where

$$K_a^{app.}=\frac{K_a^i[B]}{[B]+K_b^i} \quad (4)$$

Values of $K_a^{app.}$ were determined from direct linear plots (Eisenthal & Cornish-Bowden, 1974) of initial rates against concentration of 2-oxoglutarate (A) at different fixed concentrations of aspartate (B) for each difluoro-oxaloacetate concentration. Similar plots of $K_a^{app.}$ against aspartate concentration allowed

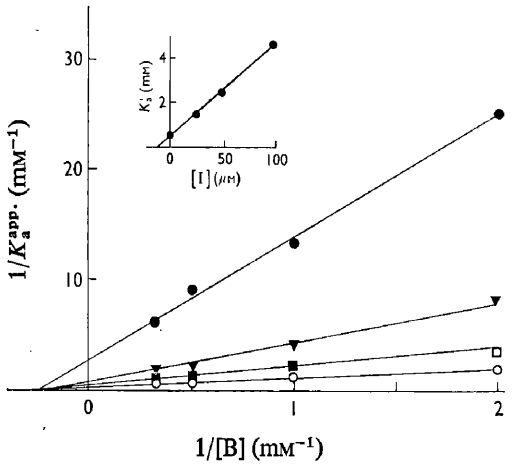

Fig. 1. *Secondary plot of effect of aspartate concentration [B] on $K_a^{app.}$ at various inhibitor concentrations*
Primary kinetic data were obtained from initial-rate measurements at 2-oxoglutarate concentrations of 0.1, 0.25, 0.5 and 1.0mM; difluoro-oxaloacetate concentrations: ●, 0; ▼, 25μM; ■, 50μM; ○, 100μM. Lines are drawn by using parameters calculated as described in the text. Inset: variation of K_a^1 as a function of difluoro-oxaloacetate concentration [I].

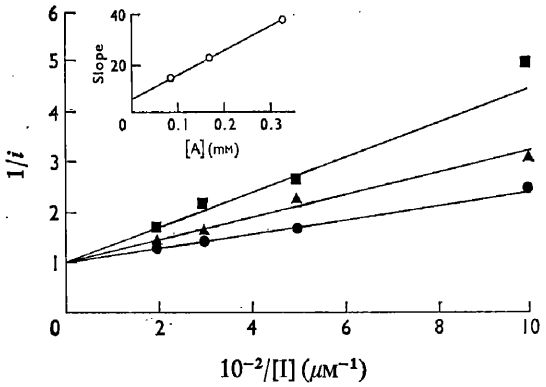

Fig. 2. *Effect of difluoro-oxaloacetate on fractional inhibition of transaminase*
Double-reciprocal plot of fractional inhibition (i) against difluoro-oxaloacetate concentration ([I]). Aspartate was held constant at 2.0mM; 2-oxoglutarate concentration: ●, 0.083mM; ▲, 0.166mM; ■, 0.33mM. The enzyme concentration was 1.0nM. The lines were drawn by using parameters estimated from direct linear plots (Eisenthal & Cornish-Bowden, 1974) of i against [I]. Inset: variation of the slope as a function of 2-oxoglutarate concentration ([A]).

determination of K_a^1 and K_b^1 (eqn. 4). These are displayed in Fig. 1 as plots of $1/K_a^{app.}$ against 1/[B] for each value of [I]. In such a plot the ordinate intercept is $1/K_a^1$ and the abscissa intercept $-1/K_b^1$. The lines in Fig. 1 share a common abscissa intercept, but the ordinate intercepts show a linear dependence on [I] (Fig. 1, inset), showing that K_a^1 but not K_b^1 depends on the concentration of inhibitor. It thus appears that the EI complex makes a negligible contribution to the observed rates under the experimental conditions used and suggests that terms in eqn. (1) containing K_i be neglected. This leads to eqn. (5):

$$v = \frac{V[A][B]}{[A][B]+K_a[B](1+[I]/K_i')+K_b[A]} \quad (5)$$

which adequately describes the results. From this it can be seen that inhibition by difluoro-oxaloacetate is competitive with respect to the oxo acid substrate and uncompetitive with respect to the amino acid substrate. It follows that the species responsible for inhibition is the complex of the inhibitor with the aminic form of aspartate transaminase (E'I in Scheme 1).

Justification for eqn. (5) was provided by a separate series of experiments on the effect of various inhibitor concentrations on the fractional inhibition, i, at different fixed concentrations of 2-oxoglutarate and constant aspartate. The results are shown in Fig. 2 as a plot of $1/i$ against 1/[I] where $i = 1-v_i/v_0$, v_i being the velocity in the presence of inhibitor and v_0 the uninhibited velocity. The observed pattern of straight lines converging on a common ordinate intercept of unity is consistent with both competitive and mixed inhibition. These can be distinguished by a secondary plot of slope against 2-oxoglutarate concentration. Rearrangement of eqn. (1) in fractional inhibition form gives:

$$\frac{1}{i} = \frac{[A][B]+K_a[B]+K_b[A]}{(K_a[B]/K_i')+(K_b[A]/K_i)}\left(\frac{1}{[I]}\right)+1 \quad (6)$$

If eqn. (6) is applicable, the secondary plot of slope versus [A] will not be linear. However, if $K_i \gg K_i'$ values of K_a and K_b are, in this case, such that the second term in the denominator may be neglected,

$$\frac{1}{i} = \left[\frac{[A]K_i'}{K_a}\left(1+\frac{K_b}{[B]}\right)+K_i'\right]\left(\frac{1}{[I]}\right)+1 \quad (7)$$

and a secondary plot of slope against [A] is linear, as observed (Fig. 2, inset). Eqn. (7) may also be directly derived from eqn. (5).

An estimate of $K_i' = 9.2\mu M$ was obtained from the plot of K_a^1 against [I] (Fig. 1, inset). These results are in reasonable agreement with the K_i' of 5.85μM (ordinate intercept) obtained from the secondary plot of slope (Fig. 2) against 2-oxoglutarate (Fig. 2, inset). The kinetic data here, obtained by using purified cytoplasmic aspartate transaminase from pig heart, are in contrast with those obtained by using a crude mitochondrial extract of rat liver, containing aspartate transaminase (Kun *et al.*, 1963), in which difluoro-oxaloacetate was found to behave as a non-

competitive inhibitor with respect to aspartate. Preincubation of transaminase (either form) with inhibitor alone or together with aspartate or 2-oxoglutarate did not affect the initial rates, showing that difluoro-oxaloacetate does not irreversibly inactivate the enzyme.

A significant contribution to the steady-state kinetics from productive breakdown of the difluoro-oxaloacetate–aminic enzyme complex would result in non-hyperbolic variation of initial rates with variation of inhibitor or 2-oxoglutarate concentrations. In neither case was such kinetic behaviour detected, indicating that the measured K_i' is a good approximation to the true dissociation constant of the difluoro-oxaloacetate–aminic enzyme complex. When difluoro-oxaloacetate (0.2mM) was incubated with aspartate (30mM) in the presence of a relatively high concentration (30μM) of enzyme, however, a time-dependent increase in A_{260} was observed, indicative of oxaloacetate formation. Detectable rates were obtained only at enzyme concentrations 4000-fold greater than those used in the kinetic studies described above. The turnover was some five orders of magnitude less than those with 2-oxoglutarate, results which are consistent with the assumption that transamination of the fluoroanalogue does not significantly contribute to the steady state kinetics.

Direct spectrophotometric evidence of initial aminic enzyme–difluoro-oxaloacetate complex-formation followed by a very much slower transamination reaction was obtained by incubation of difluoro-oxaloacetate (100μM) with aminic enzyme (25μM) in 20mM-pyrophosphate buffer, pH7.4. An initial rapid shift ($t_{\frac{1}{2}}$ approx. 5s) of the absorption maximum of the aminic enzyme (332nm) to lower wavelength (approx. 328nm) was followed by the slow appearance of an absorption band with $\lambda_{max.}$ 360nm, characteristic of aldimine enzyme, over a period of approx. 30min.

Demonstration of the transamination of difluoro-oxaloacetate to difluoroaspartate was obtained by using cysteine sulphinate as the amino acid substrate. Difluoro-oxaloacetate (50mM), cysteine sulphinic acid (40mM) and aspartate transaminase (0.2mM) were incubated in 50mM-ammonium acetate buffer, pH7.4, for 4 days at 22°C in an n.m.r. tube. The intensity of the ^{19}F n.m.r. single t(Fig. 3) of the oxo acid decreased and a multiplet characteristic of the ABX system of difluoroaspartate (Fig. 3) appeared (J_{AX} 8, J_{BX} 21, J_{AB} 270, $\nu_A-\nu_B$ 456 Hz). Analysis of the completed reaction mixture for free F^- by using an F^--specific electrode indicated less than 5% decomposition of transaminated difluoro-oxaloacetate. This contrasts with the extensive decomposition reported (Kun *et al.*, 1960) after similar enzymic transamination of monofluoro-oxaloacetate.

Although the reactions of the aldimine form of aspartate transaminase have been extensively studied there is little corresponding knowledge about the aminic enzyme; a circumstance directly attributable to the lack of a suitable substrate analogue (Fasella & Turano, 1970). Apart from a single mention, without experimental details (Kun *et al.*, 1963), there has been no previous report of the substrate activity of difluoro-oxaloacetate with any form of aspartate transaminase, and the present finding that the fluoro analogue is slowly transaminated by the aminic enzyme suggests that difluoro-oxaloacetate may well provide the required probe for kinetic studies of the aminic enzyme.

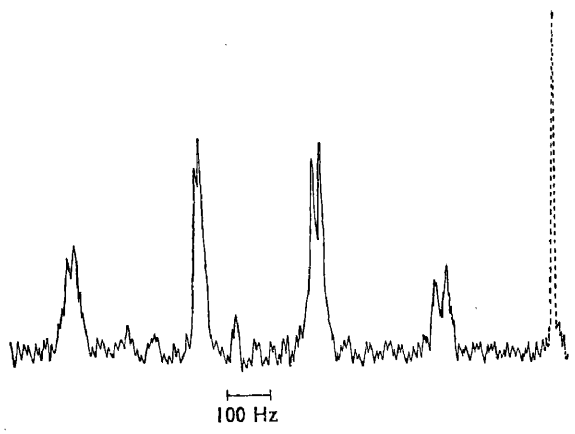

Fig. 3. *^{19}F n.m.r. spectra of difluoroaspartate and difluoro-oxaloacetate*

The spectra were obtained under the conditions described in the text and are the average of 16 spectral scans. The singlet (----) is the spectrum of unchanged difluoro-oxaloacetate.

We thank the Enzyme Chemistry and Technology Committee of the Science Research Council for a grant (to R. E. and R. H.) and a studentship (to G. D. S.).

References

Banks, B. E. C., Lawrence, A. J., Thain, E. M. & Vernon, C. A. (1963) *J. Chem. Soc.* 5799–5806

Banks, B. E. C., Doonan, S., Lawrence, A. J. & Vernon, C. A. (1968) *Eur. J. Biochem.* **5**, 528–539

Braunstein, A. E. (1973) in *The Enzymes* (Boyer, P. D., ed.), pp. 379–481, Academic Press, New York

Ciba Foundation Symposium (1972) *Carbon–Fluorine Compounds: Chem. Biochem. Biol. Activities, Ciba Found. Symp.*, Elsevier, Amsterdam

Eisenthal, R. & Cornish-Bowden, A. (1974) *Biochem. J.* **139**, 715–720

Fasella, P. & Turano, C. (1970) *Vitam. Horm. (N.Y.)* **28**, 157–194

Haarhoff, K. N. (1969) *J. Theor. Biol.* **22**, 117–150

Jenkins, W. T. & D'Ari, L. (1966) *Biochem. Biophys. Res. Commun.* **22**, 376–382

Jenkins, W. T., Yphantis, D. A. & Sizer, I. W. (1959) *J. Biol. Chem.* **234**, 51–57

Kun, E., Fanshier, D. W. & Grassetti, D. R. (1960) *J. Biol. Chem.* **235**, 416–419

Kun, E., Gottwald, L. K., Fanshier, D. W. & Ayling, J. E. (1963) *J. Biol. Chem.* **238**, 1456–1463

Ovchinnikov, Yu. A., Egorov, C. A., Aldanova, N. A., Feigina, M. Yu., Lipkin, V. M., Abdulaev, N. G., Grishin, E. V., Kiselev, A. P., Modyanov, N. N., Braunstein, A. E., Polyanovsky, O. L. & Nosikov, V. V. (1973) *FEBS Lett.* **29**, 31–34

Turano, C., Giartosio, A., Riva, F. & Fasella, P. (1964) *Biochem. Biophys. Res. Commun.* **16**, 221–226